Transatlantic Hydrogen Seagoing Aircraft

Final Report Group 21

Max van Bart	4994655	Rowan Heckmanns	4840402
Paula Méndez Chacón	5067758	Alexander Kiselev	5071909
Paloma Diaz Garcia	5015332	Julie van Nauta Lemke	5071348
Mika Doorenbosch	4868730	Thomas Potgieter	5003733
Atze Harmsen	5060346	Kato Vanaken	5006163

Delft University of Technology

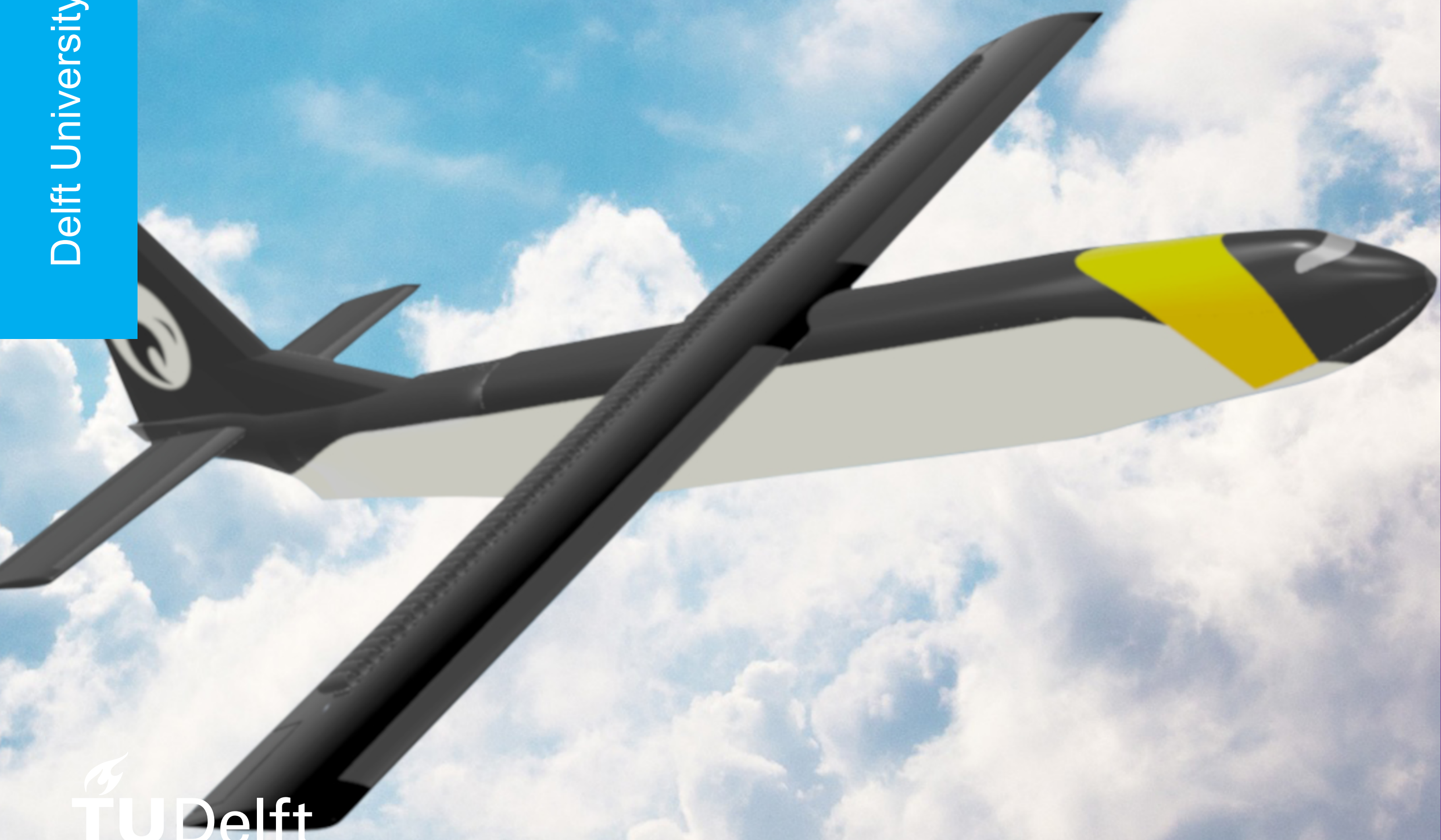

TU Delft

This page is intentionally left blank.

Transatlantic Hydrogen Seagoing Aircraft

Final Report Group 21

by

Max van Bart	4994655	Rowan Heckmanns	4840402
Paula Méndez Chacón	5067758	Alexander Kiselev	5071909
Paloma Diaz Garcia	5015332	Julie van Nauta Lemke	5071348
Mika Doorenbosch	4868730	Thomas Potgieter	5003733
Atze Harmsen	5060346	Kato Vanaken	5006163

AE3200 - Design Synthesis Exercise

at the Delft University of Technology,

Project duration:	April 19, 2022 – June 23, 2022	
DSE committee:	Ir. R.N.H.W. van Gent,	TU Delft, Tutor
	Ir. E.C. Bunschoten,	TU Delft, Coach
	Ir. G. Zoppini,	TU Delft, Coach

Delft University of Technology

Executive Overview

"An emphasis on sustainability and sustainable design is critical to enable future generations to enjoy a similar quality-of-life as in the present day. In the aviation sector, sustainable solutions are proving to be difficult to realise. Recently, there has been a significant amount of interest in battery-powered flight. However, this option is only viable for short range flights due to the excessive weight of batteries. For longer distance flights, such as the transatlantic route, which is one of the busiest in the world, it is of great importance to explore alternative options."[1] One such alternative is the transatlantic, hydrogen, seagoing aircraft summarised in this report, called the 'Emperor', which is propelled by fans driven from electricity generated by cryogenic liquid hydrogen in fuel cells. The sea-based Emperor is a zero-emission alternative to present-day aviation, excelling in payload capacity.

This executive overview serves as a stand-alone document, summarising the report and presenting a total overview of the design of the transatlantic hydrogen seagoing aircraft called the Emperor.

Project Objectives and Requirements

The mission statement for the project is, "Provide a sustainable, transatlantic air travel alternative to present-day civil aviation, competitive in payload capacity, travel time, ticket price, safety and reliability." [1]. The project objective is to, "Develop a design for a sustainable, transatlantic aircraft as a group of 10 students in 10 weeks in order to gain experience in complex engineering processes and explore an interesting alternative air travel solution." [1]. These statements are the basis for the design. A set of requirements are determined by the stakeholders, of which various system and subsystem requirements are derived. This is done with the aid of a requirement discovery tree in order to constrain the full design and the key requirements for the stakeholders are provided below.

- **HHA-Sys-T01-01** The Emperor shall have a minimum cruise speed of 500 [km/h].
- **HHA-Sys-T03-01** The Emperor shall be able to carry a minimum of 500 passengers.
- **HHA-Sys-T11-01** The cost per passenger for the airline shall be comparable to present day transoceanic flight.
- **HHA-Sys-T06-01** The Emperor shall emit no greenhouse gases during operation.

From the full set of system requirements, the driving requirements are identified to be the following.

- **HHA-Sys-T01-01** The Emperor shall have a minimum cruise speed of 500 [km/h].
- **HHA-Sys-T06-01** The Emperor shall emit no greenhouse gases during operation.
- **HHA-Sys-T03-01** The Emperor shall be able to carry a minimum of 500 passengers.
- **HHA-Sys-T02-01** The Emperor shall have a minimum range of 8,000 [km].
- **HHA-Sys-T10-01** The Emperor shall be able to take-off from the sea.
- **HHA-Sys-T10-02** The Emperor shall be able to land in the sea.

Functional Analysis

Apart from the actual flights themselves, there are several other tasks vital in performing transoceanic air travel in a safe and sustainable manner. These start with the designing and manufacturing of the aircraft, and also include the handling of pre- and post-flight logistics, communicating during the flight and the transportation of the payload. Maintenance has to be performed regularly and the aircraft will get scrapped at the end of life. A functional analysis breaks this operational life down into multiple (sub)functions, and displays the sequential order of performing these tasks.

Preliminary Design and Trade-off Summary

The original concept provided by the client was an electrically powered combination of a seaplane and an airship, where hydrogen would both be used as fuel in fuel cells and would generate lift as a buoyancy gas. It was thought that this combination may lead to an efficient solution to long range, yet sufficiently fast and cost effective, passenger travel.

It was found that in order to assure that the hydrogen produces lift at take-off, the pressure of the gas had to be kept lower than 14 times sea-level pressure. Preliminary results indicated that any concepts using pressures lower than and around this value were estimated to require exceptionally larger fuel containers which have would resulted in large amounts of drag. This severely limited their achievable speeds. Therefore, concepts using hydrogen stored at higher pressures were explored further. After further research and after consulting several hydrogen experts, a cryogenic liquid hydrogen concept was investigated. By means of a trade-off, the final concept was chosen to be the cryogenic, liquid hydrogen, electrically powered aircraft.

Initialising the Detailed Design

Before iterating over the detailed design, it was necessary to estimate some initial values as a starting point for the iteration. This was done by developing a statistical relation between different concepts for hydrogen aircraft which are in an advanced development stage. This resulted in a 1,500 passenger aircraft with an estimated operating empty mass of 661 $[tons]$. This was then incorporated into a constraint diagram in order to produce an initial estimate of the required power and main wing surface area, given the flight mission profile as prescribed by the requirements.

Design Characteristics

An in depth analysis and sizing was done for the final design concept, for a mission consisting of a 8000 $[km]$ cruise and a 30 $[min]$ loiter, all at an altitude of 3000 $[m]$. After an aerodynamics analysis, the wing has been sized to have a surface area of 1977 $[m^2]$ and a span of 126 $[m]$. On the other hand, stability analyses have proven that a vertical tailplane of 302.34 $[m^2]$ and horizontal tailplane of 745 $[m^2]$ are required for longitudinal and lateral stability. Regarding airfoils, the NACA $65_1 412$ was selected for the main wing and the NACA 0010 for the tailplanes.

Being a sea-based aircraft, the hydrodynamics at take-off had to be addressed. Studies have been done into drag reduction technologies, such as hydrofoils, and it was found that the most effective solution would be to use the NACA TN-2481 seaplane hull without hydrofoils. The power required at take-off was found not to be a limiting condition for the aircraft, with regular operations being able to take place safely with wave heights of up to 2.99 $[m]$. The take off speed was found to be 79.47 $[m/s]$. In order to ensure longitudinal static stability on water, the use of mid-wing floats was required.

The aircraft utilizes 82 fans powered by electric motors. Each fan is attached to a 4 $[MW]$ electric motor, which includes an inverter. The fans are distributed along the top side of the wing, at a small distance above the wing surface. This placement allows for a phenomenon called boundary layer ingestion (BLI) to occur. Due to BLI, the propulsive efficiency is expected to be increased by 10%. The total mass of the propulsion system, including all fans, motors, inverters, cabling and the integration structure is 99.1 [$tons$].

Fuel cells use gaseous hydrogen and oxygen to generate water vapour and electricity. With the required peak power of the entire aircraft calculated to be 484 [MW] and assuming a future mass power density of 8000 [W/kg], a total size of 66.9 [m^3] and weight of 80297 [kg] have been found. This sizing is valid for the PEM fuel cells of the type VLS II Pro-165, which will be used in the Emperor.

The hydrogen fuel system supplies the fuel cells with gaseous hydrogen, but the fuel is stored as a liquid. Storing liquid hydrogen implies cryogenic temperatures and as such, special attention was paid to the fuel containment system. It was found that 5.8 [mm] thick aluminium tanks with an additional 2.2 [mm] of multi-layer insulation were sufficient to contain the fuel, deal with stresses involved and limit hydrogen boil-off. The complete fuel containment system was split up into three different tanks; forward, mid and aft. The forward tank, located above the cabin and in front of the wingbox, is the largest and contains 91.34 [$tons$] of hydrogen. The mid tank, located aft of the wingbox but still above the cabin, contains 28.45 [$tons$] of hydrogen and the final aft fuel container, located in the tail section after the cabin, was designed to hold 17.65 [$tons$]. This division was done to improve the stability of the aircraft as well as its safety features.

The choice of materials has a large influence on the weight, performance and cost of the Emperor. A qualitative analysis resulted in the exterior of the Emperor existing mainly out of carbon reinforced composites and aluminium 6063. A structural analysis has proven that these materials lead to reasonable thicknesses of the fuselage and an acceptable amount of stringers in the wing.

After being designed, the subsystems had to be connected to each other and fitted into the Emperor. From the fuel cells located in the wings, electricity is guided to the electro-mechaninical actuators of the moving surfaces, the environmental control system and the propulsion system.

Design Analysis and Summary

The final configuration can be seen in Figure 1. The final MTOW is 1169 [$tons$] and the total fuel mass is 137 [$tons$]. The total length of the aircraft is 133.6 [m], with a fuselage height of 14.4 [m] and a width of 9.7 [m]. The wing span is 125.78 [m] with a surface area of 1977 [m^2]. The component that takes up the most mass is the fuselage, taking up 21.99 % of the mass, followed by a combination of miscellaneous components such as the internal systems, furnishings and extra weight added by the hull and floats which take up 19.81 %. This is followed by the wing, fuel cells, engines, horizontal tail, fuel containers and vertical tails in a decreasing order.

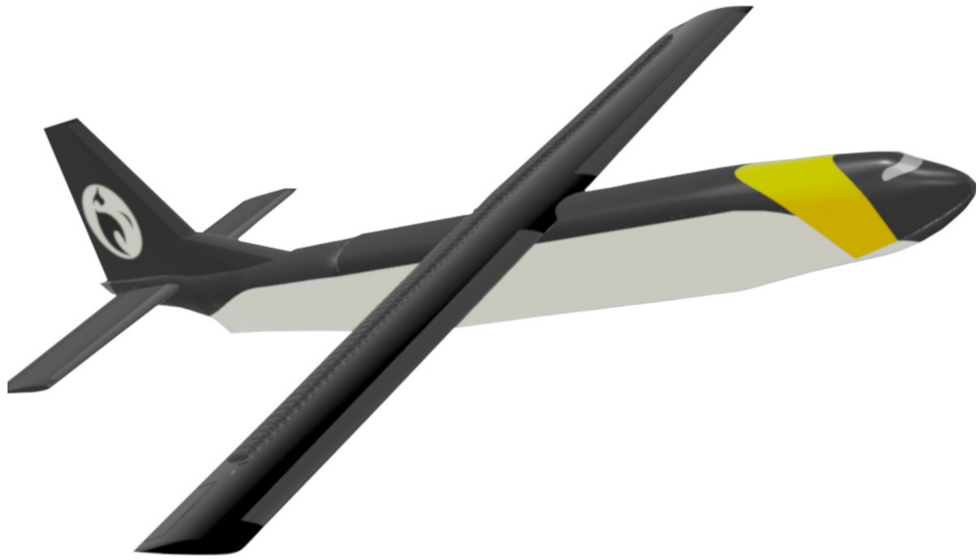

Figure 1: *Render of the Emperor*

The aircraft flies at an altitude of 3,000 $[m]$ which enables comfortable flight without pressurizing the cabin and avoids the design challenges that come with a non-circular pressurized cabin. The maximum range at maximum fuel is 8,000 $[km]$ and at zero payload is 10,000 $[km]$. The optimal climb velocity at take-off is 14.1 $[m/s]$ and the climb angle for this is 7.3 $[\mathrm{deg}]$. At cruise conditions, the optimal climb velocity is 7.94 $[m/s]$ with a climb angle of 8.4 $[\mathrm{deg}]$. The higher the altitude, the higher the speed required to stay above stall limit and achieve maximum rates of climb. However, there is a limit to how fast the Emperor can fly at a certain altitude due to increased drag in the transonic speed regime. Nevertheless, these effects at higher altitudes will not be experienced by the Emperor due to a service ceiling of 3,810 $[m]$ since the cabin is non-pressurized.

For the approximation of the noise produced by the Emperor, only that caused by the exhaust of the fans is considered. For an exhaust velocity of 229 $[m/s]$ at maximum power setting and taking into account the use of distributed electric propulsion, the noise produced is deemed to be 3.2 $[dB]$ more than the A320 at take-off and 5.2 $[dB]$ more at landing, this however is a very conservative approach.

While performance requirements must be satisfied, the Emperor must also be reliable, available, maintainable and safe. Reliability is ensured by the use of redundancy and maintenance in systems and operations that are deemed less reliable. These are the refueling logistics, sea-based take-off and landing procedures, and the electric systems. The biggest challenge to availability is the dependence on favorable weather conditions, which is due to the low cruising altitude and the take-off and landing on water. Due to the large size of the Emperor, maintenance will take longer than for typical commercial aircraft. Maintenance shall also be carried out by a larger crew and will likely more difficult to do due to the sea-based operations. Regular automated inspection using drones is suggested to help remedy this. Safety is ensured by allowing for venting of hydrogen tanks in the case of a fire or of an important leakage as detected by hydrogen concentration sensors. The tanks are placed above the passengers to avoid asphyxiation in the case of leakage, since hydrogen is less dense than air and will rapidly rise. In addition, the case of the main (forward) fuel tank being lost was considered, from which it was concluded that the Emperor would have enough extra fuel to safely land close to the coastline at any point in a typical transatlantic crossing.

After all characteristics of the design were established, the compliance of the aircraft to the requirements as set previously had to be assessed. It was deemed that the Emperor is able to meet the speed, range, number of passengers, reliability, safety, zero emission, stability, controllability, sea-based, ticket cost and noise requirements. However, there were a series of aspects that could not fully be assessed yet due to a lack of information. These are the recyclability/reusability of the aircraft, its availability, maintainability, compliance with all applicable laws and regulations and its ensuring of a comfortable flight.

Verification, Validation and Sensitivity

Verification and validation was done throughout the design process to ensure the accuracy of the computational models being used. Unit tests, subsystem tests and system tests were able to identify many errors, which were subsequently fixed, resulting in a model in which one can have confidence. Proving the robustness of the design, a sensitivity analysis was done which shows the deviation of several parameters given a 1% change in the value of certain key input parameters. A noteworthy result was that a 1% change in the operating empty mass contingency factor resulted in a 2.47 % change in estimated operating empty mass of the system, a 1.29% increase in estimated fuel mass and a 1.33% increase in normalised direct operating costs.

Data diagrams

The integration and interactions between (sub)systems can be visualised with the use of diagrams. The software diagram focuses on the surveillance, communication and navigation of the Emperor and how they differ from conventional aircraft due to being sea-based and flying transatlantic routes. The hardware block diagram shows how the fuel cells and flight computers regulate the electricity that is to be provided to all systems, such as the engines and flight controls. The electrical block diagram goes more in depth into the fuel cells, how the oxygen and liquid hydrogen get provided and how the electricity first passes through converters and inverters before reaching the systems. The data handling block diagram describes the central position of the flight management and flight control computers (FMS and FCC) and how they feed all of the data through the systems. Finally, the communication flow diagram shows the specifics of aircraft communications via GNSS, ground stations and other aircraft.

Production, Operations and Logistics

After the Design Synthesis Exercise (DSE) has been finalized, the project would still have to undergo a series of steps in order to reach the market. A year of further designing is expected. After other phases, such as funding and marketing, prototype testing is expected to start in 2028 and the production in 2035, having the first deliveries in late 2036.

For the manufacturing of the Emperor, the wing, fuselage, nosecone and tailcone assembly are performed in parallel. Once these are integrated, the cabin and cargo related elements are installed as well as the power and propulsion systems, finalising the assembly.

Operations will take place in specially developed sea-ports. The Emperor will dock in a floating dock where passengers, cargo and fuel will be loaded. Between one flight and another, maintenance and checks will be performed to ensure safety. The turnaround time is estimated to be 2.90 [h]. The aircraft is towed using boats to the runway and constantly communicates with sea-port and air authorities.

Sustainability

"Sustainability is defined as "development that meets the needs of the present without compromising the ability of future generations to meet their own needs" [2]. This means that in the environmental, social and economic fields, care should be taken that sustainability is applied in the design and development of the Emperor." [1]

To this goal, green hydrogen is used to generate the necessary electricity to power both the engines and the internal electric systems. Exhaust of pure hydrogen is minimised by regular maintenance and reliable refueling, and greenhouse gas emissions are avoided by liquefaction of the water vapour expelled by the fuel cells. Regarding the material choice, the focus is put on the minimisation of material waste and their reusability and recyclability at the end of life. The zero-emissions Emperor will thus contribute to the global decrease in CO_2 emissions, by leading the transition to green aviation alternatives. Economic and social sustainability will be achieved by the strict implementation of lean manufacturing, whilst ensuring fair wages and a respectful treatment of the employees, customers and passengers.

Market Analysis

The area of focus for the Emperor is mass transatlantic passenger travel, making it compete with other wide bodied aircraft. Set apart from the competition in terms of sustainability, cruise velocity and payload capacity, it is assumed that the Emperor will be able to take a 25% market share of the 500+ seat aircraft which would lead to a production run of 119 units. When analysing existing aircraft prices in the context of available range and payload, it was found that a competitive price for the Emperor would be 1,240.60 [$M\$$].

Cost and Revenue Analysis

The costs can be broken down into the areas of development, production, operations and organisation. Development makes up the non-recurring cost elements of the program such as the engineer wages, software, certification and tool design and was estimated to cost 37,231.12 [$M\$$]. Production costs form the recurring costs of the program and are made up of a combination of the labour and material costs for each aircraft. Considering a learning curve and the 119 unit production run, the average cost to produce each aircraft was estimated to be 807.71 [$M\$$]. When added, the capital expenditure for a prospective operator was estimated and when the direct operating costs were added as well, the final delivery price of the Emperor was estimated to be 1,465.75 [$M\$$].

Revenues of the program are generated by selling the aircraft, the revenues of operators are generated from ticket sales and from transporting additional cargo. Ticket and freight prices are kept low to remain competitive. Including a 20% subsidy for the manufacturer, the program is estimated to have an ROI of 12.44 % with an operational ROI of 40.30 %.

Risks

"Assessing risks throughout the design process is essential to grant the feasibility of the design and avoid detrimental unforeseen circumstances. The technical risks can be split up into risks occurring during the design phase such as the overestimation of material properties or verification errors, and risks during the operational lifetime such as the leakage of hydrogen or engine failure.

These risks can be reduced by introducing a mitigation and contingency plan. A mitigation plan aims to avoid the occurrence of the risk, i.e. decrease the likelihood, by taking measures in advance. An example is the introduction of a safety factor to account for errors in the design. In case the risk that occurs is still unacceptable, a contingency plan aims to reduce the impact it has on the design. An example is the redesigning or going back to alternative options when a risk is unacceptable." [1]

Limitations and Recommendations

This report presents the detailed design of the Emperor, however the design process has its limitations and can be optimised further. Further analysis is required for the hydrodynamics, due to the unpredictable nature of the sea and uncertainty how the Emperor will respond to disturbances. This can aid both in improving the drag estimation at take-off, and ensuring stability and controllability during water operations. Furthermore, more research is required for the hydrogen fuel aspects, and especially its storage methods, as this component has the lowest technological readiness level. Some general limitations of the design include the wingbox design and the availability, maintainability, reusability and recyclability of materials, which require further analysis to ensure proper compliance with current requirements. It is recommended to perform a computational fluid dynamic (CFD) study, finite element methods (FEM), wind tunnel and water tunnel testing on a scale model to improve the overall confidence in the design and more accurately analyse the structure.

Reflection

The Emperor comes with both advantages and disadvantages. The main drawbacks are the large development costs, the uncertainty of passenger demand and the need for new infrastructure due to sea-based operations. On the other hand, sea operations allow for flexible port locations, and the flight schedules can be optimized to profit from its large passenger capacity. The Emperor is emission-free and implements sustainability over the entire range of operations and manufacturing, which makes it attractive for airlines and passengers. In order to overcome the aforementioned weaknesses an option is to develop a cargo version or a down scaled land-based version.

As a conclusion, the main limiting factors are financial resources. If sufficient government funding is redirected towards sustainable initiatives such as the Emperor, a sustainable society will become possible. The Emperor can be seen as a step forward in achieving long-range, zero-emission aviation, allowing airlines and passengers to play a larger role in the green energy transition. As a group, we hope that this project contributes to the survival of future generations and opens a door to pursue innovative, green aviation alternatives.

Contents

List of Symbols

Abbreviations

AAIM	Aircraft Autonomous Integrity Monitoring
ABAS	Aircraft-Based Augmentation System
ACARS	Aircraft Communications Addressing and Reporting System
ADF	Automatic Direction Finding
ADS-B	Automatic Dependent Surveillance - Broadcast
AFCS/AFGS	Automatic Flight Control/Guidance System
ASAS	Airborne Separation Assurance Systems
ATC	Air Traffic Control
DLR	German Aerospace Center
DME	Distance Measuring Equipment
EFIS	Electronic Flight Instrument System
EICAS	Engine Indication and Crew Alerting System
FCS	Fuel containment system
FMC	Flight Management Computer
FMS	Flight Management System
GNSS	Global Navigation Satellite System
HF	High Frequency
HUD	Heads Up Display
ILS	Instrument Landing System
INS	Inertial Navigation System
MFD	Multi-Function Display
NAV	Navigation
PFD	Primary Flight Display
RAIM	Receiver Autonomous Integrity Monitoring
SATCOM	Satellite Communications
SDU	Satellite Data Unit
SFD	Secundary Flight Display
TCAS	Traffic collision Avoidance System
UHBR	Ultra-High Bypass Ratio
VHF	Very High Frequency
VOR	VHF Omnidirectional Range

Greek Symbols

α	Angle of Attack	deg
β	Sideslip angle	deg
Δ	Hydrostatic force	N
η	Efficiency	-
$\frac{d\epsilon}{d\alpha}$	Downwash gradient	-
γ	Specific weight of water	N/m^3
Λ	Sweep angle	deg
λ	Tail taper ratio	-
∇	Immersed hull volume	-
ν	Poisson's ratio	-
ω	Angular velocity	RPM
Φ	Flow coefficient at tip	-
ρ	Density	kg/m^3
σ	Stress	Pa
τ	Shear Stress	Pa

θ	Climb angle	deg
θ	Small heel angles	deg

Latin Symbols

$\bar{U}_t$	Peripheral speed	m/s
$\dot{m}$	Mass flow	kg/s
A	Area	m^2
AR	Aspect Ratio	-
b	Span	m
c	Chord	m
C_d	Drag coefficient	-
C_l	Lift coefficient	-
C_m	Moment coefficient	-
D	Diameter	m
E	Young's modulus	Pa
g	Gravitational constant	m/s^2
I	Second moment of Inertia	m^4
J	Polar moment of Inertia	m^4
L	Lift	N
L	Load waterline length	m
l	Length	m
l_h	Tail arm	m
M	Moment	Nm
MAC	Mean Aerodynamic Chord	m
P	Power	W
P	Pressure	Pa
Q	First Moment of Area	m^3
R	Radius	m
ROC	Rate of Climb	m/s
S	Shear Force	N
S	Surface area	m^2
T	Thrust	N
T	Torque	Nm
t	Thickness	m
V	Velocity	m/s

1 Introduction

”An emphasis on sustainability and sustainable design is critical to enable future generations to enjoy a similar quality-of-life as available in present day. In the aviation sector, sustainable solutions are proving to be difficult to realise. Recently, there has been significant research into battery-powered flight, however this option is only viable for short flights due to the weight of the batteries. For longer flights, such as the transatlantic route which is one of the busiest in operation, it is of great importance to explore alternative options.” [1]. One such alternative is the transatlantic hydrogen seagoing aircraft presented in this report, called the ’Emperor’. Using hydrogen fuel cells to generate electricity and drive the fans, the sea-based Emperor is a zero-emission alternative to present-day aviation which excels in its payload capacity.

”The aim of this report is to present the design process for the design of a sustainable, heavier-than-air, transoceanic aircraft as done by a group of 10 students in 10 weeks in order to gain experience in complex engineering processes and explore an interesting alternative air travel solution. This alternative must be competitive in payload capacity, travel time, cost, reliability, and safety.” [1] The report serves as a final summary of the project, where the characteristics of the final design choice have been traded off, researched and determined in design iterations.

The report has the following structure. Firstly, Chapter 2 describes the project objectives and requirements which serve as a starting point for the design. Then, the operational life of the Emperor is broken down in Chapter 3. The development of the design process and a trade-off between concepts is shown in Chapter 4. Furthermore, the detailed design is initialised in Chapter 5. Chapter 6 continues by providing technical subsystem design characteristics. Moreover, an overview of the design and its performance, along with the noise and RAMS characteristics is explained in Chapter 7. The validation & verification procedures and the sensitivity analysis are presented in Chapter 8, where a link to the model source code can be found. Afterwards, Chapter 9 shows multiple diagrams visualising the interaction between the various systems. The production, operation and logistics are explained in Chapter 10. Chapter 11 highlights the sustainability approach taken into the design. This is followed by a market and cost analysis in Chapter 12 and Chapter 13, respectively. Additionally, the risks are presented in Chapter 14. Finally, a discussion and conclusion are given in Chapter 15 and Chapter 16 respectively.

2

Project Objectives and Requirements

"Sustainable alternatives for transatlantic transport are essential to reduce the impact of humans on nature and to ensure a viable future for coming generations. This chapter presents the mission need statement and the project objectives behind the design of such an alternative. This can be found in Section 2.1. Moreover, the stakeholder, system and subsystem requirements developed in order to achieve this mission are presented in Section 2.2" [1], along with the means to implement validation and verification for these requirements.

2.1. General Mission Description

"The product to be designed is an electrical hydrogen powered aircraft with a focus on transatlantic passenger flight that will perform sea-based operations. In order to be a competitive alternative to conventional solutions, the design will need to be further constrained in several different areas from cruise velocity to payload capacity. From this need to be competitive with existing technologies, the mission statement is defined as the following:" [1]

> *Provide a sustainable, heavier-than-air, transatlantic air travel alternative to present-day civil aviation, competitive in payload capacity, travel time, ticket price, safety and reliability.*

"The project objective is derived from the need of a design executed by a group of students and should satisfy the mission statement. The project objective is defined as the following:" [1]

> *Develop a design for a sustainable, transatlantic aircraft as a group of 10 students in 10 weeks in order to gain experience in complex engineering processes and explore an interesting alternative air travel solution.*

2.2. Requirements

"The stakeholder requirements are identified and shown in Table 2.2. From the stakeholder requirements, the system and subsystem requirements are derived, as indicated in Table 2.3 and Table 2.4, respectively. All requirements are given a unique identifier. The labelling for the stakeholder requirements is done using the following format: Mission abbreviation - Stakeholder - Number. An example is: HHA-Tut-01, where HHA stands for Heavier-than-air Hydrogen Emperor, Tut for the tutor, and 1 referring to the first requirement for this stakeholder. Furthermore, the abbreviation Arl refers to Airlines, Pax to passengers and Env to environment. For the system requirements, the format used is: Mission abbreviation - System - Stakeholder requirement - Number. An example is HHA-Sys-T01-01, which is a system requirement derived from the first stakeholder requirement of the tutor. The subsystem requirements use the following format: Mission abbreviation - System - Stakeholder requirement - Number system requirement - Subsystem - Number. For example, HHA-Sys-T06-01-Prop-02, which is the second subsystem requirement for propulsion, derived from the first system requirement which has been derived from the sixth tutor stakeholder requirement. Moreover, the abbreviation Struct refers to the structural subsystem, Int to internal systems, Oper to operations and Perf to performance. The reasoning behind labelling requirements in such a way is to clearly be able to see the origin of each requirement, easing their traceability for future phases of the design process. ” [3].

”The requirements are generated using the VALID criteria: they have to be Verifiable, Achievable, Logical, Integral and Definitive [4]. The requirements are quantitative and objective, thus established to be verifiable. The requirements are deemed to be obtainable thus achievable. The requirements flow down from the top level requirements thus are said to be logical. Moreover, the requirements are considered integral as they describe the complete system. The requirements are viewed to be definitive since no unambiguous language is used.

The requirements shall be verified by using one of the following four methods in Table 2.1 [4]. The method used for each requirement, including stakeholder, system and subsystem ones, is given in the third column of Table 2.2, Table 2.3 and Table 2.4.” [1].

Table 2.1: *Verification methods for the requirements*

Inspection (I)	Used to inspect documentation or product for agreement with the requirement.
Analysis (A)	Uses a mathematical or numerical analysis technique to show compliance with the requirement.
Demonstration (D)	Done by showing that the product is able to perform compliance with the requirement.
Test (T)	Used to establish accordance with the requirement by testing under representative settings.

Table 2.2: *Stakeholder requirements*

Label	**Stakeholder requirement**	**Verification**
HHA-Tut-01	The Emperor shall have a minimum cruise speed of 500 $[km/h]$.	D
HHA-Tut-02	The Emperor shall have a minimum range of 8,000 $[km]$.	A
HHA-Tut-03	The Emperor shall be able to carry a minimum of 500 passengers.	I
HHA-Tut-04	The Emperor shall have a reliability comparable to present day transatlantic civil aviation.	A
HHA-Tut-05	The Emperor shall have a safety comparable to present day transatlantic civil aviation.	A
HHA-Tut-06	The Emperor shall emit no greenhouse gases during operation.	T
HHA-Tut-07	The Emperor shall be at least 95% reusable/recyclable.	I
HHA-Tut-08	The Emperor shall be stable in nominal conditions.	A/T
HHA-Tut-09	The Emperor shall be controllable.	A/T
HHA-Tut-10	The Emperor shall be sea-based.	D
HHA-Tut-11	The ticket cost of the Emperor shall be comparable to present day transatlantic civil aviation.	A
HHA-Arl-02	The Emperor shall have an availability comparable to present day transatlantic civil aviation.	A/D
HHA-Arl-03	The Emperor shall have a maintainability comparable to present day transatlantic civil aviation.	A/D
HHA-Arl-04	The Emperor shall comply with all of the applicable laws.	I/A/D/T
HHA-Arl-05	The Emperor shall comply with all of the applicable regulations.	I/A/D/T
HHA-Pax-01	The passengers shall experience a comfortable flight, comparable to present day civil aviation.	D
HHA-Env-01	The Emperor shall produce a maximum of 110 $[dB]$ of noise during operation.	D

Table 2.3: *System requirements*

Label	System requirement	Verification
HHA-Sys-T01-01	The Emperor shall have a minimum cruise speed of 500 [km/h].	I
HHA-Sys-T02-01	The Emperor shall have a minimum range of 8,000 [km].	A
HHA-Sys-T03-01	The Emperor shall be able to carry a minimum of 500 passengers.	I
HHA-Sys-T04-01	The Emperor shall have a reliability comparable to present day transatlantic civil aviation.	A
HHA-Sys-T05-01	The Emperor shall have a safety comparable to present day transatlantic civil aviation.	A
HHA-Sys-T06-01	The Emperor shall emit no greenhouse gases during operation.	T
HHA-Sys-T06-02	The Emperor shall use green hydrogen as fuel.	I
HHA-Sys-T07-01	The Emperor shall be at least 95% reusable or recyclable.	I
HHA-Sys-T08-01	The Emperor shall be stable over the complete speed regime.	A/T
HHA-Sys-T09-01	The Emperor shall be controllable over the complete speed regime.	A/T
HHA-Sys-T10-01	The Emperor shall be able to take-off from the sea.	D
HHA-Sys-T10-02	The Emperor shall be able to land in the sea.	D
HHA-Sys-T11-01	The cost per passenger for the airline shall be comparable to present day transatlantic flight.	A
HHA-Sys-T11-05	The Emperor shall have a delivery time comparable to current transatlantic civil Aircraft.	I/A
HHA-Sys-T11-06	The aircraft shall have a DOC/ASK of no more than 0.089 [$\$/passenger/km$].	A
HHA-Sys-A03-01	Components with a higher risk of failure shall be easily replaceable.	I
HHA-Sys-A04-02	The Emperor shall be accessible for handicapped passengers.	D
HHA-Sys-A04-03	During the design and production of the Emperor workers shall receive at least minimum wages as specified by Dutch law.	I
HHA-Sys-A05-01	The Emperor shall comply with CS-25 large Aircraft European regulations.	I/A/D/T
HHA-Sys-A05-02	The Emperor shall comply with the applicable sea-base regulations.	I/A/D/T
HHA-Sys-A05-03	The Emperor shall be granted an Airworthiness and Environmental certification.	I
HHA-Sys-P01-01	The passengers shall experience a comfortable flight comparable to present day civil aviation.	D
HHA-Sys-P01-02	The ride quality shall be maintained in rough air conditions.	A
HHA-Sys-P01-03	The ride quality shall be maintained in rough sea conditions.	A
HHA-Sys-E01-01	The Emperor shall produce a maximum of 110 [dB] of noise during operation.	D
HHA-Sys-01	The Emperor shall have an operational life of at least 20 years.	A
HHA-Sys-02	The Emperor shall have a maximum take-off distance of 10 [km].	D
HHA-Sys-03	The Emperor shall have a maximum landing distance of 10 [km].	D
HHA-Sys-04	The Emperor structure shall withstand the operational loads without experiencing damage.	A
HHA-Sys-05	The turn-around time shall be comparable to present day transatlantic civil aviation.	A/D
HHA-Sys-06	The Emperor shall be able to communicate with the ground support.	D

Table 2.4: *Subsystem requirements*

Label	Subsystem requirement	Verification
HHA-Sys-P01-01-Int-01	The pressure in the cabin and cockpit shall remain between the pressure that is present at sea level and 8,000 [ft].	T
HHA-Sys-P01-01-Int-02	The temperature in the cabin and cockpit shall remain between 20 and 26 degrees Celsius throughout the flight.	T
HHA-Sys-P01-01-Int-03	The Emperor shall be equipped with a ventilation system for the cabin and cockpit.	I
HHA-Sys-P01-01-Int-04	The cabin shall be equipped with at most 60 passengers per lavatory.	I
HHA-Sys-T10-01-Oper-01	The Emperor shall include means to allow for taxiing.	D
HHA-Sys-A05-02-Oper-02	The pilots shall receive the necessary training for sea-based operations.	I
HHA-Sys-T09-01-Perf-01	The Emperor shall include means for active control.	D
HHA-Sys-05-Prop-01	The fuel storage fill inlet shall be easily accessible.	I
HHA-Sys-T06-01-Prop-02	The propulsion medium shall use fuel cells to provide electricity.	I/T
HHA-Sys-T06-01-Prop-03	The engines shall be electrically powered.	T
HHA-Sys-T11-04-Prop-06	The fuel cell shall have an efficiency of at least 60 %.	A
HHA-Sys-E01-01-Prop-08	The engines shall produce a maximum of 110 [dB] of noise during operation.	T
HHA-Sys-T02-01-Prop-09	The Emperor shall be able to store excess hydrogen sufficient for one hour of loitering.	D
HHA-Sys-05-Struct-01	The cargo compartments shall be easily accessible.	I
HHA-Sys-04-Struct-02	The applied materials shall withstand the operational loads without experiencing damage.	A
HHA-Sys-T03-01-Struct-03	The cabin shall house seats for at least 500 passengers.	I
HHA-Sys-T03-01-Struct-04	The Emperor shall be able to carry passengers, including carry-on and check-in luggage, considering a mass of 120 kg per passenger.	A
HHA-Sys-T06-01-Struct-05	The Emperor shall not allow the escape of hydrogen from the fuel storage.	T
HHA-Sys-T10-01-Struct-06	The Emperor shall be layered with materials able to sustain a corrosive environment.	I
HHA-Sys-T10-01-Struct-07	Exterior structural joints shall be watertight.	T
HHA-Sys-T10-01-Struct-08	The exterior paint shall be non-toxic to sea-life.	I
HHA-Sys-T10-01-Struct-09	The Emperor shall be able to stay afloat in water.	D/T
HHA-Sys-T10-02-Struct-10	The Emperor structure shall resist the impact of landing against the sea.	D
HHA-Sys-01-Struct-12	The structure shall be able to resist fatigue loading during its entire operational life.	A
HHA-Sys-05-Struct-13	The Emperor shall be easily accessible for the passengers.	I

”The key requirements are **HHA-Sys-T01-01**, **HHA-Sys-T03-01**, **HHA-Sys-T11-01** and **HHA-Sys-T06-01**. For the stakeholders, the cruise speed, amount of passengers, and comparable ticket cost to current transoceanic flight are most significant. Furthermore, no greenhouse gas emissions during operation is a main objective representative of the sustainability goal.”[3]

Killer requirements are those which drive the design to an unattainable extent, thus causing the design to become unrealisable. Any killer requirements that were identified have been discussed with the stakeholders and modified to be able to comply with these requirements.

”The driving requirements will have the most substantial influence on the design. The driving requirements are **HHA-Sys-T01-01**, as this cruise speed largely determined the necessary thrust and fuel; **HHA-Sys-T06-01**, **HHA-Sys-T03-01**, and **HHA-Sys-T02-01**, since carrying hydrogen as fuel, 500 passengers, and a 8,000 [km] range are the main factors that determine the required sized of the cabin and the fuel storage compartment; and finally **HHA-Sys-T10-01** and **HHA-Sys-T10-02**, since take-off and landing on water highly influence the landing gear, possible configurations and stability and control capabilities. ” [3].

3 Functional Analysis

This chapter presents the main functions that the Emperor shall perform during its lifetime. These functions directly flow down from the mission need statement presented in Section 2.1. They are presented in two forms, first as a functional breakdown structure in Figure 3.1 and then as a functional flow diagram in Figure 3.2 and 3.3 respectively. The breakdown diagram was generated by compiling all of the functions which were found while specifying the order of the functions to be performed in the flow diagram. All the functions were compared with the requirements list in order to ensure that the Emperor is able to fulfil them.

Design The design phase of the Emperor consists of three main phases as it can be seen in Figure 3.1. Before actual designing can start however, one needs to identify a problem to which the design will provide a solution. This problem will be the focus of the design. The next step is to figure out a way to solve this problem. This solution will be worked out into a final design. When the design is complete, a manufacturing plan is designed. The intermediate steps can be seen more in detail in the third level of Figure 3.2.

Manufacture The manufacturing will consist of three phases, the last one being the delivery of the aircraft to the client as seen in Figure 3.1. The first step is the production of the different subsystems. When the required parts are complete, the subsystems can be assembled into subassemblies and then brought together in the final assembly. It should be noted that for both phases, special facilities like large hangers and sea docks are needed.

Normal Mission Loop The normal mission loop includes pre-flight logistics, transport, communications and post flight logistics, which when looking at Level 1 of Figure 3.2, comprises blocks 3 to 6. This phase is the most important because it is when the product will fulfil its mission. The general structure of this section is to perform checks, load, travel, unload and repeat until the aircraft's end of life. The details can be found in Figure 3.3.

Maintenance "The Emperor may also be serviced, either when damage is noticed during nominal operations, or on a regularly scheduled service interval. For the latter, which occurs after completing a nominal mission, it will be moved to a service area. There it will be inspected and repaired. If the repair does not appear economically feasible then the Emperor may be scrapped. Otherwise, it will be moved back to dock in order to resume the nominal missions."[3]

Scrapping "At the end of life, the Emperor must be scrapped, all while following the correct procedures in order to ensure maximal sustainability. It will be decided after an inspection, during the service phase, whether or not it should be scrapped. After the decision is made, the scrapping process begins. This includes disassembly and the reuse/recycling of individual parts."[3]

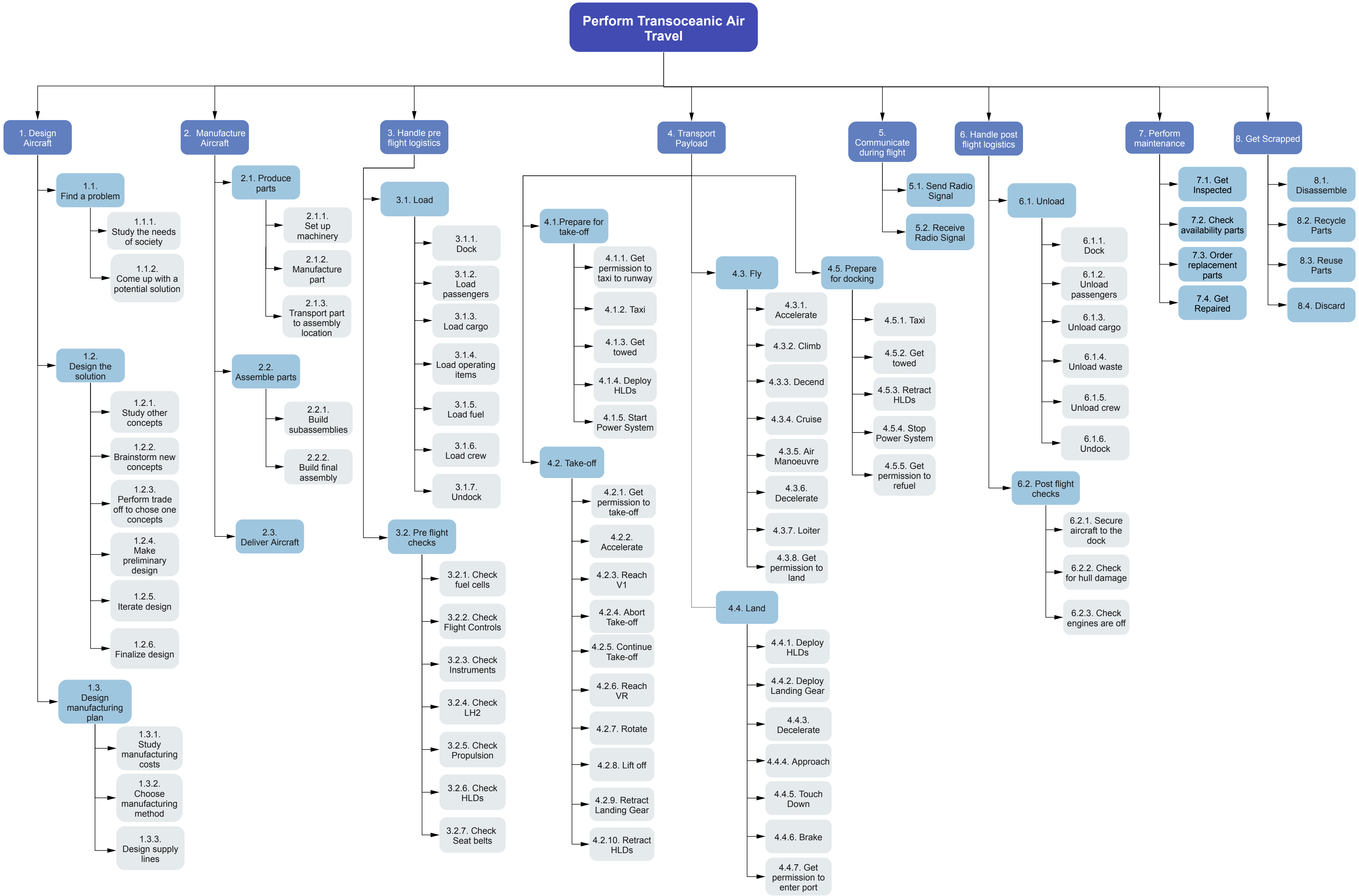

Figure 3.1: *Functional Breakdown Diagram*

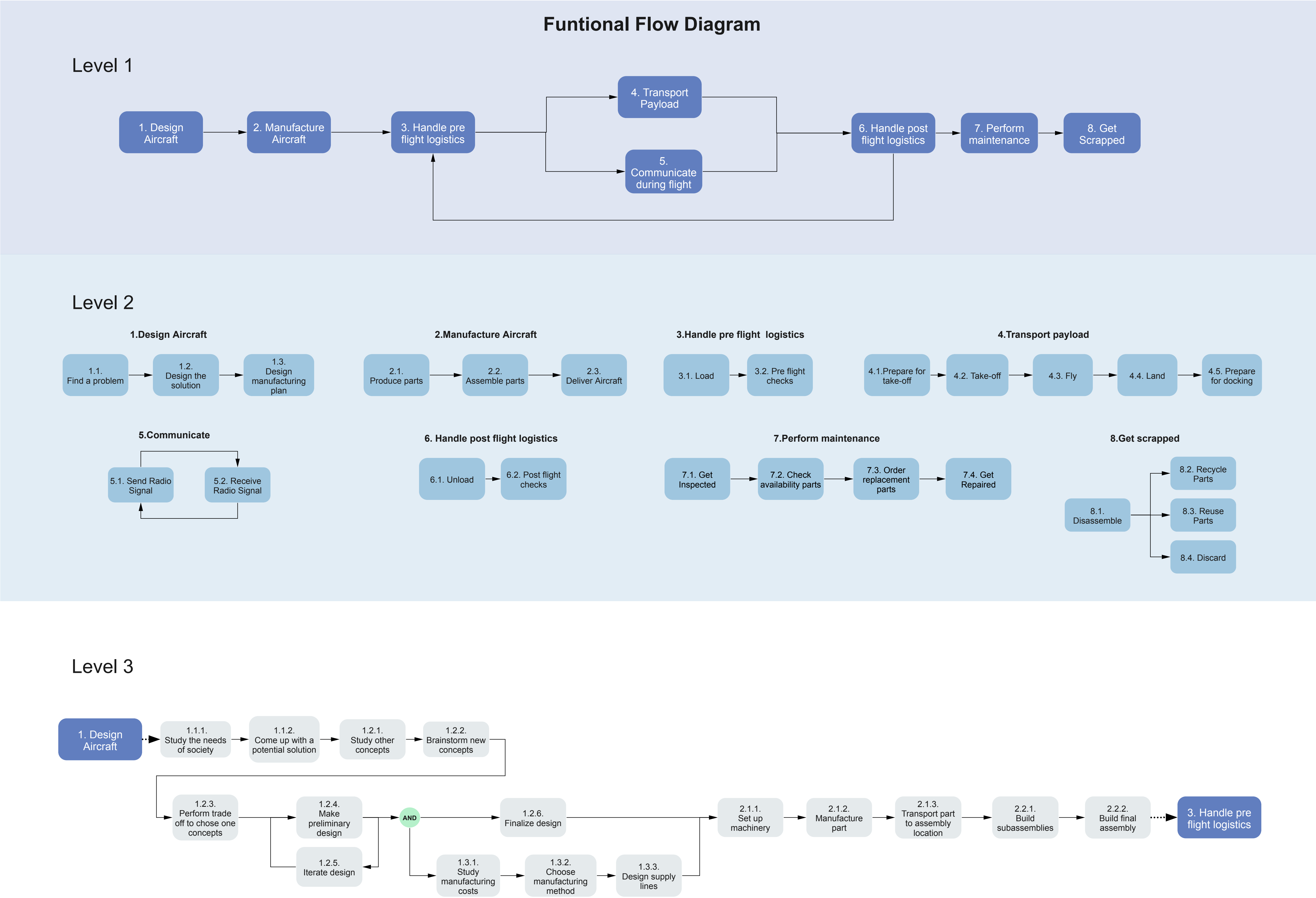

Figure 3.2: *Functional Flow Diagram part 1*

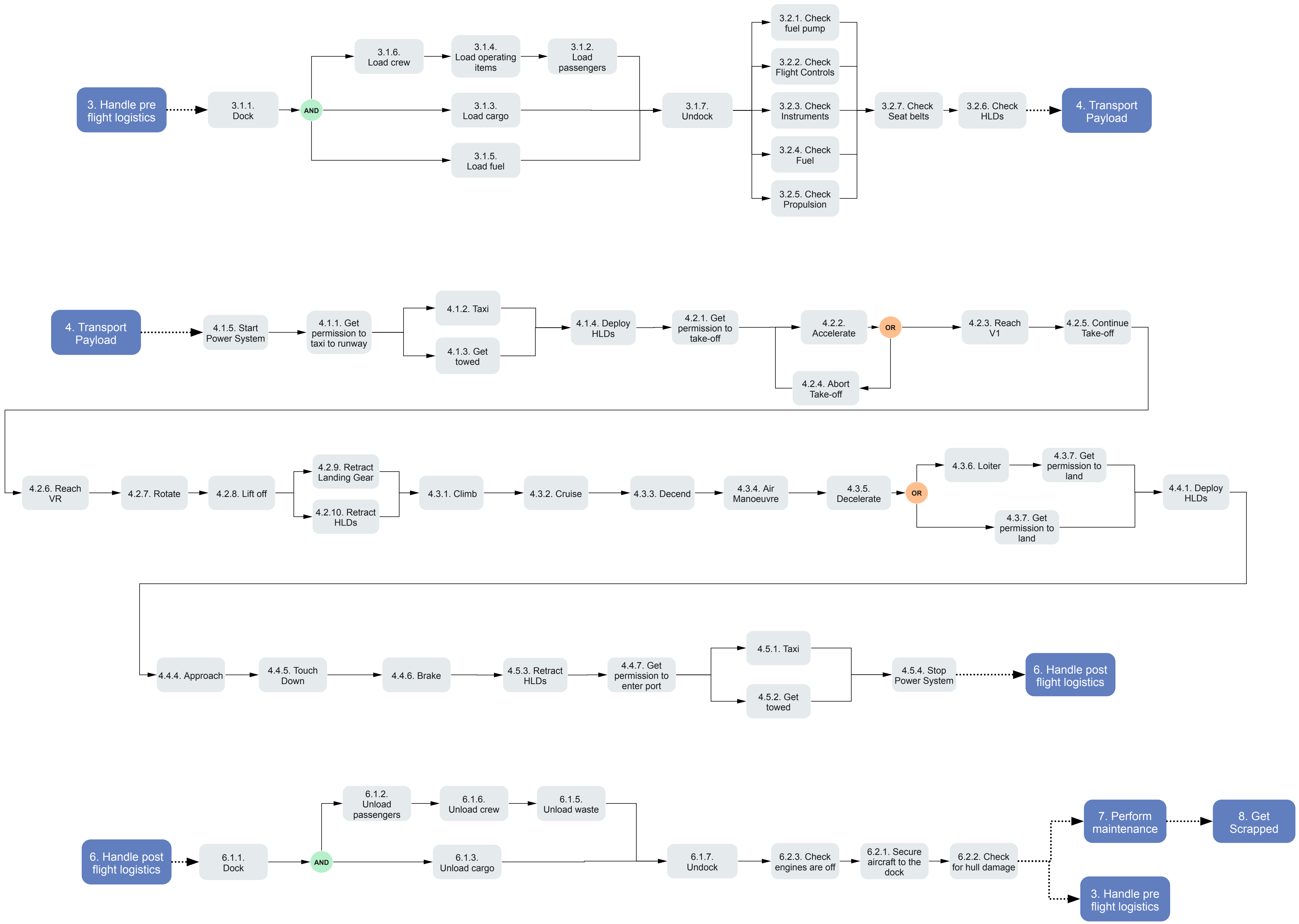

Figure 3.3: *Functional Flow Diagram part 2*

4

Preliminary Design and Trade-off Summary

This chapter aims to present the process, including the final trade-off, which was used to arrive to the final design concept. The chapter starts by explaining the original mission of this Design Synthesis Exercise in Section 4.1. It continues by highlighting the preliminary concepts and a feasibility analysis in Section 4.2. The trade-off method is described in Section 4.3, while the trade criteria and weights are presented in Section 4.4. The trade-off matrix along with its discussion is shown in Section 4.5. Moreover, the sensitivity analysis for the trade-off is given in Section 4.6. Finally, Section 4.7 discusses the final concept.

4.1. Original Mission

The vision of the mission was to think outside of convention and develop a sustainable, alternative solution to long range air travel. The original goal was set to develop a transatlantic, heavier than air, fast, hydrogen seagoing airship. The aim was to use gaseous hydrogen in fuel cells for electrical propulsion as well as for generating lift due to its buoyancy in air, while also implementing wings for the remaining required lift. Through this, it was expected that an efficient balance could be found where long ranges could be reached, high speeds could be achieved and competitive economics would make it a viable option for airlines and passengers. During the preliminary phases of development, extensive studies were conducted to assess the feasibility of this idea and many interesting conclusions were reached regarding both airship technology and hydrogen as a propulsion medium.

The main conclusion was that given their large size, in order to achieve the speed and range required, airships with uncompressed gaseous hydrogen would generate an unacceptable amount of drag. Generating this excessive drag would lead to an increase in the fuel required which would increase the size and mass of the fuel containment system (FCS) which would again increase the drag. This negative reflexive loop ultimately would result in not being able to converge to a design due to being far too heavy. A logical conclusion was to try and reduce the size of the FCS.

The volume of the fuel containment system could be decreased by compressing the hydrogen. However, as hydrogen is compressed, the lift it generates is decreased as it approaches the density of the surrounding air and the buoyancy force approaches zero. Naturally, this loss in lift would require larger wings to be used such as to maintain flight. Another issue of increasing compression is that the thickness of the fuel tank walls would also need to increase in order to handle the pressure required. This would also increase the mass of the system. Factoring in these considerations, studies were conducted to attempt to find the most efficient design point. Due to the aforementioned challenges that occur with higher compression ratios, another option considered is liquid hydrogen. The proposal of varying compression ratios while also including liquid hydrogen to produce different concepts is discussed further in Section 4.2.

4.2. Preliminary Concepts

Multiple concepts were established during the initial design stages of this project, based on various design possibilities [1]. An initial computational model was set up to allow preliminary calculations and iterations for, amongst others, the sizing and mass of the fuselage, wings, fuel tanks and propulsion system. These calculations have been done for varying compression ratios. Compression ratio refers to how much the hydrogen gas is compressed with respect to its standard sea level pressure. After an initial investigation, four concepts have been established to use for the trade-off process, which is described in Section 4.3. The four concepts used are a Zeppelin, Mega-lifter, Beluga and a liquid hydrogen concept. The Zeppelin and Mega-lifter use gaseous hydrogen as both a fuel and a lifting gas while the Zeppelin, Mega-lifter and Beluga concepts all use compressed gaseous hydrogen as fuel, at compression ratios of 3, 14 and 200, respectively. The liquid hydrogen concept stores the liquid hydrogen fuel cryogenically.

4.2.1. Zeppelin Concept

The Zeppelin concept aims to have a hydrogen compression ratio of 3, at which the gas will stay lighter than air and generates lift. This concept aims to minimize the required wing area in favor of generating lift using the gaseous hydrogen. Preliminary calculations regarding this concept show that this concept performs well for long ranges at low speeds. However, it experiences large amounts of drag at higher speeds due to the large fuel containment system required for the hydrogen gas, limiting the flight velocity of this design.

4.2.2. Mega-lifter Concept

The Mega-lifter-like concept aims to mimic the Mega-lifter proposed by Peter Lobner as seen in Figure 4.1[5]. This concept uses a compression ratio of 14, which allows the gaseous hydrogen to still generate lift at take-off. Furthermore, the higher compression ratio decreases the frontal area, which reduces drag and gives it a significant performance boost over the Zeppelin concept at higher speeds. However, this concept has a considerably large volume and mass, thus it has similar shortcomings as the Zeppelin concept when compared to the other proposed concepts.

4.2.3. Beluga Concept

The Beluga-like concept aims to be comparable to a Beluga aircraft as seen in Figure 4.2[1], where it uses the large cargo space of the Beluga to store the hydrogen. The concept can be greatly reduced in size by storing the gaseous hydrogen at a compression ratio of 200. This does increase the thickness of the tank wall to be able to sustain these high pressures. Due to the decrease in frontal area, the overall drag will be decreased. However, due to the large compression ratio, the gaseous hydrogen does not provide lift thus the concept will require larger wings.

4.2.4. Liquid Hydrogen Concept

The cryogenic, liquid hydrogen concept is the logical extension of a highly compressed gaseous aircraft design. Using the more dense liquid fuel, the overall size can be decreased the most and thus resembles a more conventional aircraft. The cryogenic liquid hydrogen is stored close to atmospheric pressures at approximately 20 $[K]$ [2]. To handle this pressure and temperature, the tank requires only a low thickness but must have sufficient insulation.

[1] https://aircraft.airbus.com/en/aircraft/freighters/belugaxl, accessed on 20/06/2022
[2] https://h2tools.org/bestpractices/handling-cryogenic-liquid, accessed on 05-06-2022

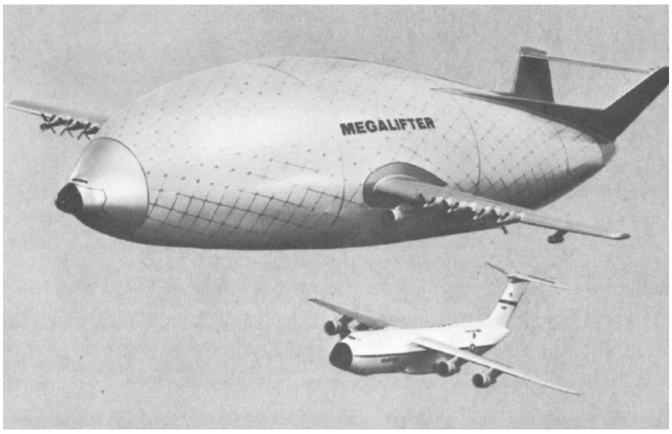

Figure 4.1: *Megalifter, compared to a C-5 Galaxy [5]*

Figure 4.2: *Airbus A330 BelugaXL*

4.2.5. Initial Feasibility Analysis

In order to compare these four concepts for the trade-off, various parameters have been calculated for a range of 5,800 [km], which all concepts can achieve, and are presented in Table 4.1. Some characteristic values from this table are used for the trade-off in Section 4.5.

Table 4.1: *Performance of the concepts used for the trade-off*

	Zeppelin	**Megalifter**	**Beluga**	**Cryogenic**
Compression Ratio [-]	*CR = 3*	*CR = 14*	*CR = 200*	*Liquid*
Velocity [m/s]	50	164	200	200
Fuel Mass [kg]	20,003	148,243	22,854	16,206
Mass Efficiency [-]	0.23	0.05	0.26	0.33
Total Mass [kg]	263,075	1,215,289	229,140	183,658
Tank Volume [m^3]	119,423	136,159	1,371	276
Wing Area [m^2]	1,265	1,711	233	188
Operational Cost [$\$/pax$]	181	766	134	101

The outcomes of the model as presented in Table 4.1 call for further investigation into varying the compression ratios. The primary questions to be answered are with respect to lift, drag, mass and fuel consumption as a function of the compression ratio (CR). This was explored within the context of the aircraft traveling at 120 [m/s] for 5,000 [km]. The blue lines in Figure 4.3 and Figure 4.4 at CR = 14 represent the point at which no lift at take-off is generated by the hydrogen gas. After this point, all lift is generated by the wings of the aircraft and the design can no longer be considered an ”airship”.

The first plot, Figure 4.3 shows how the lift over drag ratio changes with an increasing compression ratio. The ratio is shown to increase from an L/D of around 8 at CR 1 to an L/D of over 12 at CR 250. The decrease in volume rapidly helps to decrease drag and the loss in buoyancy lift is easily compensated by the lift generated by the wings.

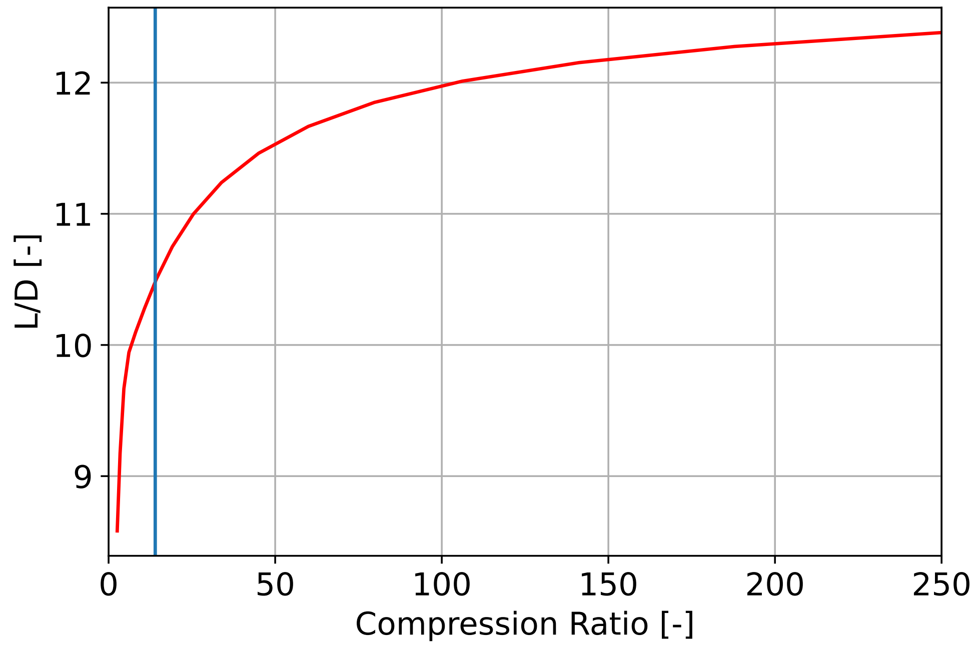

Figure 4.3: *Lift/Drag vs compression ratio at 120 $[m/s]$ for 5,000 $[km]$*

The next result, Figure 4.4 shows how the total required fuel mass of the Emperor decreases with increasing compression ratio. The mass savings are exponential as the size decreases. This is also a good proxy to visualise what was found to happen with the aircraft structure as a whole. When fuel mass is high, the rigid tank structure is large and is inherently very heavy. What has also been incorporated into the analysis is how the tank walls need to increase in thickness to be able to withstand the increased pressures as compression increases. Despite the thicker walls, the decrease in tank size made for a reduction in overall system mass.

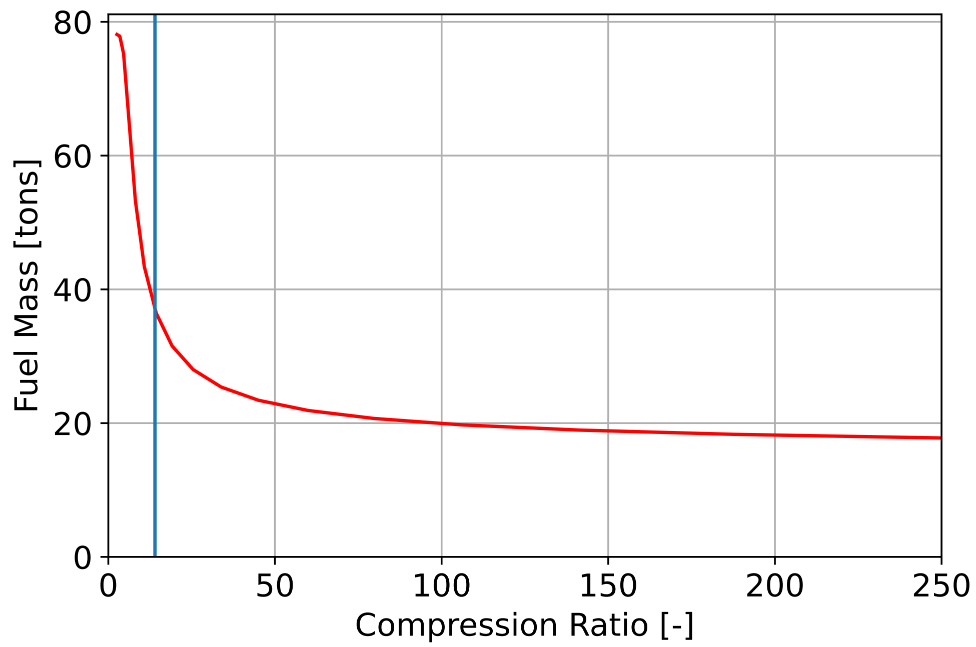

Figure 4.4: *Total fuel mass vs compression ratio at 120 $[m/s]$ for 5,000 $[km]$*

Clearly, from these figures it can be concluded that decreasing the overall volume of the Emperor has performance benefits that far outweigh the loss in lift from the hydrogen as a buoyancy gas. From another perspective, cost analyses were also done on all designs and once again, given the amount of material required, as the size decreases, the cost of the complete aircraft system also decreases. By the same token of using less material and fuel, sustainability and environmental consciousness improves as the design becomes smaller.

Extending the idea of reducing the overall system size, liquid hydrogen has a density of 71 $[kg/m^3]$ while hydrogen gas at 700 $[bar]$ (or a compression ratio of about 250) is only 42 $[kg/m^3]$[3]. Moreover, for liquid hydrogen the fuel tanks could be thinner, and therefore lighter, as they are kept close to atmospheric pressure.

4.3. Trade-off Method

In order to perform the trade-off of the concepts described in Section 4.2, the weighted criteria method is used and a trade-off matrix is constructed. For this, concepts are shown in the left column and criteria are presented across the top row. "The column width of the criteria is proportional to their weight, and the weight for each criteria is also mentioned in the bottom row. The options are evaluated and labelled for each criteria, using the following defined scale, with the associated colours and points in brackets: excellent (dark green, 3), good (light green, 2), correctable deficiency (orange, 1) and unacceptable (red, 0). The unacceptable label for any criteria causes the design option to be disregarded. Correctable deficiency is used when a criterion causes difficulties, but can still be corrected for. Good satisfies the requirements, while excellent significantly exceeds these. Once all options are labelled, the scale and weights are used to calculate a score for each option. Finally, the colours specified previously are used for visual presentation and shown in Figure 4.5. " [1].

Criteria	unacceptable	correctable deficiency	good	excellent
Score	0	1	2	3

Figure 4.5: *Trade-off labels (figure created using Excel)*

4.4. Trade-off Criteria and Weights

"The trade-off criteria can be split up in two categories, these are the primary and secondary criteria. The primary criteria are the ones considered in the trade-off. These have been analysed to be most influential on the design. The secondary criteria are unable to be considered for a trade-off, due to them being a product of primary criteria, or there not being a difference between the designs. The weights allocated to the primary trade-off criteria are assigned according to the importance of the associated trade criteria. The weights used are the values 2, 3 and 4. A more important trade criteria is associated with a larger weight.

4.4.1. Primary Criteria

The primary criteria, along with their assigned weights, were determined to best quantify the challenges the design will face. Most of these options are criteria which also provide an indication of costs in the design:

- **Fuel consumption** The fuel consumption regards the amount of hydrogen used per distance travelled. Hydrogen can be produced completely sustainable, but this does not

[3] https://energies.airliquide.com/resources-planet-hydrogen/how-hydrogen-stored, accessed 01/06/2022

mean that fuel consumption is not important. From both a sustainability and cost perspective it is desirable to minimize fuel consumption. Even considering future hydrogen being cheaper, there will still be a price. Thus consuming more fuel would increase operating costs. From a sustainability point of view using as little hydrogen as possible is an advantage, as the green energy required to produce the hydrogen could be used elsewhere. Since fuel consumption is one of the main indicators for operational costs, it is of great importance and therefore given a weight of 4.

- **Mass Efficiency** The mass efficiency is defined as the payload mass divided by the total mass. Thus a higher mass efficiency corresponds to having less structural mass to carry the same amount of payload. Therefore, this parameter is related to manufacturing costs as well, as it relates to the amount of material needed to manufacture a concept. This relates to the construction cost of the aircraft, as using more materials will be more expensive. In addition not all materials used in the construction will be recyclable. Thus a larger mass efficiency would indicate a more sustainable aircraft. Due to this relation to both cost and sustainability, the mass efficiency is given a weight of 3.
- **Refuelling Logistics** The refuelling logistics refer to the refuelling of the tanks in the Emperor to prepare for the next flight. The refuelling of the concepts differs in the state of hydrogen being gaseous or liquid and the pressure of storing the gaseous form. These options will create differences in the refuelling system being used. This criterion refers purely to the difficulty, costs and time associated with the refuelling method. The refuelling logistics is related to various difficulties, which have less influence than the other discussed criteria, and therefore given a weight of 2.
- **Ground Operation Logistics** The ground operation logistics refers to the take-off and landing operations being performed land-based or sea-based. This is mainly related to the size of the Emperor. The land-based operations are limited by the capability of currently existing airports. The sea-based operations will include more new infrastructure such as building airports at the coasts and providing means of transporting both passengers and cargo from airport into the Emperor at sea. Minimizing the additional infrastructure to be arranged would be preferable in order to minimize costs. Furthermore, as the ground operations have great influence on the costs, this criteria is deemed critical. Therefore, the ground operations is assigned a weight of 4.
- **Velocity** The velocity refers to the cruise speed of the aircraft. This influences two things related to the total flight time. The first reason is that shorter flight times result in proportionally less money spent on wages. This is relevant since the ticket price has a pretty set competitive price point. Secondly, longer travel times would obligate the airline to provide alternative benefits in order to compete in the current market. As the velocity is a key requirement, it is of importance to meet this requirement. However, it is not deemed to be the most critical criterion since it would still be amenable if the Emperor is able to perform slightly lower than the velocity requirement. Therefore, velocity is assigned a weight of 2.

4.4.2. Secondary Criteria

The secondary criteria were not considered due to their inability to contribute to a proper comparison. They are shortly elaborated upon to give reason for not including these criteria in the trade-off." [1]. These criteria are not considered as there were no adequately accurate estimations available at the time of trade-off, or the criteria do not sufficiently differentiate between the options.

- "**Range** The range of the Emperor dictates the flights it can make. This is important for its position in the market. However, since the concepts for this trade-off were chosen for a single range, there is no comparison to be made here.

- **Operating Costs** The operating costs are a key number to minimize, as it will be very important to be able to provide a competitive ticket price. The problem with this criterion is that no accurate estimate could be made at the time of the trade-off. In order to make sure the best option will still provide a competitive operational cost, the fuel consumption and velocity are considered in the trade-off. These two parameters were deemed sufficient to predict the comparative operational costs of the designs.
- **Total Costs** The total costs is also a key parameter to minimize, as the cost of the aircraft needs to be recouped during its operational life. The total cost has the same problem as the operational cost, which is the lack of any accurate estimation at this time of the model. The mass efficiency and ground operation criteria should be able to predict the relative difference in total cost between the models.
- **Recyclability and Reusability of Materials** The reusability and recyclability of materials is of critical importance to ensure sustainability in the design. However, the materials used for the various concepts will be very similar thus this cannot be used as a proper criteria for the trade-off." [1].

4.5. Trade-off Matrix

The trade-off matrix for the concepts presented in Section 4.2 is shown in Figure 4.6. Each criteria is assessed for all of the design concepts. This trade-off was performed using the trade-off method presented in Section 4.3.

Design\Criteria	Fuel Consumption	Mass Efficiency	Refuelling	Ground Operations	Velocity	Total Score
Zeppelin	excellent	good	good	correctable deficiency	unacceptable	26
Beluga	excellent	good	correctable deficiency	good	excellent	34
Megalifter	correctable deficiency	correctable deficiency	good	correctable deficiency	good	19
Liquid Hydrogen	good	excellent	good	good	excellent	35
Weights (x/4)	4	3	2	4	2	

Figure 4.6: *Trade-off matrix for the final concept (figure created using Excel)*

"Firstly the fuel consumption is considered. These values are calculated using the model described in Section 4.2 and presented in Table 4.1. It can be seen that the zeppelin-like and Beluga-like concept have the lowest fuel consumption, thus score excellent. The liquid hydrogen concept has very low fuel consumption however due to the large amount of energy required to store the liquid hydrogen [6] the aircraft has been assigned a score of good. Moreover, the Megalifter-like concept has a quite high fuel consumption, but it would still be possible to use thus it is labelled correctable deficiency.

Secondly, the mass efficiency is also calculated using the model and the values are presented in Table 4.1. The mass efficiency for the liquid hydrogen concept is the largest number, thus is labelled excellent. The zeppelin-like concept and Beluga-like concept have values a bit smaller than the liquid hydrogen concept thus are labelled good. The Megalifter-like concept has a low mass efficiency, which results in the use of more material and thus higher costs. However, it is still feasible to use and therefore is labelled correctable deficiency.

Thirdly, the refuelling logistics are determined based on the storage of the hydrogen. As the zeppelin-like concept and the Megalifter-like concept use hydrogen gas stored at lower pressure, it will be less challenging to allow for refilling the tanks, by taking advantage of the pressure difference between the tanks and the hydrogen storage compartment. Therefore these two concepts are labelled good. For the Beluga-like concept this will be more challenging as the hydrogen will be stored in the tanks at relatively high pressure. However, it is still found to be doable thus it is labelled correctable deficiency." [1]. Refuelling the cryogenic liquid hydrogen concept comes with its own challenges but after consulting a hydrogen expert was found to be relatively fast when compared to the hydrogen at higher pressure, and is therefore labelled good.

"Moreover, the ground operations are based on the size of the aircraft and the wingspan, as calculated using the model as described in Section 4.2. For the Beluga-like concept and the liquid hydrogen concept, the size and wingspan are estimated to be in the larger range of current-day civil aviation, but still able to fit in regular airports thus these concepts are land-based and thus labelled good. The zeppelin-like and Megalifter-like concepts will have sizes far too large to be able to operate them in regular airports, thus the ground operations will be sea-based. This results in needing new infrastructure and thus is more costly. However, it is still possible to perform these operations thus they are labelled correctable deficiency.

Furthermore, the velocity is again calculated using the model as described in Section 4.2 and the values are presented in Table 4.1. The zeppelin-like concept is deemed unacceptable as the concept is unable to meet the velocity requirement as specified by the tutor. The other three concepts are all able to meet the velocity requirement. The Beluga-like and liquid hydrogen concept are able to obtain a higher speed than the Megalifter-like concept thus these are labelled excellent and good, respectively.

The weights and scale of the labels are used to obtain the total score of all four concepts, as given in the final column." [1]. The zeppelin-like concept is labelled unacceptable with regards to a certain criteria, thus provides the score in red and is disregarded. The Megalifter-like concept scores 19 points, the Beluga-like concept scores 34 points, and the Liquid Hydrogen concept scores 35 points. By examining this score and the visual presentation in the trade-off matrix, the Liquid Hydrogen concept is shown to be the best option.

4.6. Sensitivity Analysis

"In order to ensure the trade-off to be both verified and unbiased, a sensitivity analysis is done. In this analysis all possible criteria weight combinations are analyzed, with the weights ranging from 1 to 5. In addition, the scores of all labels are varied, using intervals from 1 to 3 between them. A python script is used to perform the analysis and compare all options. In the analysis 100,000 different trade-offs are performed, using the various weights and label scores as explained previously. For this analysis an unacceptable label is not instantly dismissed, as is done in the trade-off explained in Figure 4.6. In the analysis, the best design is chosen simply by comparing the final score." [1]. Out of the 100,000 trade-offs, the liquid hydrogen concept came out as the best design option in 84% of the trade-offs. In second place was the Beluga-like concept, turning out to be the best design option in 16% of the cases. The zeppelin-like concept was the best design option in 36 out of 100,000 trade-offs, which effectively results in a percentage of 0%. The Megalifter-like concept was the best design option in 0% of the trade-offs. From this sensitivity analysis, it is clear that when varying the weights and scores, the liquid hydrogen remains the best design option in a majority of the trade-offs. Thus the performed trade-off is concluded to be verified [1].

4.7. Final concept

With the trade-off concluding that a cryogenic, liquid hydrogen concept is the best option, the engineering team concluded that the original design goal for the project would be unfeasible, as the initial design goal was more akin to the Megalifter-like concept or the Beluga-like concept. With this realization, the team set up a meeting with the client and the limitations of the heavier-than-air airship and gaseous hydrogen proposals were discussed. Subsequently, the two parties discussed the underlying goal of the project and a clear direction for the project was defined. This discussion resulted in adjustments to the requirements of the cryogenic, liquid hydrogen concept and this was used for further development [1].

The new concept was a scaled up liquid hydrogen concept, able to carry 1,500 passengers across the Atlantic while remaining competitive with present day aviation. ”The design will then be optimized for minimizing the operational cost per passenger. By scaling up the design, more passengers and/or cargo can provide increased revenue to balance out the operational costs. This will allow the design to be more competitive in the current transatlantic market, not relying solely on the sustainability to carve out it’s spot in the market. Due to increasing the amount of passengers and/or cargo, the design will have to operate sea-based to eliminate any sizing constraints due to the limits of current day airports. The cruise speed of 500 [km/h] and range of 8,000 [km] are kept as minimum requirements.” [1].

5

Initialising the Detailed Design

The design which will be further developed in the upcoming chapters, is based on the final concept which has been described in Section 4.7. This chapter aims to describe the initial parameters used for the final design and how they will be iterated upon. A statistical relation between existing hydrogen aircraft will be presented in Section 5.1 which aims to provide an initial mass estimate. Section 5.2 will then present the constraint diagram which has been made for the final design conditions. Furthermore Section 5.3 will present the cabin layout which shall be used in the final design. Finally Section 5.4 will describe the iterative model which is used in order to iterate over the design using the relations in Chapter 6.

5.1. LH2 Aircraft Statistical Relations

As an input of the model, an initial estimation of the Maximum Takeoff Weight (MTOW) in order to estimate the wing area and power required using the constraint diagram. Given that there are currently no liquid hydrogen aircraft in operation, the MTOW of various detailed concept aircraft, as generated by Brewer [7], were plotted against their passenger count and a statistical relation was created as can be seen in Figure 5.1.

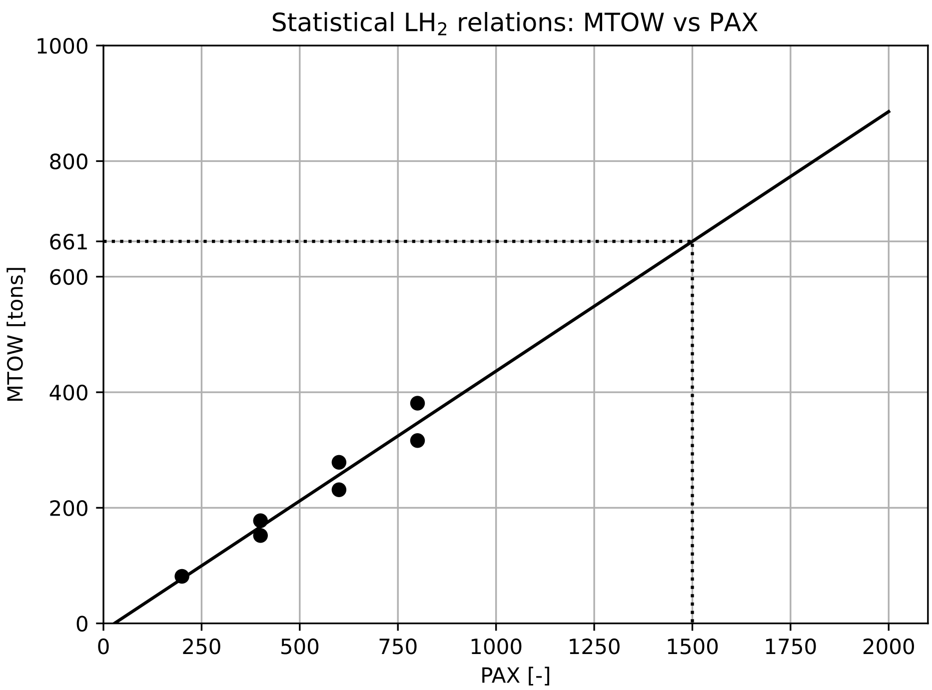

Figure 5.1: *MTOW vs passenger count [7]*

When inputting a passenger count of 1,500, an estimated MTOW was found to be 661 [$tons$]. This value is used as the initial MTOW estimation.

5.2. Constraint Diagram

In order to find the optimum design point for power and wing surface area, a constraint diagram is constructed. As can be seen in Figure 5.2, the constraining conditions are considered to be when the aircraft is in cruise, a constant turn and its required climb rate. Also factored in is its take-off and stalling conditions. These conditions were chosen as they are typically the constraining conditions in other aircraft designs[8].

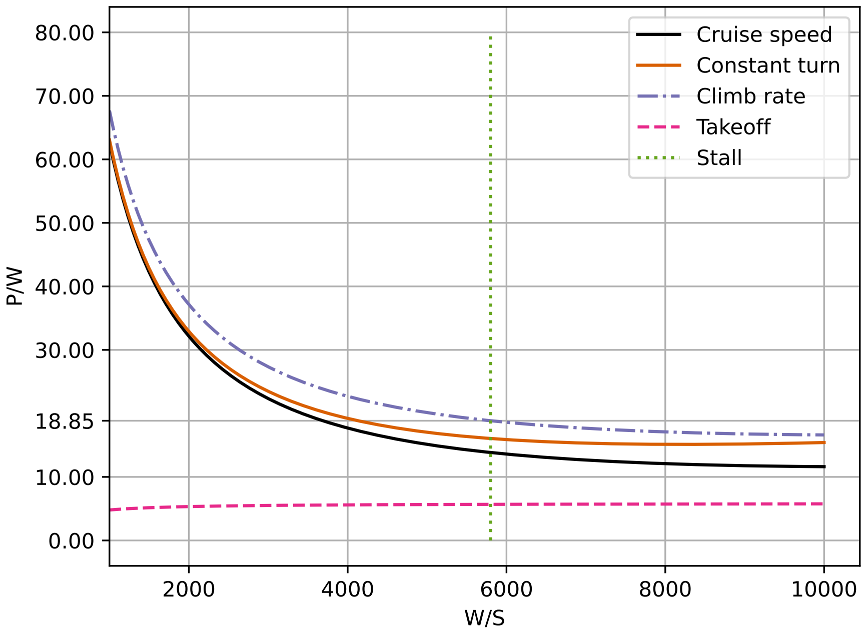

Figure 5.2: *Constraint diagram*

After plotting the requirements of these conditions, it was found that the constraining point gives a P/W of 18.85 [W/N] and a W/S of 5,800 [N/m^2]. The takeoff condition was not a limiting constraint as while the thrust required there was greater than in the cruise and climb condition, the airspeed was also much lower which lead to a lower power requirement.

5.3. Fuselage and Cabin Layout

The fuselage of a sea-based aircraft differs greatly from regular aircraft due to the required added feature of a boat-shaped hull for landing and take-off on water. To aid with water landing, the underside of the aircraft is shaped similarly to a boat hull. The shape has to be hydrodynamically efficient while also maintaining both static and dynamic stability during take-off and landing. This can be achieved by shaping the hull to minimise drag and by adding floats or stabilizers to aid with stability and for water drag reduction [9]. For this aircraft, the NACA TN-2481 conventional hull shape was selected. It was chosen as it has known drag characteristics [10] and due to the large internal volume available once the cabin is fitted inside the fuselage. The space is necessary to store the required volume of liquid hydrogen in the top part of the fuselage. The hull shape was scaled to match the required dimensions based on the fixed cabin cross-section. The original hull design shown in Figure 5.3 and Figure 5.4 gives the cross sections of the hull at certain locations along the fuselage. When compared to the original NACA TN-2481 it can be noted that our hull-shape has been lengthened. This resulted in a larger carrying capacity for both passengers and fuel, while not severely affecting the relative water resistance drag of the aircraft. In fact, a longer length to width ratio of the hull results in a more hydrodynamically efficient design [8]. A conventional hull shape has also been chosen over the planing-tail hull shape, as the conventional hull offers the most internal space for the amount of passengers and fuel in exchange for more water resistance Figure 6.1. Since water resistance is not the critical design case for which the propulsion system is designed, this was deemed to be an acceptable consequence. The hydrodynamics of the hull shape and the aircraft are further described in detail in Section 6.2.

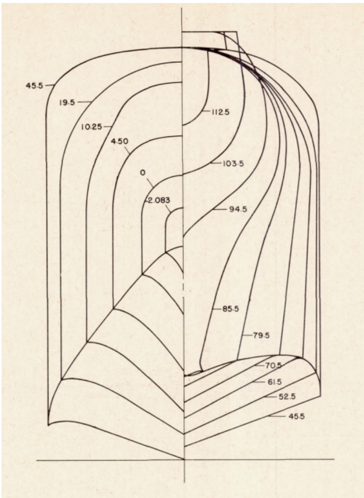

Figure 5.3: *NACA TN 2481 cross-section view*

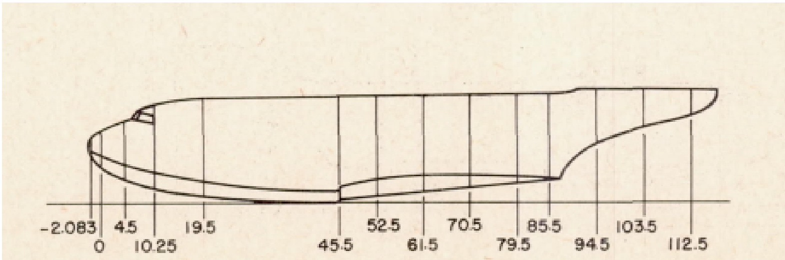

Figure 5.4: *NACA TN 2481 side view*

The fuselage layout was first designed by considering 3 main components, namely the passenger cabin, the cargo bay area and the hydrogen fuel tank. To design the cabin, the passenger layout and amount of passengers were chosen, as detailed optimisation of the cabin layout was deemed outside the scope of the current design. The chosen layout was 2 floors of 12 seats abreast each, for a total of 1500 passengers leading to 63 rows per floor.

In the iterative model described in Section 5.4, the required fuel volume was computed using an initial given passenger amount, seat configuration and cabin length. The fuel tank is also split into at least two parts to make room for the wing box. In order to allow for further flexibility in positioning, and to fill the volume of the aft section behind the cabin, the final design features 3 fuel tanks; two tanks constrained by the length of the cabin and the length of the wing box, and a third aft tank placed behind the cabin. The tanks are called the Forward, Mid, and Aft Fuel Containers for the remainder of the report. The wing box dimensions are also outputted by the same iterative model to take into account the reduction in available fuel volume. A side view of the aircraft and it's main components can be seen below in Figure 5.5.

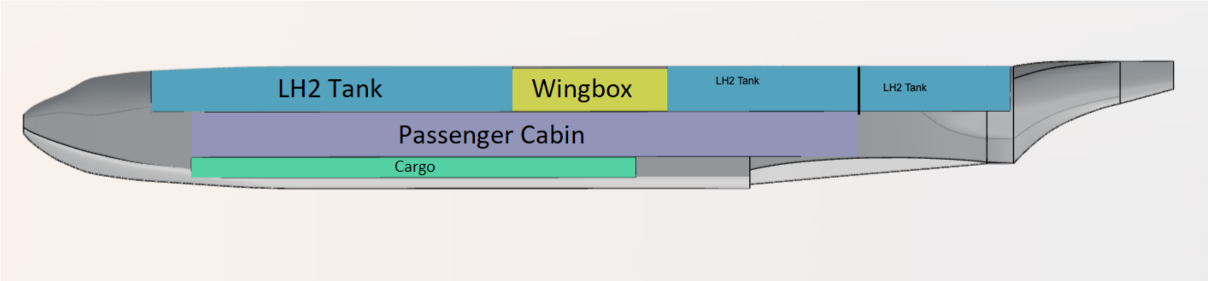

Figure 5.5: *Aircraft side view*

As mentioned, the optimal passenger configuration which best fits the hull shape was found to be a 12 seat wide cabin with two floors, carrying 1500 passengers in 63 rows. The optimal layout was determined by considering which layout provided sufficient room for the fuel tanks and the cargo while limiting unused space. The sufficiency was tested by comparing the volume available for fuel, with the volume of fuel required. Due to the hull being a rectangular shape, the floor plan design differs from traditional aircraft. For example, a single floor or triple floor configuration would result in either too much or too little fuel capacity respectively, due to the fact that the height-to-width ratio stays the same for this hull shape.

Reducing the width and number of seats abreast would result in insufficient hydrogen storage, as the hull shape would not be tall nor wide enough due to the narrow shape cabin, reducing the overall fuselage volume. Increasing width would also increase hydrodynamic and aerodynamic drag. Moreover, going for a size larger than a 12 seat wide cabin leads to an aircraft size that would exceed the limits of practicality. There is then a balance in optimal amount of passenger compartment floors and seats abreast, resulting in a good passenger amount and fuel capacity to meet the range requirement, while not causing access drag by being larger than needed. The outputted required fuel from the model would be compared to the amount of fuel volume that could be stored in the remaining fuselage volume in the 3D fuselage model. The 3D model was made in such a way that fast changes in size were quick to implement, making it easy and accurate to iterate the fuselage size, while keeping it's original shape, and automatically outputting the fuel volume available.

The fuselage cross section can be seen in Figure 5.6. Furthermore, the floor plan can be seen in Figure 5.7 which is used for both floors as they are identical. For storage, the standard LD-29 air cargo ULD container [11] was selected. It is the largest of the standard containers, and is able to fit in the given cross-section, leading to the greatest cargo carrying capacity possible. Due to the low position of the cargo hold and the large probability of the side access being submerged, the cargo door will be located in the back of the Emperor.

The fuel tank is placed on top of the passenger cabin, with the cargo being kept below the passengers. Due to the Emperor flying at 3000 $[m]$ altitude, it will not be pressurized, and hence a shape optimised for pressure differences is not required. This allows for the space given by the hull shape to be optimally used. The required sizes for each section are performed using standard sizing methods [11]. The width of the fuselage is found using Equation 5.1, for the height of the cabin the standard height of one layer of the passenger compartment was taken as 2.5 $[m]$ [11]. The height of the fuselage itself was determined from the fixed width due to the cabin, and the shape given by the NACA hull.

While the cross section of the fuselage was fixed, the tail cone length was a variable input parameter used to achieve longitudinal stability, and the length of the section aft of the cabin was determined from the length required by the Aft Fuel Container. The weight of the fuselage was estimated using Raymer's methods [12].

$$W_{\text{cabin}} = 0.6n_{\text{passengers}} + 0.7n_{\text{aisles}} \tag{5.1}$$

For twelve seats and two aisles this results in a cabin width of 8.6 [m]. This design is the most efficient design that allows for ticket prices to be kept low, which will also be discussed further in Chapter 13. If 6 seats abreast is found to be uncomfortable for passengers during a long flight, the amount of seats can be reduced or an extra aisle can be placed depending on the wishes of the airline operating the aircraft.

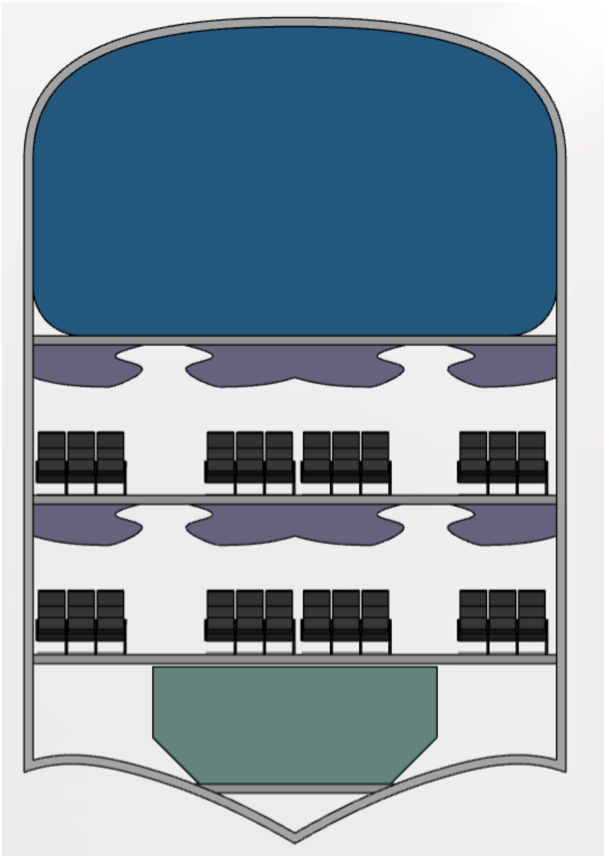

Figure 5.6: *Cabin cross-section*

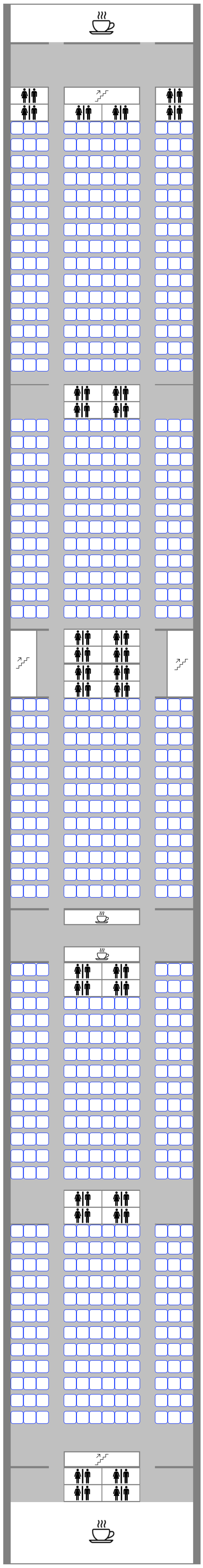

Figure 5.7: *Cabin floor plan - both floors*

5.4. Iterative Model

After performing the initial parts of the sizing for the aircraft, it is necessary to iterate over some of the design parameters. This iteration is done by looping over the different components represented in Figure 5.9 and then updating their design parameters in order to satisfy the new constraints. The components in the loop will update one-by-one using the previous values from the other components whenever necessary. This allows for iteration over the different components which rely on values from other components. This process can be seen as an iterative constraint satisfaction problem, which if it converges, guarantees the satisfaction of the all constraints inputted into it.

The iterative loop has multiple functions which output the size, weight and location of the different components that make up the aircraft. The sizing is done using empiric methods from the ADSEE I [11] course of TU Delft which represent the best methods available for the current design stage.

The initial weight estimations of the different components also takes place in this iterative loop. This is mainly done using the Raymer methods [12]. However, some of the weighing methods do not work for the large size of the aircraft being designed. As an example, it was found that the weight of the passenger cabin air conditioning unit was being estimated at around 27 $[tons]$ whereas a B747 air conditioning system is just 2 $[tons]$ [13]. Hence it was decided to replace the Raymer formulas which cause unreasonable results with their respective Torenbeek equivalents [14].

Finally, it was also necessary to estimate the centres of gravity for the different components of the aircraft. For this, a coordinate system was defined which has its origin at the nose of the aircraft. This means that the x-coordinate describes the longitudinal position with respect to the aircraft nose and the y coordinate represents the span-wise placement of a component oriented towards the right wing when seen from the front. Finally the z-axis completes the right handed coordinate system which is being made. This coordinate system can be seen in Figure 5.8.

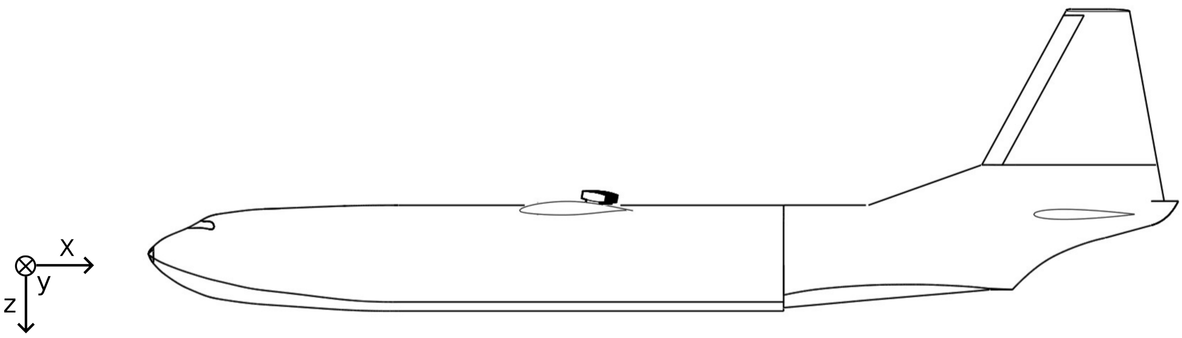

Figure 5.8: *Default coordinate system*

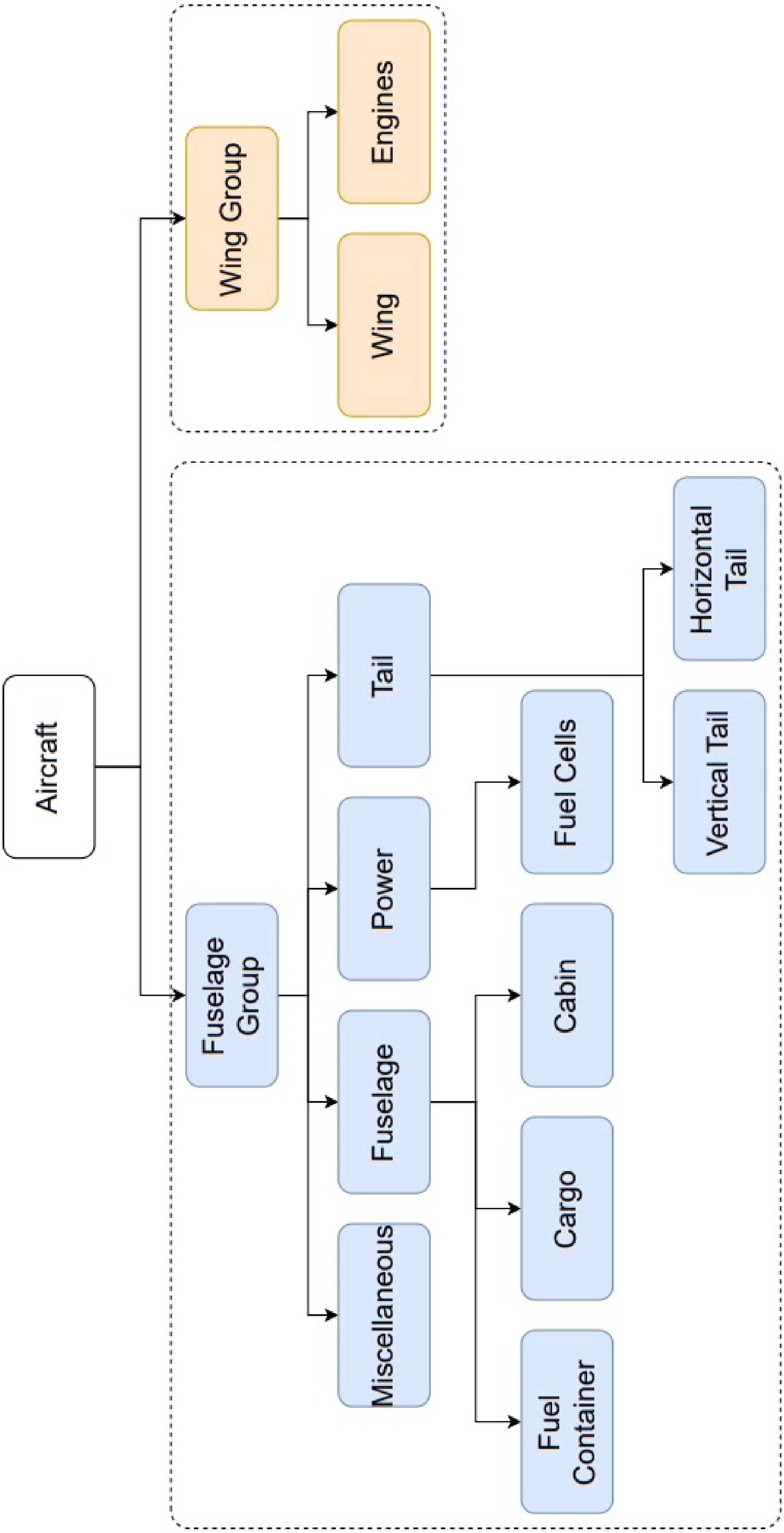

Figure 5.9: *Iteration Loop*

6

Design Characteristics

To design and develop an aircraft that accomplishes the requirements and mission profile, its subsystems must be designed in detail. This chapter presents the characteristics of the different subsystems and the methods used to generate these results, these methods were applied as constraints in the iterative model. First, the aerodynamic characteristics are detailed in Section 6.1, namely the wing design, lift and drag estimations. Section 6.2 presents the hydrodynamic characteristics of the Emperor, which play an important role for take-off and landing on water. The propulsion design can be found in Section 6.3, followed by the description of power generation in Section 6.4. Next, the fuel storage system is presented in Section 6.5 and the material characteristics in Section 6.6. The stability and control characteristics are shown in Section 6.9. Finally the fuel system layout, actuator layout, auxiliary power and environmental control can be found in Section 6.10.

6.1. Aerodynamic Characteristics

This section presents the aerodynamic characteristics of the Emperor. It was decided that it will have a single wing at a high position. The high position is due to the location of engines on the wing, which due to the sea-based operations requires clearance between the engines and bottom of the aircraft to avoid being submerged or affected by the water. Further detail on the design of the wing can be found in Subsection 6.1.1. The lift and drag characteristics of the aircraft are detailed in Subsection 6.1.2 and Subsection 6.1.3 respectively.

6.1.1. Wing Design

When designing a wing, an airfoil must first be chosen. This affects various aerodynamic characteristics such as lift, drag and stall speed. As the Emperor is flying below transonic speeds at M = 0.61, supercritical airfoils do not need to be considered. The airfoil selection was limited to NACA airfoils, due to their detailed characteristics being readily available. Ultimately, the NACA 65_1412 was chosen due to its high $C_{l\max}$ at 1.64 and low $c_{d\min}$ of 0.0038 at which at C_l of 0.38 is achieved [8].

The next step is designing the wing planform. As stated before, the Emperor will be flying at subsonic speeds and therefore there is no need for a swept wing. The taper ratio was taken from the Lockheed C-130 Hercules [8] to be 0.85. This was done because the Hercules performs a similar mission, with a unswept wing and powered by propellers which behave similarly to the fans selected for the Emperor as will be addressed in Section 6.3. At the current point in the design no wing twist has been set yet. This value is important for stall characteristics but to properly implement this, windtunnel testing should be done which lies outside of the scope of the current design. The dihedral was set at -2.5 $[\mathrm{deg}]$ as similar fan aircraft with a high-wing configuration, like the C130 Hercules and the ATR-72, use the same value[8].

The optimal effective aspect ratio for a certain range can be found by the following formula:

$$\mathrm{AR}_e = \frac{C_{LC}^2}{\pi} \frac{1}{\left(\frac{V_C}{R}\frac{C_{LC}}{c_t}\ln\left(\frac{W_{\mathrm{ini}}}{W_{\mathrm{fin}}}\right) - C_{D\mathrm{min}}\right)} \tag{6.1}$$

The effective aspect ratio is the product of the aspect ratio and the Oswald efficiency factor. C_{LC} is the average lift coefficient over the cruise. V_C is the cruise speed, R is the range, c_t is the thrust specific fuel consumption in $[1/s]$. W_{ini} and W_{fin} are the weights at start of cruise and end of cruise respectively. Lastly $C_{D\mathrm{min}}$ is the minimum drag coefficient.

There are more considerations to be made regarding the aspect ratio besides this theoretical optimum. Most importantly the wing needs to be able to carry the propulsion system. It also needs to be wide enough to fit all the fans and all the motors powering them. Taking all the considerations into account a final wing planform is designed, with all the characteristics stated in Table 6.1.

The weight of the wing planform was estimated using the empirical weight relations given by Raymer [12].

Table 6.1: *Sizing of main wing*

Symbol	Value	Unit
Airfoil	NACA 65_1412	
S	1,977	$[m^2]$
MAC	15.76	$[m]$
b	126	$[m]$
λ	0.85	-
$\Lambda_{c/4}$	0.0	$[rad]$
AR	8	-
e	0.81	$[m]$

6.1.2. Lift Estimation

With the airfoil and wing planform chosen, the analysis of the lift characteristics can be done. The lift curve slope is constructed and the general slope can be approximated by the following formula [8]:

$$C_{L\alpha} = \frac{2\pi AR}{2 + \sqrt{\left(\frac{AR\beta}{\kappa}\right)^2 \left(1 + \frac{\tan^2 \Lambda_{C/2}}{\beta^2}\right) + 4}} \tag{6.2}$$

In this formula, AR is the aspect ratio, β is the Prandtl-Glauert Mach number parameter, and κ is the ratio of two-dimensional lift curve slope to 2π, which for the NACA 65_1412 is about 0.95. The $\Lambda_{C/2}$ is the half chord sweep.

The next step is to find the C_{L0}, or the lift coefficient at zero angle of attack. From the airfoil, it is known that no lift is generated at an angle of attack of -3 $[\mathrm{deg}]$. Thus C_{L0} is $3 \cdot C_{L\alpha}$. And with this Equation 6.3] can be established.

$$C_L = C_{L0} + \alpha C_{L\alpha} \tag{6.3}$$

In order to estimate the $C_{L\max}$, the DATCOM 2 method was used [8]. This method is an empirical method which relates the airfoil $C_{l\max}$ to the wings $C_{L\max}$ for high aspect ratio wings. For an unswept wing with a taper ratio of 0.85, a wing is considered to be high aspect ratio if it has an aspect ratio of at least 4. Then depending on the airfoil, the maximum lift ratio ($\frac{C_{L\max}}{C_{l\max}}$) is found, which is 0.9 for the NACA 65_1412.

Lastly, the mach number correction factor ($\Delta C_{L\max}$) is approximated. This factor is based on the airfoil, sweep and the mach number and is approximated to be -0.2. The result of combining these factors is Equation 6.4. This equation, considering an aircraft flying at M = 0.61 results in a $C_{L\max}$ in clean configuration of 1.276.

$$C_{L\max} = C_{l\max}\left(\frac{C_{L\max}}{C_{l\max}}\right) + \Delta C_{L\max} \tag{6.4}$$

6.1.3. Drag Estimation

To estimate the drag, an analytical drag component build-up method was used [8] and the results of this are stated in Table 6.2. To calculate the drag per element, the Reynolds number and cutoff Reynolds number are calculated. From those, the smallest is chosen [8, 15], which is $167 \cdot 10^6$ for the wing.

The transition location is of great importance for the skin friction drag. For surfaces like the wing and tail, a transition point at 35% of the chord is chosen [16]. For the fuselage, a fully turbulent flow is assumed, in part due to the size and in part due to the boat hull shape. The friction coefficient, c_f, can be calculated and combining this with the proper reference area, in this case the wing area, the C_{Df} is obtained. For the form factors (FF) of the aircraft parts, the formulas from Raymer are used for compressible flow [12]. The interference factors (IF) are obtained from [8] where the IF of the fuselage is changed from 1 to 1.5 due to additional drag due to the hull shape [17]. Now the C_{Df}, the FF, and IF can be multiplied together for each part to get the individual $C_{D\min}$. Adding those together, and adding 0.0025 to account for miscellaneous drag like antennas, the total $C_{D\min}$ of the Emperor is obtained and can be seen in Table 6.2. The C_D of the Emperor consists of a fixed part, $C_{D\min}$, and an induced part, C_{Di}, which is dependent on the lift coefficient, and the effective aspect ratio. The C_{Di} is calculated to be 0.0180 in cruise condition at maximum fuel and payload. This leads to the scenario of the largest lift coefficient required. This results in a total drag coefficient of 0.0322.

Table 6.2: *C_{Dmin} for different parts of the Emperor and the total C_{Dmin}*

	Wing	Fuselage	Vertical Tail	Horizontal Tail	Miscellaneous	Total
C_{Df}	0.0021	0.0047	0.00020	0.00055	-	-
FF	1.472	1.055	1.483	1.483	-	-
IF	1	1.5	1.04	1.04	-	-
$C_{D\min}$	0.0031	0.0074	0.00030	0.00084	0.0025	0.0142

6.2. Hydrodynamic Characteristics

When designing an aircraft that takes off and lands in water, one must account for the water-based operations during its design. This brings an extra challenge when compared to a conventional aircraft, since the aircraft must also be stable and controllable while being partly submerged in water, a medium thousand times denser than air. Therefore, ground operations stability needs to be considered. As opposed to land-based aircraft, an aircraft in the water could easily tip over when turning, which will be further explored in Section 6.9. In addition, the take-off from water needs to be considered. If ignored, the hydrodynamic drag might result in an inability to take off due to the higher resistance offered by sea-water when compared to air.

The goal of the take-off procedure is to get the Emperor out of the water and airborne. The main difference between a take-off from water as compared to land, is that in water the aircraft needs to displace the water it is moving through. On land, wheels provide a low-resistance solution. In water however, there is no such efficient solution. There are two approaches to stay afloat on the water. The first option is to use the fuselage itself as a boat hull; this is most commonly seen with larger flying boats[1]. The second approach is to support the Emperor with floats, so that only part of the floats are submerged in water and the fuselage is completely out of the water. This has the added effect that less of the Emperor is in contact with the water, thus requiring less water specific adaptations. In practice however, this option is only used on small sport aircraft. This is because as the mass of the aircraft becomes larger, the floats required to carry that weight get larger as well. Larger floats are heavier and cause more drag and given that the Emperor is extremely large compared to any aircraft currently available, the option of using floats has been discarded. It was decided to use the already existing conventional NACA TN-2481 hull, scaled up.

In order to take off, a certain speed (V_{TO}) has to be achieved. As water is about 800 times more dense than air and an aircraft of this size would be submerged quite deep, the drag of moving through the water becomes very high as speed increases. It thus is essential to get out of the water as soon as possible.

One possible solution that was considered for this was the use of hydrofoils which generate lift much in the same way as airfoils do. However, it was found that typically hydrofoils are only effective up to speeds of around 50 - 60 $[kts]$ (25.72 - 30.87 $[m/s]$) [2]. At higher water speeds, the low pressure flow over the top of the hydrofoil drops below the vapor pressure of water, causing gaseous bubbles to appear and interfere with the flow. This results in a rapid deterioration of the lift to drag ratio of the hydrofoil and the total drag eventually reaches the available thrust and makes take-off impossible [18]. Since the Emperor takes off at 79.47 $[m/s]$, hydrofoils do not seem to be an option. This will be further discussed after presenting another option for take-off.

The alternative to hydrofoils is to make use of hull planing. This method uses the shape of the hull to generate hydrodynamic lift which raises the aircraft to the water's surface. When planing, the hydrodynamic lift generated from just a small contact area keeps much of the hull out of the water. Drag at this stage is far lower than it is during the displacement phase at low speeds, during which much of the hull is still submerged and lift is predominantly generated by the buoyant force [8]. If the drag during take-off is plotted against the velocity, there is a clear hump visible, illustrated in Figure 6.1. This hump is the point at which the aircraft starts lifting out of the water and here the "the pilot will rotate the airplane sharply to try to help it 'get on the step'" [8]. For the conventional NACA TN-2481, the hull being used for this design, the hump can be seen in the non-dotted line of Figure 6.1. As the Emperor makes use of a conventional hull, the hump is located at a speed coefficient, C_V, of roughly 2.8. This is converted to velocity using $C_V = \frac{V}{\sqrt{(\mathrm{gB})}}$ where g is acceleration of gravity taken to be 9.80665 $[m/s^2]$ and B is the width of the hull being 9 $[m]$. This gives a hump speed of 26.31 $[m/s]$. It should be noted that the true value may be different due to the real world complications of scaling up the hull dimensions

[1] https://wightaviationmuseum.org.uk/princess-flying-boat/, accessed 15/06/2022 and https://www.platinumfighters.com/inventory/1945-martin-jrm-3-mars/, accessed 15/06/2022

[2] https://www.sciencedirect.com/topics/engineering/hydrofoil-craft, accessed 14/06/2022

[8], hence further investigation and testing should be carried out. The total drag at the peak of the hump, including aerodynamic drag, has been taken as the critical take-off drag with which the take-off constraint was constructed. This peak drag is used to calculate the critical take-off thrust and it was found to not be a limiting constraint when sizing the propulsion system, needing a higher thrust during cruise, which is further explained in Section 6.3.

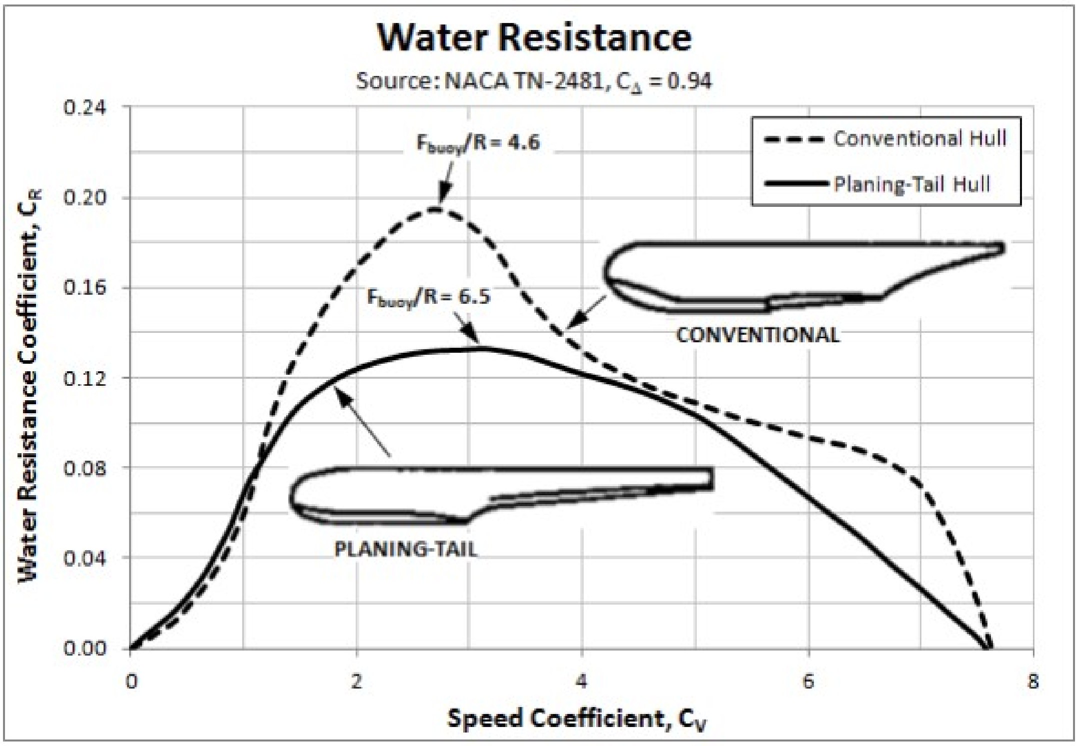

Figure 6.1: *Drag-Velocity curve [8]*

Finalising the conclusion of using a hull rather than hydrofoils for take-off and summarising the take-off conditions, a study done was found which serves as a good proxy for the Emperor [18]. The study was on the same hull as is being used for the design of this Emperor, without and with hydrofoils during take-off and their main results can be seen below in Figure 6.2 and Figure 6.3 respectively [18]. It should be noted that the aircraft that the researchers used was much smaller and lighter than the Emperor. Also incorporated in the study is the effect of aerodynamic drag and Froude resistance, which is another type of hydrodynamic drag representing the generation of waves and was found to be non-limiting. The plots show how the horizontal forces change over time during take-off. Other plots are available as well showing horizontal force versus velocity coefficient. The weight of the boat hull was estimated to be 25% of the fuselage structural mass. This factor was based on engineering judgement, selected to present a worst case scenario, as no accurate weight estimations for a boat hull of such size were available.

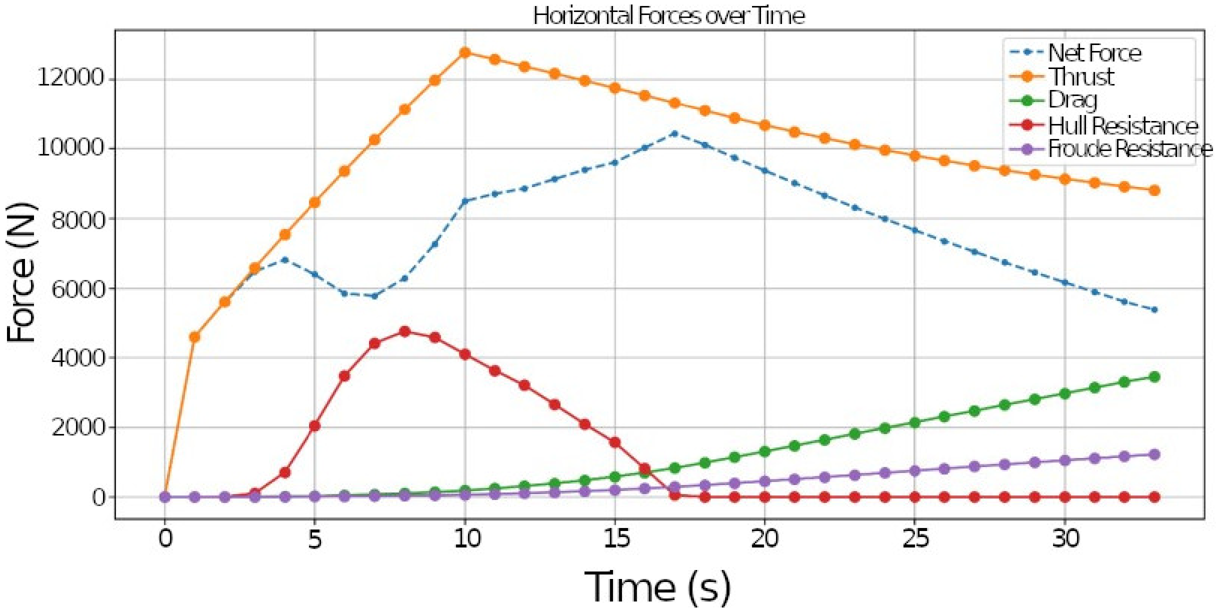

Figure 6.2: *No-hydrofoil configuration: take-off results of horizontal force over time [18]*

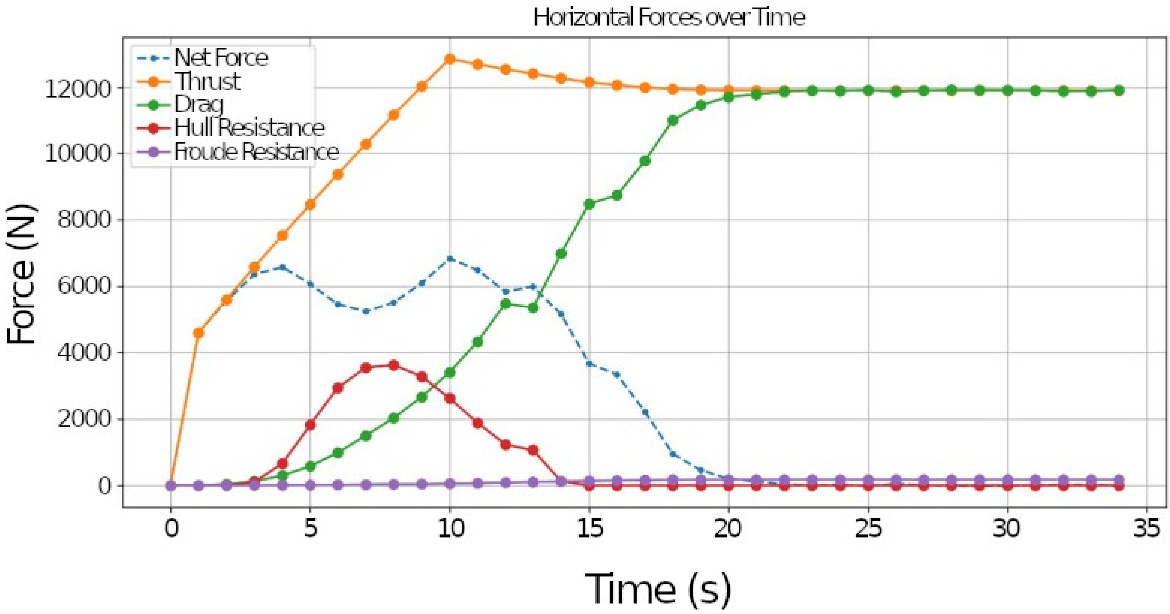

Figure 6.3: *Hydrofoil configuration: take-off results of horizontal force over time [18]*

Note in Figure 6.2 how the hump is reached and then drag rapidly decreases, allowing the aircraft to continue accelerating and to eventually take-off. In Figure 6.3 however, one can see how the hump speed is reached but due to cavitation over the hydrofoil, the overall drag continues to rapidly increase even after this point. Eventually drag equals thrust making the net force zero and at this point the aircraft is no longer accelerating and taking off is impossible. Given that the Emperor takes off at 79.47 $[m/s]$, hydrofoils would ultimately end up being more of a hindrance than a help [18]. Therefore, due to this cavitation problem, the use of hydrofoils has been dismissed as a take-off aid and the NACA TN-2481 seaplane hull alone is used.

One last aspect to consider is the impact of waves on ride comfort and mission feasibility. This was another reason why hydrofoils were initially considered as an aircraft out of the water is not as limited by waves creating a rough take-off. However, with hydrofoils being unfeasible this was no longer an option. This said, a study is recommended into employing hydrofoils to reach the hump speed and then retracting them such that the planing hull can take over. Ideally this would decrease the critical take-off drag and would improve the ride quality for passengers. The maximum wave height that a seaplane hull can safely handle is estimated using the empirical relation based on maximum take-off weight, where all values are imperial units [8]:

$$h_{\text{wave, ft}} \approx 1.25 ln(W_{\text{TO, lbs}}) - 8.6414 \tag{6.5}$$

When converted back to SI, this yields h_{wave} = 2.99 $[m]$. Given that take-off operations will be conducted close to sheltered ports, this would not limit day-to-day flights and would only become a concern in stormy conditions. It should be noted that in the period of 2020-2022, there was no day in which waves in New York were above 2 $[m]$ [3]. Hence it is assumed that due to the Emperors large size and mass of over 1000 $[tons]$ the ride quality at takeoff will be minimally impacted by waves.

6.3. Propulsion Subsystem

For the propulsion system, fans are used which are powered by electric motors. An inverter is included within the electric motor. Given the large size and large amount of thrust that was estimated during the preliminary design phase, a distributed propulsion (DP) system is utilized as a large number of fans are anticipated to be required. The fans are distributed along the wingspan and by placing the fans at a small distance above the wing, a phenomenon called boundary layer ingestion (BLI) occurs. To ingest the thickest boundary layer into the fan, the fans are placed quite aft on top of the wing. However, sufficient space is kept available for the HLD's behind the fans. BLI is known to improve the propulsive efficiency by adding up to 20% to the previous efficiency [19, 20]. However, being conservative, a BLI increase in efficiency is taken to be 10%, but the actual value of this effect should be investigated in a follow-up design study. To achieve distributed propulsion and ensure boundary layer ingestion along the wingspan, consequently the diameter of the fans needs to be smaller than conventional engine diameters, as found in conventional aircraft.

One of the characteristic parameters of a fan is the compression ratio between the inlet and the outlet pressure. The DLR UHBR performance map was used to get such value for the highest fan efficiency in cruise. In Figure 6.4, the relevant part for this design of the performance map is shown. The y-axis is the pressure ratio and x-axis is the corrected mass flow. The blue line, labeled by 'CR', represents cruise conditions. In this line, the square represents the highest efficiency point with conventional propulsion and the circle represents the highest efficiency point with BLI [21]. The pressure ratio for the blue circle, which is used to size the fan, is 1.31.

[3]`https://seatemperature.info/new-york-city-waves-forecast.html`, accessed 15/06/2022

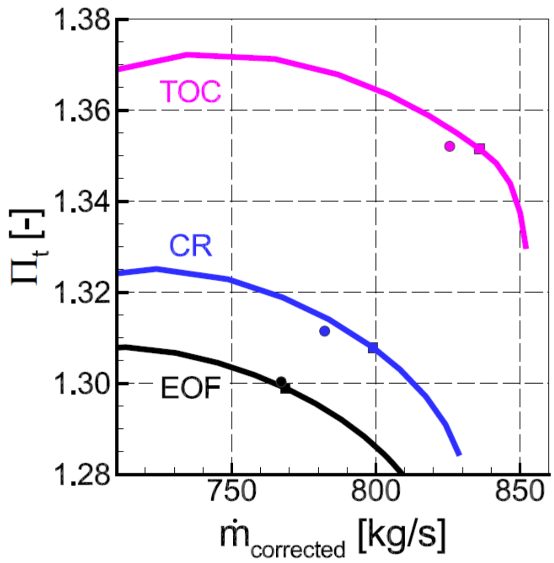

Figure 6.4: *Performance map of the DLR UHBR fan showing efficiency for regular set up and BLI [21]*

Another parameter needed to size the propulsion system is the thrust it needs to deliver. Due to the unconventional amount of engines, an engines contingency factor of 1.3 is applied to the total thrust required. This accounts for the risk of having 30% of the engines become inoperative while still maintaining the nominal cruise performance. This number was chosen based on the fact that a regular two-engine plane has to be able to take-off and cruise with one engine inoperative. The Emperor will take-off in water thus a lower margin is possible because it can always abort landing as opposed to regular aircraft, that once they reach a certain speed, take-off cannot be aborted[4].

The power of the Emperor is calculated using Equation 6.6 where P and T are the power and thrust after the contingency is applied and V is the speed. The power needed for both cruise and take-off conditions is calculated, using the thrust and velocity for cruise and take-off, respectively. The largest power required is used in the further calculations to size the propulsion system. With this critical power, the amount of fans can be found using Equation 6.7. The power of a single unit consisting of a motor and inverter is 4 $[MW]$, taken from the Saluqi Motors catalog [5]. The efficiency of the motor includes the efficiency of the motor plus the inverter and has a value of 96%. Regarding the term between brackets, the power of the motor needs to be multiplied by the propulsive efficiency of the fan, η_{prop}, taken to be 80% [22]. Due to the fact that BLI is utilized, a 10% increase in the propulsive efficiency is included, as mentioned previously.

$$P = TV \qquad (6.6)$$

$$N_{\text{fans}} = \frac{P}{P_{\text{motor}}\eta_{\text{motor}}(\eta_{\text{prop}} + \eta_{\text{BLI}})} \qquad (6.7)$$

The thrust each fan needs to provide is calculated by dividing the total thrust over the number of fans. The total pressure at the inlet of the fan is calculated with Equation 6.8 using ISA to calculate the static pressure at cruise altitude using the cruise speed. By using the pressure ratio obtained from Figure 6.4 and the total pressure at the inlet, the total pressure at the outlet can be obtained.

[4] https://skybrary.aero/articles/v1, accessed 03/06/2022
[5] https://www.saluqimotors.com/products/, accessed 01/06/2022

$$P_t = P_s + \frac{1}{2}\rho V^2 \tag{6.8}$$

The speed behind the fan changes due to the change in total pressure. The speed at the outlet can be calculated by rewriting Equation 6.8, using the total pressure at the outlet, while the static pressure and density remain identical to those previously used for the inlet. The mass flow can be calculated by rewriting Equation 6.9 and using the speed difference at the inlet and outlet of the fan.

$$T_{\text{fan}} = \dot{m}(V_1 - V_0) \tag{6.9}$$

$$\dot{m} = \Phi \rho A_{\text{inlet}} \bar{U}_t \tag{6.10}$$

The mass flow can then be used to calculate the radius of the fan, by substituting Equation 6.11 for peripheral speed at the tip and Equation 6.12 for the area of the fan inlet into Equation 6.10 and solving for the radius. Φ refers to the flow coefficient at the tip, taken to be 0.5 [21], ρ is the density at the cruise altitude, ω is the angular speed, taken to be 4500 RPM. This angular speed is the rated speed for the electric motor and inverter combination from Saluqi, which is connected to the fan. The peripheral speed at the tip for fans regularly are designed to be supersonic [6]. However, the tip speed for the Emperor is found to be subsonic, as can be seen in Table 6.3. This subsonic tip speed causes the fan to produce less noise and heat, and the fan is exposed to smaller structural loads [23].

$$\bar{U}_t = \omega r_{\text{fan}} \tag{6.11}$$

$$A_{\text{inlet}} = \pi r_{\text{fan}}^2 \tag{6.12}$$

Once the radius is calculated, the placement of the fans is determined. Due to the high-wing configuration, fans can be distributed along the entire wing span. However, to avoid interference, no fans are placed in front of the ailerons at both ends of the wing. The spacing is determined using Equation 6.13, while ensuring that the spacing is at least 5% of the fan diameter. This spacing is defined as the minimum distance between adjacent fan casings.

$$S = 2l_{\text{ailerons}} + n_{\text{fans}} D_{\text{fan}} + \text{spacing}(n_{\text{fans}} - 1) \tag{6.13}$$

Finally, the mass and size of the propulsion system is determined. The mass of the fans is determined by performing a regression using data of fans for tunnel ventilation [24]. The fans for this application have very extensive casings, thus to represent more accurately the length and weight of an aircraft fan, one third of both the length and mass is taken for each corresponding diameter. This reduced length and mass, along with the corresponding diameters is then used to make two regressions, where the reduced length is plotted against the diameter, and the reduced mass is plotted against the diameter. From this regression the mass of the fan blades and length of the casing is estimated. Another regression using this data is performed to estimate the length of the casing, corresponding to the diameter of the used fan. The resultant values can be found in Table 6.3. The combined mass and dimensions of the electric motor and inverter is determined using information provided by Saluqi. The electric motor and inverter will be placed behind the blades of the fan, inside of the fan casing. To account for the integration of the fan with the wing or fuselage and the cabling, a contingency factor of 1.15 is included on the total mass of all motors, inverters and fans. A propulsion unit, as mentioned in Table 6.3, consists of a fan, an electric motor, an inverter, the integration and cabling contingency. The motors remaining at operational temperatures will be ensured by cooling using air taken in from the surroundings of the aircraft.

The previously explained method is used to find the parameters summarised in Table 6.3. It should be noted that the diameter of the fan is relatively small and the number of fans is large,

[6] `https://www.mcnallyinstitute.com/what-is-the-fan-speed-of-a-jet-engine/`, accessed on 02/06/2022

compared to current conventional aircraft. As mentioned before, this is designed as such to achieve the benefits of both distributed propulsion and boundary layer ingestion.

Table 6.3: *Results of the propulsion system*

Parameter	Value	Unit
Number of fans on wing	82	[-]
Diameter fan	1.20	$[m]$
Length fan casing	2.59	$[m]$
Blade tip speed	283.8	$[m/s]$
Spacing between fans	0.13	$[m]$
Mass propulsion unit	1209	$[kg]$
Total mass propulsion system	99.1	$[tons]$

6.4. Power Subsystem

In order to determine the power requirements of the Emperor, it is important to consider that power should be provided both for the propulsion system and also for the rest of the systems that require electricity. Furthermore, it was established that this power will be obtained by the use of fuel cells due to the fact that the Emperor will be a zero greenhouse gas emission aircraft. Other options of generating power with hydrogen do exist, such as through combustion, but this is discarded as it would generate greenhouse gases and would make the aircraft not fully sustainable.

The power to be delivered to the fans can be either the average power or the peak power. The average power for the fan is calculated using the assumption that at cruise thrust is equal to drag, as shown in Equation 6.14. But the peak power must be used to size the fuel cells, as that is the power they must be capable of delivering.

$$P_{\text{average fan}} = T_{\text{cruise}} V_{\text{cruise}} \quad (6.14) \qquad P_{\text{peak fan}} = n_{\text{motors}} P_{\text{motor}} \quad (6.15)$$

Besides the power being delivered to the fans, much of other subsystems of the aircraft also uses power. The average power being delivered to the fans is assumed to be 95% of the total power of the aircraft [25], thus 5% is needed for various other subsystems. This 5% can be calculated from the average power required for the fans. The peak power for the fans is calculated by taking into account the amount of power the total number of motors is able to deliver, as shown in Equation 6.15, based on the power required obtained through the constraint diagram. The peak power for the Emperor is calculated by adding the power of the rest of the systems of the aircraft, mentioned previously, and the peak power for the fans. The peak power for the complete aircraft is divided by the efficiency of the converter, and multiplied by a contingency for cable losses, which are shown in Table 6.4. On top of this, an extra engine power contingency of 1.3, also stated in Table 6.4, was added as a safety factor to account for the possibility of the failure of some fuel cells, and the value was taken to match the power redundancy of the fans. This contingency would also aid in situations of peak power by lowering the stress on each individual fuel cell and could increase system longevity. This peak power for the total aircraft, as shown in Table 6.4, is used to determine the amount of fuel cells needed to deliver this power.

Table 6.4: *Values utilized to size power system*

Parameter	Value	Unit
Average power aircraft	185	$[MW]$
Efficiency converter	0.95	[-]
Contingency cable losses	1.05	[-]
Contingency failure & peak power	1.30	[-]
Peak power aircraft	484	$[MW]$

Fuel cells generate electricity when gaseous hydrogen and oxygen pass over the anode and cathode respectively. There is a flow of electrons from the anode to the cathode, creating a flow of electricity, and the gases react to form water as waste product in the electrolyte[7]. When comparing fuel cell types, Proton-Echange Membrane (PEM) fuel cells have been chosen for their high power-density, cold-start capability, versatility and lightweight nature [8].

To decide on a specific PEM fuel cell, multiple state-of-the-art fuel cells are compared and their properties analysed[9]. From this initial study, the VLS II Pro-165 fuel cell stack was found to be the best in terms of mass and volume power density and will thus be used for further calculations. Since the Emperor will have a peak power required of 484 $[MW]$ and given a present day mass power density of 2800 $[W/kg]$ and a present day stack density of 1200 $[kg/m^3]$, it would lead to a total size of 373.91 $[m^3]$ and a weight of 448.70 $[tons]$ if build today. However, [26] predicts a future mass power density of 8000 $[W/kg]$. Incorporating the future estimated fuel cell performance but still assuming the present stack density, a total weight of 100.69 $[tons]$ and size of 83.91 $[m^3]$ are found which are the values that will be further used in the design. For this it is assumed that the density of fuel cells (stack density) does not improve in the future, which while being a pessimistic assumption, serves as a worst-case scenario for the fuel cell design. While the use of the highest predicted future mass power density may be questioned, considering the fact that the Emperor will be produced far into the future, and considering the pace of development for the use of hydrogen as fuel, it is believed to be a justified assumption to make[27].

Regarding the voltage of the stack, the VLS II Pro-165 has an output of 300 $[V]$. This will be converted and inverted to the correct voltage before it reaches the energy-consuming systems. Finally, the heat generated in the cells from the production of electricity should also be addressed. Given the operating speeds of the aircraft, cooling can be achieved from a sufficient flow of air over the cells. This will keep the cells at normal operating conditions. A study into liquid cooling could be done as future research but these complications are out of the scope of this report. This could perhaps be done by using the cold H2 fuel to cool a liquid through a heat exchanger which can then be used to cool the cells.

The fuel cells are located in the wings. This way, they are located in a central location, close to the main electricity user namely the propulsion unit. Additionally, they provide bending relief for the wings. The exact locations are shown in the aircraft layout overviews in Section 6.10.

6.5. Fuel Storage

The liquid hydrogen tanks need to be able to efficiently fit within the aircraft frame and also keep the fuel at cryogenic temperatures throughout the duration of the flight. The fuel tanks are

[7] https://www.energy.gov/eere/fuelcells/fuel-cells
[8] https://nedstack.com/en/pem-fcs-stack-technology
[9] https://www.horizonfuelcell.com/fuelcellstacks

placed inside the fuselage and not in the wings, where they are placed in conventional aircraft. This is due to the wings having a limited volume and also a relatively large surface area which would require significantly more insulation. This section discusses the design and sizing of the tanks.

6.5.1. Liquid Hydrogen Tanks Characteristics

When designing a fuel containment system, multiple aspects have to first be considered such as whether the tank will be integral or not, the type of insulation that will be used, and at what location that insulation will be located. These are important as they influence the strength requirements, the general service life of the tank, and the total size and mass of the tanks.

Regarding the integration of the fuel tank in the fuselage, the difference between integral and non-integral tanks is that integral tanks are load bearing structures of the airframe. This implies that they serve as part of the aircraft structure and carry the same loads as the fuselage in addition to containing the required fuel. Non-integral tanks on the other hand only contain the fuel, and are supported by the external airframe structure. The advantage of the integral tank is its higher volumetric and weight efficiency. However, because of the importance of the tank not failing due to unexpected loads, the choice was made for non-integral tanks to be used. This said, while not load bearing, the shape of the tanks closely follow the shape of the internal fuselage layout making them comparably space efficient. A study was done regarding the use of removable, standard shipping container sized fuel tanks which could be loaded and unloaded after each flight and could improve refuelling times. As will be discussed later in Section 10.4, conventional pump operated refueling times were found to not be a limiting factor in the turnaround time of the aircraft and therefore speeding up the process through the use of ”tanktainers” was unnecessary. Given that they had to be standard size, the use of these kinds of tanks was also found to be highly space and mass inefficient.

One vital design consideration of the tank insulation is to limit the boil-off of hydrogen. This refers to LH2 that has reached boiling temperatures within the tank and needs to be released in order to keep the pressure of the tank below the operating level of 1.2 $[bar]$ [28]. The boil-off must be released in order to prevent a build up of pressure which could lead to an explosion. Since boil-off occurs at a temperature of 20.28 $[K]$, it is possible to convert it back to liquid hydrogen with little extra energy input for cooling. This process should be minimised however given that the process is only about 30% efficient and the systems are heavy and complicated. Venting boil-off to the atmosphere should not occur and it should instead be used to supply the fuel cells. During non-flight operations it could be used to power other subsystems.

For the insulation itself, the choice between internal and external insulation must be made. Internal insulation has strict demands on the permeability of the material, such that the gaseous hydrogen due to the boil-off cannot diffuse through the tank wall and decrease the insulation effectiveness. Even though no such material exists that fully insulates, it is an interesting option to explore, since it minimizes differential thermal expansion by keeping the tank walls at a near-ambient temperature. External insulation however must only be impervious to air and as such the most demanding requirement is that it can handle a certain amount mechanical damage. Additionally, due to differential thermal expansion, the tank will contract and expand during refuelling which creates attachment concerns. On the other hand, maintenance becomes easier, and the reliability in terms of insulation are higher. Ultimately for simplicity and reliability, the design choice was made to use external insulation [7].

As a choice of insulation materials, aerogels, polymer foams and multilayer insulation (MLI) were considered. While aerogels were found to be promising, their brittleness makes them only

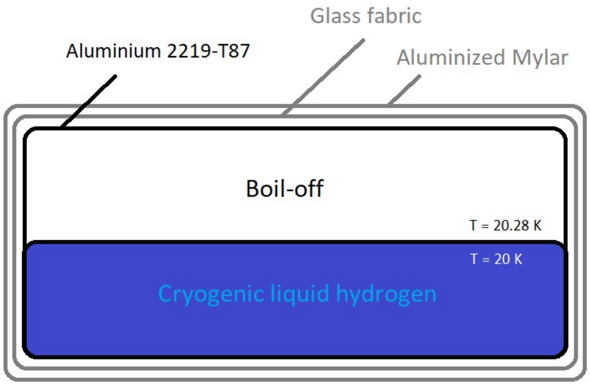

Figure 6.5: *Fuel tank*

valid for small scale applications. With a thermal conductivity as low as 10^{-5} $[W/(mK)]$ and with sufficient material properties, MLI was found to be the best insulation technique currently available. The way it works is that warm air from the environment makes contact with the outer layer, where part of the heat is reflected away while the rest heats up this outer layer. This process continues through the layers until almost no temperature gradient is present. The optimum combination for the MLI was found to consist of overlapping layers of glass fabric and aluminized Mylar [29] with a total thickness of 2.2 $[mm]$, as further discussed with Figure 6.6. With these design choices established, the tanks can be sized, and are shown in Figure 6.5.

6.5.2. Tank Sizing

The first step in tank sizing is to find the required amount fuel that is needed. This is based on the mission profile and incorporates the electrical conversion efficiency of the fuel cell stack. This method for sizing liquid hydrogen storage results in a fuel tank and insulation size and mass. It also accounts for the total hydrogen storage, the wall thickness required to contain the pressure and handle the fatigue, the insulation material thickness and weight to minimize boil off [30].

The Forward and Mid fuel containers have a maximum length dictated by the length of the cabin, the length of the wing box and the position of the wing. The maximum available volume for these is calculated as cylinders with spherical end caps, assuming that the cross sectional area is equal to the cross sectional area available in the 3D model in those locations, using Equation 6.16.

$$V_t = \frac{4}{3}\pi r^3 + \pi r^2 L \tag{6.16}$$

Having obtained the volumes of the two containers, the mass of hydrogen that can be stored in each was calculated using Equation 6.17. Where V_i is 7.2 % and is a contingency factor that incorporates the additional volume required to accommodate a certain amount of boil-off. Using the inner cabin radius as a first estimate of the tank radius, the length of the tank is found using Equation 6.16.

$$V_t = M_H \frac{1 + V_i}{\rho_{LH}} \tag{6.17}$$

The remaining required mass of hydrogen shall be stored in the Aft Fuel container, located behind the cabin. The cross sectional area of it was also estimated from the 3D model, and the volume required was computed using the same method but in reverse, leading to the required length.

Materials used for the construction of liquid hydrogen tanks must be impermeable to gaseous hydrogen, resistant to hydrogen embrittlement and must retain satisfactory fracture resistance and ductility at cryogenic temperatures [7]. Aluminium alloy 2219-T87 is chosen as the material for the fuel tank because of its excellent strength characteristics and high brittleness resistance under cryogenic conditions [31]. Using the material properties displayed in Table 6.6, the wall thickness and tank mass are calculated. Equation 6.18 gives the required thickness for a given yield stress or fatigue strength. The fatigue strength is found to be the limiting in this case, the yield under fatigue is used to calculate the minimum required wall thickness for a cylinder with hemispherical end caps [30].

$$t_w = \frac{PrSF}{2\sigma_{\text{fatigue}}} \tag{6.18}$$

For a pressure of 1.2 bar [28] the minimum required thickness is 5.8 $[mm]$ using an added safety factor of 1.5. However, this is not the total thickness of the fuel tank: the insulation still has to be added.

Using the properties of MLI as discussed in Subsection 6.5.1, the thickness of the insulation was found iteratively for a minimal total tank and boil-off mass and is equal to 2.2 $[mm]$. The relation between the thickness and tank mass is shown in Figure 6.6.

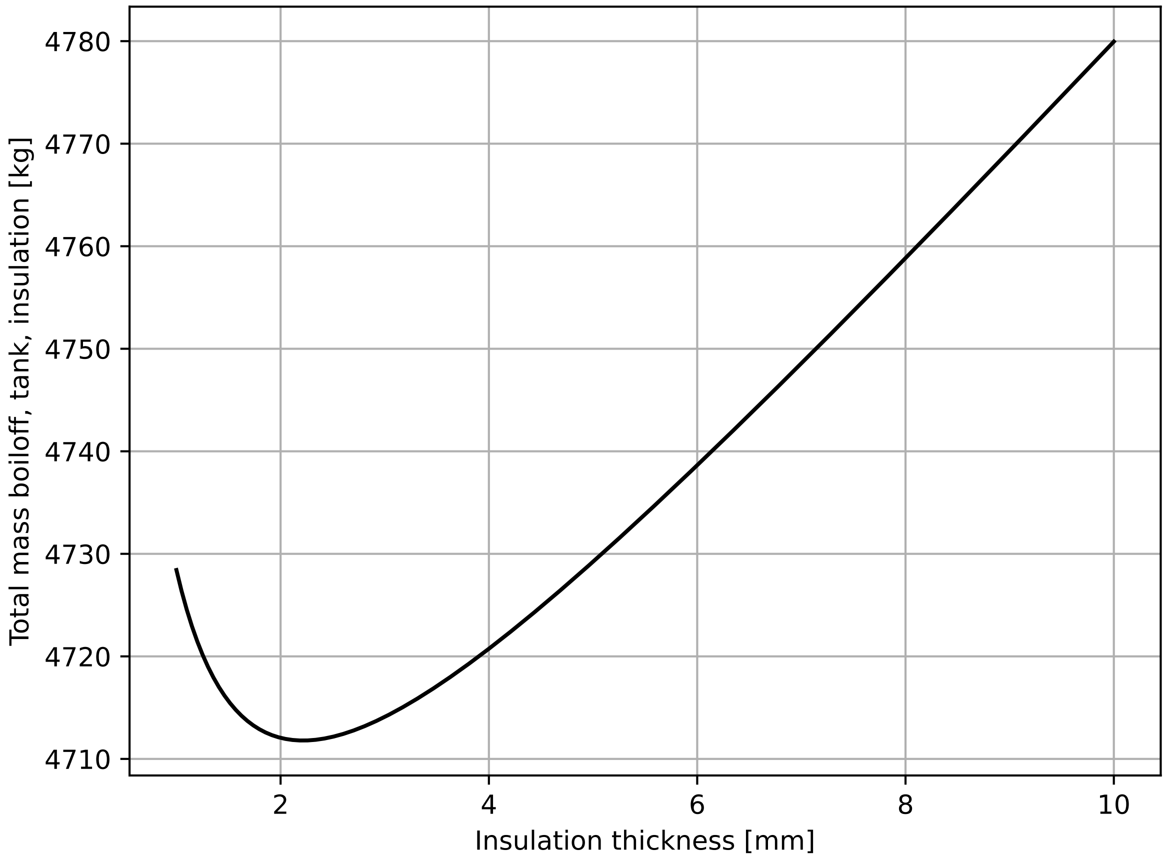

Figure 6.6: *Relationship insulation thickness vs total tank mass*

Finally the mass of the fuel tanks must be estimated. This mass should account for the thickness of the aluminium walls of the tank, the mass of the insulation and the mass of the hydrogen which will boil off. The mass of the aluminium walls was estimated by subtracting the internal volume of the fuel container from the external volume of the fuel container, and multiplying the volume by the density of the selected aluminium at 2840 $[kg/m^3]$. The thickness of the insulation which minimizes the total mass of the fuel container including the boil-off was found as described previously.

To summarise the characteristics of the fuel tanks, Table 6.5 gives several of the most noteworthy results, including the masses.

Table 6.5: *Fuel container properties*

Parameter	Value	Unit
Forward Fuel Container		
Length	42	$[m]$
Volume	1383	$[m^3]$
Fuel Mass	91378	$[kg]$
Fuel Container Mass	18320	$[kg]$
Mid Fuel Container		
Length	15	$[m]$
Volume	430	$[m^3]$
Fuel Mass	28448	$[kg]$
Fuel Container Mass	6369	$[kg]$
Aft Fuel Container		
Length	13	$[m]$
Volume	267	$[m^3]$
Fuel Mass	17649	$[kg]$
Fuel Container Mass	4712	$[kg]$

6.6. Material Characteristics

The choice of materials has a big influence on the weight, strength and performance, and cost of the Emperor. Due to its large and sea-based nature, some additions such as a seawater-resistant coating, or extra strong material to deal with bending have to be considered. This section first deals with the distribution of the materials over the different aircraft sections, and then continues with a qualitative comparison between the different materials that are used.

6.6.1. Material Distribution

In general the material distribution along the Emperor will be the same as for the B787, with some small variations when going more into depth. See Figure 6.7[10] for this distribution, which is consistent with other current aircraft.

"In general, the use of composites has gained domain to the point where it is used for 50 % of almost all current large aircraft. This because of its desirable lightweight and strength properties. The corrosion resistance is also an advantage.

Even though the Emperor will be a huge seaplane, it has been decided that the material distribution can be the same as current conventional aircraft. Using composites over 50 % of the body will allow the Emperor to carry its weight, aerodynamic loads and impact shocks whilst keeping it as light as possible. This is a challenge due to its huge size. The second most used material is aluminium. Aluminium is also a strong, lightweight material, and is considerable cheaper than carbon fibres. However, it gets corroded by salt water, but this can be delayed sufficiently by applying coating. Titanium has excellent strength and weight characteristics, but is only used in the most critical regions (such as the pylons) due to its cost.[1]

[10] https://aerocorner.com/blog/what-are-planes-made-of/#why-are-planes-made-of-aluminium

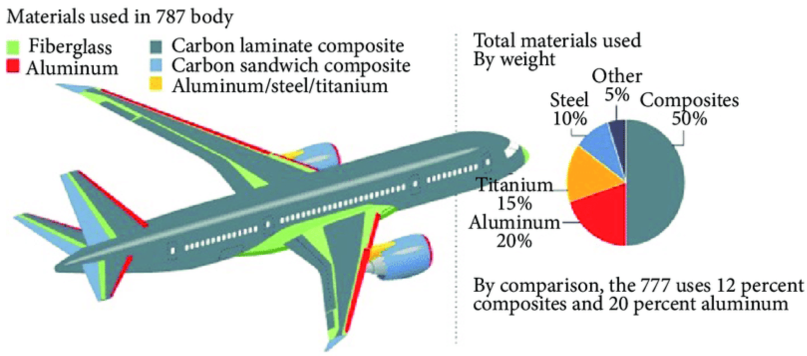

Figure 6.7: *Layout aircraft with material application [32]*

6.6.2. Comparison Materials

Multiple sub-classes exist within the material categories of Figure 6.7, which are described in this subsection along with a qualitative comparison between the different materials. The specific properties of the respective materials can be found in Table 6.6.

Aluminium is widely used in the aerospace industry due its excellent material properties, such as being lightweight and still remaining strong, while also being highly corrosion-resistant. Aluminium does need some special attention when being applied in sea-based operations since salt water has a high corroding effect to non-treated aluminium. Regular maintenance and the application of coatings are vital for the durability of aluminium. While possessing all these great properties, aluminium is a relatively cheap material. Thanks to its good heat transfer capacities and impact strength, aluminium can be used on the leading edges of the wings to protect the Emperor from icing and bird impacts. It is sufficient to also cover the body of the Emperor, but more advantageous composites are preferred due to the lighter weight of these composites compared to aluminium.

Aluminium alloys widely used in the aerospace industry are 7075, 6063, 6061, 5052 and 2024 [33]. From this section onward only the 7075 and 6063 aluminium alloys are considered. 2024 while being widely used in aerospace and being stronger than for example type 6061 or type 6063 aluminium alloy is sensitive to corrosion due to its high copper concentration. This can be mitigated by coating the material, but for marine operations a generally better corrosion resistant alloy is preferred. While type 6063 aluminium is harder to machine and shape, it is more corrosion resistant than type 6061 which is why it is preferred for the purposes of this product. Type 5052 aluminium is also highly corrosion resistant like 6063, but type 6063 is preferred for its stronger material properties. Type 7075 aluminium is to be used due to being by far one of the strongest aluminium alloys, even though it is harder to form and shape into a final product. All these aluminium alloys could be coated to further improve corrosion resistance.

Even though composites with e.g. carbon fibre are more expensive than aluminium, they are also stronger and even lighter. Additionally, they are better at bearing tension loads and vibrations. Their properties vary wildly depending on the fibre orientation, and fibre type and density. Depending on the strength and stiffness requirements, a specific type of fibres and resin can be chosen. The properties listed in Table 6.6 originate from pure carbon fibres, and they will change depending on the resin.

Fiberglass is used in the aviation sector due to its environmental friendliness and lightweight nature. It is a robust and corrosion-resistant material. It is basically a less strong, but cheaper version of carbon fibres. Fiberglass is mostly used for secondary structures on aircraft.

Titanium is a desired material with the highest specific properties out of all the metal alloys and the highest strength out of all the considered materials, but it sees limited used due to its high reactivity and cost.

Glare is a material developed at the TU Delft with a low density, good impact resistance, and fatigue, fire and corrosion resistance. All elements that are especially important in seaplane design and thus shows great potential.” [1]

It should be noted that for the estimations of the weights of the systems using the Raymer method, advanced material choices were not considered. Hence the OEM calculated is the worst case scenario that will be improved with the application of advanced materials during the next design phase.

Table 6.6: *Material characteristics*

Material	**Yield strength** $[MPa]$	**Ultimate strength** $[MPa]$	**Fatigue** $[MPa]$	**Young’s Modulus** $[MPa]$	**Density** $[kg/m^3]$
Glare	284	620	-	58100	620
Aluminium 6063-T6	214	241	68.9 at $5 \cdot 10^8$ cycles	68900	2700
Aluminium 7075	503	572	159 at $5 \cdot 10^8$ cycles	71700	2810
Aluminium 2219-T87	393	476	103 at $5 \cdot 10^8$ cycles	73100	2840
Fiberglass	207	3033	-	7200	1950-2050
Carbon fibres	2500	4000	-	500000	2000
Titanium Ti-6AI-4V	880	950	240-510 at $1 \cdot 10^7$ cycles	113000	862-1200

6.7. Static Loading Fuselage

The static loading of the fuselage due to bending, shear and buckling is analysed in this section to determine the required thickness for the different parts of the fuselage. For simplicity, the fuselage is divided into three sections with every point in a section carrying the maximum load present in that section. The material considered for the fuselage structure is aluminium 7075 due to its high performance. Aluminium 7075 is not designed to withstand the marine conditions the Emperor is operating, therefore an additional coating of corrosion resistant paint is added to the fuselage. For the purposes of this analysis the fuselage was considered as a series of ellipses with matching heights and widths of the NACA hull. A more thorough FEM based analysis of the loads is recommended for the next stage of the design process.

6.7.1. Loading

In order to design the fuselage it is necessary to examine loads that the fuselage will be carrying. This is done by creating the shear and bending moment diagrams which can be seen in Figure 6.8. These loads are found from the centres of gravity of the different components of the aircraft by introducing them as either distributed or points loads based on the size of the component and the nature of the load. Additionally the moment generated by the moment coefficients C_m of the wing and horizontal tail are also incorporated in the moment diagram by modeling them as a point moments at the same location as the lift forces.

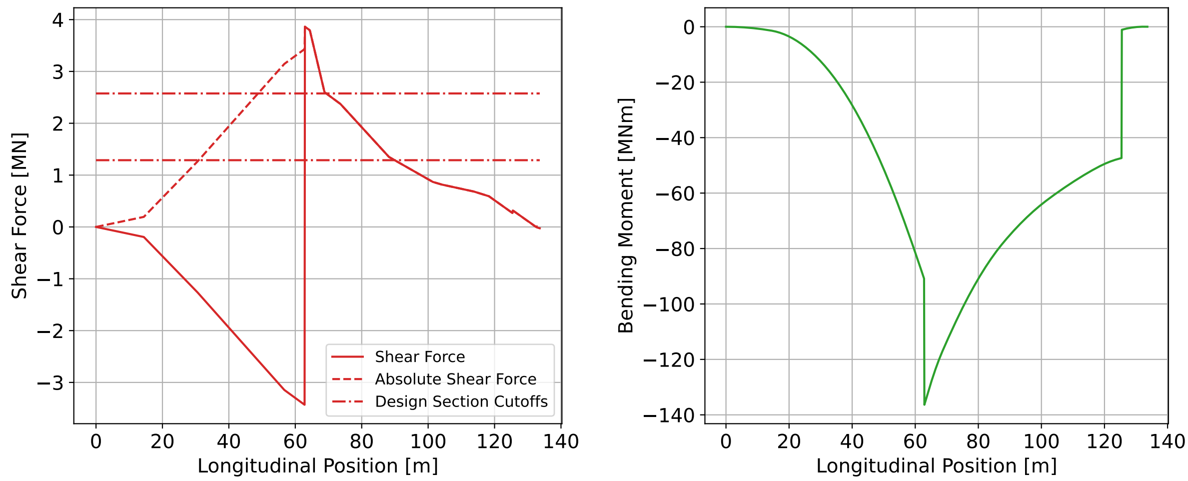

(a) *Fuselage shear force diagram*

(b) *Fuselage bending moment diagram*

Figure 6.8: *Shear and moment diagrams for the fuselage*

6.7.2. Bending and Shear Stresses

To find the optimal thickness of the fuselage, some structural analysis is performed to optimise the thickness for minimum bending and shear stresses. This is done for the hollow elliptical shape of the fuselage which is subjected to loads in the z- and y-directions.

Since the fuselage is elliptical, the bending stress can be found through Equation 6.19. This equation includes the contribution of the pressurisation of the fuselage. Due to this pressurisation, there is also a stress contribution acting in the circumferential direction given by Equation 6.20. These stresses are calculated at two extreme locations: on top of the fuselage where z = max and y = 0, and on the left of the fuselage where z = 0 and y = max. Although it should be noted that the final design is not pressurised due to the cruise altitude being 3000 $[m]$, hence the term describing how the pressure difference contributes to the stress will be zero.

$$\sigma_x = \frac{M_z}{I_{zz}} y + \frac{M_y}{I_{yy}} z + \frac{\Delta P R}{t} \tag{6.19}$$

$$\sigma_y = \frac{2 \Delta P R}{t} \tag{6.20}$$

The shear stress is shown in Equation 6.21, where S_y and S_z represent the loading in y- and z-directions, J the polar moment of inertia and T the torque acting on the fuselage due to the contribution of the vertical tailplane.

$$\tau = -\frac{S_y Q_z}{I_{zz} t} - \frac{S_z Q_y}{I_{yy} t} + \frac{TR}{J} \tag{6.21}$$

Since multiple loads and stresses work on the fuselage simultaneously, they have to be combined using Mohr's circle. The maximum in plane shear stress and principle stresses can then be found through Equation 6.22 and Equation 6.23. These design stresses should be less than the shear and yield strength of the material, for the structure not to fail.

$$\tau_{max} = \sqrt{\left(\frac{\sigma_x - \sigma_y}{2}\right)^2 + \tau^2} \tag{6.22}$$

$$\sigma_{1,2} = \frac{\sigma_x + \sigma_y}{2} \pm \tau_{max} \tag{6.23}$$

6.7.3. Buckling Analysis

The fuselage will also need to be checked for possible buckling. This is done after performing the bending and shear analysis in order to limit the amount of variables to design for.

The buckling will thus be considered with the skin thickness chosen in Subsection 6.7.2. This skin thickness will be used along with the spacing of the longitudinal stringers in order to find the crippling load of the panels using Equation 6.24. Here, the constant C represents the support type of the panel, which is found from Figure 6.9 knowing that the panels are simply clamped on all sides. α and n are correction factors equal to 0.8 and 0.6.

$$\sigma_{cr} = C\frac{\pi^2 E}{12(1-\nu^2)}\left(\frac{t}{b}\right)^2 \tag{6.24}$$

For the stringers it was chosen to use a simple hat stringer design for its high buckling resistance and wide design range. The stringer design can be seen in Figure 6.10, whose dimensions will be further analysed in the buckling analysis. The stringer will consist of aluminium alloy 7075 for its high strength, resistance to fatigue, toughness and good ductility. Its properties can be found in Table 6.6. Using this stringer design it is possible to find the crippling strength of the stringer using Equation 6.25 and Equation 6.26.

$$\frac{\sigma_{cc}^{(i)}}{\sigma_y} == \alpha\left[\frac{C}{\sigma_y}\frac{\pi^2 E}{12(1-\nu^2)}\left(\frac{t}{b}\right)^2\right]^{1-n} \tag{6.25}$$

$$\sigma_{cc} = \frac{\sum \sigma_{cc}^{(i)} A_i}{\sum A_i} \tag{6.26}$$

After finding the crippling strengths for both the plate and the stringers it is possible to calculate the crippling strength of the complete panel. This can be done using Equation 6.27 where the buckling strengths of both the panel and stringer are combined in accordance with their areas.

$$\sigma_{cc_{\text{panel}}} = \frac{\sum \sigma A_i}{\sum A_i} \tag{6.27}$$

It was found that the buckling strength of the panel is 2.61 $[GPa]$. This indicates that the buckling is not a critical factor which should be designed for as the panel will start yielding before it reaches the buckling load.

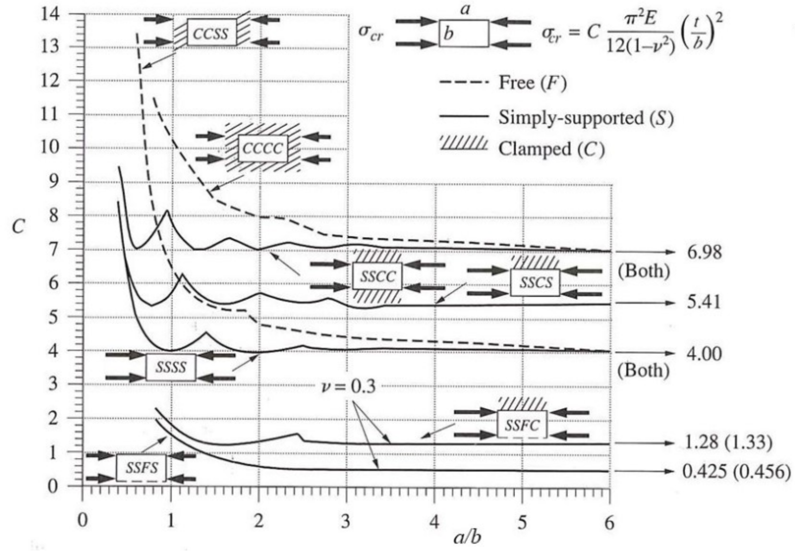

Figure 6.9: *Coefficient C versus aspect ratio for several different boundary conditions. Only the bottommost curves depend on Poisson's ratio, and their asymptotes for ν = 0.25 are shown in parentheses [34]*

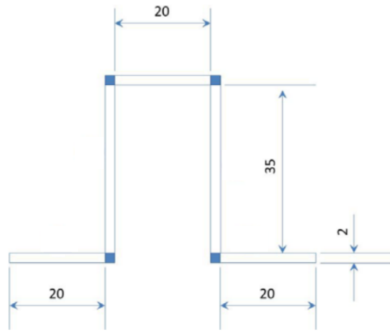

Figure 6.10: *Dimensions and layout of the hat stringer*

6.7.4. Final Fuselage Structure

A multiple section fuselage was designed after analyzing the fuselage for all loads present. This fuselage consists of 3 different sections: heavy, medium and light. In this configuration the heavy section will be the strongest and have a skin thickness of 7 $[mm]$, the light section will be the weakest and have a skin thickness of 3 $[mm]$. The final medium section will be an in-between option for the other two sections having a skin thickness of 5 $[mm]$. The distribution of these 3 fuselage sections can be seen in Figure 6.11 by cross-checking with the skin thicknesses of the different sections.

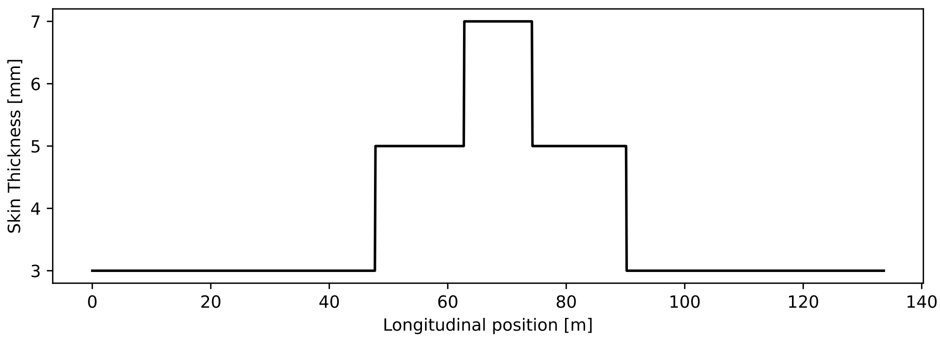

Figure 6.11: *Fuselage skin thickness against the longitudinal position in the fuselage*

6.8. Static Loading Wing

Similarly to the calculations for the static loading of the fuselage, the wing box thickness and stringer specifics are calculated in this section by analysing the internal loads.

6.8.1. Loading

Knowing the loads which shall be acting on a wingbox is essential to designing it. For this purpose a wing loading diagram can be made containing both the shear and bending moments which shall be carried by the wingbox in the span-wise direction. This is shown in Figure 6.12. In this section only shear forces parallel to the lift force are considered. The distribution were generated by analysing the aerodynamic loading on the wing in cruise conditions utilising AVL.

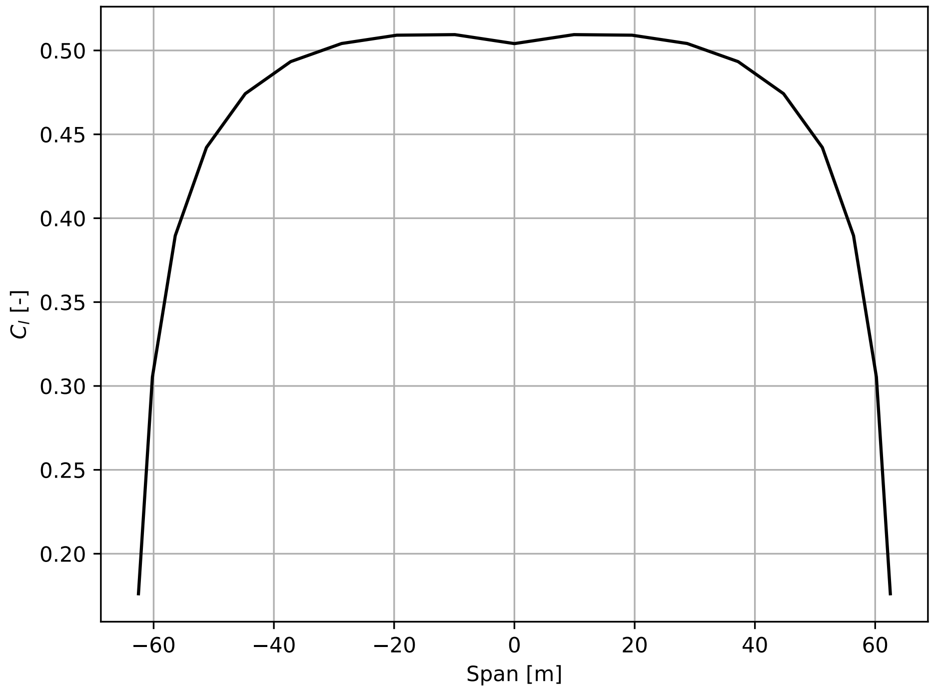

Figure 6.12: *Lift distribution over the wing*

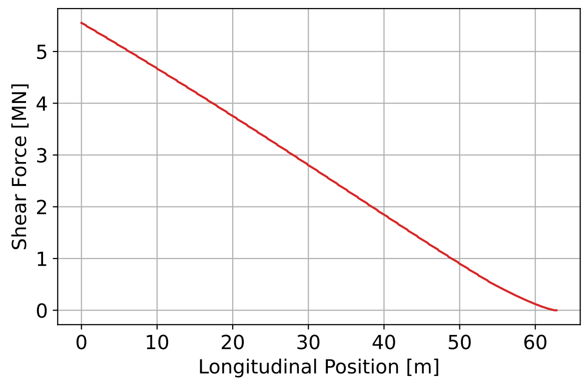

(a) *Wing shear force diagram*

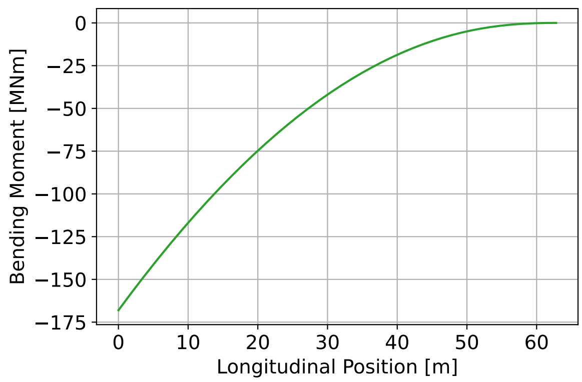

(b) *Wing bending moment diagram*

Figure 6.13: *Shear and moment diagrams for the wing*

6.8.2. Wing Box Design

The wing box is made of Aluminium 7075 which has a yield strength of 503 $[MPa]$ and a shear strength of 331 $[MPa]$ both with a safety margin of 1.5. The wing box front spar is located at 15% of the chord and the aft spar is located at 65% of the chord. These locations are chosen so that spars do not interfere with the HLD's or ailerons. The height of the wing box is equal to the thickness of the airfoil at 15% of the chord, which is 8.76% of the chord. An analysis is done for the shear stress and the bending moment acting on the wing, for which it is assumed that the wing box carries all the loads. The sign convention used for the wing box can be found in Figure 6.15[35]. The stringer design chosen to be used in the wing box of the Emperor is a U-stringer, the main reason being the simplicity of the stringer and the relative larger area when compared to an L-stringer. As a result of the analysis of the loads on the wing box, it is concluded that the stringers need to have an area of 0.012 $[m^2]$. The stringer in Figure 6.14 is designed for this area.

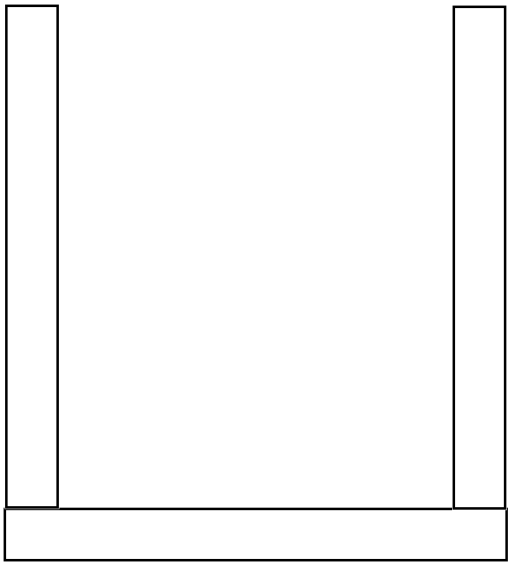

Figure 6.14: *Shape of the stringer, the boxes have a length of 200 $[mm]$ an a thickness of 20 $[mm]$*

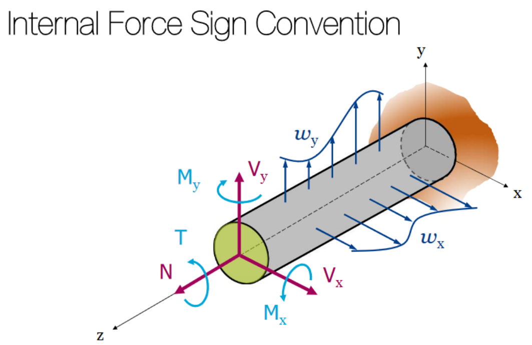

Figure 6.15: *Sign convention used in designing the wing box*

The shear in a thin walled section such as a wing box can be calculated using Equation 6.28[35]. To simplify Equation 6.28, multiple assumptions are made. Firstly, it is assumed that the wing box is symmetric, causing I_{xy} to be 0 and making the shear center coincide with the centroid of the wing box. Secondly, the loading due to drag is neglected so $V_x = 0$, as it is small compared to the lift loading. Thirdly, the thickness of the wing box is assumed to be non-varying for simplicity. Finally, the lift and weight are assumed to act in the centroid and therefore in the shear centre, which results in $q_{s0} = 0$. This is a big assumption, because the torsion induced in the wing box due to the lift actually acting in the centre of pressure is completely neglected. An additional safety factor of 20 % is thus included to take care of the additional shear due to torsion. Applying these assumptions together with $\tau = \frac{q}{t}$ gives Equation 6.29.

$$q_s = q_b + q_{s0} = -\frac{V_y I_{yy} - V_x I_{xy}}{I_{xx} I_{yy} - I_{xy}^2} \int_0^s tyds - \frac{V_x I_{xx} - V_y I_{xy}}{I_{xx} I_{yy} - I_{xy}^2} \int_0^s txds + q_{s0} \tag{6.28}$$

$$\tau = -\frac{V_y}{I_{xx}} \int_0^s yds \tag{6.29}$$

Using the loading diagram from Subsection 6.8.1 and the outer geometry of the wing box, I_{xx} can be determined for every location on the span. In order to meet this I_{xx} some stringers needed to be added this can be found in Figure 6.16.

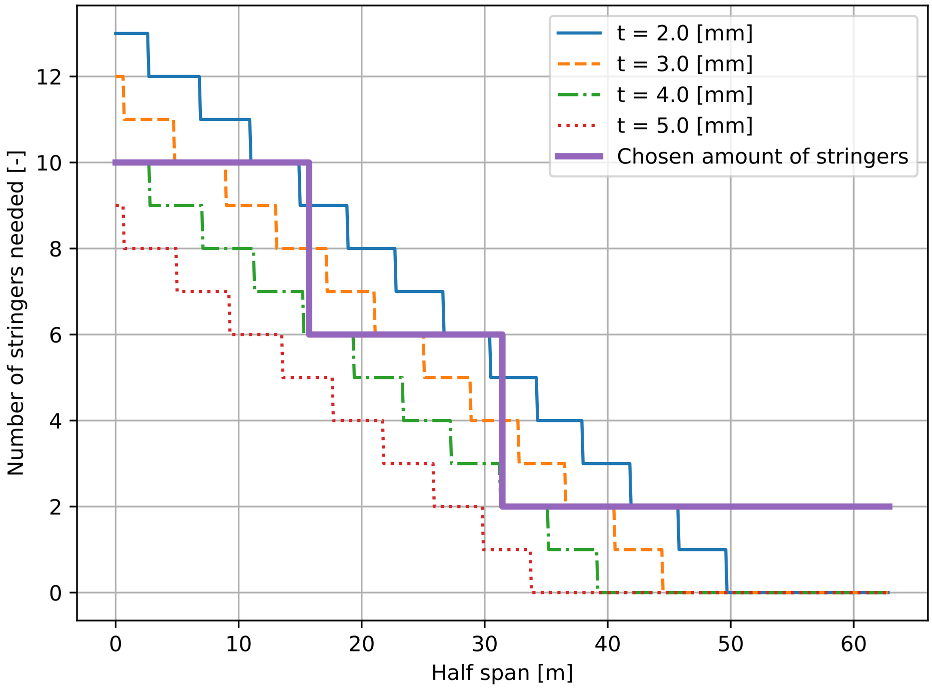

Figure 6.16: *Number of stringers needed due to shear loading. t is an abbreviation for the thickness of the wing box.*

To determine the total number of stringers the required number is incremented by one, which is assumed to introduce a sufficient safety margin, and is rounded up to the an even number such that the wing box is symmetric. The thickness of the wing box is chosen to be 5 $[mm]$, mostly due to the normal loading following from the bending moment acting on the wing. Furthermore, the wing box is split in 4 sections of equal length for which the most critical case is chosen. This causes the final design to have 10, 6, 2 and 2 stringers in the different sections of the wing box stated from root to tip, as can be seen in Table 6.7. The stringers are evenly divided between the top and bottom and placed equidistantly.

In order to calculate the stress due to bending moment a standard analytical structural analysis method is used [35]. Using the same assumptions as when calculating the shear, and in addition the assumption that there is no bending moment around the y-axis ($M_y = 0$), Equation 6.30 can be rewritten to Equation 6.31. Now the I_{xx} needed to withstand the bending moment can be determined and can be linked to an amount of stringers needed, the amount of stringers needed can be found in Figure 6.17, where the chosen amount is again incremented by one for safety and rounded up to the nearest even integer. This leads to four spanwise wing box sections with 50, 28, 8 and 2 stringers per section from root to tip as can be seen in Table 6.7. In Table 6.7 also the total moment of inertia is stated for the four different wing box sections.

$$\sigma_z = \frac{\left(M_x I_{yy} - M_y I_{xy}\right) y + \left(M_y I_{xx} - M_x I_{xy}\right) x}{I_{xx} I_{yy} - I_{xy}^2} \tag{6.30}$$

$$\sigma_z = \frac{M_x y}{I_{xx}} \tag{6.31}$$

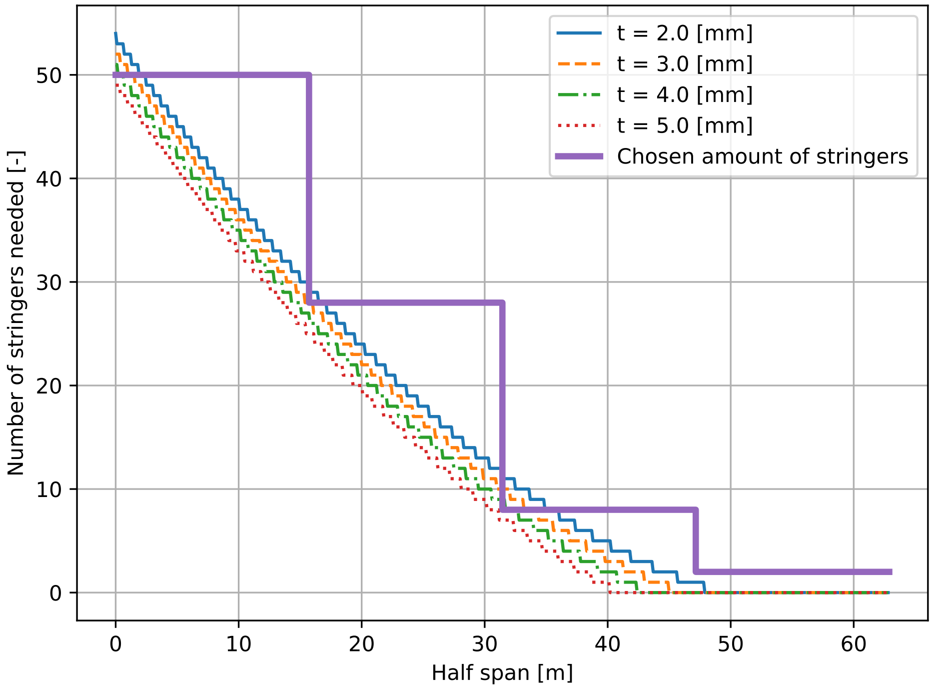

Figure 6.17: *Number of stringers needed due to bending moment*

To make sure the wing box can withstand these loads simultaneously, the number of stringers for both load cases are added together. The final result can be seen in Table 6.7, where the distance 0 $[m]$ is at the root and 62.89 $[m]$ is at the tip of the wing. The stringers are evenly divided over the top and bottom and are first placed in the corners of the wing box, after which they are located equidistant to each other. The wing box design can be optimized further by performing the following analyses: Mohr's circle to optimize the combination of the two types of loading, torsion due to the lift can be taken into account to get a more accurate estimate of the shear so that the contingency can be discarded, a buckling analysis should be included to get to the most critical failure mode. In the case considered the Emperor is at cruise at the maximum load factor. However it might be that landing is the most critical case, this should be further investigated in the next iteration of the design process. Finally, the division of the wing box in four spanwise sections should be investigated more, which can be done by means of an investigation of the ribs.

Table 6.7: *Amount of stringers due to different types of loading, the total amount of stringers chosen and the total moment of inertia for the different wing box sections along the wing span.*

	0 to 15.72 $[m]$	**15.72 to 31.44 $[m]$**	**31.44 to 47.16 $[m]$**	**47.16 to 62.89 $[m]$**
Shear	10	6	2	2
Normal	50	28	8	2
Total	60	34	10	4
Total I_{xx} $[m^4]$	0.4479	0.2536	0.0964	0.0559

6.9. Stability and Control Characteristics

This section deals with the sizing of the vertical and horizontal tail for the Emperor and its stability and controllability in the water and air. To size the empennage and determine the stability the cg position is determined in Subsection 6.9.1. In the sizing of the horizontal tail, the air longitudinal stability is considered as a determining factor, and the size of the horizontal tail and position of the main wing are chosen such that longitudinal stability is achieved. This is explained in Subsection 6.9.2. All coordinates shall be used with respect to the global coordinate system given in Figure 5.8 where the yz-plane coincides with the nose of the aircraft.

For detailed sizing of the vertical tail, lateral stability should be considered. However, due to the complexities of obtaining the required coefficients, this was deemed out of the scope at this stage of the project and it should be considered in further iterations of the design, as explained in Subsection 6.9.3. For now, the vertical tail is sized using a preliminary approach where a vertical tail volume coefficient is selected based on similar aircraft at 0.07. The method used for tail sizing is presented in Subsection 6.9.4 where the final tail dimensions can be found. After determining the tail size, the mobile surfaces on the wing which provide the needed controllability, are described in Subsection 6.9.5. Now the Emperor is designed to be stable and controllable in air, the stability and controllability in the water is investigated, this is done in Subsection 6.9.6.

6.9.1. Loading Diagram

In order to estimate the stability and controllability characteristics of the Emperor, the variations in cg position need to be determined. This is done by making a loading diagram, which gives the most forward and most aft cg positions. This is done by first estimating the cg position of the OEM using the cg location and mass of all components and Equation 6.32. These values can be found in Table 6.8. Secondly the shifting in cg position is calculated by loading the cargo. After the cargo the passengers are loaded. This is done by first loading the four window rows and continue loading four seats at the time from front to back and from back to front. this results in the ”potatoes” in Figure 6.18. Finally, the hydrogen is loaded in the three fuel containers, those can be loaded in the order of first the forward fuel container and then the aft fuel container or reversed, but here a proportional loading of the fuel containers was considered. The variations in cg position are calculated using Equation 6.32 and are displayed in Figure 6.18. From Figure 6.18 the cg range of the Emperor can be seen to range from 35% to 74% of the mean aerodynamic chord (MAC) of the wing. A safety margin of 2% of the MAC is included, to account for uncertainties and non-ideal loading [36]. This cg range is optimised by positioning the wing ensuring the minimal structural mass of the aircraft while maintaining stability and controlability. This gives a position of the wing at 56.5 [m] from the tip of the nose.

$$x_{cg_{OEM}} = \frac{\sum_i x_{cg_i} m_i}{\sum_i m_i} \tag{6.32}$$

Table 6.8: *cg locations and masses of different elements*

Elements	Xcg $[m]$	Mass $[tons]$
Wing	62.8	136.24
HT	125.4	38.15
VT	124.26	13.23
Motors	64.38	99.1
Fuselage	66.8	157.49
Forward Fuel Container	35.46	18.32
Mid Fuel Container	80.8	6.37
Aft Fuel Container	94.65	4.71
Fuel Cells	66.58	100.69
Miscellaneous	60.57	141.9
OEM	61.36	7.52

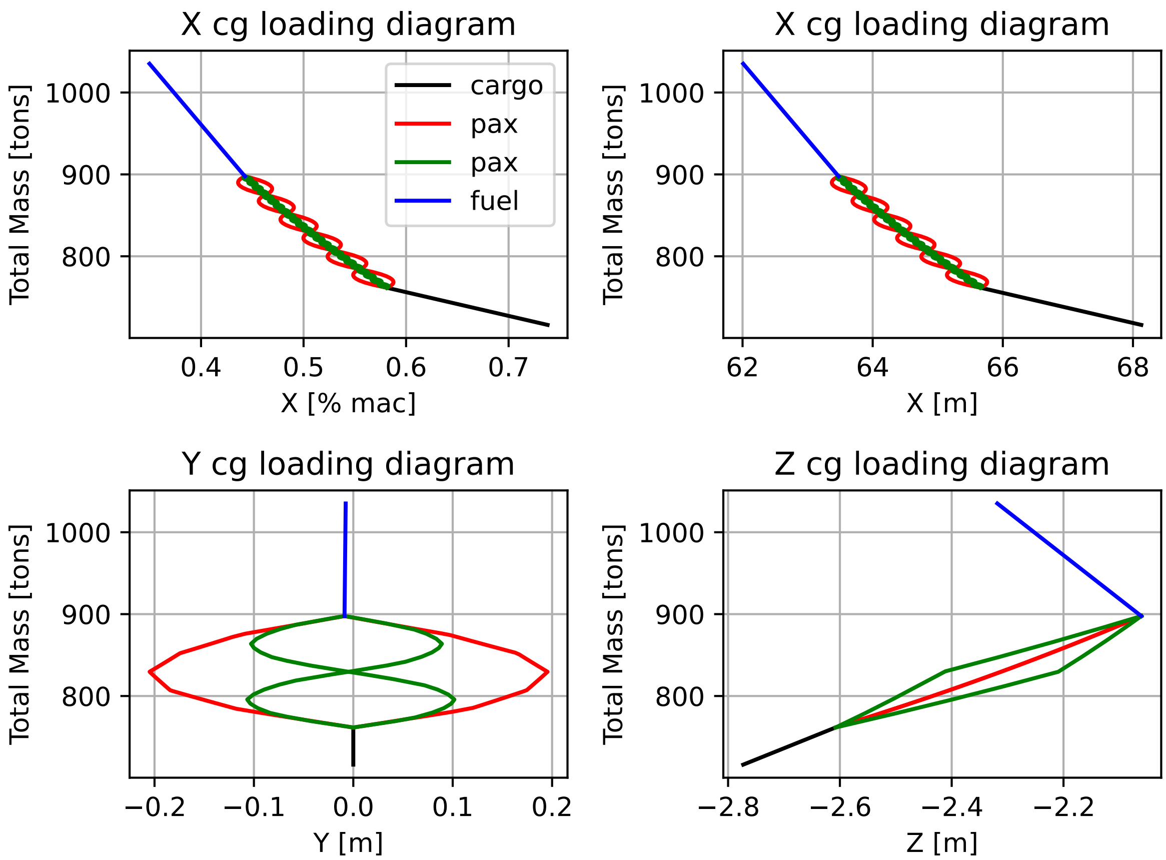

Figure 6.18: *Loading Diagram*

6.9.2. Longitudinal Stability

In order to fly an aircraft it needs to be both controllable and stable. For an aircraft to be controllable, it needs to be able to fly at the cruise angle of attack without experiencing a pitching moment. This requires the horizontal tail to provide sufficient lift. The lift required for the tail can be calculated using Equation 6.33.

$$M_{cg} = L_w(X_{cg} - X_{\text{acw}}) + M_{\alpha_w}\alpha + M_{\alpha_{\text{fus}}}\alpha - L_h(X_{\text{ach}} - X_{cg}) + Tz_T \tag{6.33}$$

By calculating this for different angles of attack that the Emperor would want to fly in, the controllability of the Emperor can be verified.

The stability is the behaviour of the aircraft due to a small change in the angle of attack. The desired behaviour is for the Emperor to returned to the trimmed angle of attack on its own, viz. oppose the change in the angle of attack. In order to achieve this the center of gravity of the aircraft should lie in front of the neutral point, and therefore C_{m_α} should be negative. In practice this means that when the aircraft pitches up its moment becomes negative, resulting in a pitch down moment and vice versa when pitching down. The C_{m_α} can be calculated using Equation 6.34 below. It should be noted that stability was only ensured for the cg range obtained from proportional depletion of the fuel from all fuel tanks. The whole cg range including the variations due to passenger and cargo loading was not considered, as in an under-loaded scenario, the payload may be placed more forward.

$$C_{m_\alpha} = C_{L_\alpha}\left(\frac{X_{cg} - X_{\mathrm{ac}_w}}{MAC}\right) + C_{m_{\alpha_{\mathrm{fus}}}} - \eta_h \frac{S_h}{S_w} C_{L_{\alpha_h}} \frac{\partial \alpha_h}{\partial \alpha}\left(\frac{X_{\mathrm{ac}_h} - X_{cg}}{MAC}\right) \tag{6.34}$$

Where $\frac{S_h}{S_w}$ is the ratio of horizontal stabilizer to the main wing surface area, η_h is the effectiveness of the horizontal tail, and $\frac{\partial \alpha_h}{\partial \alpha}$ is the ratio of change of wing angle of attack to tail angle of attack due to downwash effects.

Equation 6.33 and Equation 6.34 can be rewritten as Equation 6.35 and Equation 6.36, which represent the controllability and stability curve respectively. This allows these lines to be plotted in a scissor plot as seen in Figure 6.19. In the scissor plot the c.g. location is related to the relative surface area of the tail against the reference area. This is helpful to size the horizontal tail more precisely than what was done before. For the Emperor however, the optimal value from the scissor plot did not prove to be the most optimal solution. Nevertheless the final result was within a reasonable range in the scissor plot, resulting in a final S_h/S of 37%.

$$\bar{x}_{cg} = \bar{x}_{ac} - \frac{C_{m_{ac}}}{C_{L_{A-h}}} + \frac{C_{L_h}}{C_{L_{A-h}}} \frac{S_h l_h}{S\bar{c}} \left(\frac{V_h}{V}\right)^2 \tag{6.35}$$

$$\bar{x}_{cg} = \bar{x}_{ac} + \frac{C_{L\alpha_h}}{C_{L\alpha_{A-h}}} \left(1 - \frac{d\varepsilon}{d\alpha}\right) \frac{S_h l_h}{S\bar{c}} \left(\frac{V_h}{V}\right)^2 - S.M. \tag{6.36}$$

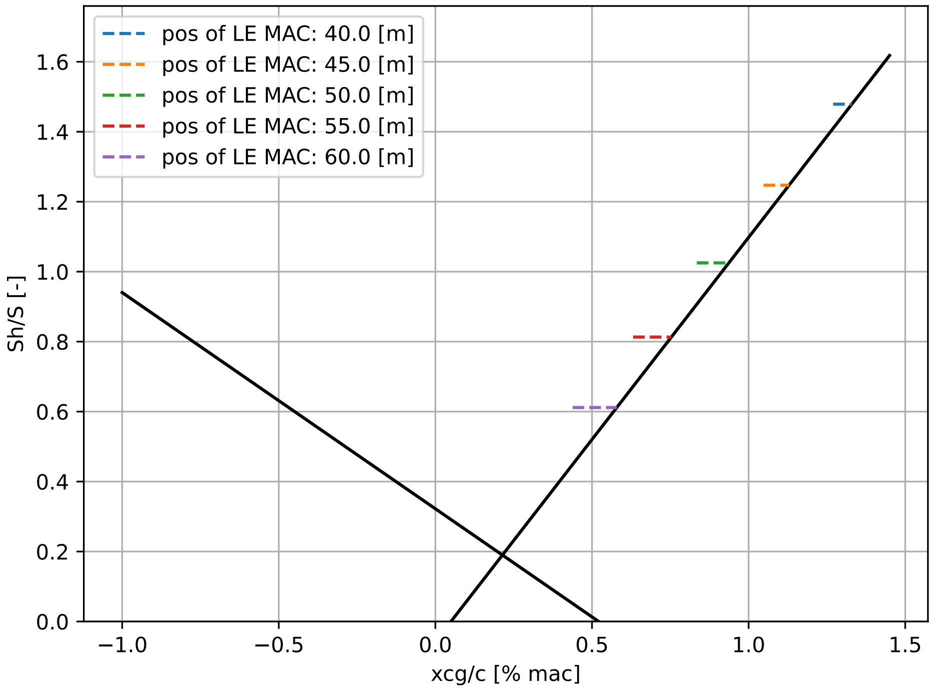

Figure 6.19: *Scissor plot*

Using the tail ratio and the cg range (Subsection 6.9.1) Equation 6.33 and Equation 6.34 can be filled in and C_{m_α} can be found. Additionally the required lift of the horizontal tail the angle at which it should be fitted for minimal drag in cruise can be calculated. Using the C_{m_α} the neutral point can be found with Equation 6.37.

$$X_{np} = -\frac{C_{m_\alpha}}{C_{L_\alpha}} + X_{cg} \tag{6.37}$$

From Equation 6.37 it can be seen that as long as C_{m_α} is negative the neutral point will lie behind the center of gravity, thus satisfying the stability requirements. The final value of C_{m_α} is -0.069, measured per degree of α, and the neutral point is located 0.2 $[m]$ behind the most aft c.g.

6.9.3. Lateral Stability

As mentioned in the introduction of this section, the lateral stability has not yet been considered in detail, and its exploration is left for further iterations of the design process. This decision was made because for the analysis of lateral stability a variety of aerodynamic coefficients must be estimated, for which no simple analytical solution exists. Hence either wind tunnel testing or CFD methods are required to accurately estimated them, both of which lie outside of the scope of the current design. For that future iteration, the factor that would be considered to influence the lateral stability is the size of the vertical tailplane. This vertical tail will be sized in correspondence with four requirements: crosswinds on landing, directional stability, control after engine failure and spin. Of these, control after engine failure is expected to be determining for the case of the Emperor, since the big size of the fuselage causes natural yaw damping which improves the directional stability.

6.9.4. Tail Sizing

The method used for tail sizing is based on the one presented by Snorri Gudmundsson [8]. The method consists of determining the tail length, meaning the distance from the quarter MAC point of the wing to the quarter MAC point of the tail. Using that, the area S, span b and average chord c_{avg} can be determined as seen in Equation 6.38, Equation 6.39, and Equation 6.40 respectively. These dimensions are calculated for tailplanes which have the airfoil NACA 0010 as a basis.

$$S = \frac{S_{\text{REF}} C_{\text{REF}} \text{Volume Coefficient}}{l} \tag{6.38}$$

$$b = \sqrt{ARS} \tag{6.39}$$

$$c_{\text{avg}} = \frac{b}{AR} \tag{6.40}$$

In these equations, 'REF' refers to the fact that it is the area and mean aerodynamic chord of a reference which is the main wing. The volume coefficient is an empirical relation that can be chosen from existing aircraft and tweaked to optimize longitudinal stability for the horizontal tail.

The tail length for both tails was determined by locating the end of the root chord of the tails at the end of the tailcone. This position is a value that, together with the volume of the horizontal tail and the position of the wing, will be optimized in order to achieve longitudinal stability. The tail length is modified by tweaking the dimensions of the tailcone. The volume coefficient for the vertical tail is chosen from past data to equal 0.07 [8]. The final dimensions for the tails are presented in Table 6.9 and Table 6.10.

To acquire yaw and pitch control, an initial sizing was carried out for the rudder, elevators and trim tabs using historical data. For the vertical tail, the rudder chord has been sized to equal $0.3 * MAC_V$ to have optimal control over the lateral stability [8]. The elevator surface over horizontal tail surface ratio is chosen to be 0.48 [37]. Moreover, the vertical tail has a dorsal fin which adds directional stability and prevents rudder-lock [8].

Table 6.9: *Sizing of vertical tailplane*

Symbol	Value	Unit
S_V	302.34	m^2
MAC_V	15.57	m
b_V	21.29	m
λ_V	0.3	-
Λ_{LE_V}	0.5	rad
AR_V	1.5	-
c_{rudder}	4.671	m

Table 6.10: *Sizing of horizontal tailplane*

Symbol	Value	Unit
S_H	745	m^2
b_H	54.6	m
λ_H	0.9	-
Λ_{LE_H}	0.04	rad
AR_H	4	-
c_{root_H}	14.4	m

6.9.5. Mobile Surfaces on the Wing

To ensure adequate controllability and lift generation, HLD are needed. Multiple leading and trailing edge HLD were compared and the design decision was made to implement the hinged leading edge (droop nose) and single-slotted flap shown in Figure 6.22. The hinged leading edge is a mechanically simple device with negligible impact on drag [8]. The hinged leading edge increases the $\Delta C_{l_{\max}}$ with 0.56, and $\Delta\alpha_{\max}$ with 7°-8°. [8]

The single-slotted flap combines the motions of rotation and translation which increases the airfoil chord length with 5-10%. It is able to deflect 40 ° and increases the $\Delta C_{l_{\max}}$ with 1.45. It is important to note that, as explained in Section 6.3, the fans are currently located on the top surface of the wing right before the flapped area. This means that the exhaust of the fans, which is at a higher velocity that the flow around, goes over the flaps, meaning that in reality the flaps are more effective than what it has just been presented. This would entail that for the same flap area considered now the increase in $C_{l_{\max}}$ is larger, which allows the possibility of reducing the take-off speed. However, this has not yet been considered for this stage of the design so further exploration of this effect is recommended for future stages.

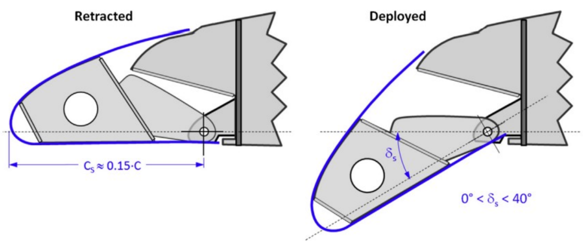

Figure 6.20: *Hinged leading edge (droop nose)*

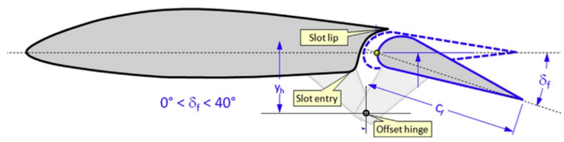

Figure 6.21: *Single-Slotted flap*

Figure 6.22: *HLD [8]*

Furthermore, in order to allow roll control of the aircraft, the wing is also equipped with ailerons. The chosen type of ailerons are plain flap ailerons, since they are very effective and inexpensive to manufacture [8]. For a cargo or Heavy-Lift aircraft like the Emperor, the required helix angle made by the wing at a certain speed, namely $\frac{pb}{2V}$, is typically larger than 0.07 [8]. It was determined that ailerons, which take 30 % of the chord length, span from a distance of 53.39 $[m]$ to a distance of 61.89 $[m]$ from the central longitudinal axis of the aircraft in each wing resulting in a length of 8.5 $[m]$ per wing. The maximum deflection of the ailerons is 20 ° both up and down. This results in an theoretical instantaneous roll rate of 12 $[rad/s]$, which by far exceeds the helix angle requirement and therefore also the roll control requirement. Furthermore, the wing will also be equipped with spoilers. However, their sizing is deemed out of the scope of this stage of the process.

6.9.6. Water Stability and Controllability

The Emperor takes-off and lands on water. In order to ensure these operations are possible, the Emperor must be stable when docking at port and also when moving through water.

In order to assess the stability while docking, the static stability of the Emperor on still water will be assessed. A boat is considered to be in static equilibrium when it returns to its original position after experiencing a slight inclination with respect to its rest condition [38]. This inclination can happen both around the longitudinal and transverse axes, generating the need to investigate stability around both axes. The stability of a boat is determined by the relative position of the metacenter (M) and the center of gravity (CG) of the boat, also known as the metacentric height (h). If M is above CG the configuration is stable, if they coincide, the equilibrium is indifferent and if M is below CG it is unstable [38].

For the case of the Emperor, to find the location of the transverse and longitudinal metacen-

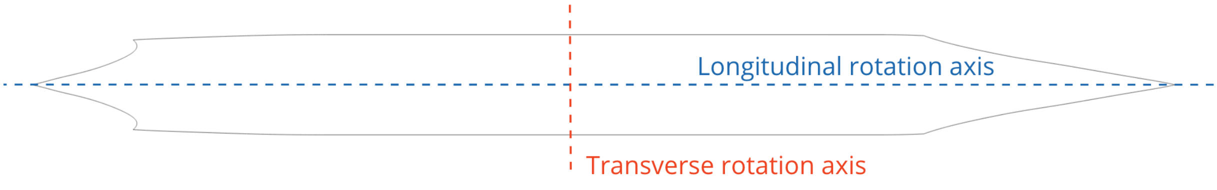

Figure 6.24: *Top view showing the axes of rotation on the wetted surface considered for the longitudinal and lateral stability moment of area calculation*

ters, the least stable loading scenarios should be considered. This occurs when the center of gravity is located as high as possible. In terms of the longitudinal position of the CG, the most critical positions that will be considered are the most aft and forward locations which occur during the loading of the passengers, cargo and fuel. Therefore, two different scenarios will be used to assess the stability of the Emperor, evaluating transversal and longitudinal stability for both.

For every option, the same method to find the location of the metacenter will be followed. The aforementioned metacentric height (h) can be found by taking the difference between the metacentric radius (r), namely the distance between metacenter and center of buoyancy (B), and the distance between the B and the center of gravity (G), referred to as 'a', as shown in Figure 6.23, where WL represents the waterline. It should be noted however that this figure is used to illustrate the aforementioned distances and points, and it does not reflect the Emperor itself.

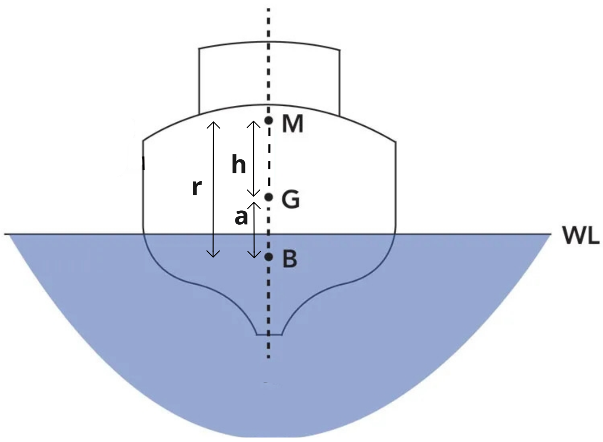

Figure 6.23

$$r = \frac{I(\text{AWP})}{\nabla} \tag{6.41}$$

The metacentric radius is calculated using Equation 6.41. I(AWP) is the second moment of inertia of the wetted surface, and is done around the transverse or longitudinal axis for transversal and longitudinal stability, respectively. These directions are visualized in Figure 6.24.

The second moment of inertia is calculated using an estimation of the hull shape. The immersed hull volume is represented by ∇ [38], which is computed using Archimedes' principle. At maximum take-off weight, and using sea water density of 1027 $[kg/m^3]$ [39], the immersed hull volume is determined to be 1139 $[m^3]$. The distance 'a' can be calculated by finding the position of the center of buoyancy by retrieving the geometric centroid of the submerged part of the planar section where the CG is located. The centroids were computed with the assistance of the Emperor's model in 3D Experience. Several other loading cases should be considered, but this consideration is left for the next iteration of the design process.

By subtracting 'a' from 'r', the metacentric height is determined. If this result is larger than zero, the Emperor is stable at that condition. For the transverse rotation, it was found that the metacentric height is a large positive number, thus transverse stability is ensured. For longitudinal rotation, the metacentric height is calculated to be a negative number, thus longitudinal stability is not ensured when considering the highest cg position. To ensure longitudinal stability, floats shall be added to the wings, a means commonly used to assure stability in flying boats such as the Hughes H-4 Hercules[11]. The decision behind putting the floats on the wings is that a larger distance from the fuselage allows a smaller float size.

Longitudinal instability affects the capability of the Emperor to generate a righting moment that counteracts the disturbances experienced. When disturbed longitudinally the response is an increase of this disturbance, which is equivalent to the generation of a negative righting moment around the longitudinal axis. The floats must be sized such that they generate a positive counteracting righting moment to compensate the negative one created by the hull. The righting moment is calculated using [38].

$$R_{\mathrm{M}} = MTOW(r-a)sin\theta \tag{6.42}$$

Here θ is the angle of heel required to completely submerge a lateral float [17], which is chosen to be 7 $[\deg]$ [40]. The result is that the wing floats required should provide a righting moment of 552,717 $[kgm]$ per float.

Two floats are placed along the wingspan, one on each side of the fuselage, approximately mid-wing at 40 $[m]$. To obtain the buoyancy, the righting moment is divided by this length of 40 $[m]$. From the buoyancy, the volume of the floats is acquired by dividing it through the density of seawater. A contingency of 1.2 is applied to ensure the floats will be able to provide sufficient buoyancy to manage disturbances. The volume of the floats is estimated to be 16.1 $[m^3]$. A first estimation of the dimensions could be approximately 8 $[m]$ length, 2 $[m]$ width, and 1 $[m]$ height, from which it can be seen that the floats fit comfortably under the wing when deployed. The shape of the floats will be aerodynamic and hydrodynamic, to avoid an excessive amount of additional drag. After take-off, the wing floats will be retracted into the wings. However, further analysis is required to determine the exact dimensions, shape and retracting mechanism of the floats.

For the taxiing phase, the optimal speed would be relatively fast, without creating excessive drag and loss of stability. This speed is determined to be the hull speed. The hull speed is the speed at which the wave speed and boat speed are identical, thus causing the wavelength and boat length to be approximately equal. At this speed, the bow-wave cycle and stern-wave cycle have merged. The hull speed for sufficiently deep waters can be calculated using Equation 6.43[12], where L is the load waterline length. The load waterline length is the hull's horizontal length at the surface of the water, determined to be 102.8 $[m]$ by making use of the Emperor's model in 3D Experience. The hull speed is then evaluated to be 12.7 $[m/s]$.

$$V_{hull} = \sqrt{\frac{gL}{2\pi}} \tag{6.43}$$

When increasing the speed further than the hull speed, the wavelength becomes even larger, which pushes the stern-wave further aft. This causes a large trough of the bow-wave at the

[11] https://simpleflying.com/h-4-hercules-flying-boat/, accessed on 10/06/2022

[12] https://www.dmsonline.us/the-truth-of-hull-speed-how-to-break-the-sailing-speed-limit/, accessed on 10/06/2022

back of the hull, leaving the Emperor to climb the crest on its own bow-wave[13]. This excessively increases the power needed to increase the speed, thus taxiing is decided to be performed at the hull speed.

To ensure stability over the entire range of sea-based operations, thus including taxiing, take-off and landing, further analysis is needed in a more detailed design phase. However, stability systems are able to assist in assuring stability. A variety of stability systems are available, of which fin stabilizers, a rudder and floats are deemed suitable options for the Emperor. Even though floats on the wings are already used to ensure static stability, it might be possible that additional stability systems are necessary to assure stability through all sea-based operations.

Fin stabilizers operate in a similar manner as ailerons in aircraft, and they can be used to remain stable by opposing any rolling motion of the boat[14]. These fin stabilizers are commonly retractable and powered by electrical power units. A boat rudder is used to be able to turn the Emperor in the water[15], which operates in similar fashion as the rudder for aircraft. However, it should be noted that it might be sufficient to steer in the water by using the vertical tail and a thrust differential to create a turning moment. This thrust differential can be obtained by turning off a number of fans on one side to create a turning moment. The functions of the fin stabilizers and rudder are combined in the Rudder Roll Stabilisation System. This system consists of a rudder which through a control algorithm is able to both change heading and reduce roll motion [41]. This is used for steering, while assuring stability. This system is expected to have more optimal performance as it combines the other two means, meanwhile remaining more economically attractive [41]. Lastly, a different way of ensuring stability would be the use of a device known as a sponson, which is a flange used to increase the beam of the hull, improving stability and providing additional lift when taking off. Whether these stability systems are required to assure stability in water, and what the most efficient means is must be established during further analysis of these sea-based operations. For the design of the Emperor, the possible need for stability systems is taken into account as an extra mass with the value of 5% of the fuselage mass.

6.10. Internal System Characteristics

The Emperor requires a series of systems that ensure its proper functioning, from taking the fuel from the tanks to the fuel cells, to providing passenger comfort. This section tackles the layout of the fuel system in Subsection 6.10.1. Subsection 6.10.2 presents the chosen type of actuators and their location in the aircraft. Then, a brief explanation on the auxiliary power estimate is presented in Subsection 6.10.3. Finally, the environmental control is described in Subsection 6.10.4.

6.10.1. Fuel System Layout

As detailed in Section 6.5, the fuel used is cryogenic liquid hydrogen, which will be stored in insulated tanks. This section will focus on the distribution of the fuel and its transportation to the power unit, where it will be used to generate the electricity required by all the subsystems of the aircraft.

The hydrogen must be taken from the interior of the tanks, where it is mainly in liquid state and

[13] https://www.boats.com/reviews/crunching-numbers-hull-speed-boat-length/, accessed on 10/06/2022

[14] https://www.imtra.com/learning-center/articleid/48/fins-vs-gyros-boat-stabilizers, accessed on 10/06/2022

[15] https://www.marineinsight.com/naval-architecture/rudder-ship-turning/, accessed on 10/06/2022

partly in gaseous state due to the boil-off. This hydrogen is transported in gaseous state to the fuel cell, at a regulated pressure. The fuel cell also receives the air from an intake, which contains the O_2 required for the chemical reaction inside. More detail into the power generation process can be found in Section 9.2.

The fuel will be pumped though different pipelines in a gaseous state, since the cryogenic temperatures can't be assured in the pipelines which causes the hydrogen to heat up. The layout of this fuel and power system is visualized in Figure 6.25. As seen in this diagram there are three main tanks where the fuel is stored in liquid state. It should be noted that while in the figure they are box shaped, in reality the tanks would have hemispherical end caps. The tanks are refueled through a series of holes along the fuselage directly from an external pump. More detail in refueling can be found in Section 10.4. The hydrogen is pumped directly to the fuel cells, where it reacts with the oxygen to become two new products: water vapour and electricity, finishing here the flow of hydrogen through the aircraft.

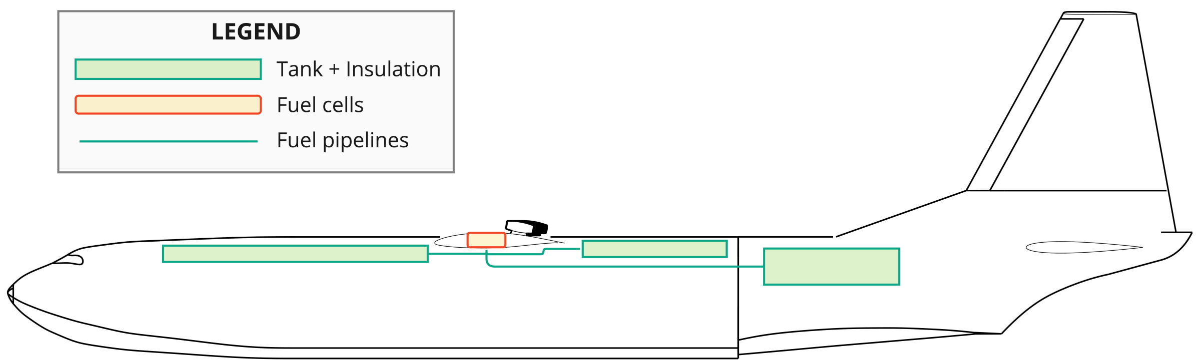

Figure 6.25: *Fuel system layout*

6.10.2. Actuators for Moving Surfaces

In order to control the moving surfaces of the Emperor it was decided to use Electro-Mechanical Actuators (EMA). This decision was made based on the fact that the Emperor already generates electricity for all the systems and therefore the implementation of electric actuators requires less additional material and volume compared to using hydraulic actuators, which would require a reservoir and pumps, in addition to other components, for the hydraulic fluid. The electric actuator system would be made up of just the actuator itself, an electric motor with required converters and gearbox for rotary EMAs, and a small control cabinet located at the point of use [42].

Furthermore, despite requiring a larger initial investment and higher installations costs, electric actuators require lower maintenance, just re-greasing for demanding performance applications, to remain accurate and consistent versus the high maintenance demanded by hydraulic systems [43]. Leaks from hydraulic systems are a hazard for the environment and are completely avoided by the use of an electric system. Moreover, when at rest, electric actuators require little current to hold position, having an increased energy efficiency versus hydraulic systems, which require continuous pressurization of the fluid[16].

The only issue behind the use of EMAs is the lack of accumulated knowledge regarding this type of actuators, reducing their reliability, and their increasing jamming possibility. Therefore,

[16] https://www.powermotiontech.com/technologies/cylinders-actuators/article/21163135/comparing-electric-and-fluidpower-actuators, accessed 14/06/2022

detailed experimental tests will be carried out to ensure their performance [44]. Redundancy will be implemented in the design of the actuating system to account for remaining uncertainties.

The moving surfaces that need the use of actuators are the control surfaces, namely ailerons, elevators, trim tabs and rudder, spoilers, flaps, slats, cargo doors and water stability devices. The general layout of the actuator system is visualized in the Figure 6.26. It should be noted that due to the uncertainty around water stability devices they have not been included in this figure. If included they will be connected in the same manner as other surfaces and operated by electric actuation systems. It can be observed in the diagram that the different electric actuator systems receive the electricity from the fuel cells. The actuators are connected to the right or left fuel cells depending on whether they are on the right or left half of the Emperor. However, the fuel cell systems are interconnected to avoid the situation where one side stops working and therefore half the surfaces lose electricity. In such a case the electricity will be obtained from the other side's fuel cells.

6.10.3. Auxiliary Power

It was decided that the Emperor would not contain a classic Auxiliary Power Unit (APU) since the fuel cells themselves are able to provide the electrical power needed for starting up the engines. This is achieved by the use of fan intake that starts to pump air when the aircraft is still and the ram air intake does not intake air yet. This fan intake would be powered by connecting the Emperor to the electricity of the airport, which will also use green energy. The pumped air will be used to start generating power at the fuel cells to start moving the engines and turning on all electric systems. Once the Emperor starts moving, air would start coming from the ram air intake and regular operations can proceed.

6.10.4. Environmental Control

Due to the fact that the Emperor flies at an altitude of 3,000 $[m]$ there is no need for pressurizing the cabin[17]. However, passenger comfort must still be ensured by keeping an adequate temperature and ventilating the cabin. In order to do so the Emperor has an Environmental Control Unit (ECU). This system intakes air from the external environment and modifies its temperature to maintain it between 20 and 26 degrees throughout the flight. This system also regulates the flow of air to the cabin, and serves as ventilation since air keeps being exhausted and new air comes in continuously. A schematic representation of the functioning of this unit can be visualized in Figure 6.27. It is important to note that this system is also present in the cockpit and cargo hold, the first to ensure comfort of pilots and the second to account for the possibility of animal transportation.

The flow of air starts at the ram intake installed on the sides of the Emperor, where air enters from the environment. A valve controls the flow of air, to achieve the desired quantity for ventilation and temperature regulation. This air, usually at lower temperatures than the desired conditions, flows through a heat exchanger, where it is heated to the required temperature using the heat produced by the fuel cells. Right after, it passes through a mechanical water separator, which removes liquid water from the air [45], most useful at low altitudes. Although not visualised in the diagram, the water removed is fed to the water exhaust system used by the fuel cells. Then, the air is fed to the cabin, flight station and cargo holds. Finally, the air is exhausted into the environment via outflow valves. As it is seen in this diagram, no cooling of the air takes place. This is due to the fact that during cruise, the air will always be colder than needed inside the

[17] https://aerospace.honeywell.com/us/en/learn/about-us/blogs/why-do-aircraft-use-cabin-pressurization, accessed on 13/06/2022

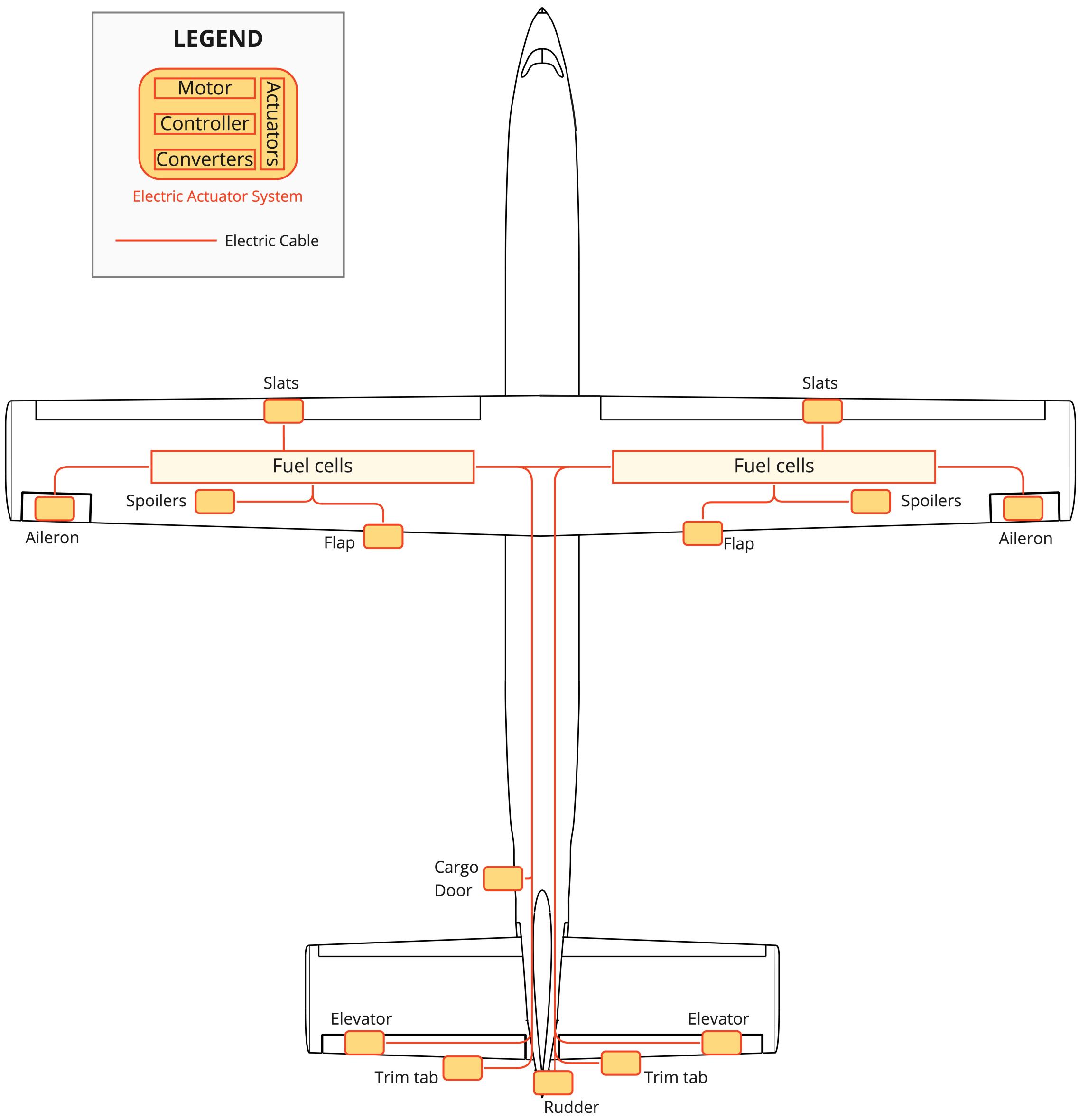

Figure 6.26: *Electric Actuator System for Moving Surfaces on the Emperor*

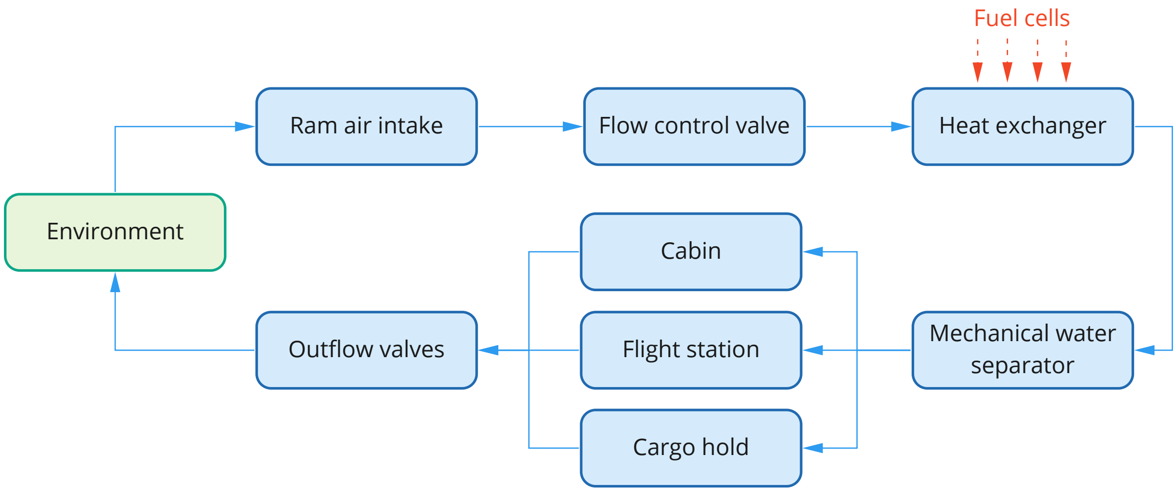

Figure 6.27: *Flow of air through the Environmental Control Unit (ECU)*

cabin, and during take-off and landing it is assumed that the highest ambient temperature will be comfortable for the passengers and only heating would have to take place in some areas or seasons.

Since the Emperor is flying at a low altitude, the oxygen quantity in the external air is sufficient. Nevertheless, sensors to measure oxygen level in the cabin will still be needed to regulate oxygen mask deployment for emergencies like fire or smoke. Along these lines, the Emperor will include a fire detection system that uses heat and smoke sensors. Heat sensing will be used in cargo holds, engines, and toilet bins. Smoke detection is used in cargo holds, avionic bays, and toilet compartments[18]. A fire extinguishing system is also essential for the safety of the Emperor, the passengers and the crew. Engine and cargo hold extinguishers are activated by the crew when abnormal heat detection or fire take place. Toilet waste bin extinguishers are activated automatically if the heat detectors there are activated[19]. Finally, there are also portable fire extinguishers installed in the cabin and the flight deck. According to EASA regulation AMC 25.851(a)(1), at least 8 hand fire extinguishers must be conveniently located and evenly distributed in passenger compartments and under AMC 25.851(a)(2), at least one hand fire extinguisher must be conveniently located in the pilot compartment [46].

It should be noted that the weights of all these auxilary systems have been accounted for using statistical weight estimation formulae taken from Torenbeek [14].

[18] https://skybrary.aero/articles/aircraft-fire-detection-systems, accessed 13/06/2022
[19] https://skybrary.aero/articles/aircraft-fire-extinguishing-systems, accessed 13/06/2022

7

Design Analysis and Summary

This chapter aims to describe the final configuration of the design. This will be done by presenting the final configuration of the aircraft in Section 7.1. After this the system characteristics, mass breakdown and performance analysis will be presented in Section 7.2 and Section 7.3. Furthermore, the noise characteristics of the aircraft will be briefly discussed in Section 7.4. Finally, the Reliability, Availability, Maintainability and Safety (RAMS) will be discussed in Section 7.5.

7.1. Configuration

This section contains the final configuration, render and the three-view drawings. The final configuration, which resulted from the iterations, can be seen in Figure 7.1, it should be noted that the floats needed to ensure the static stability of the aircraft in water are not shown, their exact design and position lies in the next iteration of the design. For the three-view drawings, technical drawings of the final design are shown in Figure 7.2. In this drawing, only the most relevant sizes are presented. On the front view, the half span of the wing and horizontal tail as well as the position of the float is shown. Regarding the top view, the width of the fuselage is presented together with the position of the leading edge of the mean aerodynamic cord of the wing and horizontal tail. Moreover, the MAC of the wing and horizontal tail is shown. The length of the fuselage is also shown in the top view. Finally, the side view indicates the height of the fuselage and the size of the vertical tail.

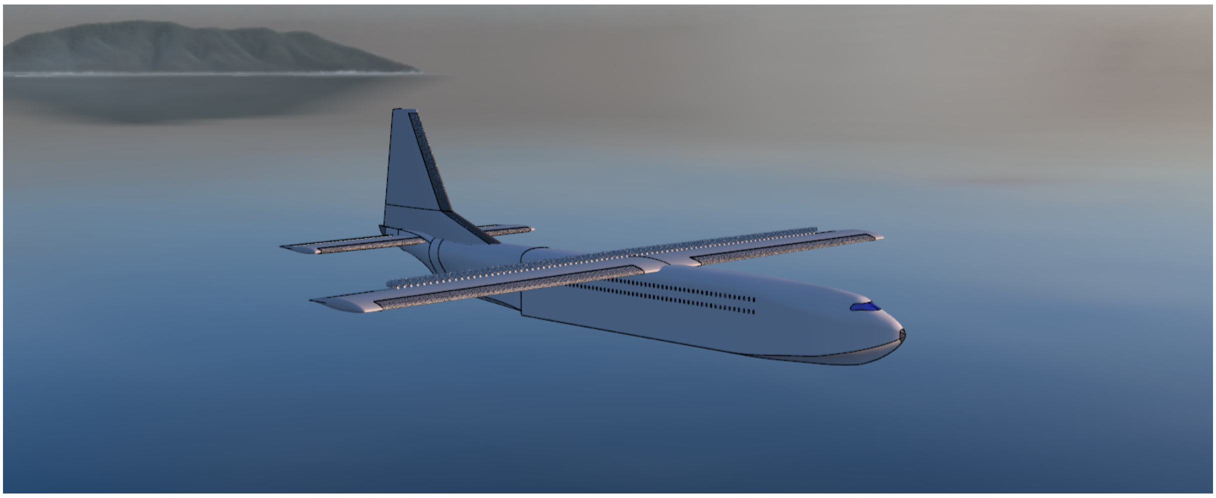

Figure 7.1: *Render of the Emperor*

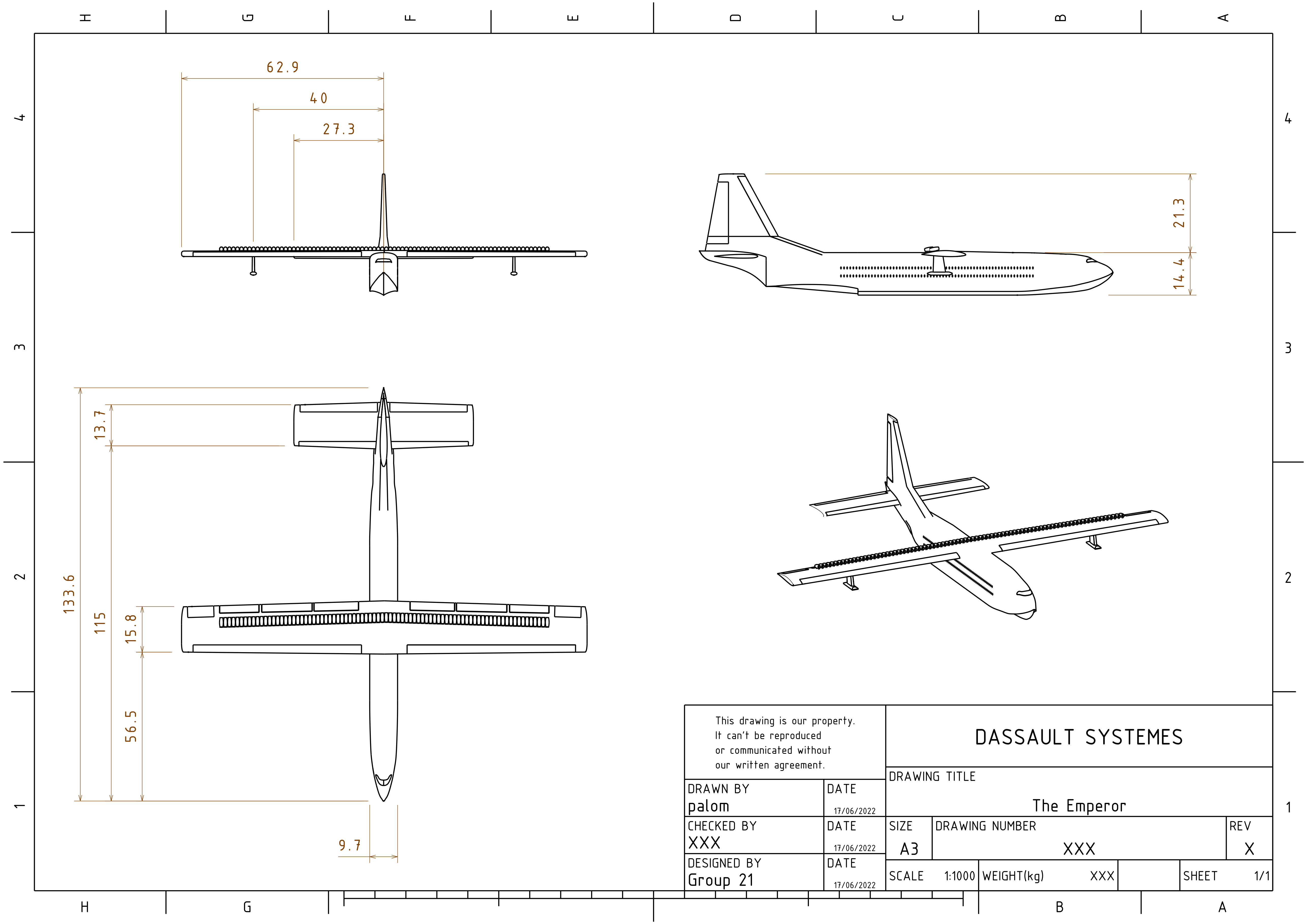

Figure 7.2: *Technical drawing of the Emperor with the most important dimensions in meters*

7.2. System Parameters and Mass Breakdown

Given that a final design has been researched, the key parameters of the aircraft can be summarised. The system characteristics breakdown includes all the major values from the most important subsystems and any parameters that may be considered noteworthy. These are all listed in Table 7.1.

Table 7.1: *Characteristics breakdown for the main subsystems*

Parameter	Value	Unit	Parameter	Value	Unit
General					
MTOM	1169	$[tons]$	Take-off speed	79.47	$[m/s]$
OEM	752	$[tons]$	Peak Power	484	$[MW]$
Total Fuel Mass	137	$[tons]$			
			Wing		
Fuselage			Airfoil	NACA651412	–
Length	133.6	$[m]$	Surface Area	1977	$[m^2]$
Height	14.4	$[m]$	Span	125.78	$[m]$
Width	9.7	$[m]$	MAC	15.76	$[m]$
Max. Thickness	350	$[mm]$	Aspect Ratio	8	–
Cockpit Length	14.4	$[m]$	Taper Ratio	0.852	–
Tailcone Length	32.4	$[m]$	Aileron Length	8.5	$[m]$
			Volume wing float	16.1	$[m^3]$
Horizontal Tail			**Vertical Tail**		
Airfoil	NACA0010	–	Airfoil	NACA0010	–
Surface Area	745	$[m^2]$	Surface Area	302.34	$[m^2]$
Span	54.59	$[m]$	Span	21.3	$[m]$
MAC	13.66	$[m]$	MAC	15.57	$[m]$
Aspect Ratio	4	–	Aspect Ratio	1.5	–
Taper Ratio	0.9	–	Taper Ratio	0.3	–
Engines			**Forward Fuel Container**		
Amount	82	–	Length	42.12	$[m]$
Power per Engine	4	$[MW]$	Volume	1382.61	$[m^3]$
Thrust per Engine	17.13	$[kN]$	Forward Fuel Mass	91.38	$[tons]$
Fan Diameter	1.20	$[m]$	Forward Container Mass	18.32	$[tons]$
Length	2.59	$[m]$			
			Aft Fuel Container		
Mid Fuel Container			Length	13.09	$[m]$
Length	14.65	$[m]$	Volume	267.03	$[m^3]$
Volume	430.43	$[m^3]$	Aft Fuel Mass	17.65	$[tons]$
Mid Fuel mass	28.45	$[tons]$	Aft Container Mass	4.71	$[tons]$
Mid Container Mass	6.39	$[tons]$			

Another essential summary of the system is the mass breakdown. This summarises the allocated mass budgets for the different subsystems of the final design. This can be seen in Table 7.2. It is important to note that these masses are based on the empirical methods which have been mentioned in Section 5.4. The miscellaneous group includes the several internal systems, such as ventilation, electric systems, instruments, or actuators. Additionally, it also includes the furnishing and the weight added by the boat hull and floats. Lastly, another important remark is that the numbers presented in the table below are still subject to changes, as the design still needs to be further developed, and more precise mass estimations will be available.

Table 7.2: *Mass breakdown of the aircraft*

Component	**Mass [tons]**	**Mass Percentage [%]**
Fuselage	157.49	21.99
Wing	136.24	19.02
Engines	99.1	13.84
Fuel Cells	100.69	14.06
Fuel Containers	29.4	4.1
Horizontal Tail	38.15	5.33
Vertical Tail	13.23	1.85
Miscellaneous	141.9	19.81
Total	**716.2**	**100**

7.3. Performance Analysis

The performance of the Emperor was analysed for a nominal mission. The mission was selected as it represents one of the longer transatlantic routes and fulfills the range requirements of the Emperor. The altitude for the mission was fixed at 3.0 $[km]$ as that is the highest altitude that an aircraft may fly at without pressuring the cabin, enabling the Emperor to have lower fuselage structural loads and not require a circular fuselage. The exact profile of the mission is shown in Figure 7.3. The fuel used for the loiter duration was calculated at cruise altitude.

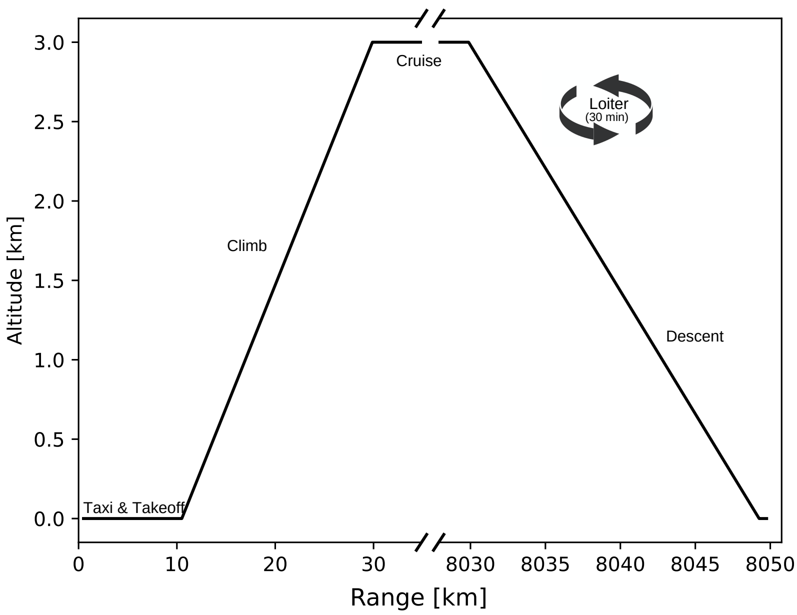

Figure 7.3: *Flight Profile Diagram*

7.3.1. Flight Envelope

The flight envelope, also called V-n diagram, shows the airspeed versus load factor, and is used to assess the structural limits of the aircraft for various airspeeds [8]. The flight envelope is specified for cruise in Figure 7.4, and take-off and landing conditions in Figure 7.5, along with their corresponding altitudes and weights. The V-n diagram consists of maneuvering and gust loading, which are superimposed to obtain the constructed diagram. The method as explained in the CS-25 regulations [47], includes establishing the load factors, design stall speed, design cruising speed, design dive speed, design maneuvering speed, and gust load factors. The diagram is completed by examining the critical points and constructing the lines which compose the outlines of the flight envelope. From the flight envelope the limit loads are determined, and by multiplying these by a safety factor of 1.5, the ultimate load factors are obtained.

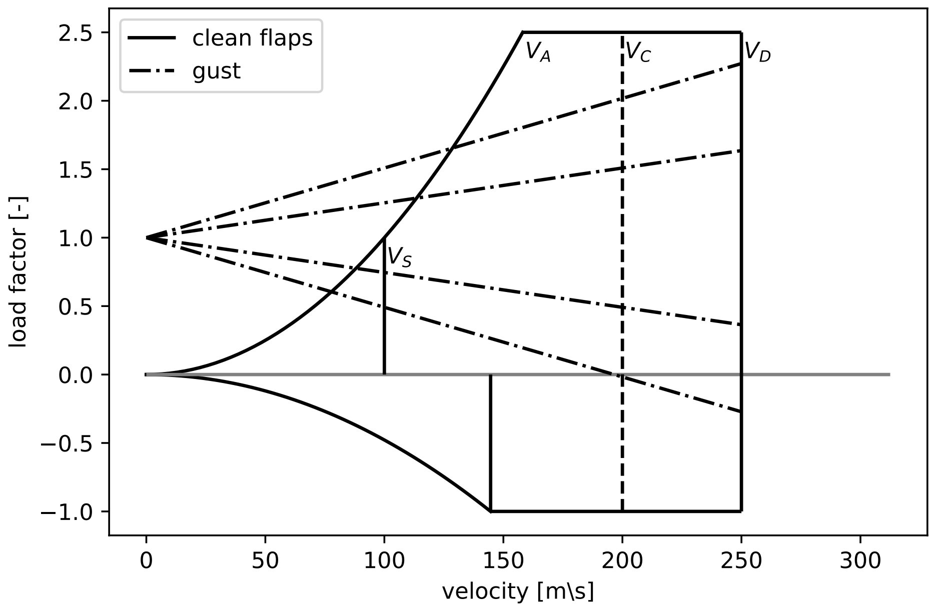

Figure 7.4: *Flight envelope Cruise*

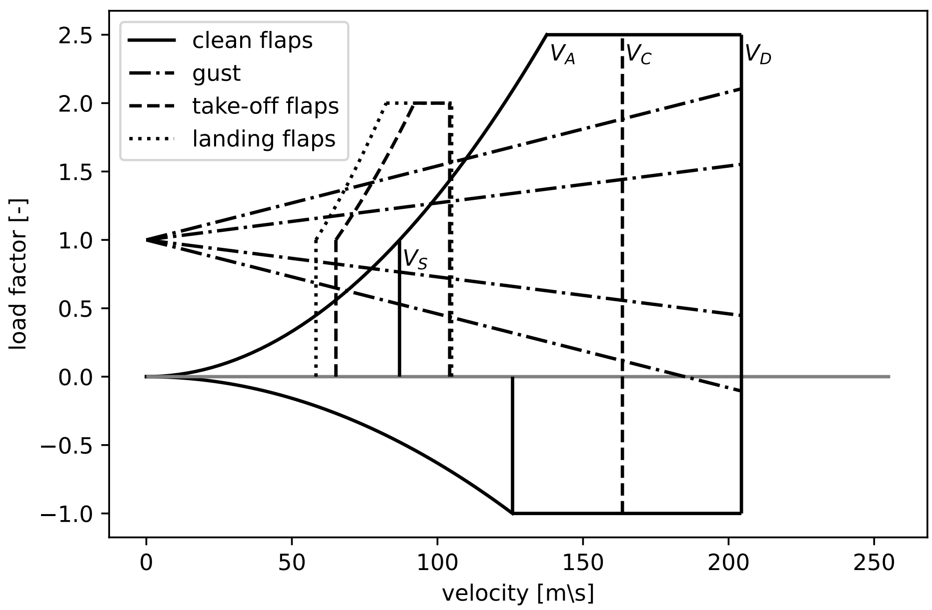

Figure 7.5: *Flight envelope Take-off and Landing*

7.3.2. Payload Range Diagram

The payload-range diagram gives an indication on some of the most important characteristics of an aircraft: the payload and the range. These characteristics are closely related to one another. For this reason they tend to be plotted against each other for different cases.

The airline flying the Emperor is capable of using this diagram in order to exchange some of the payload capacity for additional range or exchange some of the range for more payload. This passenger count can easily be changed by implementing a multi-classed layout since the aircraft is currently designed for a full economy layout. This would result however in a decrease in payload if some of the economy seats are exchanged for larger business or first class seats.

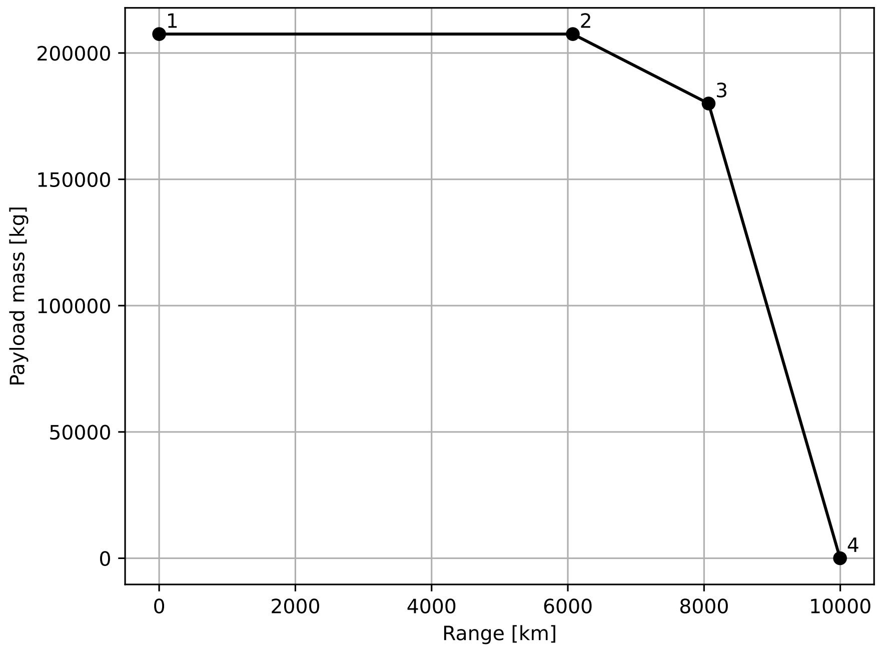

Figure 7.6: *Payload-range diagram for the final aircraft design*

There are multiple critical points in the payload range diagram as seen in Figure 7.6. These points are: maximum payload at zero fuel (1), maximum range at maximum payload (2), maximum range at maximum fuel (3) and maximum range at zero payload (4).

The locations of these points were found by finding the take-off mass and the fuel mass for these different points. Using these values it is possible to use the Breguet range equations [11] in conjunction with the aircraft characteristics in order to find the ranges at the different points. The value used for maximum payload was a 20% increase in the current payload. This was an estimation based on the cargo volume available in the 3D model, although a more accurate fuselage design should be conducted in order to further refine the mass of payload at maximum payload capacity.

The maximum range at maximum fuel point lies around 8000 [km] as expected. This point should be in this general area since the inverse of the Breguet range equations was used in order to determine the required fuel mass.

7.3.3. Climb Performance

The climb performance is an important aspect of the Emperor as it influences how fast the Emperor can reach its cruise altitude and how the noise is perceived on ground. Climb performance includes different aspects, namely the climb angle, the rate of climb (ROC) and the optimal velocity for those two. The climb performance is dependent on the power available and the power required. To get the maximum ROC the excess power $(\eta_p P - DV)$ needs to be maximal. This can be seen in Figure 7.8. Using Equation 7.1[8] the velocity for maximum rate of climb can be determined. Implementing this in Equation 7.2[8] the maximum rate of climb is calculated. The maximum climb angle (θ) can be found by solving Equation 7.3[8] for θ. The optimal climb velocity is found by differentiating with respect to V and then finding the optimum. All results are displayed in Table 7.3, where it should be noted that all the values are computed using the MTOW as the weight. With a decrease in weight, the ROC increases and the related velocity decreases. The maximal climb angle stays the same with the decrease of the weight.

On the other hand, an increase in height (and thus decrease in density) leads to a decrease in the maximum ROC which can only be reached at an increased velocity, as shown in Figure 7.7. This graph shows the service ceiling where the maximum ROC is still 0.5 m/s and an absolute ceiling at which the maximum ROC equals zero. For the Emperor the service ceiling and absolute ceiling can not be reached due to the absence of pressurization of the cabin.

$$V_{\text{ROCmax}} = \sqrt{\frac{2}{\rho}\left(\frac{W}{S}\right)\sqrt{\frac{k}{3C_{D_{min}}}}} \tag{7.1}$$

$$ROC = \frac{\eta_p P - DV}{W} \tag{7.2}$$

$$sin(\theta) + k\left(\frac{W}{S}\right)\frac{cos^2(\theta)}{\frac{1}{2}\rho V^2} = \frac{T}{W} - \frac{1}{2}\rho V^2\left(\frac{W}{S}\right)C_{D_{min}} \tag{7.3}$$

Table 7.3: *Climb Performance*

ROC_{cruise} (V = 200 $[m/s]$)	7.94 $[m/s]$	θ_{cruise} (V=200 $[m/s]$)	8.4°
$ROC_{\text{max cruise}}$ (V=115 $[m/s]$)	13.3 $[m/s]$	$\theta_{\text{max cruise}}$ (V=130 $[m/s]$)	8.9°
$ROC_{\text{take-off}}$ (V=79.4 $[m/s]$)	14.1 $[m/s]$	$\theta_{\text{take-off}}$ (V=79.4 $[m/s]$)	7.3°
$ROC_{\text{max take-off}}$ (V= 99 $[m/s]$)	14.4 $[m/s]$	$\theta_{\text{max take-off}}$ (V= 106 $[m/s]$)	9.0°

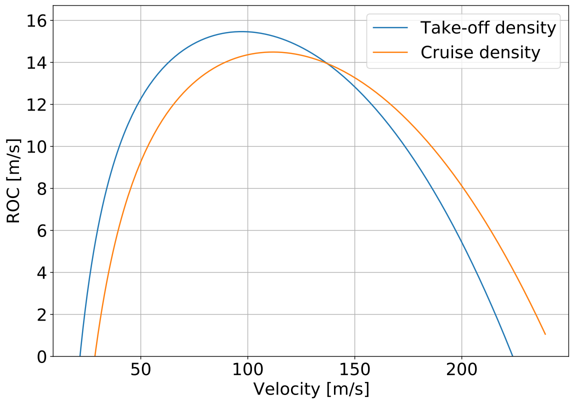

Figure 7.7: *Influence of velocity on ROC for take-off and cruise conditions*

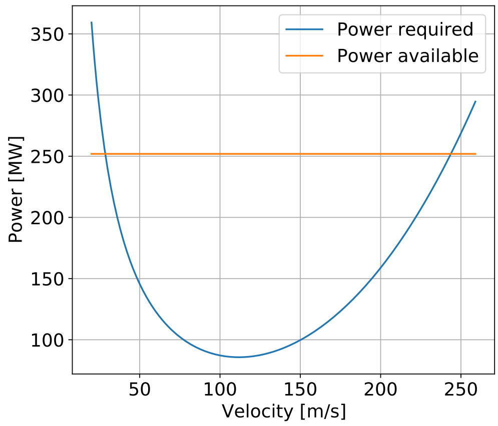

Figure 7.8: *Influence of velocity on power at cruise level*

Even though the cruise velocity is fixed at only 3000 $[m]$, the climb performance at higher altitudes is shown in Figure 7.9 to analyse the influence of a decrease in density on the climb performance and velocity. Here, the stall limit is the minimum speed the aircraft can fly and the Mach limit the limit due to the mach number becoming too high causing extra drag. The 'Limit due to the cabin being non-pressurized' is located at an altitude of 3810 $[m]$, above which it is mandatory to implement pressurization for the safety and comfort of the passengers and pilots.

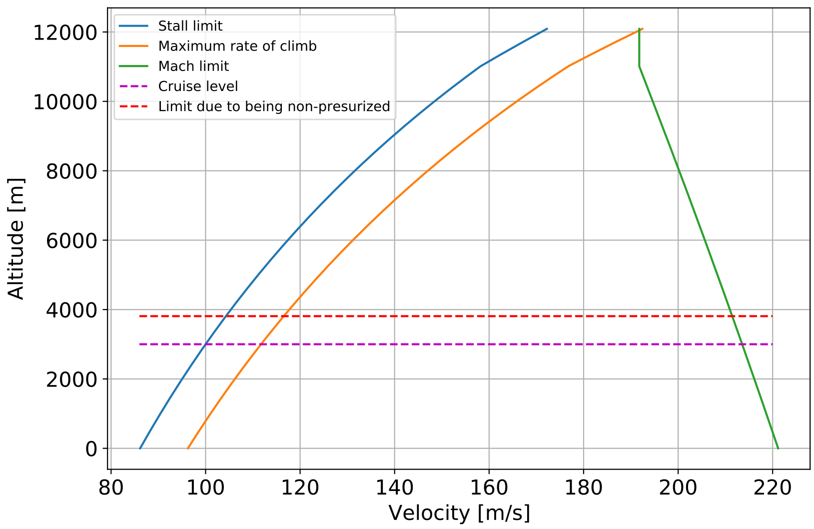

Figure 7.9: *Influence of velocity on climb performance*

7.4. Noise

Aircraft noise has a great influence on the environment and should thus be minimized. Estimating noise values for aircraft is a complex task and providing an exact measurement is not yet possible. However, based on reference values a preliminary estimation can be made. The reference for this estimate is a paper where an Airbus A320 has been modified with distributed electric propulsion (called A320MOD in this report) [48], this reference is chosen as the Emperor also uses distributed electric propulsion. Aircraft noise consists normally of three parts: jet noise from the exhaust velocity, motor noise from mechanical movements and configuration noise from flaps, landing gear and wingtips. For this analysis only the jet noise is considered to differ between the A320MOD and the Emperor. The jet noise is dependent on the exhaust velocity, which for the Emperor equals 229 $[m/s]$ at full power. The A320MOD (with ten engines) has an exhaust velocity of 243 $[m/s]$[48]. Thus, the noise per engine is likely a little smaller for the Emperor, but this is neglected. For the A320MOD the noise level is 4 $[dB]$ lower at take-off and 2 $[dB]$ lower at landing compared to the actual A320. However, the Emperor has 53 engines instead of 10 so the noise must be scaled with a factor 5.3. In decibels this equals +7.2 $[dB]$. Combining this increase with the reduction of being a distributed propulsion electric aircraft, the total noise of the Emperor is 3.2 $[dB]$ more than the A320 at take-off and 5.2 $[dB]$ more at landing. The most noise pollution happens at take-off, at which stage the Emperor is just 3.2 $[dB]$ worse than the A320. As the A320 is a relatively quiet plane in the modern day market [49]. Furthermore, it should be noted that this estimation is conservative as there are effects that are not taken into account. Some effects that are not considered are the shielding of the wing due to the engines being on top and the relatively low fan blade tip speed. Concluding, the Emperor is deemed to have an acceptable noise level and in a following stage a proper analysis should be done to obtain more accurate values.

7.5. RAMS Characteristics

RAMS is the acronym for reliability, availability, maintainability and safety. These aspects are described in the following subsections respectively. All these aspects will be touched upon in this section.

7.5.1. Reliability

"Reducing the likelihood of operational downtime as a results of technical or organisational faults is the essence of aircraft reliability. The aircraft has to be reliable in order to reduce cost for the airliner operating the aircraft due to operational downtime. Additionally, an airline operating a notoriously unreliable aircraft will likely have a lower social reputation as a result, which could lead to less customers using their services.

One of the subsystems that should have excellent reliability is the hydrogen refuelling system. An error in the refuelling system could lead to insufficient propellant entering the aircraft, meaning delays or even cancellation of the flight. Also the liquid hydrogen has to be kept under the right (cryogenic) conditions. If these conditions shows signs of large or unexpected deviations, the source of these problems first has to solved since cryogenic hydrogen can be dangerous when handled improperly.

Sea-based operations are also more difficult than land-based operations when it comes to reliability. Corrosion due to seawater can lead to more structural wear. If this wear goes unnoticed for too long the aircraft may have to be repaired or maintained at an unexpected time.

Electric subsystems, just like in normal aircraft have to have high reliability. Failure during flight without the correct back-up systems could lead to catastrophic failure. In the case of the Emperor, with its fuel cell stacks, electric motors and corresponding electronic systems, the number of total areas of failure is substantially higher than other aircraft due to the large number of electronic components. All these systems should have high reliability and if possible have some sort of redundancy element. "[1] This is ensured by including a contingency in all the fore mentioned systems, and by connecting them in parallel, where the failure of one unit still allows others to continue functioning. In this way the risk of failure the whole Emperor system is reduced, hence increasing reliability.

7.5.2. Availability

Availability of an aircraft depends on several factors. Before flight, the aircraft has to loaded with passengers, cargo, flight services and fuel. Due to the large nature of the Emperor, the amount of cargo that will be transported for extra revenues takes the longest to load. Note that the loading of cryogenic hydrogen is not a bottleneck on availability, since the addition of multiple refuelling hoses drastically decreases the refuelling time. Before refuelling, the hydrogen tanks have to be pre-cooled which does influence the availability. Increasing the pre-cooling pipe diameter decreases this time, as explained in Section 10.4.

The weather will also impact the aircraft's operation availability. With a cruise altitude of 3000 $[m]$, in case of rough storms where the weather may be too rough to fly, the flight may have to be cancelled in some instances. The maximum allowed strength of the storm will be higher than for regular aircraft, due to the large size and weight, thanks to which it is less influenced by weather conditions. Additionally, taking off will not be the biggest problem thanks to the relatively quiet bays, which would serve as the sea ports for the Emperor.

The Emperor is designed to fly only transatlantic flights, and can also only be operated at the coast. For efficiency, it would be best to depart close to larger cities or infrastructure, similar to land based aircraft. The main difference with conventional aircraft is that now only coastal cities can be considered for this method of transport.

7.5.3. Maintainability

"Maintainability of the Emperor is made more difficult due to the sea-based operational factor. The constant contact with seawater will lead to increased corrosion and wear if not properly accounted for. Maintaining the Emperor by repair and maintenance crew is also made more difficult if the Emperor is not regularly stored in a hanger, where access would be easier. Sometimes, ships are maintained using a dry dock. The Emperor will require a custom dry dock as well because of its shape and size being unconventional compared to regular ships.

Because of the size of the Emperor the maintenance will likely take longer compared to regular aircraft, while also needing more space for the inspection to take place. It will also require a large crew to repair, maintain and inspect the vehicle. Automated inspection using drones could be used to inspect the large outer surface of the aircraft to cut down on manual crew inspection time." [1]

Optimising the maintenance schedule improves the maintainability as well. By locating the custom dry dock at a strategic location where the Emperor can easily reach, as well as setting up an efficient maintenance schedule where as little time is lost, the maintainability can be improved to be comparable to modern day aircraft.

7.5.4. Safety

"When using hydrogen in any state there should always be an additional focus on safety. Hydrogen in a liquid form is extremely flammable in low concentrations, requiring only 4% volumetric ratio in the air to ignite. It also requires ten times less ignition energy to ignite compared to gasoline-air mixtures. Besides being flammable, it is also stored at an extremely low temperature of 20 $[K]$. If the cryogenic hydrogen heats up, it expands, increases pressure and might cause the tank to explode with dramatic consequences. To avoid this, sufficient insulation and protection should be present over all the length of the fuel system (incl. tanks, fuel lines etc.).

In case of a localised fire, it would be best if the remaining hydrogen could be vented out of the propellant tank far away from the cause of the fire. Multiple venting points would be required. The hydrogen will almost immediately exit the aircraft because of the extremely low density of hydrogen of 0.090 $[kg/m^3]$ at atmospheric pressure compared to surrounding air at sea level with a density of 1.225 $[kg/m^3]$. In case of fire, the hydrogen gas will escape quicker than can be ignited[1]. Even though hydrogen is a greenhouse gas when released into the atmosphere, the necessity of removing the hydrogen to ensure the passengers safety is deemed to be an essential measure to take. In the case of a ordinary hydrogen leak, with no risk of fire the propellant will slowly be depleted. To detect this leak as quickly as possible sensors should be used throughout the aircraft to measure hydrogen concentration in the air. This will allow the pilots to quickly but safely land the plane and if they deem it needed, vent the remaining hydrogen safely to reduce the chance of a fire near or inside the aircraft. This scenario has also been accounted for when deciding upon the best location to store the hydrogen propellant, which should not be stored below the passengers. In the case of a leak, the less dense hydrogen will rise. If this would rise to the passenger compartment there may be a risk of asphyxiation. Also, passenger concerns with the safety of hydrogen should be considered, as the public is likely not keen on sitting next to a hydrogen storage tank. Even though this tank is designed to survive any load with any scenario in mind, making an accident almost impossible, for passengers comfort sake they should be separated from any discomforting feeling or worry. Making the propellant tanks or high pressure lines not visible in the cabin would be such an example of removing this discomfort.

Of course, if the hydrogen has to be discarded, the achievable range decreases and might prove to be insufficient to get to a safe shore. That's why the most critical case has been researched: a flight starting from New York and losing the remaining hydrogen in the biggest (forward) fuel tank, at the most critical point. The critical point is the point during flight which is furthest from any shore. It is indicated in Figure 7.10 as the critical point. To study this condition it was assumed that the Emperor was fully filled with fuel when leaving from New York, and flew for a range of 3760 $[km]$ until reaching the critical point. The fuel used to fly to that point was calculated using the fuel fractions method and Breguet range equation subtracted from the initial fuel. It was assumed that the fuel was used from all the fuel tanks in a proportional manner. Next it was assumed that all the fuel in the forward fuel tank is gone, in order to simulate an emergency venting. The range remaining without that fuel was calculated, again using the same equation. That range was 1657 $[km]$, more than sufficient to reach the nearest port located 1060 $[km]$ further in Ireland which can serve as a backup airport for deboarding the passengers. The initial fuel would be lower in a real mission as it would be optimised for the minimal amount of fuel possible, but these optimisations lie outside the scope of the current design, and this investigation shows that indeed a backup airport can be reached in all conditions.

Due to the sea-based nature of the Emperor, it is advised against flying land-based routes, due to the incapability of making an on-land emergency landing. In the case of an emergency water landing there should be facilities to rescue the passengers and crew in such a scenario. Neighbouring countries should be aware of the location of the aircraft. In case of an emergency, air-sea rescue could be launched to help evacuate the passengers. However, due to the large number of passengers, air-sea rescue or Coastguard from neighbouring countries is likely not sufficient to rescue all passengers in a short amount of time. Also, if the emergency would happen in the middle of the Atlantic ocean it is probably out of range of these services, thus

[1] https://www1.eere.energy.gov/hydrogenandfuelcells/pdfs/h2_safety_fsheet.pdf, accessed 12/05/2022

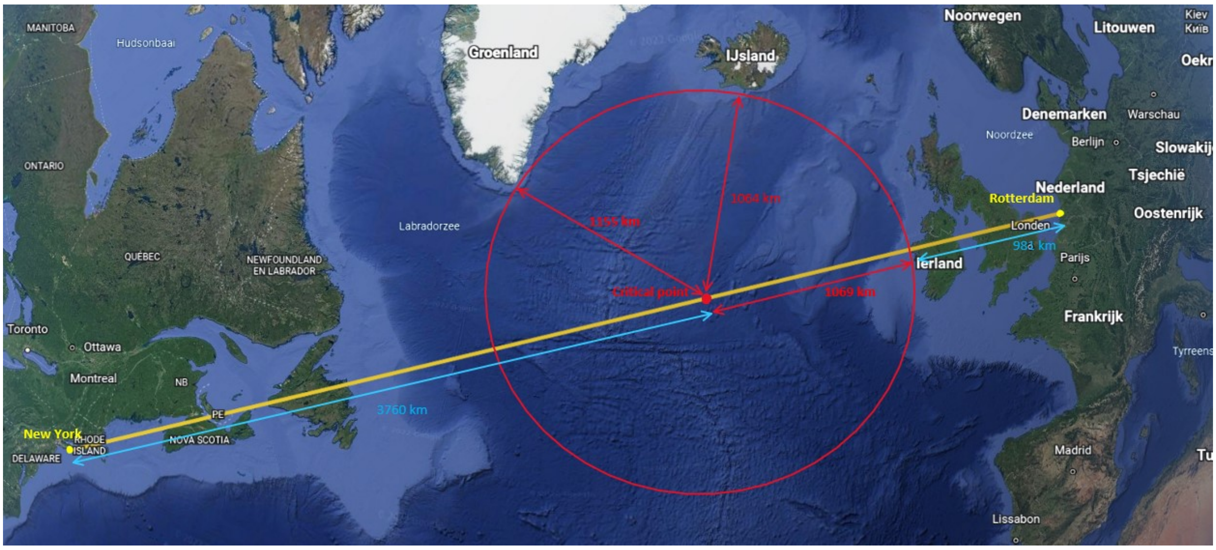

Figure 7.10: *Critical point in terms of fuel tank damage*

the Emperor should stay close to the busiest shipping lanes. In case of an emergency water landing a distress signal to cargo ships crossing the Atlantic can provide help to the nearby passengers in distress. Navy vessels could then take over the passengers from these cargo ships and provide the necessary care whilst getting everyone safely to the coast.

The fuel cell stacks will provide the engines with power, so there should be consideration for high voltage systems and wiring. When dealing with high voltage combined with water, additional case is evidently needed. To ensure the safety of maintenance crew, passengers and flight crew during regular operations and in emergency scenarios, the systems should be insulated sufficiently." [1]

7.6. Compliance Matrix

As the design has been thoroughly analysed and the parameters are finalised for the current design iteration, a compliance matrix for the stakeholder requirements previously presented in Chapter 2 is shown in Table 7.4. This compliance matrix details whether the stakeholder requirement is met, by indicating Y for yes, N for no and U for undetermined, and presents the actual achieved value when necessary. The compliance matrix is followed by a feasibility analysis, which explains the reason for any undetermined compliance and provides a rationale on how to ensure the requirement could be met.

Table 7.4: *Compliance Matrix*

Label	Stakeholder requirement	Compliance
HHA-Tut-01	The Emperor shall have a minimum cruise speed of 500 $[km/h]$.	Y - 720 $[km/h]$
HHA-Tut-02	The Emperor shall have a minimum range of 8,000 $[km]$.	Y - 8,000 $[km]$
HHA-Tut-03	The Emperor shall be able to carry a minimum of 500 passengers.	Y - 1,500 pax
HHA-Tut-04	The Emperor shall have a reliability comparable to present day transatlantic civil aviation.	Y
HHA-Tut-05	The Emperor shall have a safety comparable to present day transatlantic civil aviation.	Y
HHA-Tut-06	The Emperor shall emit no greenhouse gases during operation.	Y
HHA-Tut-07	The Emperor shall be at least 95% reusable/recyclable.	U
HHA-Tut-08	The Emperor shall be stable in nominal conditions.	Y
HHA-Tut-09	The Emperor shall be controllable.	Y
HHA-Tut-10	The Emperor shall be sea-based.	Y
HHA-Tut-11	The ticket cost of the Emperor shall be comparable to present day transatlantic civil aviation.	Y
HHA-Arl-02	The Emperor shall have an availability comparable to present day transatlantic civil aviation.	U
HHA-Arl-03	The Emperor shall have a maintainability comparable to present day transatlantic civil aviation.	U
HHA-Arl-04	The Emperor shall comply with all of the applicable laws.	U
HHA-Arl-05	The Emperor shall comply with all of the applicable regulations.	U
HHA-Pax-01	The passengers shall experience a comfortable flight, comparable to present day civil aviation.	U
HHA-Env-01	The Emperor shall produce a maximum of 110 $[dB]$ of noise during operation.	Y

It can be seen that most of the stakeholder requirements have been met, or even exceeded the minimum required value, as for cruise speed and number of passengers. However, some requirements have not yet been confirmed to be fully met, thus have been labelled undetermined. These requirements will be discussed further to give a rationale as to why they have not been fully met, and what needs to be executed to ensure compliance. The compliance with **HHA-Tut-07** has not been determined thus far. Current day aircraft are able to recycle approximately 85-90%[2], thus the Emperor will strive to perform better. Various tactics are applied to obtain this target percentage, as explained in Chapter 11. However, further analysis is needed in a more detailed design stage to ensure that this requirement is complied with. The availability, as mentioned in **HHA-Arl-02**, is striven to be comparable to current day transatlantic civil aviation, as explained in Section 7.5. The Emperor flies at a lower altitude than current transatlantic aircraft, thus a storm will have a larger effect at this lower altitude. However, due to the large size and weight of the Emperor, storms will have relatively less impact than on current aircraft. Therefore, availability should be further analysed in the extension of the current detailed design. The maintainability, as stated in **HHA-Arl-03**, is also aimed to be comparable to current day transatlantic aviation. As explained in Section 7.5, the large size of the Emperor and sea-based conditions create more difficulties for maintainability than for current aircraft. A dry dock and automated inspection drones are implemented to decrease maintenance time and efforts. Nonetheless, further investigation is required to examine if the requirement is met.

The compliance with **HHA-Arl-04** and **HHA-Arl-05** has already been partly taken into account

[2] `https://aviationbenefits.org/environmental-efficiency/circular-economy`, accessed on 08/06/2022

in the design through various means such as performance diagrams and calculation methods as shown in Chapter 7 and Chapter 6. However, only by further detailed design and testing as explained in Chapter 10 can these two requirements be met completely. The comfortableness for the passengers, as described in **HHA-Pax-01**, has been taken into account by ensuring static water stability, air stability and controllability, and temperature in the cabin, as explained in Chapter 6. Nevertheless, stability in water during take-off and landing, and thus comfort for passengers, will need to be investigated further in an extension of the detailed design. Therefore it remains undetermined if this requirement has been met.

8

Verification, Validation and Sensitivity

This chapter aims to verify, validate and establish the robustness of the computational model which has been used for the designing process of the Emperor, along with validating the robustness of the design to changes in input parameters. Verification and validation methods are discussed in Section 8.1, after sensitivity of the model is analysed in Section 8.2.

The source code of the model is made publicly available [1] for any future work which wishes to build upon the design model.

8.1. Verification and Validation Procedures

Verification and validation (V&V) procedures aim to ensure a certain level of correctness of the models used in the design of the final product. It should be noted that these procedures were performed throughout the design process and were vital in ensuring the trust-worthiness of the results. The verification of the code was done using unit tests which is further described in Subsection 8.1.1. The validation methods which have been used for the final design are then presented in Subsection 8.1.2. Validation of the different sub-systems was not possible due to the limited time available and the lack of available, proven resources but some validation methods for the sub-systems are suggested in Subsection 8.1.3.

8.1.1. Code Verification

The code which has been used to iterate over the design is verified in order to be considered correct. This is done by implementing unit tests into the Python code which compare analytical solutions to those that the code outputs for different functions or smaller units. Once all unit tests have passed, subsystems can be verified in a subsystem test and after which system tests can be performed to verify the correct implementation of all subsystems. For this model, the different classes written for each component need to be verified in order to ensure that their sub-functions and methods are capable of correctly performing the sizing of the different sub-components of the aircraft. Furthermore, they also need to be verified in an environment that proves that they correctly interact with the other sub-components of the aircraft which would be a system test.

These unit tests are made by running the different functions with some seed variables. These same variables are then used in hand calculations to find the expected output. This output is then compared against the output of the function which is being tested, after which the comparison should point to any errors in the tested function. In order to ensure sufficient accuracy of the code, it is always tested in multiple cases which can test all aspects of the code to find any potential incorrect output.

The blocks of code chosen to be considered units were individual methods on classes, such as calculating the system's weight with the current state of the design, with each class representing

[1] https://github.com/maxvanbart/AE3200DSE

a separate system. Other units that were tested were the smaller function which make up the class methods, such as the calculation of the Reynolds number in the drag module. After running unit tests on such blocks throughout the design process, it can be concluded that methods and functions in the code have been correctly implemented. This can be said since many unit tests have been implemented for different parts of the code and all bugs which have been found during the verification process have been fixed.

An additional verification step was taken when integrating together the various classes that represent the systems. As all these classes took part in the iterative loop, individual integration tests were difficult to perform, due to the interdependence of all systems. Each piece of code which was not subject to verification by unit tests on separate methods was peer reviewed in order to assure higher quality. Peer reviews were used as the method of choice for system tests. The verification consisted of a detailed walk though of the code written by another member of the design team, with the logic behind the code being elaborately explained. This step helps to catch any errors with both the flow of the execution of the code, and any false assumptions made from the engineering side. This ensured that the computational model was matching the mathematical model, along with the mathematical model being based on reasonable assumptions, grounded in literature.

Despite the confidence in the output of the model, it is possible that some errors have been overlooked. However, even if this is the case, the model has been found to be fairly robust as will be discussed in Section 8.2, and it is likely that further refinements in the accuracy of the model will lead to a more optimal design.

8.1.2. Validation

The validation of the final model is done by comparing it to already existing concepts. This is done to validate whether the results are realistic or not. A significant deviation from existing aircraft could indicate that the design is overly ambitious and may be unfeasible. This method of validation is not ideal as it assumes the final design is similar to already existing designs. While capable of identifying large, pervasive issues, this method will not be able to examine the more complex details of the subsystem design. However, while validation should be analysed in greater detail, it is still considered to be sufficient at this stage of the design process. In later stages, it will improved through several recommended procedures as will be discussed in Subsection 8.1.3.

8.1.3. Suggested V&V Procedures

As was discussed, while verified to a sufficient extent, the budget for extensive verification and validation methods was limited during this project. Many methods for validation were unfeasible but if given enough time, money and resources, employing several could increase the confidence in the results.

The first validation method recommended is the usage of an industry standard Computational Fluid Dynamics (CFD) tool in order to validate the aerodynamic model. This is due to the relative inaccuracy of the currently used analytical methods for the drag and lift calculations, and its limitations when accounting for the drag due to the boat hull. In a further stage of the design, wind-tunnel testing can be done on a scale model to further validate the aerodynamic model and the CFD analysis. This method would give reliable results for the real world aerodynamics of the unconventional design, along with providing information on all of the aerodynamic coefficients needed for further analysis. However, at this stage in development, CFD is the preferred choice as it is less expensive and would still provide insights to better fit the model to reality.

Secondly, it is recommended to perform a finite-element (FEM) analysis on the structure of the design. Performing FEM on the design will allow for the evaluation of weak points and will also allow for the examination of points which could be made lighter by decreasing the structural support.

Finally, it is recommended to do some very specific examinations on some of the more complex sub-systems which are required for the final design. These include, but are not limited to, the engines and the cryogenic fuel tanks. As these sub-systems are deemed quite complex and have a lower technological readiness level, they should be examined and designed with more care. This might require the organisation of research and development teams which specifically work on these sub-systems according to requirements set for the final design.

8.2. Sensitivity Analysis

Typically, computational models of this scale are validated via a sensitivity analysis in order to not only identify potential errors in the code and the underlying mathematical model, but also to calibrate it and exploit it as a tool to investigate the relations between the inputs and the outputs [50]. As the perfect model fit to the underlying data cannot be guaranteed due to the uncertain nature of the engineering process, it is up to the designer to ensure that the model is calibrated. A sensitivity analysis is a typical tool for this purpose which allows for the exploration of the design space. It can be argued that this validation method is the only method available when a model is developing an untried design such is the case of the Emperor, where there is a distinct gap in both historical and experimental data.

A sensitivity analysis is performed by selecting a variety of input design parameters that are deemed to be representative the design. These inputs may and probably should be altered during the design process, as more engineering insight into the problem at hand is gained. An example of such a parameter would be the position of the wing along the fuselage - X_{LEMAC}. These parameters are varied by a small factor, here selected as 1%, and the outputs measured.

The outputs for such an analysis would be key metrics describing the design. For example, when analysing the aircraft as a whole, the maximum takeoff weight may be a parameter of interest but when testing subsystems such as the tail, the surface area of the horizontal tail may be more relevant output. The relative change in the output metrics compared to baseline are computed for a 1% variation in each of the input parameters.

Along with validating the model, such an analysis gives insight into the effect of the contingencies selected for the design. If it is observed that a small change in a contingency factor leads to a significantly different design then that area of the design must be carefully monitored in the future to ensure that it does not exceed the allotted resource budgets. The threshold was selected at a 5% change in an output parameter due to a 1% change in an input parameter. This serves as a trigger for a technical risk. Hence this analysis serves as a system level validation procedure.

8.2.1. System Level

To assess how the complete system responds to changes in input parameters the Operating Empty Mass, the fuel mass and the operating costs per passenger kilometer were measured as outputs. These were measured at the baseline design, and with a 1% increase in each one of the input parameters. The input parameters deemed the most representative at the system level were the velocity, range, number of passengers, OEM contingency and cruise drag contingency. Here the OEM contingency refers to the factor by which the OEM is multiplied for mass estimation, and cruise drag contingency refers to the multiplier of the cruise drag when calculating thrust and fuel consumption requirements. The results are presented in Figure 8.1. Do note that all the changes in the output parameters are presented as a percentage change relative to their baseline values.

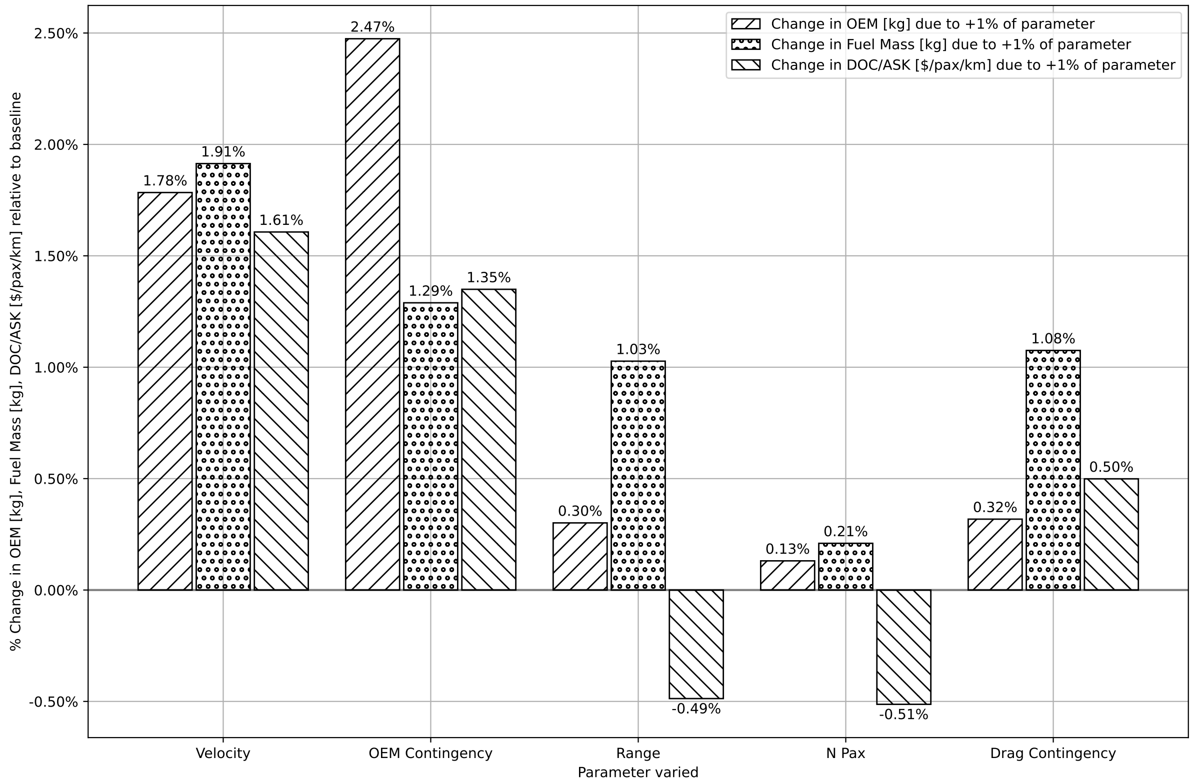

Figure 8.1: *Sensitivity Analysis - Aircraft*

It is interesting to note that an increase in passenger count or the range leads to a decrease in the direct operating costs per passenger per kilometer (DOC/ASK) which implies that the aircraft becomes more economically competitive. DOC/ASK can be decreased primarily by decreasing the size of the aircraft (which reduces fuel and manufacturing costs) or by increasing the range or passenger count. This result indicates that an increase in range or passenger count does not lead to a proportionately large increase in total operating costs and so the DOC/ASK decreases. This suggests that further cost optimisation can be achieved. Despite this intriguing result, all changes are still below 5% and hence they do not indicate any concerns with the model itself, neither with the robustness of the design.

8.2.2. Power and Propulsion

Subsequently, the responses of several key output characteristics describing the power and propulsion group were examined for their sensitivity to the changes in crucial input parameters. The characteristics considered were the mass of the whole system group, the number of fans, and again the fuel mass. The parameters varied were the velocity and the cruise drag contingency along with the fuel cell specific power and the power contingency. Here the power contingency is the multiplier of the maximum power of the engines when calculating the number of engines required. The results are presented in Figure 8.2.

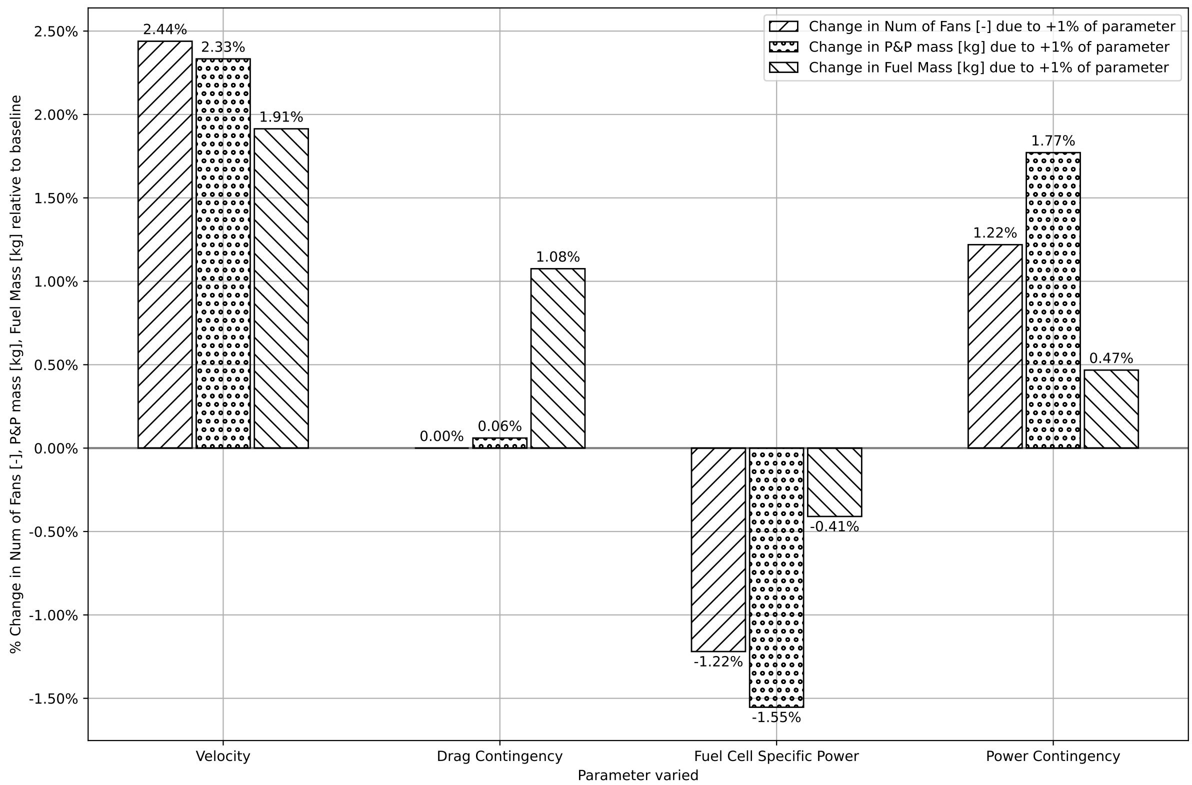

Figure 8.2: *Sensitivity Analysis - Power and Propulsion*

This sensitivity analysis again reaffirms the confidence in the design tool and the design itself, as the changes in all the outputs remain small, below 5%. One note that can be made is the fact that the number of engines does not increase when the drag contingency is increased. At first one may find this suspicious as increasing drag should lead to a larger power system requirement, but one should consider the fact that the number of fans may only be an integer number, which is rounded up. Hence a small increase in the power required from the engines does not necessarily translate to the need of an additional fan.

8.2.3. Wing

The same sensitivity analysis procedure was also repeated for the wing. The main outputs considered were the wing mass, along with its area and the installation angle. The velocity, drag and OEM contingency, along with the aspect and taper ratio of the wing are the input parameters. The results are presented in Figure 8.3.

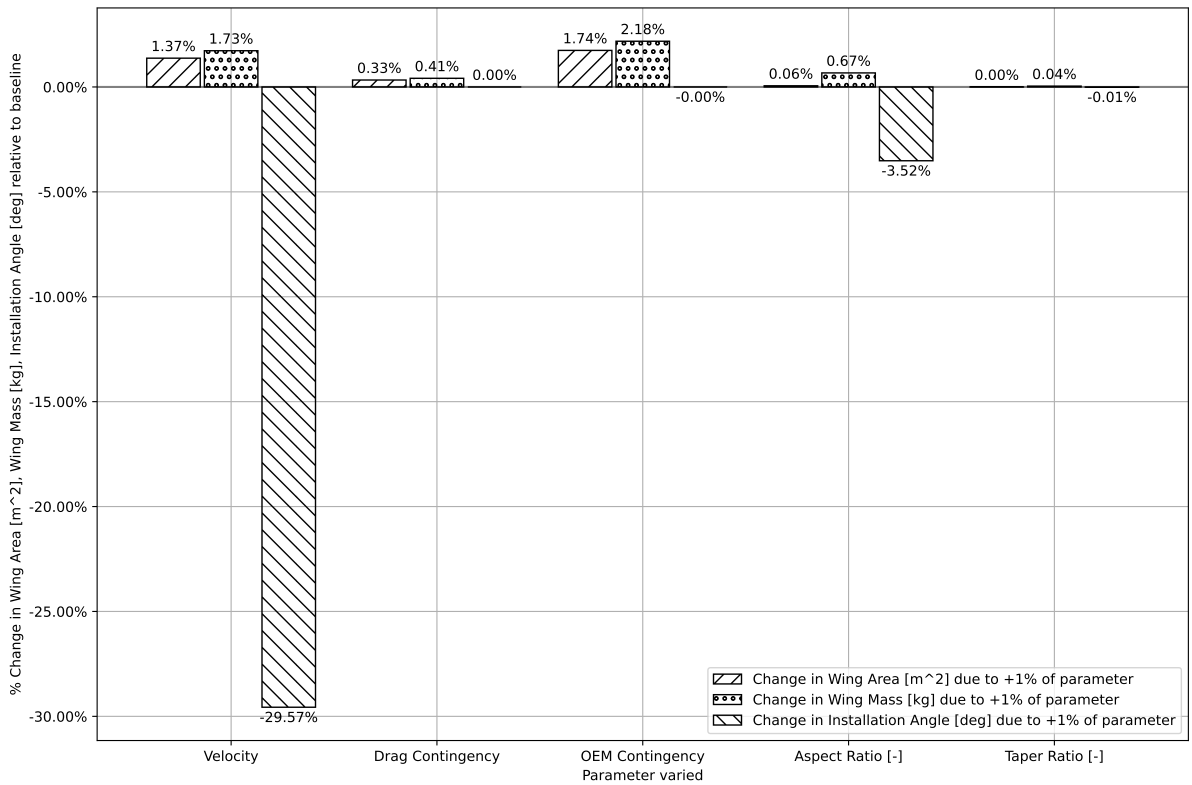

Figure 8.3: *Sensitivity Analysis - Wing*

This analysis further establishes the confidence in the model and in the design. The only aspect of note is the large decrease in the installation angle. While at first sight this may indicate a concern, as this is above the 5% threshold, the actual values should be considered, which were in this case 0.26 $[\mathrm{deg}]$ and 0.17 $[\mathrm{deg}]$, a small change in absolute terms. Hence this large variation in the output is not a concern for the confidence in the model.

8.2.4. Tail

The last system to be considered was the tail, consisting of the Horizontal (H) and Vertical (V) tails. Here the velocity, the H tail volume coefficient, the H tail aspect ratio, along with the tail cone length and the position of the leading edge of the wings mean aerodynamic chord were considered as input. The outputs measured were the total mass of the tails, and the H tail area. In addition the value of C_{m_α} was reported. But it was reported as its value instead of a percent change. This was due to the fact that the sign of it indicated the stability and a relative change would not provide useful insight. The results are presented in Figure 8.4. It should be noted that a baseline C_{m_α} is also reported.

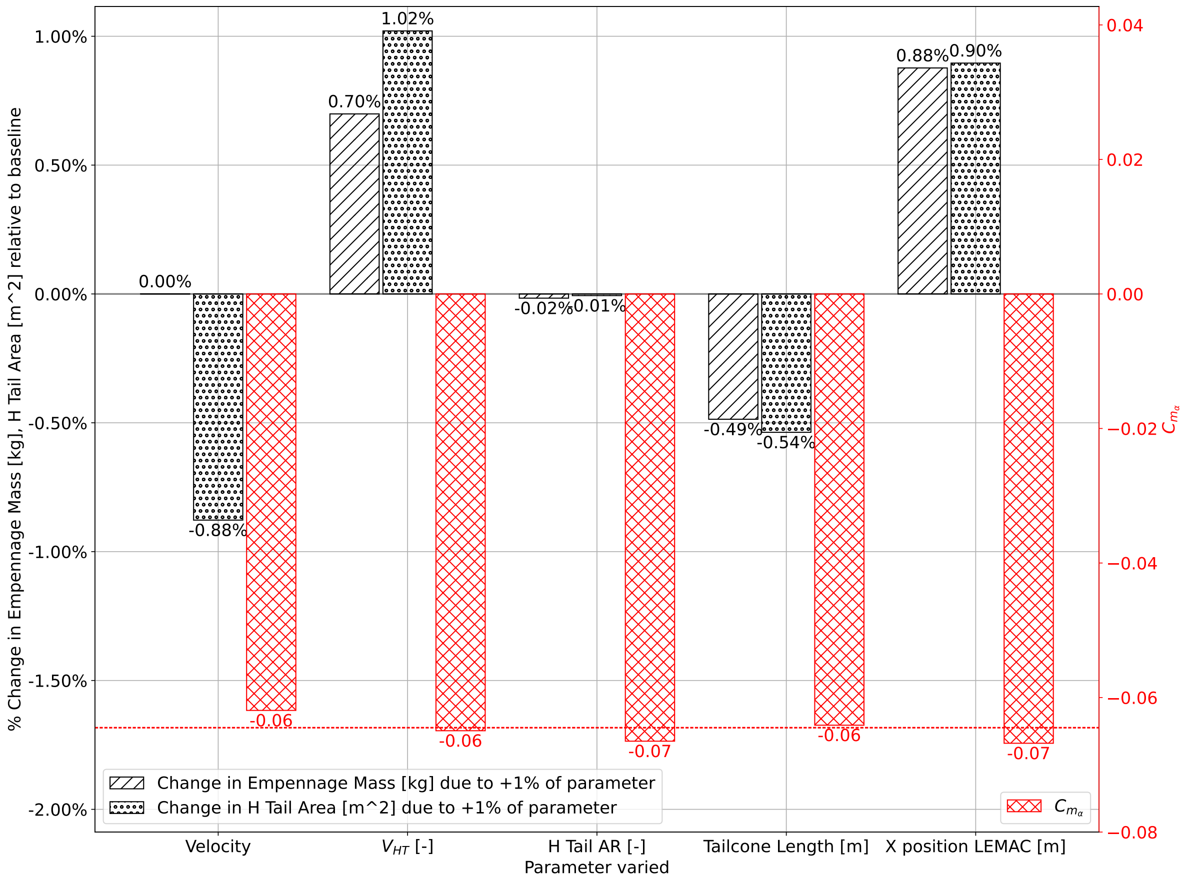

Figure 8.4: *Sensitivity Analysis - Tail*

Once again, due to the fact that the changes in the outputs are of a similar order of magnitude as the change in the input parameters, and occur in the foreseen directions, more confidence in the model is obtained. These sensitivity analyses should be repeated, especially once the design is at a higher fidelity, and more complex tools such as CFD are introduced. It is recommended that the choice of input and output parameters be further expanded, in order to investigate the sensitivity of the more detailed design. Furthermore once more engineering insight is gained into the problem at hand, the choice of inputs could be further refined.

9
Data Diagrams

Where the previous chapters explained all of the different systems and subsystems, this chapter will go deeper into how they are all integrated and how they relate with each other. To this goal, a hardware and software block diagram is shown in Section 9.1. Section 9.2 continues by presenting the electrical block diagram. The data handling block diagram is introduced in Section 9.3, while the communication flow diagram is displayed in Section 9.4.

9.1. Hardware and Software Block Diagrams

The interaction between the software of the multiple subsystems are shown in the software diagram in Figure 9.1. The main focus lies on the CNS of the Emperor, together with the FMS which is of vital importance for piloting an aircraft.

For the communications block, it must be noted that even though the output to the ATC and GNSS are drawn to start from the CPDLC and ACARS, in reality they first pass the SATCOM or VHF datalinks. However, this has not been visualised as such for clarity's sake.

Regarding the navigation system, not all existing methods (such as the ILS, ADF or simply an extensive use of radio navaids) can be used due to the nature of the Emperor being a seaplane flying on transatlantic routes. To increase the reliability, the GPS signal from the GNSS is compared to the inertial navigation system (INS) of the ABAS, after which this integrated data is sent to the RNAV which sends the position information to the FMS. The INS can be used as a backup in case the GNSS signal is lost or corrupted. Lastly, there are also the navaids which can be consulted when close to a coastal area. Radio navigation is not possible when flying over the transatlantic ocean.

For surveillance, the automatic dependent surveillance - broadcast (ADS-B) receives its position information from the GNSS, which it periodically broadcasts. The ATC or other aircraft can then pick this signal up and improves their situational awareness. Additionally, the airborne separation assurance system (ACAS) together with the TCAS aim to prevent collisions by communicating with the ATC and other aircraft, using its own position information from the FMS as a basis.

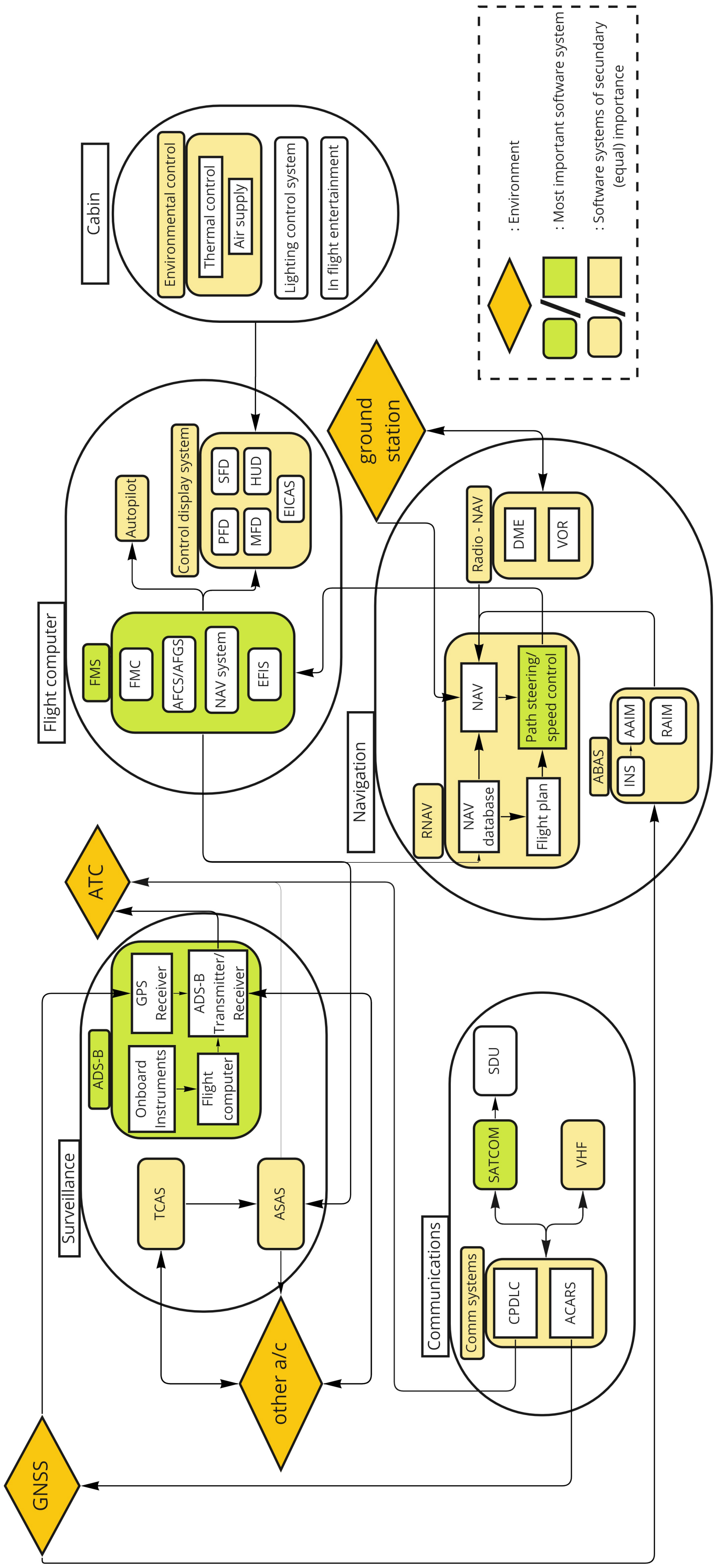

Figure 9.1: *Software block diagram*

The hardware block diagram is shown in Figure 9.2. The choice was made not to go too much into depth, since the other diagrams in this chapter aid sufficiently in the clarification of the system interactions. That is why only the data flow and the electrical flow are shown. A thing of note is the electrically driven flight controls, for which the choice has been made due to the ease of implementation as well as their high load bearing capabilities and reliability comparable to their hydraulically driven counterpart.

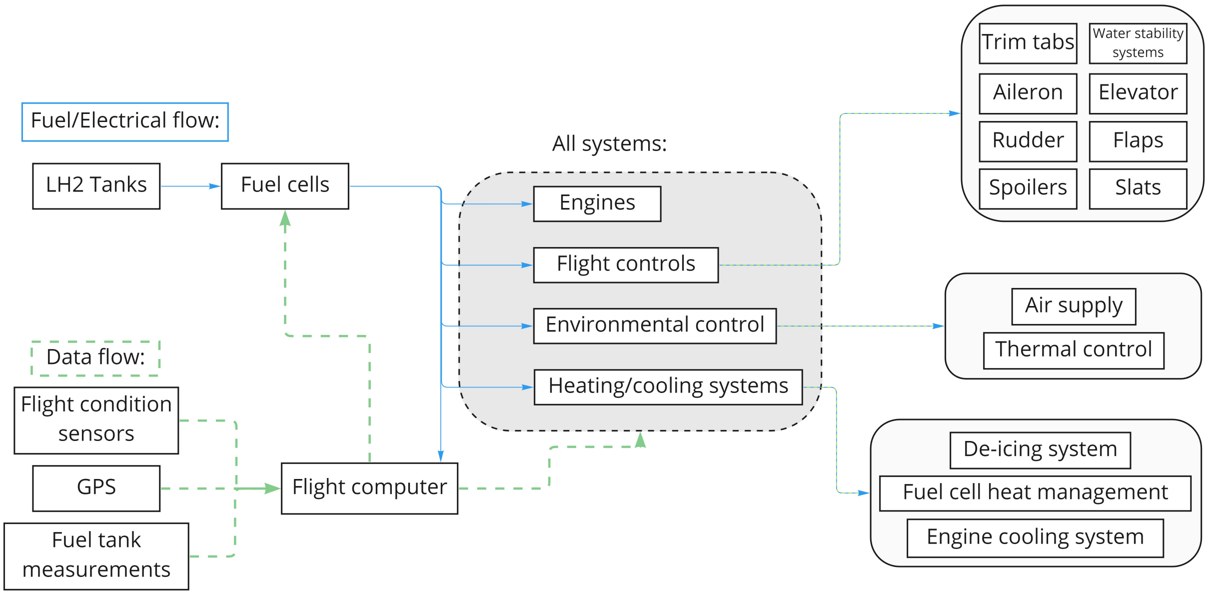

Figure 9.2: *Hardware block diagram*

9.2. Electrical Block Diagram

Figure 9.3 shows the electrical block diagram of the Emperor. It visualises the relations and interactions of the electrical equipment of the systems. It all starts with the fuel cells which generate the electrical power. The fuel cells convert the chemical energy that comes free during the electrochemical reaction of hydrogen and oxygen to electrical energy. However, before the hydrogen and oxygen are provided, they first have to be temperature and pressure controlled such that the fuel cell can work in optimal conditions. Regarding the hydrogen, it's stored in the tank at a pressure of 1.2 $[bar]$, whilst the optimal operating pressure of fuel cells is 3-4 $[bar]$ [51]. For the oxygen, the air is less dense and colder at high altitudes, so air supply fans have to be installed to increase the oxygen intake. However, these are limited since the cruise altitude is only at 3,000 $[m]$. After the electrolysis in the fuel cells, the only waste product is water vapour which is then liquefied, which makes this an environmentally friendly power generation system.

The electrical power that is acquired will be converted to have the correct current, since the power exits the fuel cells with a voltage of 300 $[V]$. This has to be lowered to protect the systems. After this the Power distribution system (PDU) sends the power to the systems that need it. The systems work on both AC and DC, so the electricity first has to be inverted to the desired format. This is done by the AC/DC inverter. The choice has been made to build in redundant fuel cells instead of batteries/APU to make up for power loss in case of fuel stack failure or increased power needs during peak periods. These specific power cells can simply be turned off by stopping the hydrogen flow leading to them.

An important system for the whole process is the cooling/heating system, since it energises the thermal control systems which make sure the fuel cell can keep working in its normal operation mode. This cooling is performed mainly by cooling water and passing air. The remaining heat waste can be used for a variety of functions such as on-board heat uses like food preparation, the heating of water and the pre-heating of hydrogen before it enters the fuel cell.

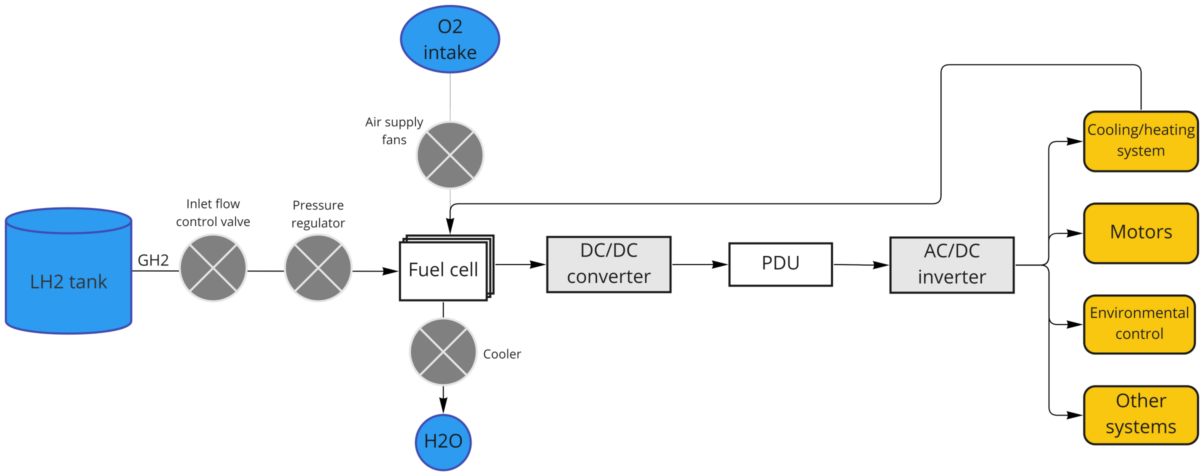

Figure 9.3: *Electrical block diagram*

9.3. Data Handling Block Diagram

In order ensure the proper functioning of the Emperor, data from different systems must be collected, transported and processed. In order to do so, it has been decided that the Emperor will use Avionics Full-Duplex Switched Ethernet (ARINC 664) to connect avionics equipment with one another and allow the exchange of data. This has been visualized in Figure 9.4. It is important to note that the different arrows and shapes used are explained in the legend.

Two main computers, the Flight Management Computer (FMC) and the Flight Control Computer (FCC), process and handle the data. The flight management computer allows routes to be pre-programmed and fed into the system. It constantly receives position, attitude and weather conditions information from the navigation system, which includes Attitude Heading and Reference Systems (AHRS) and Global Navigation Satellite System (GNSS). Furthermore, it also receives and displays the information obtained by different sensors located both on the outside and inside of the aircraft. The sensors, namely a AOA/Pitot tube and a static port, allow the computation of the horizontal and vertical airspeed. Also, sensors on the inside of the aircraft measure the conditions inside the cabin to monitor passenger comfort, whilst the FMC commands changes in the heating and ventilation systems to maintain the desired conditions. The water stability system and hull also include sensors to measure water depth, submerged level of the hull and force and vibration. The FMC receives this information and commands the activation of the electric actuators of water stability systems when needed. All relevant information processed by the FMC, including control-related data provided by the FCC, is displayed in the Electronic Flight Instrument System (EFIS) and the Multi-Function Control and Display Unit (MCDU). The pilot uses these displays to read this information and the MCDU also receives inputs from the pilot. All of the data is collected in the Flight Data Acquisition Unit (FDAU), which records it in the Flight Data Recorder (FDR) and the Quick Access Recorded (QAR). The latter is designed to access raw flight data quickly and easily[1]. Furthermore, the Cockpit Voice Recorder (CVR)

[1] https://skybrary.aero/articles/quick-access-recorder-qar, accessed 13/06/2022

records the audio environment in the flight deck for incidents investigation purposes[2].

The Flight Control Computer (FCC) is part of the Automatic Flight Control System (AFCS), which also includes the autopilot, yaw damper and Flight Director (FD). The FCC receives data from the fuel tanks, power unit, and propulsion unit through a series of sensors that measure important parameters such as temperature, pressure, revolutions or liquid level. A Flight

Control Unit (FCU) receives inputs from the pilot for the automatic flight controls, which are an input for the AFCS. The FCC exerts commands to the propulsion unit to regulate thrust as desired and also commands to deflect or deploy control surfaces and high lift devices such as the rudder, ailerons, elevators, flaps, slats, and spoilers, and is aware of their deflection through the use of sensors.

Only when information properly flows and is processed, can the aircraft perform its mission. For this reason, the existence of redundancy is important, ensuring that even with the failure of some components, the success of the mission is not compromised. For example, at least a couple of static ports and pitot tubes should be included. Furthermore, at least both FMC and FCC should be duplicated as well.

[2] https://skybrary.aero/articles/cockpit-voice-recorder-cvr, accessed 13/06/2022

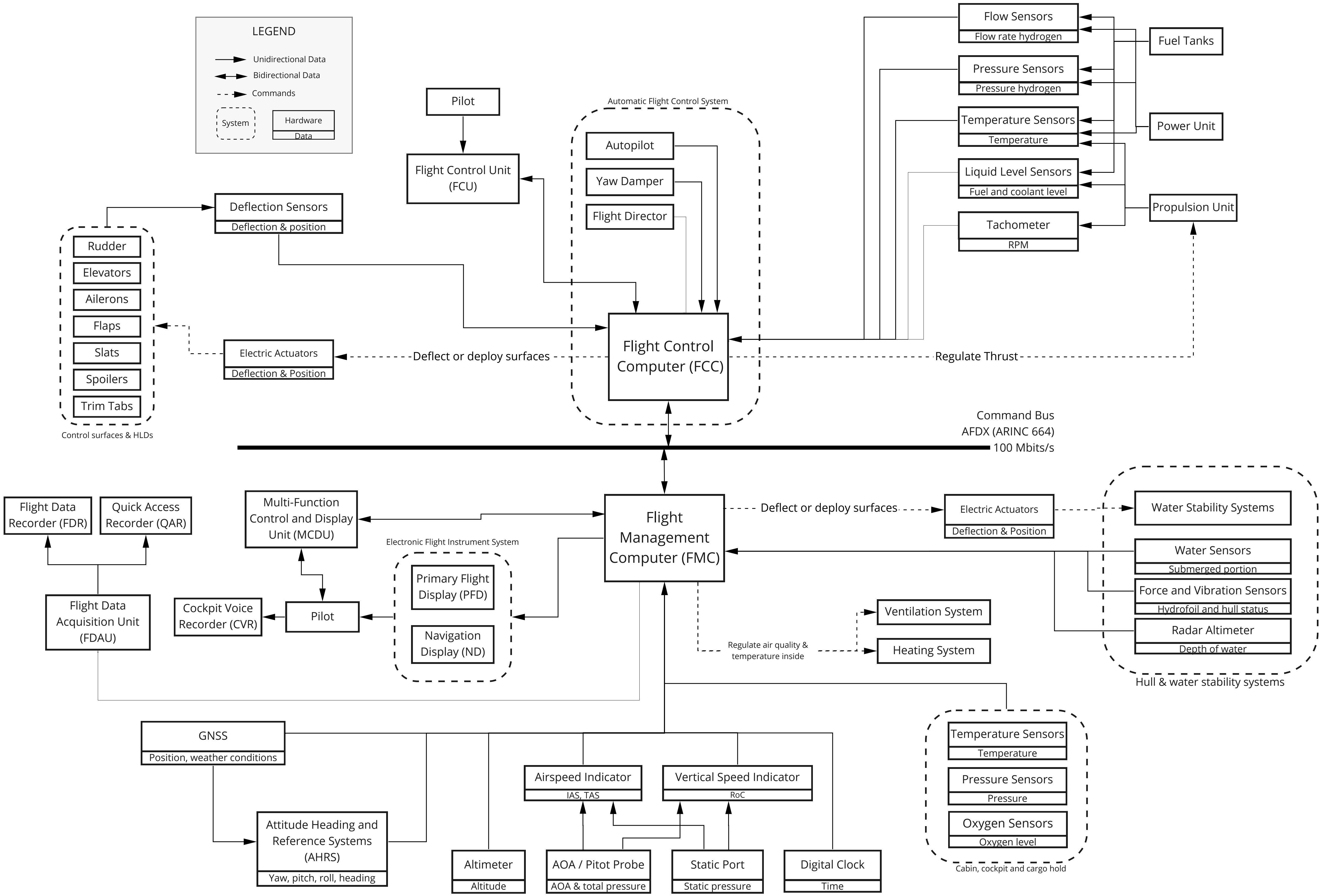

Figure 9.4: *Data handling block diagram*

9.4. Communication Flow Diagram

The Communication Flow Diagram in Figure 9.5 provides a visual representation of how the Emperor will communicate with either the ground or with the surrounding aircraft. When the Emperor is at port or flying in its proximity, the pilot will communicate with the port control to get permission to do a maneuver. He/she will also receive instruction from the port control regarding any unexpected maneuvers he/she may need to perform. Once the Emperor is crossing the Atlantic, ground control radars cannot track their position for most of the time they are cruising. Therefore, pilots are obliged to communicate every fourteen minutes with a control station and provide their position and status. In order to get their position, aircraft use GPS and receive signals from the satellites. Moreover, four ground stations control the Atlantic airspace and when the aircraft crosses from one area to the other, the ground stations inform each other. This is called handover. As well as communicating with the ground, aircraft also communicate with close by aircraft. To avoid collision, they are equipped with an Airborne Collision Avoidance System, ACAS, which in Europe reduces the risk of collision by a factor of around five[3]. This system has been implemented in the Emperor for additional safety, but little traffic is expected at the cruise altitude of 3,000 $[m]$.

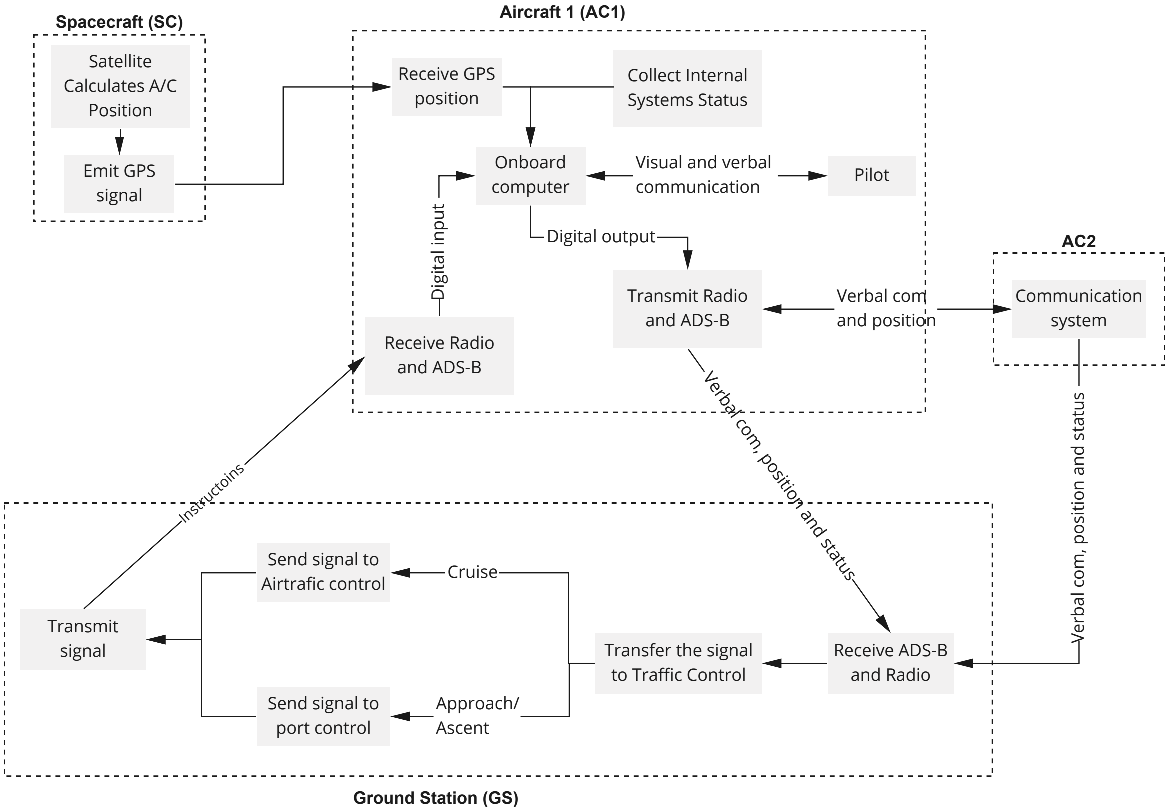

Figure 9.5: *Communication Flow Diagram*

[3]https://www.eurocontrol.int/system/acas, accesed 31/05/2022

10

Production, Operations and Logistics

After the design has been finalised during the DSE, the Emperor will go into the production phase and ultimately become operational. This chapter describes the activities to be executed in the post-DSE stage. Section 10.1 elaborates on the securing of funding, certification and manufacturing of the Emperor. A production plan is then set out in Section 10.2 and the activities are given a timeline and order in a Gantt-chart in Section 10.3. Finally, the anticipated operations are given in Section 10.4 as a flow diagram and on-ground handling is also discussed.

10.1. Project Design & Development Logic

"The Project Design & Development (PD&D) logic shows the logical order of activities to be executed in the post-DSE phases of the project. Figure 10.1 represents the post-DSE phases starting from an extension of the detailed design, continuing to proof of concept and ending with the first delivery. The goal of this chart is to present a path to the market aimed at parties interested in taking over the project." [1].

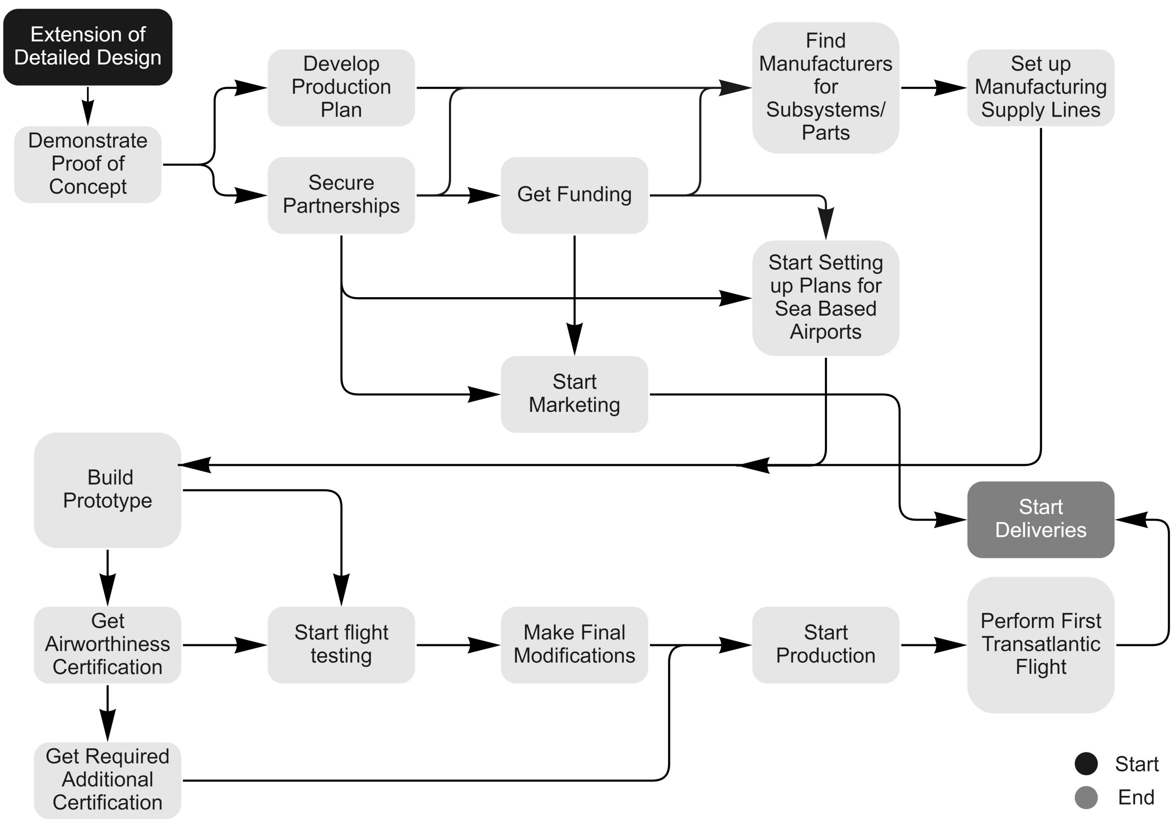

Figure 10.1: *Project design & Development logic*

Once the Design Synthesis Exercise is finished, further development in the design phase is required. This will include an even further detailed design, making use of amongst other further calculations, CFD, and wind tunnel testing. Once the detailed design is completed, the main concern is bringing it to market.

The primary steps needed to complete the detailed design phase include:

- Detailed design and integration of the floats into the wing structure.
- Manufacturing and wind tunnel testing of a scale model.
- Analysis of takeoff and landing procedures using CFD to understand the air, water, aircraft interactions, along with forces experienced by aircraft.
- Analysis of active control systems for ensuring passenger comfort.
- Determination of exact material choice for every component.
- CFD analysis of aerodynamic forces and moments in every configuration of the Emperor.
- Testing of the engine unit to confirm properties at sea-level and altitude.
- Testing of fuel tank units to confirm their properties.
- FEM analysis of the fuselage hull structure to determine the desired thickness.
- Sizing of Vertical Tail for critical condition.
- Water tunnel testing of the scale model.

”The first thing that needs to be generated is some sort of proof of concept. This is necessary to attract outside parties to the project. After generating some interest in the project, the next step would be to form partnerships. These partnerships are vital with regards to funding, marketing, operational and production needs. At the same time, a final production plan needs to be developed.

Financial partners are crucial for obtaining funding. As the manufacturing process starts, various costs start to develop. Thus far, the development has been very cheap, by employing unpaid aerospace engineering students to design the Emperor. Furthermore there will be marketing and certification expenses. As the design is a one-of-a-kind solution to the sustainability problem of transatlantic flight, everything has to be certified thoroughly.

Another challenge the Emperor has to deal with is the lack of facilities for sea-based operation. Therefore, plans should be set up with current airports and/or governments to produce the required facilities for the operations. This is a very important part of the process, as without the facilities available it is highly unlikely anyone would be willing to buy the Emperor.

With the funding secured the Emperor can get advertised to airlines, especially those operating transatlantic flights. Furthermore, the project needs to look for manufacturers for parts, and if needed specialized factories may be set up. Since the parts and materials need to come from various factories, a detailed supply logistics plan needs to be set up. With the supply lines set up the assembly of a prototype can start.

After the prototype has been built it needs to get certified. When the airworthiness certification is given, test flights can start. During the test flights the final modifications will be made to the design. When all certifications are in and the final design is complete, the production can start and the first transatlantic test mission can be flown. After a successful test mission, orders can start getting fulfilled. ” [1]

10.2. Manufacturing, Assembly & Integration plan

"The manufacturing, assembly and integration plan shows the necessary steps to produce the Emperor, as shown in Figure 10.2. It includes parallel and sequential activities to manufacture and assemble the final product. The wing, fuselage, nosecone and tailcone assembly are performed in parallel, as can be seen on the left of the diagram. Once these four components are assembled and integrated, various subsystems are further integrated into the assembly. The categories cabin/cargo and power system can be done in parallel and show various tasks that need to be performed. These two categories flow into the main branch, which continues to the assembly of the propulsion system. The propulsion system is integrated lastly to minimise risk for this costly subsystem. Ultimately, the Emperor gets painted and the flow results into the final assembly."[1]

10.3. Project Gantt Chart

Figure 10.3 shows the post-DSE timeline of the project from further detailed design to the beginning of aircraft deliveries. The main steps of this process to delivery and their relations have already been shown in the Project Design & Development Logic in Figure 10.1.

Firstly, the Extended Detailed Design is specified as this is required for further development of the Emperor. This includes the Computational Fluid Dynamics (CFD) analysis of both the aircraft's hydrodynamics and aerodynamics. In this stage, a singular propulsion unit will also be tested and it's performance will be analysed. Furthermore, in this early stage the structural testing of the fuel tank can start, as the fuel tank design and materials are unlikely to change significantly. Securing the safety certification of the hydrogen fuel tanks will be a long process due to the many safety standards it has to comply with in order to ensure safe hydrogen storage. This will include destructive and life cycle testing.

Before the production of the Emperor can begin, some form of partnership or governmental funding will have to be arranged. Methods of production are also to be developed together with the manufacturing companies and partners.

As the Emperor will use a sea-based airport which will be a new innovation in the aviation sector, further research and development has to be conducted to ensure its successful implementation. More specifically, its construction, location, functionality, demand and surrounding infrastructure have to be further analysed.

The final stage of development will consist of the prototyping and flight testing. The results of these tests will be used to make further modifications and improvements to the Emperor to increase its overall performance. Once the prototype shows acceptable flight performance, the aircraft can enter the production and delivery stage.

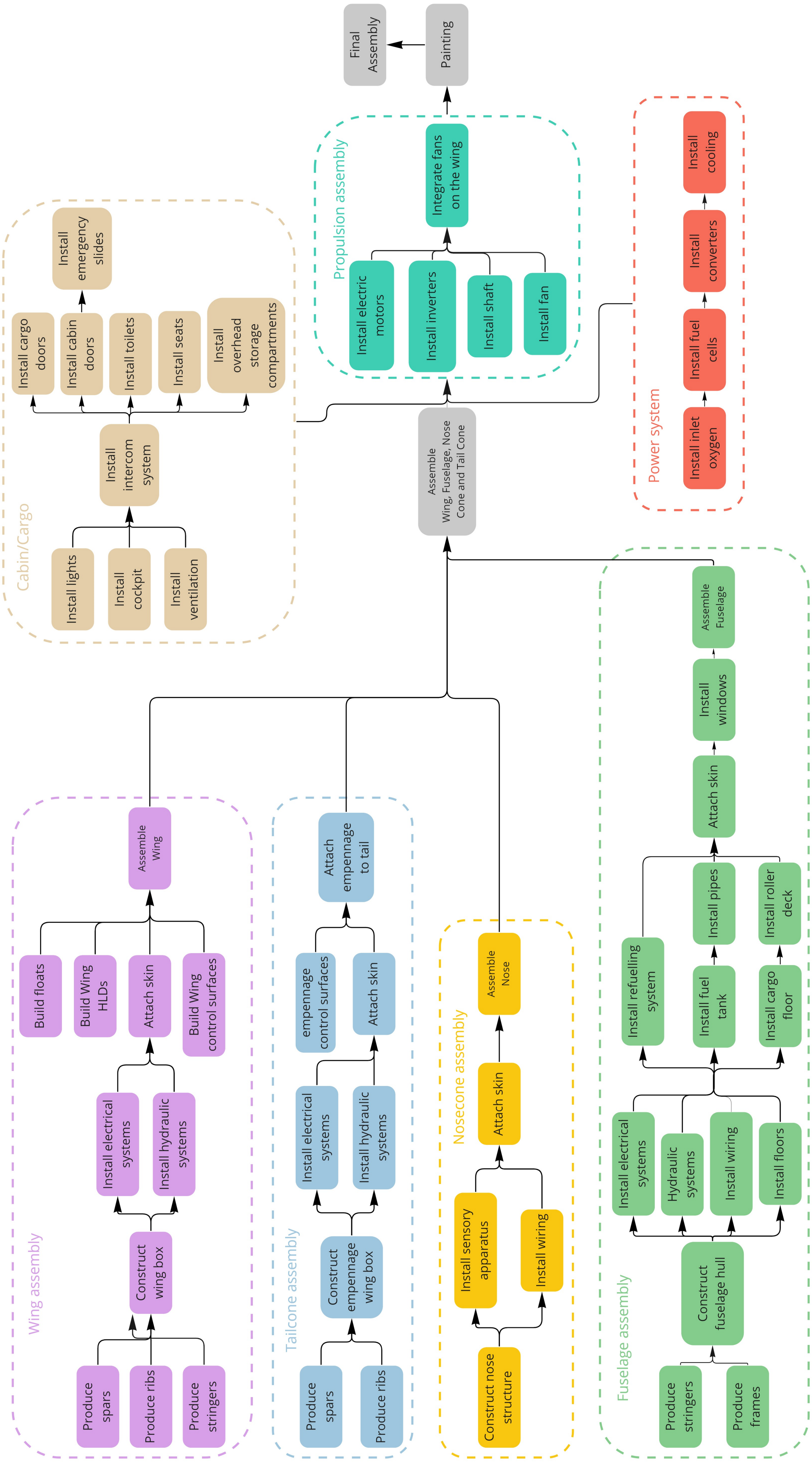

Figure 10.2: *Manufacturing, Assembly and Integration Plan*

ID	Task Name	Duration	Start	Finish
1	**Extended Detailed Design**	**920 days**	**13-6-2022**	**19-12-2025**
2	Further Detailed Design	200 days	13-6-2022	17-3-2023
3	Wing Float integration	120 days	13-6-2022	25-11-2022
4	Scale model production	28 days	20-3-2023	26-4-2023
5	Wind tunnel Testing	120 days	27-4-2023	11-10-2023
6	CFD Analysis for Take-Off Performance	30 days	20-3-2023	28-4-2023
7	Analyse Active Control Systems	100 days	13-6-2022	28-10-2022
8	Determine exact material choice components	120 days	13-6-2022	25-11-2022
9	CFD Analysis for Aerodynamic Forces and Moments	30 days	1-5-2023	9-6-2023
10	Propulsion Unit Power Test	720 days	20-3-2023	19-12-2025
11	Fuel tank Integrity testing	720 days	20-3-2023	19-12-2025
12	Demonstrate Proof of Concept	120 days	20-3-2023	1-9-2023
13	Develop Production Plan	200 days	13-6-2022	17-3-2023
14	**Secure Partnerships**	**555 days**	**4-9-2023**	**17-10-2025**
15	Develop Partnership approach	90 days	4-9-2023	5-1-2024
16	Approach Governmental organisations	300 days	8-1-2024	28-2-2025
17	Approach Airlines	125 days	8-1-2024	28-6-2024
18	Approach Manufacturing Companies	125 days	8-1-2024	28-6-2024
19	Secure Partnerships	165 days	3-3-2025	17-10-2025
20	Secure Funding	600 days	20-10-2025	4-2-2028
21	**Set up production**	**900 days**	**20-3-2023**	**28-8-2026**
22	Find Manufacturers	300 days	20-3-2023	10-5-2024
23	Set up Manufacturing Supply Lines	180 days	13-5-2024	17-1-2025
24	Design / Set up Manufacturing Equipment	600 days	13-5-2024	28-8-2026
25	**Marketing Campaign**	**60 days**	**20-10-2025**	**9-1-2026**
26	Develop Marketing Strategy	40 days	20-10-2025	12-12-2025
27	Launch Marketing Campaign	60 days	20-10-2025	9-1-2026
28	**Sea Based Airport Development**	**2360 days**	**12-1-2026**	**26-1-2035**
29	Define possible Sea-Based Airport Locations	30 days	12-1-2026	20-2-2026
30	Analyse Sea-Based Airport locations	285 days	23-2-2026	26-3-2027
31	Research surrounding Infrastructure Oppurtunities and Risks	180 days	29-3-2027	3-12-2027
32	Determine Sea-Based Airport Locations	165 days	6-12-2027	21-7-2028
33	Start Setting up Plans for Sea Based Airports	270 days	12-1-2026	22-1-2027
34	Construct Sea Based Airport Proof of concept	350 days	25-1-2027	26-5-2028
35	Design Sea Based Airport	1100 days	29-5-2028	13-8-2032
36	Construction Sea Based Airport	640 days	16-8-2032	26-1-2035
37	Expected completion Sea Based Airport	0 days	26-1-2035	26-1-2035
38	**Build Prototype**	**730 days**	**25-1-2027**	**9-11-2029**
39	Prototype design	140 days	25-1-2027	6-8-2027
40	Prototype production	320 days	9-8-2027	27-10-2028
41	Protorype Testing	180 days	30-10-2028	6-7-2029
42	Testing results verification & validation	90 days	9-7-2029	9-11-2029
43	Get Airworthiness Certification	1625 days	25-1-2027	15-4-2033
44	**Start flight testing**	**500 days**	**18-4-2033**	**16-3-2035**
45	Subsystem Testing	300 days	18-4-2033	9-6-2034
46	System Testing	200 days	12-6-2034	16-3-2035
47	Structural Tests	400 days	18-4-2033	27-10-2034
48	Flight Performance Testing	100 days	12-6-2034	27-10-2034
49	Testing results Verification & Validation	500 days	18-4-2033	16-3-2035
50	Make Final Modifications	100 days	19-3-2035	3-8-2035
51	Get Required Additional Certification	500 days	18-4-2033	16-3-2035
52	**Start Production**	**340 days**	**6-8-2035**	**21-11-2036**
53	Produce Parts	140 days	6-8-2035	15-2-2036
54	Parts Assembly	90 days	18-2-2036	20-6-2036
55	Final Assembly	20 days	23-6-2036	18-7-2036
56	Final System Testing	90 days	21-7-2036	21-11-2036
57	Perform First Transatlantic Flight	14 days	24-11-2036	11-12-2036
58	Start Deliveries	0 days	11-12-2036	11-12-2036

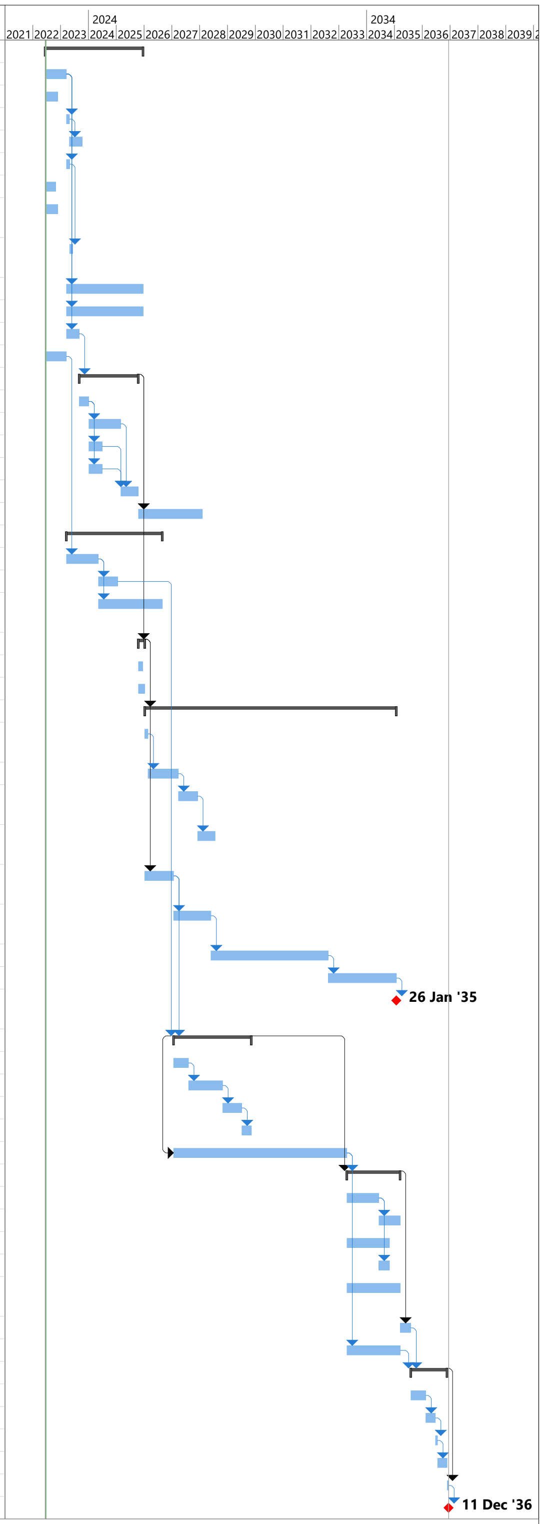

Project: Post_DSE5
Date: 21-6-2022

Task | Split | Milestone | Multiple Task Subset

Figure 10.3: *Project Gantt chart*

10.4. Operations and Logistics

Operations and logistics are an essential part to take into account when developing a design concept. Details about the operations allow determining a more accurate operational cost estimation and also help assessing the feasibility of the design. The flow of operations and the logistics around operating a large sea-based aircraft are addressed and summarized in a flow diagram containing the relevant steps to be followed. Then, a potential layout of the water port is presented. Next, the refueling operations are considered in more detail. Finally, a small note regarding the training of the pilots is included [1].

As it has been already presented, the Emperor will require water operations due to its large size. Therefore, operations and logistics differ from those of conventional aircraft and will share similarities with those of large cargo or cruise ships. Figure 10.5 shows the flow of the operations for the entire life-cycle of the Emperor. The flow starts when the Emperor is already at the dock. Weather and sea conditions are checked in order to ensure that the Emperor can take-off and fly safely. Given its large size, it was found that waves up to 2.99 $[m]$ could be safely handled as was explained at the end of Section 6.2. When conditions are deemed acceptable, the loading of the Emperor can begin.

The turnaround time of the Emperor is estimated to be 2.9 $[h]$ (or 174 $[mins]$). This has been estimated given a refuelling rate of 35500 $[kg/h/\mathrm{pump}]$ with 3 pumps being used (given that there are 3 fuel tanks on board)[2], a loading/unloading cargo rate of 43.4 and 50 [containers/h] respectively and a boarding/deboarding rate of 1080 and 1680 $[pax/h/\mathrm{door}]$ [3]respectively with 8 doors in operation. The cargo containers are also separated into bag containers, which can hold 30 bags each, and cargo containers which can store 13300 $[lbs]$ or 6032 $[kg]$ of additional cargo each [4]. This results in 50 bag containers and 17 cargo containers. It should be noted that the cargo time and cabin time refers to the time it takes to both fully unload from the previous flight and then once again load for the next one. Also factored into the cabin time is the time required for cleaning, catering and any last passenger delays. It is found that the refuelling time is 1.41 $[h]$, the total cargo related time is 2.90 $[h]$ and the total cabin related time is 1.10 $[h]$. Evidently, the turnaround time is limited by the cargo time. To improve the safety aspects of the operations and make for a better passenger experience, the cargo could be unloaded/loaded first in parallel with the deboarding of passengers and the cleaning of the cabin, then in parallel with refueling and then in parallel with the boarding and catering of new passengers only once it is already refueled. A flow detailed diagram of this procedure can be seen in Figure 10.4.

Once loading is complete, the pilot can run through the pre-flight checklist and the cabin crew can prepare the cabin for take-off. If no problems are detected during the pre-flight checks the flow of operations continues. If a problem is detected but is small, it will be fixed directly such that the operations can continue. Else, the Emperor has to be unloaded and brought to maintenance. The normal flow of operations continues by getting permission to undock. A tug boat guides the Emperor out of port and onto the runway area and a check is made to ensure that rescue teams are on standby if needed. When this is verified, the Emperor is permitted to take-off. During cruise there will be ongoing communications with the sea-ports and marine control and also with regular air traffic control authorities. Flying at only 3,000 $[m]$, the Emperor

[1]Much of this section has been adapted from the Midterm Report. The original can be found in [1]

[2]https://cryostar-hydrogen-solutions.com/liquid-hydrogen-transfer-pumps/, accessed 14/06/2022

[3]https://www.researchgate.net/publication/322508783_Fast_Aircraft_Turnaround_Enabled_by_Reliable_Passenger_Boarding, accessed 15/06/2022

[4]https://aviation.stackexchange.com/questions/17564/what-is-the-average-time-taken-to-load-and-unload-the-luggage, accessed 15/06/2022

will be in a band of its own and will easily avoid other aircraft. This also allows for the potential of 24 hour flight in both directions crossing the Atlantic.

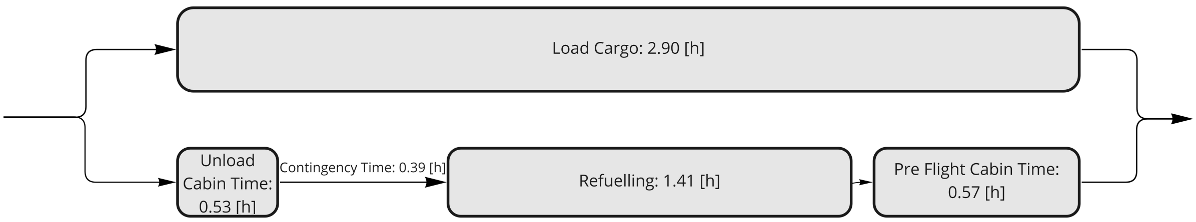

Figure 10.4: *Turnaround operations flow diagram*

Once the Emperor is approaching its destination, the pilots get permission for landing by the sea-port traffic control. Naturally, emergency services are available if needed. Once it lands, taxiing through the port is done again with the help of a tug boat and permission is received to enter and dock. Unloading of the passengers, cargo, luggage and waste happens in parallel. The unloaded waste is taken to a recycling or compost plant and water goes to a purifying plant. Cargo is taken to storage and the luggage to the luggage hall. To unload the passengers the seaport will have platforms with movable ramps, after which the passengers are transported to the luggage hall. Passengers pick up their luggage and then pass custom checks. After everything is unloaded, the cabin of the Emperor is cleaned and turn around maintenance checks and procedures are performed.

Maintenance is especially important for the Emperor given its sea-based nature. The salt water will accelerate degradation and thus being proactive is vital for the longevity of the system. If minor problems are detected they will be fixed on dock. If large problems are found, they will be fixed in a maintenance dock and if the aircraft needs to be taken out of the water to fix them, it will be taken to the custom-made sea-port hangar. If they are too significant or numerous, a decision is made to discard the Emperor, which would be the end of the operational loop. The end of life is discussed further in Chapter 11. If the problems are fixed, the Emperor is moved back to dock and normal operations continue.

As seen from Figure 10.5, the cycle of operations would require complex logistics to optimize all procedures. An efficient lay-out of the sea-port can be used to streamline ground based operations. Extensions can be made to existing ports which already have strong infrastructure in place to minimize development costs. When choosing the port at which the sea-port will be built, the proximity of an airport is an essential factor to ensure passengers from non-coastal regions can reach the sea-port. A transport network, combining trains and flights should be used to ensure easy access to flying in the Emperor.

An illustration of the sea-port can be seen in Figure 10.6. The terminal is a combination of a ground building where security, drop-off and pick-up of luggage will be preformed and a floating dock supported by pontoons, used to load passengers, cargo, fuel and supplies as well as to perform pre- and post-flight checks and maintenance. The reasoning behind using pontoons is to allow the dock to adapt to the tide level and therefore to the Emperor itself, which will also be floating. This way, the distance between the pontoon and the aircraft doors is independent of the water level and operations are more consistent and therefore easier.

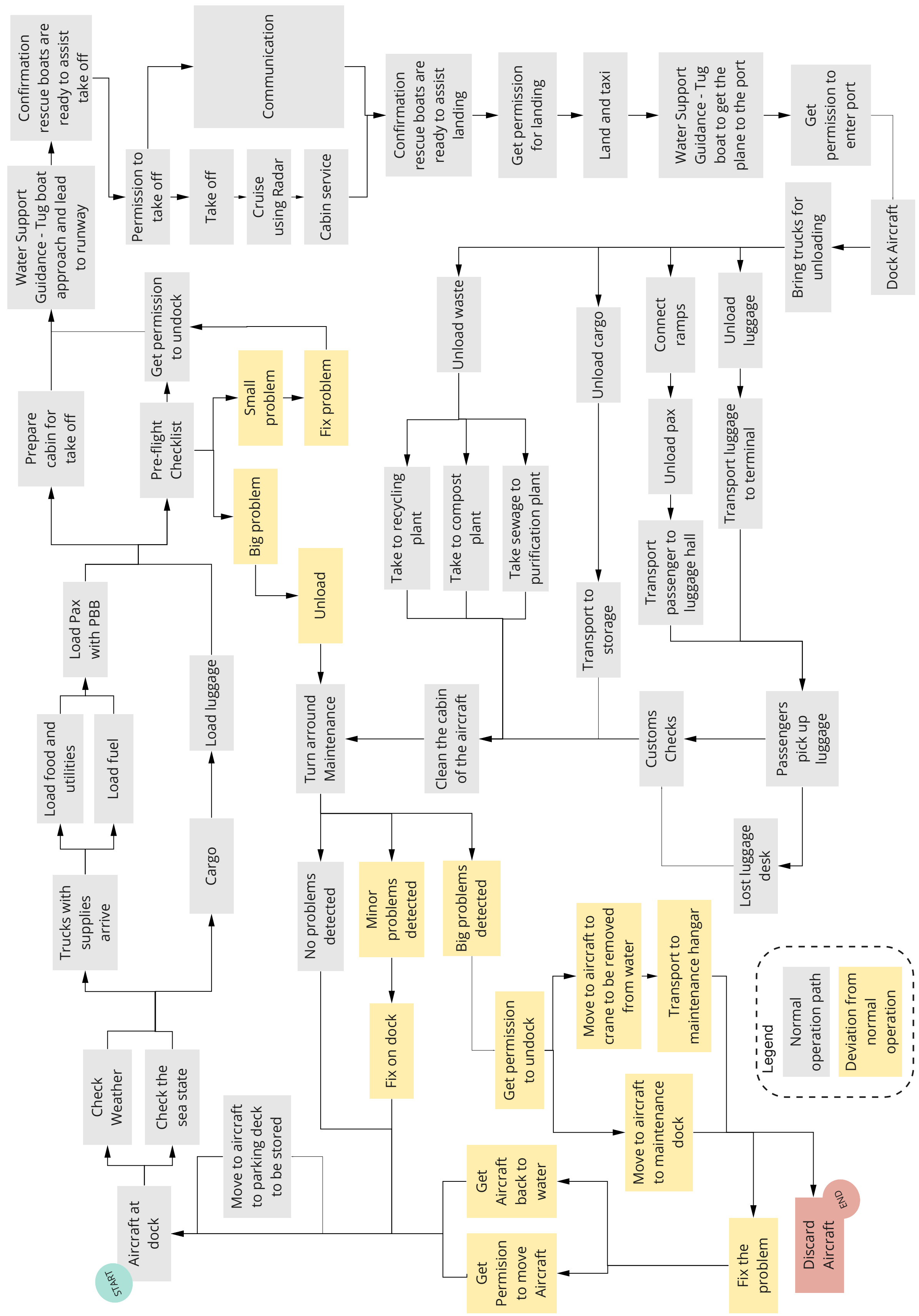

Figure 10.5: *Flow Diagram of the Operations and Logistics needed for the Emperor*

The floating dock will have a platform with two floors, which can clearly be seen in Figure 10.6. The platform will be connected to the main building through the use of pivoting joints, similar to those in an articulated bus, to allow for the movement of the floating structure. Passengers will walk on the top floor of the platform to their gate and then go to the ground floor to board. The bottom floor of the platform and the rest of the floating jetty is reserved for trucks, luggage transportation and any other sorts of transportation needed in the seaport. An important aspect to take into account is that the cargo door will be at the back of the Emperor. Since the aircraft is parked with the nose towards land, the back of the aircraft will point toward the water. For this reason, there will be two methods that can be used to load the cargo, which is using a boat with a crane to load the cargo or using a ramp from land that leads into the cargo compartment.

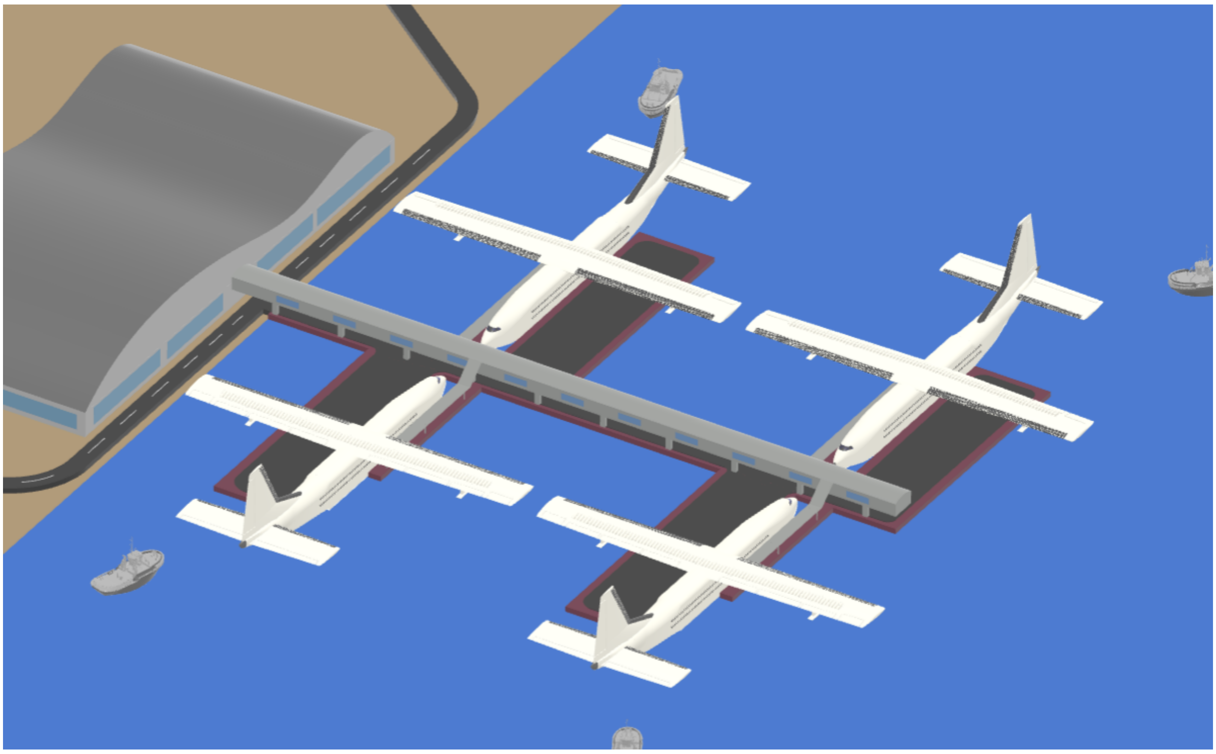

Figure 10.6: *General Seaport layout*

As explained in the flow of operations in Figure 10.5, while docked the Emperor is refuelled. A diagram of what this could look like is seen in Figure 10.7. As it was mentioned before, given that there are three tanks, three of these pumps are to be used simultaneously. Multiple studies have been done which attest to the feasibility of this concept [7]. Moreover, fuel pumped in through underground pipelines rather than from trucks or tankers would help to facilitate the large quantities required. For the Emperor, due to the consideration of a floating dock, the pipes will run though this floating structure until land is reached and therefore the dock should have a fairly thick platform that is able to house these conduits. Nevertheless, refueling operations remain a challenge using present day technology and is an active area of research. An example of what has been deemed possible by several studies can be seen in Figure 10.7 [7].

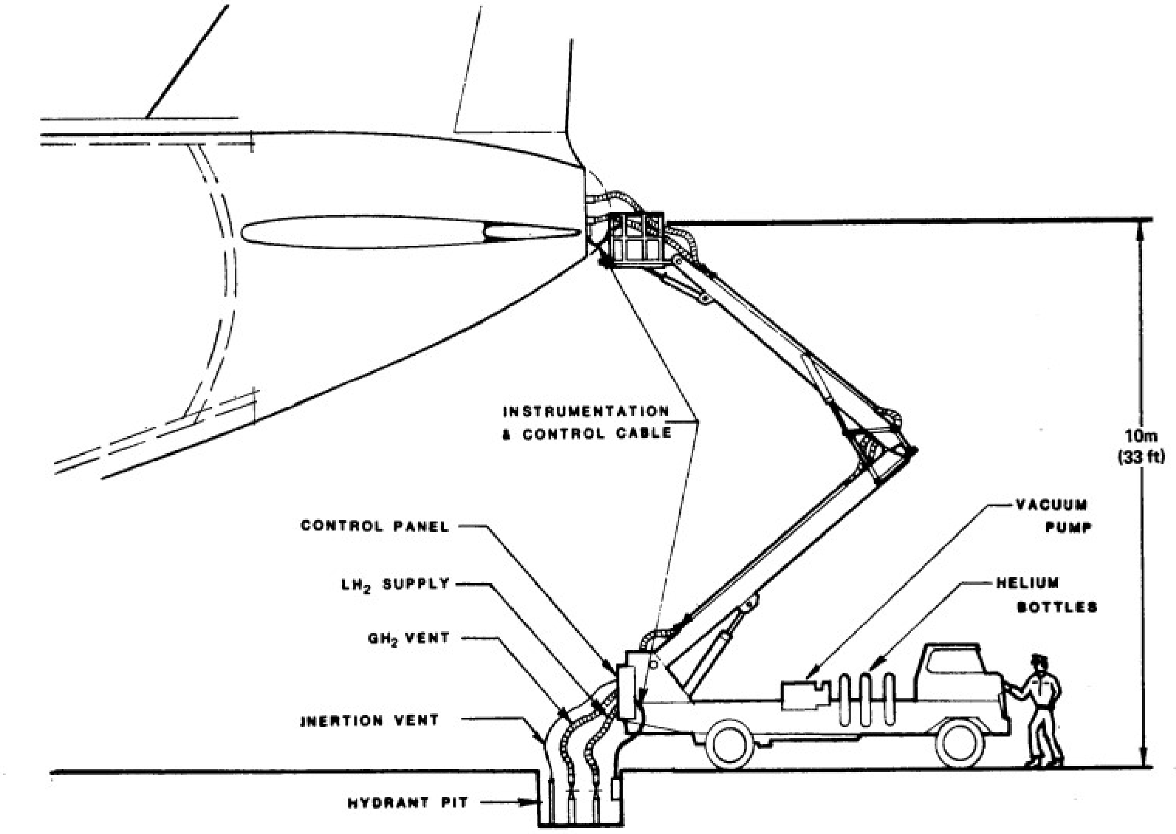

Figure 10.7: *Liquid hydrogen refuelling operations [7]*

Another challenge regarding the refuelling is the pre-cooling of the hydrogen tanks. In order to limit hydrogen waste, a closed loop will be set up including the onboard and external hydrogen storage tanks and a refrigeration system. Hydrogen will flow through this loop until the correct temperature is achieved, after which the onboard tank can be refuelled. This process can be accelerated by increasing the pipe diameter, as well as having a lower initial tank temperature [52].

Finally, the training of the pilots has to be addressed. Due to sea-based operations and docking in a port, pilots must be specially trained. They should be fully aware of the unique challenges that are present and also should be aware of the safety rules. Therefore, it will be necessary to grant special certifications in order to be allowed to pilot the Emperor. This would come as an annoyance to prospective operators but it is an unavoidable and necessary undertaking. The cabin crew must also receive special training due to the difference in safety procedures in a sea-operated aircraft.

11 Sustainability

The Brundtland Commission in 1987 defined sustainability as ”sustainable development is development that meets the needs of the present without compromising the ability of future generations to meet their own needs”[1]. The main idea behind using green liquid hydrogen as a fuel instead of kerosene is reducing the use of fossil fuels and atmospheric emissions, which is a direct contribution to the sustainability of aviation. However, in order to provide a sustainable means to cross the Atlantic, more aspects of the design and development of the Emperor have to be considered. The three pillars of sustainability are the environmental, economical and social sustainability. These three factors will be investigated and balanced in equal harmony to achieve true sustainability[1] and will be discussed in Section 11.1, Section 11.2 and Section 11.3 respectively. As a conclusion, the larger contribution of the Emperor to overall sustainability will be discussed in Section 11.4.

11.1. Environmental Sustainability

Environmental sustainability means using available resources at a sustainable rate [1]. In order to ensure that the design respects this in all of its phases, from design to operations, three different aspects have been considered: the use of hydrogen, the used materials and the operations.

The use of hydrogen as the fuel to generate electricity through fuel cells implies the avoidance of the polluting gases emitted by combustion. This ensures that during flight, the emission of carbon dioxide (CO2), nitrogen oxides (NOx), sulphur oxides (SOx), unburnt hydrocarbons (HC), carbon monoxide (CO), particulate matter (PM) and soot, which are regular products kerosene combustion [2], can completely be avoided. The energy provided by the fuel cells will not only be used to power the engines, but also to provide all electricity used in the Emperor, such as for powering the communication or data handling systems. Furthermore, it is important to note that, when generating electricity, the fuel cells also generate water vapour as a result of the internal chemical process. If this water vapour was to be released into the atmosphere, the Emperor would not be emission free. Since the resulting water vapour is pure water, it will be liquefied and mineralised in order to use it for flushing the toilets and as tap water. As a large amount of water vapour is produced, not all liquefied water will be needed for this purpose, and all excess liquefied water will be thrown out. This way, not all the water is wasted and only part of the water is emitted to the outside environment, and a more sustainable water use is accomplished.

It is also important to note that the hydrogen used as fuel must be green hydrogen, meaning

[1] https://circularecology.com/sustainability-and-sustainable-development.html#:~:text=Social%20Sustainability%3A%20Social%20sustainability%20is,maintained%20in%20the%20long%20term, accessed 07/06/2022

[2] https://www.easa.europa.eu/eaer/topics/overview-aviation-sector/emissions, accessed 20/06/2022

it was obtained by electrolysis powered by renewable energies[3]. Otherwise, despite yielding zero emissions during operations, its obtainment would not be sustainable. The final aspect regarding the hydrogen is that leakage to the atmosphere must be avoided at all cost, since it reacts with the ozone layer and breaks it down. "Due to the high flammability of hydrogen, safety protocols are higher than for natural gases[4]." [1]. This includes the refuelling and transport of liquid hydrogen in highly reliable and safe systems[5]. "Moreover, a leak detection system with sensors placed at strategic locations will quickly indicate a leak, causing venting of the hydrogen if needed and this will be repaired before next flight"[1].

Regarding the materials used in the Emperor, the largest contribution to sustainability is to use as little material as possible, therefore, the aim is to minimize material waste. In order to do so, the philosophy of lean manufacturing will be applied. For instance, the methods and techniques chosen for manufacturing the parts will be chosen optimally in the basis of minimising waste. Another measure, is that when using metal sheets to manufacture parts, they will be used in the most efficient way to minimise waste. On the other hand, the use of materials whose obtainment and processing are most harmful for the environment must be minimized and substituted for more sustainable options when possible. For example, the lubricants used in the engines can be biodegradable, or the external paint can be non-toxic to decrease harm to the surroundings.

The aim is that at the end-of-life, most parts can be reused or repurposed, if not recycled. The Emperor will be fully disassembled, easing the recyclability of parts made up of single materials, e.g. metallic parts can always be melted and re-purposed. Due to the high performance expected from materials in the aviation industry, the bulk of the parts will be reused in other industries that require lower performing materials, such as the naval industry. The materials that can not be reused or recycled for other purposes require proper disposal to minimize their impact on the environment. Parts will be taken to a controlled graveyard that minimizes the impact of waste to the environment. Finally, ideally, all manufacturing facilities will be powered using renewable energy sources.

The final aspect for environmental sustainability is to allow for sustainable operations. The noise generated must be limited to reduce impact on the surrounding ecosystem and communities. Acceptable noise emissions are ensured by the use of fans instead of propellers. Also, use of land or water should be minimized by limiting, to a possible extent, the runway length and the space used for the airport, by optimizing the layout and eliminating unnecessary parts such as the duty free store. Furthermore, the seaport infrastructure will be powered by renewable energies, such as solar panels and off-shore wind energy. The waste generated will be managed in a proper manner, taking waste water to water-waste treatment plants, and trash to recycling facilities and compost plants. Finally, the used cleaning products should not be harmful for the environment.

11.2. Economic Sustainability

Economic sustainability means using resources efficiently and responsibly such that a profitable organisation can be operated over the long term[1]. Economic sustainability is required to ensure profitable operation and sustain this profit long term. To ensure successful operation, resources have to be utilized efficiently to prevent waste of time, money and materials.

[3] https://greenhydrogensystems.com/, accessed 07/06/2022

[4] https://www.euractiv.com/section/energy/news/scientists-warn-against-global-warming-\effect-of-hydrogen-leaks/, accessed 04/05/2022

[5] https://www.linde-engineering.com/en/plant-components/hydrogen-refueling-technologies/index.html, accessed 07/06/2022

Lean manufacturing should be an integrated practice in the manufacturing process as mentioned previously, hence waste should be continuously eliminated with the goal of creating value for stakeholders [53] resulting in an increase in profitability. Transport is a source of waste, as it does not add value to a product. However, transport often cannot be eliminated completely, but it can be reduced to a viable extent. The manufacturing and assembly will be performed in Europe, which will minimise the need for long-range or overseas transport. Furthermore, the transport within Europe should be structured in such a way that it is minimized. Existing establishments will be used to avoid the need of having to build all new infrastructure for the production process. Hydrogen powered vehicles, such as trucks, boats and aircraft, are expected to evolve and be more commonly used in the future. Therefore, ideally all transport that cannot be eliminated for the production process should be performed using emission free vehicles. Within the production process in a factory, the production line should be structured such that unnecessary transport is avoided as much as feasible. Furthermore, all necessary tools and equipment should be readily available to avoid waste of time. Repairs are another source of waste, thus quality assurance during the production phase is critical to prevent the necessity for repairs and avoid the obligation to scrap parts due to defects. The Emperor shall be designed with the aim of being relatively easy and affordable to repair during operation to avoid high costs and to reduce the risk of having to discard the Emperor prematurely.

To be able to sustain profit long term, the interests of the various stakeholders have to be balanced and fulfilled. The company has to set up rules and processes by which transparency and accountability is ensured, to conserve the confidence of the stakeholders. Furthermore, proper risk management is critical to ensure profitability. Any risk that might increase costs has to be taken into account properly to assure that a company can remain profitable in the long term. Risks are further elaborated upon in Chapter 14. As mentioned in Section 11.1, the seaport, and preferably the manufacturing facilities, shall use renewable energy sources. The facilities should be energy neutral, thus all power that is utilized should be generated by these energy sources. By investing in these means for renewable energy sources, such as wind parks or solar panels, profit can be obtained in the long term by ensuring independence of energy companies and thus prices.

The Emperor is designed to have an operational life comparable to current day aircraft. The operational life should be sufficiently large to be attractive for airlines, such that it will be competitive. The price of green hydrogen is expected to decrease in the future thus assisting in making the Emperor more profitable. ”Additionally, it is expected that jet fuel will become more scarce and expensive in the future due to the decrease in available fossil fuel sources and the uncertainty introduced by e.g. wars.” [1].

11.3. Social Sustainability

”Social sustainability is the ability of society, or any social system, to persistently achieve a good social well being. Achieving social sustainability ensures that the social well being of a country, an organisation, or a community can be maintained in the long term”[1].

In order to achieve a good social well being it is essential to ensure that throughout the design and manufacturing process the employees receive fair wages, are treated with respect, and are given the rights and benefits they deserve. Manufacturing is at the moment designed to take place in Europe, and therefore regulations regarding workers rights in each country must be respected. A benefit of manufacturing in Europe is the creation of new jobs, which benefits the economy of the different countries but also boosts the reputation of the Emperor for the customers and passengers. Furthermore, when buying parts and materials from other parties, due to this social responsibility, it must be ensured that these products are not the result of child labor or worker exploitation.

Furthermore, customers and passengers must also be treated fairly and given the rights they deserve. Safety must be ensured for the passengers during flight, which will be assured by proper design and manufacturing, but also execution of proper safety protocols by airlines. The tanks and hydrogen refuelling systems are safe and reliable to avoid leakage, as mentioned in Section 11.1, thus will not pose a threat to the passengers.

In addition, the Emperor brings a lot of benefits for the airlines, as it boosts their image and they can sell it as an experience for their passengers. Airlines that use this type of aircraft will be able to show that they meet their environmental and social responsibilities. It will make airlines participants of the energy transition quest and they might even receive help through funds of governments to be able to make this transition. For the passengers, the Emperor is attractive, since it makes them feel they can make a difference for the planet which will lead to the removal of the existing guilty feelings regarding flying. The use of the Emperor will also help raise awareness for the environmental struggles of our planet.

11.4. Contribution to Sustainability

Combining all the aspects explained in this chapter, the result is a system where sustainability is regarded along all the development phases of the product. Carbon dioxide is considered as the principal greenhouse gas according to the Intergovernmental Panel on Climate Change (IPCC). Aviation represents approximately 2 to 3% of the total annual global $\mathrm{CO_2}$ emissions from human activities, and has impact on climate due its non-$\mathrm{CO_2}$ emissions[6], yielding in 2018 a 3.5% of 'effective radiating forcing', a closer measure of the impact on global warming[7].

For instance, in 2015 a total of 88 million seats were destined to transatlantic flight[8]. In the hypothetical case that the Emperor assumed a market share of 25 % during that year, 22 million passengers would have benefited from its use. Assuming that the average distanced travelled by these flights is 6,000 km, and that every traditional long-haul flight emits 195 g/km/person[9] of $\mathrm{CO_2}$, it can be approximated that, in that hypothetical case, the emissions of $\mathrm{CO_2}$ would have been reduced by $2.574 \cdot 10^{10}$ $[kg]$. In the coming years, where the number of transatlantic flights is only expected to increase, the contribution of the Emperor to a more sustainable future will become even more relevant.

The Emperor is a step forward in achieving long-range, zero-emission aviation, allowing airlines and passengers to play a large role in the green energy transition. This will also boost the production and infrastructure for the hydrogen industry, allowing the use of hydrogen to become more accessible. Hopefully, this project contributes to the survival of future generations and opens a door to pursue innovative green aviation alternatives.

[6] https://www.easa.europa.eu/eaer/topics/adapting-changing-climate/climate-change, accessed 07/06/2022

[7] https://ourworldindata.org/co2-emissions-from-aviation, accessed 07/06/2022

[8] https://www.anna.aero/2015/06/03/transatlantic-market-grows-by-6-in-2015/, accessed 09/05/2022

[9] https://www.robeco.com/en/insights/2020/02/short-haul-flights-are-the-worst-offenders-for-co2.html

12
Market Analysis

A market analysis has been performed to determine the market of the Emperor and to estimate the market share it can occupy. First, similar aircraft are found in Section 12.1 to find the specific market segment. The strengths and weaknesses of the Emperor as well as the threats and opportunities of the market are analysed in Section 12.2. Following are Section 12.3 and Section 12.4 where the specific volume and price are estimated, respectively. Finally, Section 12.5 predicts some future trends that would influence the revenues and costs of the Emperor.

12.1. Potential Market

Existing somewhere in between a long-haul passenger aircraft and a cargo ship, the Emperor is able to service a broad range of needs. This versatility grants access to several addressable market segments, all of which will benefit from a new, sustainable solution. This said, being outside of convention makes analysing and estimating the competitive landscape difficult. Undoubtedly, the area of focus for the current version of the Emperor is mass transatlantic passenger travel. As such, market share will be taken primarily from Airbus and Boeing and it will compete with other wide bodied aircraft such as the A380, A350 or the B747-8.

One evident drawback is that land-based operations would be impossible, eliminating the potential for most transcontinental travel and would for the most part bind the Emperor to only transoceanic travel. While this is not ideal, the available range allows for the access of many of the busiest passenger routes which are on the water-front anyway such as New York to the UK or even the busiest route in the world, the domestic South Korean flight Seoul to Jeju, multiple times in a day without refuelling. Extending this idea, the market appetite in South-East Asia for sea-planes is high. This is due to the vast quantity of separate islands making servicing them with airports difficult. On a single fuel load, the Emperor would be able to service multiple destinations in one round trip, allowing passengers and cargo to be loaded and unloaded at each stop before returning to a large central hub where it can be refuelled and prepared again.

Another noteworthy point would be the introduction of a competitor green energy aircraft. Hydrogen technology is developing at a rapid pace and large investments have already been made by both Airbus and Boeing which helps to indicate the market's appetite for alternative air travel solutions. While this increased competition may be concerning to some extent, the concepts being developed will not operate in the same market segment as the Emperor. In fact, perhaps the Emperor could even be developed in partnership with Airbus and Boeing given that it is a market gap that both partners would be interested in addressing and they may be interested in spreading the risk of a new, large, and unconventional project.

Lastly, given the large volume and heavy lift capabilities, there is the potential for the development of a dedicated cargo version of the Emperor. It would be able to take significantly more than the largest cargo planes while still maintaining an acceptable range and cruise speed.

12.2. SWOT Analysis

Analysing the traits of the Emperor, several strengths and weaknesses are determined. Combining it with the opportunities and threats, a SWOT diagram is made and is visualized in Figure 12.1 which helps to identify where in the market the Emperor may have the most value.

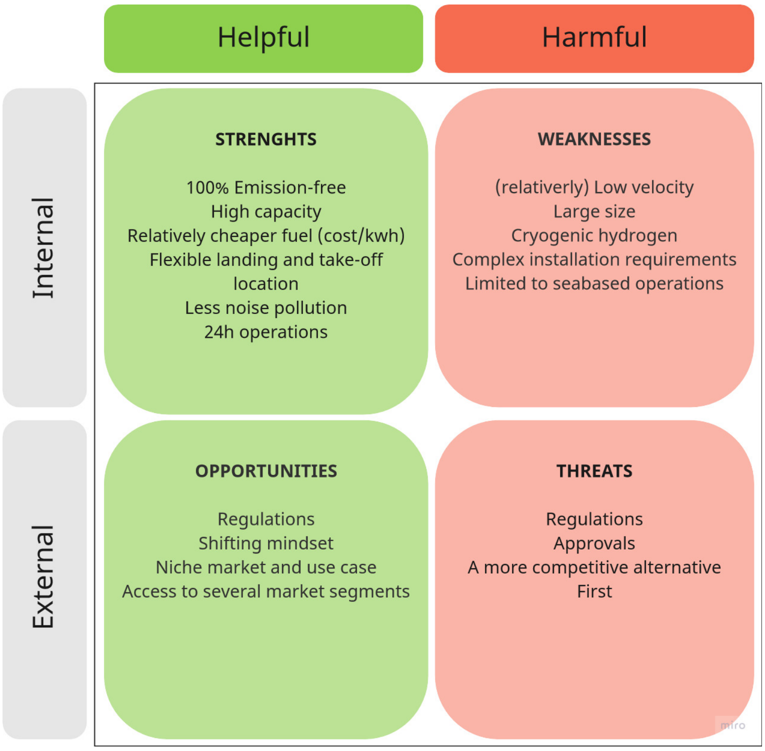

Figure 12.1: *SWOT analysis*

From Figure 12.1 it can be seen that the Emperor has more strengths than weaknesses and more opportunities than threats. Regulations are mentioned both as opportunities and as threats. For example, new regulations can be beneficial when kerosene gets taxed for instance but can also be harmful if hydrogen is deemed unsafe for aviation. A big threat is when a more competitive alternative comes to the market. At this stage there are none in development within the same market segment but as mentioned in Section 12.1, Airbus has several concepts in development [27].

12.3. Market Volume

The quantity of aircraft to be produced is found by taking an average of estimates made by Airbus, Airline Monitor and Boeing regarding 500+ seat aircraft, as seen in Figure 12.2, and assuming a 25% attainable market share as described by Markish [54]. This is seen to be a realistic market share when considering the current market share distribution of the competition within Airbus and Boeing and also factoring in the advanced technology and sustainability of the Emperor leading to increased demand. The average estimate of the 500 seat aircraft with a 50% market share was 717 and scaling it up to represent a 1500 seat aircraft with a market share of 25% lead to a potential production run of 119. Other methods were also used to estimate the quantity demanded and similar conclusions were reached which gives a certain level of confidence in the estimate. It should be noted that given the Emperor is water based, it excludes demand from landlocked regions. This said, most major transoceanic routes are easily accessible which is the target audience. Assuming a 25% market share as opposed to an often suggested 50% market share also serves as a type of contingency factor.

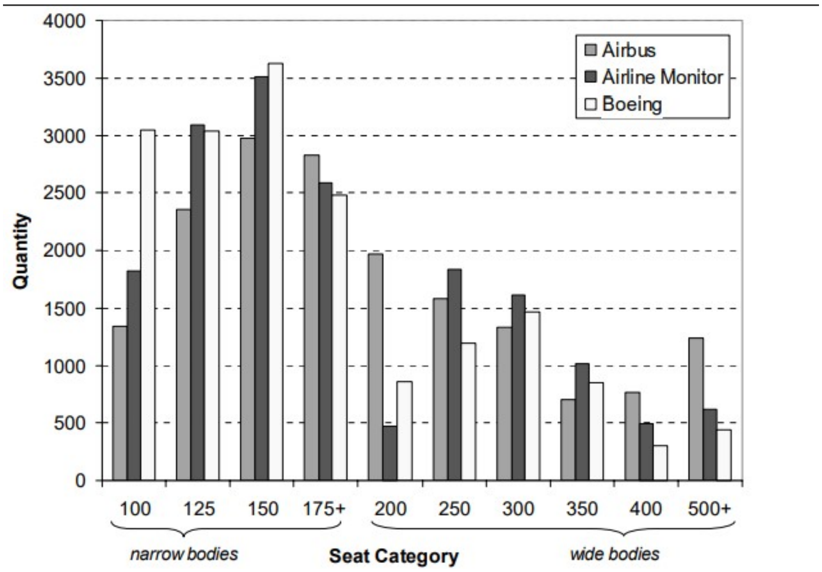

Figure 12.2: *Commercial aircraft demand forecast [54]*

12.4. Market Price

The price of the aircraft has been addressed from several perspectives. A competitive price was found once again using methods as described by Markish [54] who established a statistical relation between aircraft seat count, range and price. A figure of estimated vs actual prices is shown in Figure 12.3.

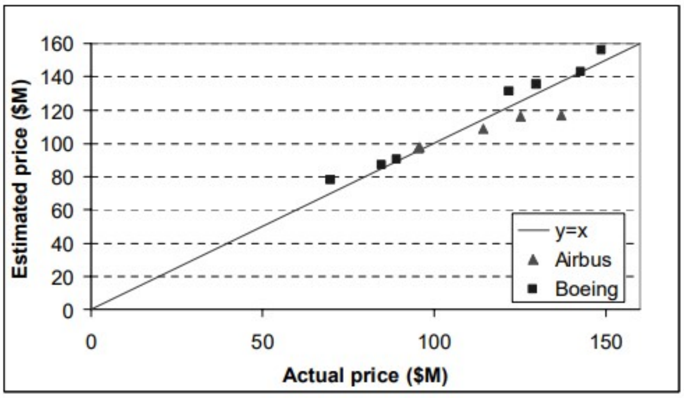

Figure 12.3: *Estimated vs actual prices of wide bodied aircraft [54]*

$$\text{Price} = \left[k_1 \frac{\text{Seats}}{\text{Seats}_{\text{ref}}}^{\alpha} + k_2 \frac{\text{Range}}{\text{Range}_{\text{ref}}} \right] \text{Price}_{\text{ref}} \tag{12.1}$$

Using the relation shown in Equation 12.1, where k_1 = 0.508, k_2 = 0.697 and α = 2.760 and the A380 being used as the reference aircraft with $\text{seats}_{\text{ref}}$ = 853, $\text{range}_{\text{ref}}$ = 15,400 $[km]$ [1] and $\text{Price}_{\text{ref}}$ = 445.60 $[M\$]$ [2]. Given that the Emperor has 1,500 seats with a range of 8,000 $[km]$,

[1] https://www.airbus.com/sites/g/files/jlcbta136/files/2021-12/EN-Airbus-A380-Facts-and-Figures-December-2021_0.pdf, accessed 09/06/2022

[2] https://aerocorner.com/aircraft/airbus-a380-800/, accessed 09/06/2022

a competitive price would be 1,240.60 [$M\$$], not adjusting for inflation and assuming a date of entry of around 2040. It should also be noted that this would be the competitive price estimate for a kerosene aircraft with the same specifications.

The actual price of the Emperor, factoring in all recurring and non-recurring costs, including additions for the implementation of the hydrogen technology is addressed in Chapter 13.

12.5. Future Market

With an ever growing weariness for contemporary aviation or more specifically for the pollution generated by it, the demand for sustainable solutions to fast long distance travel is ever increasing. As of present, the majority of sustainable aircraft in development are smaller, shorter range aircraft such as the Airbus ZeroE concepts or the TU Delft Flying V[3]. A limitation to all of these designs is the lack of payload and heavy lift capacity which is exactly the gap that the Emperor can fill, especially with a dedicated cargo version. If this gap remains, the potential market share could be much larger than the 25% estimated previously given how long it would take competitors to enter the market. Another positive to consider is the future investment into hydrogen technology which Goldman Sachs estimates could be over 5 trillion dollars [4].

From the perspective of the aviation industry as a whole, according to Airbus the global aviation market is predicted to grow with a compounded annual growth rate (CAGR) of 3.9% per year[5]. Assuming the same 25% market share from before resulting in the production of 119 units today, a CAGR of 3.9% over the next 20 years would result in a demand of 255 units. When combined with the need to replace current fleets of unsustainable aircraft, there could be a huge increase in demand. For the sake of this report however, 119 will be used as a more reasonable, perhaps even conservative, market volume going forward.

One last point to consider would be the future cost of carbon. Currently, the cost of an Aviation Industry Carbon Offset is 4.07 [$\$/\mathrm{ton\ CO_2 equivalent})$][6] but in order to meet climate goals it is expected that the price of credits will increase dramatically. As will be discussed later in Chapter 11, the annual $\mathrm{CO_2}$ savings of a complete fleet of 119 aircraft could be as much as $2.57 \cdot 10^7$ [$tons$]. If the carbon offsets could be sold at market, this would result in an additional total revenue of 102.96 [$M\$$] across the fleet at today's prices. From another perspective, if these credits cannot be sold and instead carbon emitting operators have to buy them as offsets, this would imply a cost saving potential of 0.87 [$M\$$] per aircraft. Finally, the future cost of kerosene should be addressed. While the price of green hydrogen is expected to rapidly fall as new infrastructure is developed, the price of oil is unlikely to decrease in any significant capacity. In fact, "given the international appetite for green energy projects, a significant under-investment in the traditional energy sector may lead to an increased cost of crude oil and would result in an increase in the price of jet fuel"[1]. This shift in price dynamics may lead to the hydrogen aircraft of the future being seen as legitimate competitors from an operational cost stand point, regardless of the positive sustainability impact they would bring.

[3] https://www.bbc.com/future/article/20220316-the-epic-attempts-to-power-planes-with-hydrogen, accessed 09/06/2022

[4] https://www.goldmansachs.com/insights/pages/from-briefings-17-february-2022.html, accessed 09/06/2022

[5] https://www.airbus.com/en/products-services/commercial-aircraft/market/global-market-forecast, accessed 15/06/2022

[6] https://carboncredits.com/carbon-prices-today/?gclid=Cj0KCQjwhqaVBhCxARIsAHK1tiMS_KoBPcAfYsR2Hr9MQAlEtOTF1A0cHZRg6Ann53LfUnV2iIeGdRcaAtc8EALw_wcB, accessed 15/06/2022

13
Cost and Revenue Analysis

The costs and revenues of the aircraft are analysed to give an idea of the business-case. A detailed cost breakdown is given in Section 13.1 and the revenues are given in Section 13.2, along with a discussion on the potential return on investment.

13.1. Cost Breakdown

To gain insight into where the different costs of the Emperor originate, a cost breakdown structure is shown in Figure 13.1. The specific cost elements are detailed in the following subsections. In Subsection 13.1.2 the development costs are discussed, followed by the production costs and operational costs in respectively Subsection 13.1.3 and Subsection 13.1.4.

13.1.1. Cost Breakdown Structure

From the cost break down structure, a distinction can be made separating non-recurring and recurring costs (NRC and RC). These reflect the costs and hence return on investment of the program where development makes up the NRC elements and production makes up the RC. Development is seen as NRC as any expenses are typically one-off such as building a prototype or funding research. Production costs are recurring as for each aircraft constructed, the manufacturer would need to purchase materials and pay for labour. These are addressed further in Subsection 13.1.2 and Subsection 13.1.3. Operational and organisation costs are those of the operator and logically affect the operation return on investment. Operational costs are addressed in Subsection 13.1.4 whereas organisational costs are assumed to be small in comparison to the others and a study of this is out of the scope of this report.

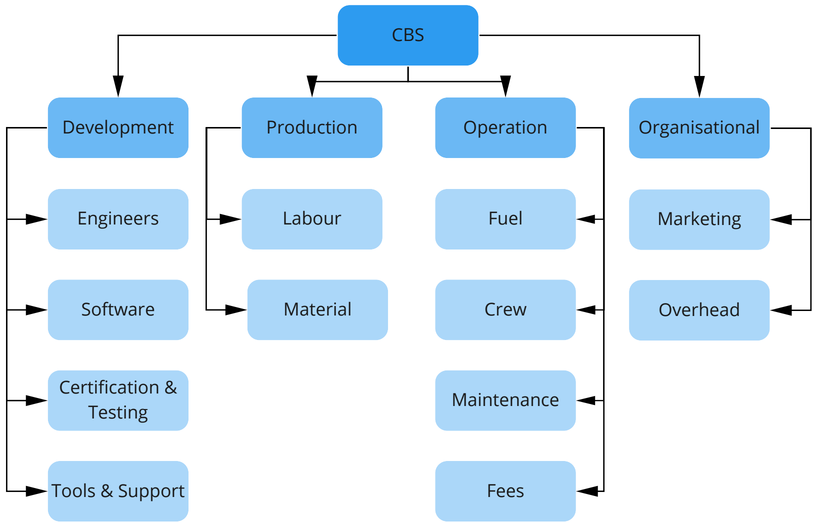

Figure 13.1: *Cost Breakdown Structure*

13.1.2. Development Cost

Development costs make up the non-recurring cost elements of the Emperor. This includes the cost of aircraft engineering, manufacturing engineering, tool design, tool fabrication and other support. This also includes the costs of testing and certification. To estimate the development costs, Markish presents another statistical method based on the weight fractions of various aircraft components normalised as a cost per pound [54] for a typical commercial aircraft. This estimate includes the cost of materials as well as the cost of wages. Applying this method to the development of the Emperor, all systems and hydrogen technology were factored in under 'Miscellaneous'. It is therefore logical that is one of the most costly areas to develop. A table is shown in Table 13.1 which shows the complete breakdown as well as the totals in [$M\$$].

Table 13.1: *Non-recurring costs [$M\$$]*

	Engineering	ME	Tool Design	Tool Fab	Support	Totals
Wing	2130.31	532.58	798.87	1853.37	250.31	5325.79
Empennage	2362.95	590.74	886.11	2055.77	277.65	5907.38
Fuselage	4457.28	1114.32	1671.48	3877.83	523.73	11143.20
Engines	759.52	189.88	284.82	660.78	89.24	1898.80
Miscellaneous	5182.38	1295.60	1943.39	4508.67	608.93	12955.96
Emperor Total	14892.45	3723.11	5584.67	12956.43	1749.86	**37231.12**

As can be seen, the total cost of development is estimated to be about 37 [$B\$$]. For reference, the final development cost of the A380 is estimated to be about 25 [$B\$$][1] which is far above Airbus's original prediction. With this historic issue of underestimation in mind and considering the new technology that is still to be developed, perhaps the true cost of development would be higher than the estimate found. The non-recurring cost breakdown is also visualised as a pie chart below in Figure 13.2.

[1] https://www.bbc.com/news/business-47231504

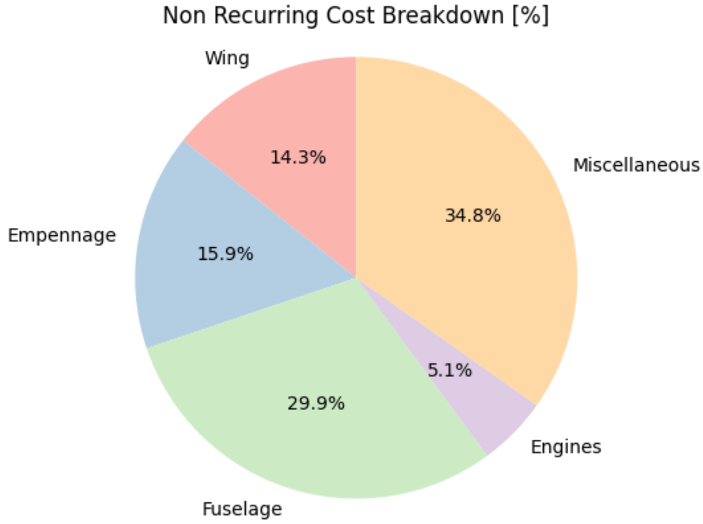

Figure 13.2: *Breakdown of the non-recurring costs*

It should be noted that the cost of building the seaports has not been taken into account in the non-recurring costs. The seaport would consist of the main terminal where security checks and luggage drop off will take place, the building of a hydrogen storage and refuelling system, the floating platforms where boarding will take place and the dry docks for maintenance. Whilst hydrogen handling requires complex systems, the cost of the runway which is normally of primary concern will be limited due to the sea-based nature of the Emperor.

13.1.3. Production Cost

The production costs are estimated in a similar way to the development costs and make up the recurring costs of the program. The method used is an elaborated version of the normalised cost per pound method used by Markish [54] which includes the cost of labour, materials and other expenses for various standard aircraft elements such as the wing, empennage, fuselage and final assembly. The values used for the various components specifically reflect the cost per pound of the materials and labour of the Boeing 777-200. The material breakdown of the 777-200 is similar to what would be expected to be used on the Emperor and as such makes for an appropriate estimate. Niche elements such as the engines, fuel cells, fuel tank and other miscellaneous aspects are incorporated using up to date and independently sourced information. More specifically, the aerospace-grade Saluqi electric motors would be 2674 [$\$/kg$] [2], the liquid hydrogen tanks would be 550 [$\$/kg$] [27] and the fuel cells would be 320 [$\$/kg$] [55]. A table of the recurring cost [$M\$$] breakdown can be seen in Table 13.2.

Table 13.2: *Recurring costs [$M\$$]*

Wing	207.33	**Engines**	155.14	**Miscellaneous**	170.70
Empennage	264.02	**Fuel Cells**	32.22	**Final Assembly**	107.76
Fuselage	335.76	**Fuel Tank**	16.17	**Total**	1352.10

[2] https://www.saluqimotors.com/products/, accessed 01/06/2022

From the table, the total recurring costs per Emperor is 1352.10 M$ and this represents the theoretical first unit-cost. While producing the assumed 119 units, a learning curve has to be factored in. This takes into account a slope coefficient of the learning curve of the labour of 85%, the material of 95% and on other costs of 95% which implies a total learning curve parameter of 91% when averaged over the total recurring cost [54]. Equation 13.1 can be used to implement the learning curve, where MC is the marginal unit cost, TFU is the theoretical first unit cost of 1352.10 [$M\$$], Q is the quantity built as of to date and s is the slope coefficient of the learning curve; 0.91.

$$\mathrm{MC} = \mathrm{TFU}\ Q^{\frac{\ln(s)}{\ln(2)}} \tag{13.1}$$

Using this relation, the final unit produced would be 700.35 [$M\$$] and would make for an average unit cost of **807.71** [$M\$$]. Clearly, the greater the production number, the greater the cost reductions. Finally, the recurring cost breakdown is also visualised in a pie chart as can be seen in Figure 13.3.

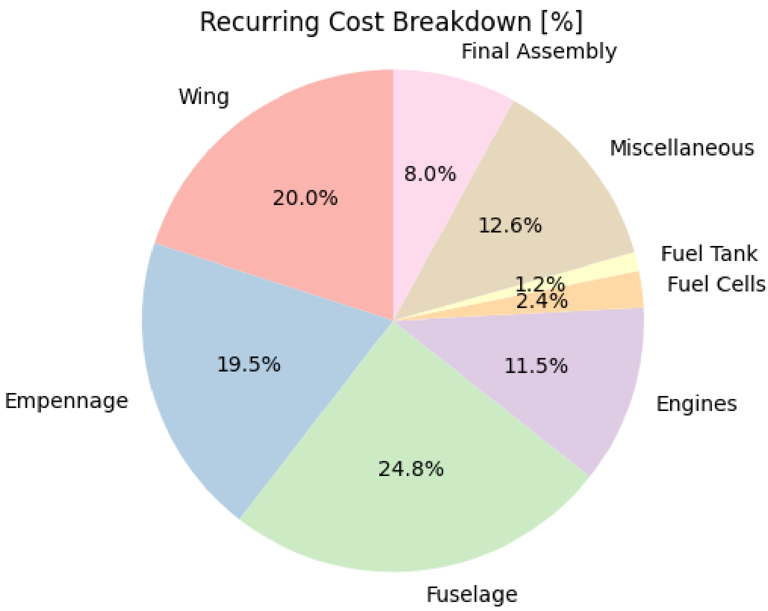

Figure 13.3: *Breakdown of the recurring costs*

13.1.4. Operational Cost

The direct operating costs (DOC) of an Emperor are estimated and normalising them as costs per passenger kilometer is a typical way to measure against competitors. Replicating the DOC method as seen in [56], as well as the constants used, an estimate of the complete operating costs is found. Adapted to factor in the hydrogen technology, DOC is calculated using Equation 13.2.

$$\begin{aligned}\mathrm{DOC}_{\text{Total, yearly}} = {} & \mathrm{DOC}_{\text{CAPEX}} + \mathrm{DOC}_{\text{Maint}} + \mathrm{DOC}_{\text{crew}} + \mathrm{DOC}_{\text{fees, ATC}} + \\ & + \mathrm{DOC}_{\text{fees, port}} + \mathrm{DOC}_{\text{energy}}\end{aligned} \tag{13.2}$$

Essentially this resembles the sum of the non recurring costs and the recurring costs of an operator which are estimated as a function of operating mass, range and speed of the Emperor. DOC_{CAPEX} reflects the cost of purchasing the Emperor itself (capital expenditure) and is a parametric relation from [56] which incorporates both the developmental and manufacturing costs as established in Subsection 13.1.2 and Subsection 13.1.3 respectively. As discussed previously, the added costs of new, niche technology is factored in here. The aircraft cost is scaled by an assumed 20% profit margin for the manufacturer along with a 5% contingency cost to account for the cost of other unforeseen new technology. An annuity factor is then applied which is a function of the depreciation period, assumed to be 14 years, an interest rate of 5% and a 10% residual value factor. Finally, a 0.5% insurance cost is added [56]. The equations of this can be seen below.

$$P_{\text{AC}} = \left(RC_{\text{AC}} + \frac{NRC}{n_{\text{AC}}}\right)(1 + PM_{\text{AC}} + f_{\text{misc}})$$

$$a = IR\frac{1 - f_{RV}\left(\frac{1}{1+IR}\right)^{DP}}{1 - \left(\frac{1}{1+IR}\right)^{DP}}$$

$$DOC_{\text{CAPEX}} = P_{\text{AC}}(a + f_{\text{ins}})$$

From this method, the final delivery price of the Emperor is estimated to be 1.46 [$B\$$]. This is 17.42 % higher than the kerosene equivalent competitive price as estimated in Section 12.4. When considering the many new technologies being implemented and the promise of green aviation, this premium can be justified.

The remaining factors in the DOC calculation reflect the recurring costs of the operator. In this, the costs of maintenance, the crew, fees and fuel are estimated as parametric functions of the number of yearly flight cycles which includes expected down time, speed, range, block time, turnaround time and other miscellaneous operations. DOC_{Maint} is the total yearly maintenance cost of the Emperor and assumes an average air-frame, including systems. It is assumed that the hydrogen fuel containment system has the same maintenance cost as that of a rest of the air-frame per kg [56]. Engine maintenance (cost per engine) and maintenance personnel fees are also included in this number. DOC_{crew} reflects the salaries of the crew. This is the same as it would be for a conventional aircraft with an estimated pilot salary of $175,000 per year, a flight attendant salary of $ 85,000 and for every 50 passengers 1 flight attendant is considered, as well as a total of 5 complete crews per aircraft. $DOC_{\text{fees, ATC}}$ is the air traffic control fees found from a function of range and maximum take off mass. $DOC_{\text{fees, port}}$ reflects the handling costs of the Emperor and include payload handling at 0.1 [$\$/kg$] [payload] as well as landing fees of 0.01 [$\$/kg$] [MTOM]. Lastly, DOC_{energy} represents the cost of the fuel of the Emperor assuming nominal operations over a year.

Along with the CAPEX, the fuel, being liquid green hydrogen, makes up another significant cost for the operator. A study has been done by the EU as a joint collaboration with Airbus, Boeing, Shell, TU Delft and others on hydrogen technology, the economics and climate impact of aviation by 2050. This indicated that the complete production, distribution, liquefaction, storage and refuelling cost of green liquid hydrogen could be in the range of 2.3 - 3.5 [$\$/kg$] by 2040 [27]. The full cost breakdown of the process can be seen in Figure 13.4.

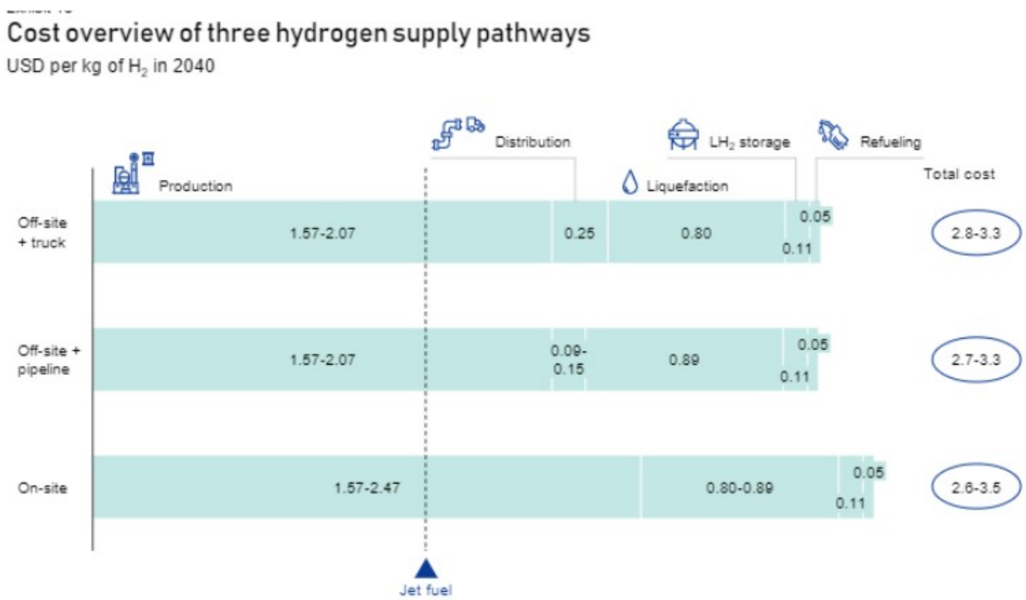

Figure 13.4: *Cost breakdown of hydrogen production and operations [27]*

When consulting with a hydrogen technology expert at TU Delft as well as a professional in the hydrogen production sector, both estimated the production cost of green hydrogen could be as low as 1 [$\$/kg$] by 2040. Factoring in the 0.89 \$ cost of liquefaction, as well as the cost of distribution through a pipeline, LH2 storage and refuelling from Figure 13.4, it would result in a complete cost of 2.14 [$\$/kg$] for green LH2. The complete breakdown of the direct operating costs is visualised in Figure 13.5.

The value of the DOC alone gives the total cost over an average year of operations but as mentioned previously, when it is normalised with respect to the available seat kilometres (ASK) of the aircraft, one is able to effectively compare costs across a range of competitors. Naturally, a lower DOC/ASK [$\$/passenger/km$] would be considered more competitive and cost effective than a higher one. ASK is calculated as follows:

$$\text{ASK} = \text{Flight cycles} * \text{Flight range} * \text{Passenger Count} \tag{13.3}$$

Given an OEM of 752.01 [$tons$], a range of 8,000 [km] and a passenger count of 1,500, an estimate of the DOC/ASK is 0.071 [$\$/pax/km$]. For reference, a medium range kerosene aircraft was estimated to have a DOC/ASK of 0.042 [$\$/pax/km$] and a medium range LH2 aircraft is estimated to have a DOC/ASK of 0.047 - 0.089 [$\$/pax/km$] depending on the degree of success of the implementation of hydrogen infrastructure in the future [56]. The Emperor is evidently less cost effective than an average medium range aircraft which is to be expected. This said, it is competitive with respect to a medium range LH2 aircraft which is a very promising result. Moreover, the DOC only factors in costs. When analysing the revenues of the program in Section 13.2, further potential for economic viability is identified.

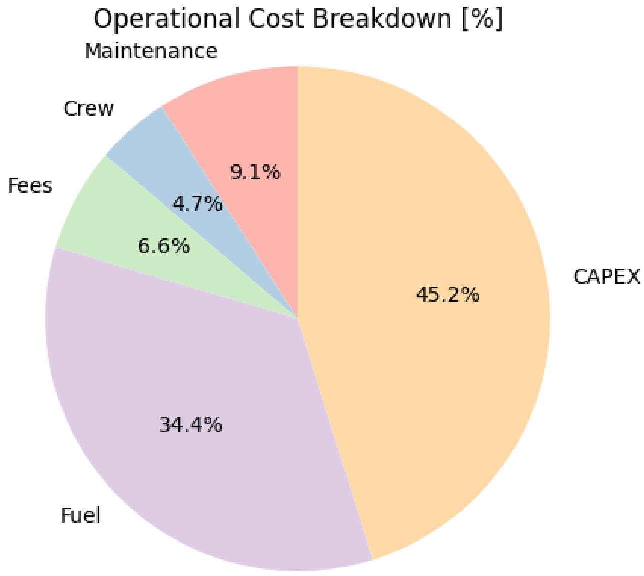

Figure 13.5: *Breakdown of direct operating costs [%]*

13.2. Revenue Analysis and Return on Investment

Revenues and return on investment can be addressed from the perspective of the program as a whole as well as that of an operator who purchased the Emperor.

13.2.1. Revenue Analysis

Revenue of the program comes from selling the complete Emperor after development and production. The sale price is 1.46 [$B\$$] as was reasoned in Subsection 13.1.4. Given a total program cost of 133.34 [$B\$$] and without additional aid, the break-even number for the program (the point at which total revenues equals total costs) would be 127 aircraft sold, which is larger than the estimated market volume of 119. With an additional 20% subsidy, the break-even point is 106 and would make the program profitable. The assumption of a subsidy is not unreasonable as the transition to green aviation is a challenge that needs to be addressed and governments would almost certainly be willing to help in the development of new technologies.

Revenue of an operator arises in the form of ticket sales and the transportation of additional cargo. To estimate this, a standard transatlantic flight was considered. To be highly competitive, ticket prices were set at just 600 [$] and cargo prices were set at 3 [$\$/kg$] [3]. It should be noted that this cargo refers to additional freight separate from the mass of passenger luggage and also that no subsidy is given to operators. The revenue per flight is found to be 1.20 [$M\$$] while the cost per flight (found as DOC divided by yearly flight cycles) is 0.86 [$M\$$]; making it a profitable venture for operators.

[3] https://www.worldbank.org/en/topic/transport/publication/air-freight-study

13.2.2. Return on Investment

To summarise the business case for the Emperor, the total return on investment (ROI) for both the program as a whole as well as the operators is addressed. ROI is calculated using Equation 13.4:

$$\mathrm{ROI} = \frac{\text{Total revenues} - \text{Total costs}}{\text{Total costs}} \tag{13.4}$$

Assuming the same standard transatlantic flight parameters discussed previously, with a 20% subsidy for the manufacturer, a final breakdown can be seen in Table 13.3 and Table 13.4.

Table 13.3: *Program profitability and ROI*

	Value [$M\$$]
Program Revenues	
Price	1456.75
Number sold [-]	119
Net revenue (incl. 20% subsidy)	149,943.43
Program Costs	
Development	
- Engineering	(14,892.45)
- ME	(3,723.11)
- Tool Design	(5,584.67)
- Tool Fab	(12,956.43)
-Support	(1,749.86)
Production	
- Total recurring	(96,117.55)
Net cost	(133,348.67)
Profit	16,594.76
ROI	12.44 %

Table 13.4: *Operational profitability and ROI*

	Value [$]
Operational Revenues	
Price per ticket	600
Number pax	1,500
Price of cargo [$\$/kg$]	3
Cargo [kg]	100,000
Net revenue	1,200,000
Operational Costs	
CAPEX	(386,425.29)
Fuel	(294,223.77)
Fees	(56,792.03)
Maintenance	(77,490.33)
Crew	(40,370.23)
Net cost per flight	(855,301.65)
Profit	344,698.35
ROI	40.30 %

The ROI of the program and of the operator is 12.44 % and 40.30 % respectively. The high operational ROI allows for some contingency in the amount of passengers that need to be taken to ensure profitability. It has been found that the break even number of passengers would be 926. While the ROI is positive for the program, the net present value would be very low considering the long time frame. Nevertheless, given the unique nature of the Emperor, this is a highly promising result and hints at the potential bright future for green aviation.

14 Risks

During design, manufacturing and operations, risks are always present. It is of vital importance to keep them in mind such as to mitigate and contain their negative effects. To that goal, they are first listed in Section 14.1 and plotted in Section 14.2. Finally, Section 14.3 proposes contingency and mitigation strategies to reduce these risks.

14.1. Technical Risk Assessment

”Table 14.1 shows a list of all technical risks. They have been divided into risks that can occur during the design process (TR-DES-X), and thus raise flags with the engineers that the design will not be desirable or optimal, and operational risks (TR-OPS-X). Operational risks are risks that can occur after the designing process, i.e. during the operational phase of the Emperor. Some overlap might be observed, but the risks are allocated as much as possible to the phase they most belong to.

All of the risks have been appointed a risk score based on their likelihood and impact, ranging from 1 to 5. For the likelihood, this represents whether the risk is almost impossible, unlikely, occasional, probable or likely to happen. Regarding the impact, its severity can be negligible, marginal, relevant, critical or catastrophic. This will be further explained in Section 14.2.”[1]

14.2. Technical Risk Map

”A list of technical risks has been analysed and assessed for their probability of occurrence and impact severity in Figure 14.1. The probability of occurrence or likelihood, visible in the vertical axis of Figure 14.1, refers to the possibility of it happening. The metrics go from 1 to 5, where 1 is the least likely to happen and 5 most likely to happen. The severity of the impact of the risks is also categorised in five levels. It refers to the consequences for the proper organisation and functioning of the group and project. These categories are seen on the horizontal axis of Figure 14.1.

The allocation of metrics to the different risks follows from experience and common sense. This is because the exact impact and likelihood of occurrence are hard to quantify for technical risks at such an early stage of the project, especially for the operational risks. For the risks during the design process, some initial estimations and calculations can be made already. The risks are organized in the map according to these metrics. Depending on their position on the map the risks can either be accepted, reduced, transferred or avoided.”[1]

14.3. Contingency Management

”The risks from Figure 14.1 should be accepted, reduced, transferred or avoided based on their severity and likelihood. Risks R12-R15 are small enough to simply be accepted as is. Risks R01-R11 are deemed to be too large and shall thus be discussed.

Table 14.1: *Technical risks*

Identifier	Risk	Likelihood	Impact
TR-DES-1	Overestimation of material properties	4	4
TR-DES-2	Faulty programming code	5	3
TR-DES-3	Validation errors	3	4
TR-DES-4	Incompatible subsystems	3	4
TR-DES-5	Simplification errors	2	2
TR-DES-6	Insufficient thrust generation	2	4
TR-DES-7	Insufficient lift generation	2	4
TR-DES-8	Verification errors	2	4
TR-DES-9	Faulty trade-off	2	4
TR-DES-10	Incomplete trade-off	3	3
TR-DES-11	Underestimation of costs	3	2
TR-DES-12	Aircraft too heavy	4	2
TR-DES-13	Passenger capacity not met	1	3
TR-OPS-1	Leakage in the hydrogen tanks	3	5
TR-OPS-2	Passenger comfort can not be assured	4	4
TR-OPS-3	Corrosion	5	3
TR-OPS-4	Aircraft can not be certified	2	5
TR-OPS-5	Excessive drag	3	4
TR-OPS-6	Aircraft is not able to take-off	2	3
TR-OPS-7	cg range wrongly defined	3	4
TR-OPS-8	Hydrogen can not be sufficiently compressed	3	4
TR-OPS-9	Velocity requirement is not achieved	4	3
TR-OPS-10	TOC are non-competitive	4	3
TR-OPS-11	Range requirements not achieved	4	2
TR-OPS-12	Aircraft can not be designed in a sustainable way	2	4
TR-OPS-13	Control surfaces failure	2	4
TR-OPS-14	Engine failure	3	3
TR-OPS-15	Fire breaks out	2	4
TR-OPS-16	Emergency landing	2	4
TR-OPS-17	Unforeseen fatigue occurs	3	4
TR-OPS-18	Load cases underestimated	3	4
TR-OPS-19	Shock waves occur	1	4
TR-OPS-20	Insulation fuel tanks get destroyed	3	5
TR-OPS-21	Delays in refuelling or boarding	3	2
TR-OPS-22	Navigation signal is jammed	3	3
TR-OPS-23	Cruise altitude exceeded without pressurization	3	3

This section proposes mitigation strategies and contingency plans to decrease the influence of the most severe and likely risks. A mitigation plan aims to reduce the likelihood or impact of the risk. However, in case the mitigated risks are still unacceptable, a contingency plan describes how to make the risk acceptable. Finally the risk map is adjusted to account for the mitigation strategies, as seen in Figure 14.2.

TR-DES-1: Overestimation of material properties
It could happen that the material properties are overestimated, such that the final design is not strong enough to carry all of the loads. To avoid this, a quality assurance engineer has been appointed to check the calculations performed. Any remaining errors are accounted for by a safety factor of 1.5.

TR-DES-2: Faulty programming code
There might be errors or inconsistencies in the programming code. Performing the proper verification and validation decreases the likelihood of it occurring.

TR-DES-3: Validation Errors
Improper validation can results in incorrect models/results. Introducing a second opinion and allocating more resources improves the quality of validation.

TR-DES-4: Incompatible subsystems
Since the designing of subsystems will be done by different groups, communication might be lacking leading to inconsistencies in the design. Having the chief engineer keep a good general overview decreases the likelihood of it happening. A contingency plan is to keep alternative designs in mind to choose from.

TR-DES-6: Insufficient thrust generation
Since the criteria related to size and weight are quite relaxed, the likelihood of insufficient thrust generation is quite low, since bigger, more or stronger engines can always be installed. Aerodynamic properties are related to each other and are each monitored during the design process, to avoid being surprised by this lack of thrust.

TR-DES-7: Insufficient lift generation
Since the criteria related to size and weight are quite relaxed, the likelihood of insufficient lift generation is quite low, since bigger wings or engines can always be installed. Aerodynamic properties are related to each other and are each monitored during the design process, to avoid being surprised by this lack of lift.

TR-DES-8: Verification errors
Improper verification can results in incorrect models/results. Introducing a second opinion and allocating more resources improves the quality of verification.

TR-DES-9: Faulty trade-off
A faulty trade-off can result in a sub-optimal design being chosen, this could result in a lacking design. In order to keep the impact of trade of mistakes limited, various design relations are monitored throughout the trade-off process. Proper trade-off validation should limit the likelihood of this happening.

TR-DES-10: Incomplete trade-off
An incomplete trade-off is an oversight on a significant criterion for the design. In order to try and prevent such an oversight a detailed project-flow and requirement breakdown has been

made. With all relevant functions and requirements clearly mapped, the likelihood of lacking trade-off criteria is reduced. In case of this still happening and the current design not being able to accommodate the forgotten criterion, alternative design options can be checked and used.

TR-DES-12: Aircraft too heavy
A non-conventional and innovative aircraft is being designed, meaning that a lot of design decisions have to be made without being sure of their influence on the weight. However, since an airship is being created added to it being energized by hydrogen which has some lifting capacity, the impact was not determined to be very severe. A solution to an excessive weight can be to use different materials or to decompress the hydrogen to increase the lifting capacity which offsets the weight. Using safety factors can also avoid unforeseen surprises.

TR-OPS-1: Leakage in the hydrogen tanks
Leaking hydrogen reacts with the atmosphere and breaks it down and must thus be avoided. Decreasing the likelihood can be done by using a double layer or a different material in the fuel tanks.

TR-OPS-2: Passenger comfort can not be assured
Even though the flight altitude is still undecided, due to the size and landing peculiarity of the Emperor, not all phases of the flight will reach the comfort standards set by modern aircraft. Flying at a higher altitude or designing the fuselage to lie within the balloon (one of the preliminary design choices) will decrease the turbulence experienced. Making the internal cabin more shock-free helps as well. Lastly, designing for a hydrofoil softens the landing.

TR-OPS-3: Corrosion
The airship will land, be stored and take off again on water, i.e. the sea. The salty seawater corrodes the Emperor and should thus be taken into account. There are multiple ways to prevent or delay corrosion. Examples are using corrosion-resistant material for the outer hull, or to introduce small patches of material that corrode before the main fuselage. Regular maintenance will fix and replace the corroded parts.

TR-OPS-4: Aircraft can not be certified
Certification companies look at whether the Emperor complies with all applicable regulations. Without certification, the Emperor won't be allowed to fly. Having a good understanding of the applicable regulations increases the odds of being certified. If lacking, redesigning and going back to alternative designs is always an option. Else, the aircraft shall have to be discarded.

TR-OPS-5: Excessive drag
Due to the large nature of the Emperor, a huge amount of drag will be generated. This is very fuel consuming and non-efficient. Designing for a more aerodynamic shape or making smart choices to make the Emperor smaller will decrease the drag. However, it is not yet known how to fully fix this problem due to the snowball effect relation of propulsion, size and mass.

TR-OPS-7: cg range wrongly defined
With a wrongly defined cg range, the aircraft becomes unstable and difficult to fly. Fixing everything in place and keeping a clear overview of the mass distribution within the plane increases the correctness of the cg range. Having only experienced pilots fly the Emperor will decrease the severity of impact since they are able to quickly react to difficult flying situations.

TR-OPS-8: Hydrogen can not be sufficiently compressed
Hydrogen has a very low density, meaning a large volume is needed to store sufficient hydrogen to fly the aircraft over its mission ratio. This large volume results in a very big Aircraft which leads to an excessive drag and is undesirable. Compressing the hydrogen decreases the size which is needed. New technologies can be used to increase the compression ratio.

TR-OPS-9: Velocity requirement is not achieved
The preliminary requirement was to have a cruise velocity of 500 $[km/h]$, which is proving to be difficult to reach. Using more efficient engines, distributed propulsion or decreasing the size of the aircraft to decrease the drag are options that can be explored to go faster. If it is still not reachable, the requirement can be renegotiated.

TR-OPS-10: TOC are non-competitive
Due to the longer duration of the flight, the total operating costs of the Emperor are higher than its faster competitors. Revenues can be increased to offset these costs and keep the aircraft competitive. This can be done by carrying more cargo or passengers since the size requirements are less stringent.

TR-OPS-11: Range requirements not achieved
The limiting factor on the range is the amount of fuel taken aboard, increasing the fuel tank volume will increase the range. Since an airship for transoceanic flights is being designed, a small shortage in range can (in emergencies) be solved by landing earlier and sailing to shore.

TR-OPS-12: Aircraft can not be designed in a sustainable way
Not only operations, but also the designing and manufacturing processes should be performed as sustainable as possible. If this is not possible, the effects should at least be minimised.

TR-OPS-13: Control surfaces failure
Control surfaces failure would make the aircraft uncontrollable. Introducing redundancies will decrease the odds of uncontrollable behaviour. This includes the secondary effects of the control surfaces that can be used to keep directing the aircraft. Performing regular maintenance is also an option to sustain the optimal operation of controls.

TR-OPS-14: Engine failure
Engine failure can be mitigated and contained by designing for one engine inoperative and by using multiple (smaller) engines to propel the aircraft.

TR-OPS-15: Fire breaks out
Since the aircraft is powered by hydrogen, a fire breaking out would be dramatic. Even just an increased temperature might cause the hydrogen to expand and explode the tank. Introducing some reserve and making the tank walls thicker and insulating delays this event. Complying or exceeding with the fire fighting measures such as the amount of extinguishers or emergency exists decreases the impact as well.

TR-OPS-16: Emergency landing
Even though it can not really be designed for, having the aircraft perform an emergency landing or crashing would be rather critical. A plan should be drafted which lists what to do. Since it is a seaplane with considerable size, it can basically land anywhere if it can handle the state of the sea. However, flying over long patches of land should be avoided, since the landing gear doesn't support a landing on land."[1]

TR-OPS-17: Unforeseen fatigue occurs
An aircraft is a complex vehicle, where fatigue occurs in multiple ways. It will definitely take place, but the trick is to introduce sufficient contingencies and research it in depth to get a clear overview and anticipate it. Regular maintenance and inspection can avoid critical consequences.

TR-OPS-18: Load cases underestimated
Due to the novel and innovative design, some load cases might be underestimated due to a lack of information available. Again, sufficient contingencies and safety factors would decrease the likelihood of failure.

TR-OPS-20: Insulation fuel tanks gets destroyed
Cryogenic hydrogen has to be stored at a temperature of 20 $[K]$, for which you need advanced insulation. If this insulation layer gets damaged or destroyed, the hydrogen will heat up, expand and explode the tanks. This can be avoided by having redundant insulation layers, or putting it in a strong and impact resistant container. Putting the insulation on the inside of the tank is also a possibility, but then it corrodes faster and is less available for maintenance. The tank should also have a quick release handle and accurate sensors to release the hydrogen in time if necessary.

TR-OPS-22: Navigation signal is jammed
When flying in the middle of the ocean, the navigation system is the only system that allows the pilot to orientate himself. If it fails, the flight track might move leading to a longer range for which the fuel might be insufficient. That's why the system is set up such that GNSS provides the primary source of information, with radio navigation as a backup. Lastly, basic orientation can be performed by a compass or looking at the location of the sun until ground stations are within reach.

TR-OPS-23: Cruise altitude exceeded without pressurization
Pressurization is required for pilots when flying for 30 minutes above 3,810 $[m]$ altitude. Even though there is a safety margin of 810 $[m]$ above our cruise altitude of 3,000 $[m]$, the risk exists of exceeding this altitude, which decreases the pilots capabilities and in the worst case leads to a crash. Installing an alerting system, setting a limit on the altitude or even installing an automatic pressurization system makes this risk disappear. This last measure will not be taken due to the high cost and complexity whilst it's not required for the mission flight profile.

Impact ↑		1 Almost impossible	2 Unlikely	3 Occasional	4 Probable	5 Likely
Catastrophic	5		TR-OPS-4	TR-OPS-1/20		
Critical	4	TR-OPS-19	TR-OPS-12/13/15/16 TR-DES-6/7/8/9	TR-OPS-5/7/8/17/18 TR-DES-3/4	TR-OPS-2 TR-DES-1	
Relevant	3	TR-DES-13	TR-OPS-6	TR-OPS-14/22/23 TR-DES-10	TR-OPS-9/10	TR-OPS-3 TR-DES-2
Marginal	2		TR-DES-5	TR-DES-11 TR-OPS-21	TR-OPS-11 TR-DES-12	
Negligible	1					
		Likelihood →				

Figure 14.1: *Technical risk map*

Impact ↑		1 Almost impossible	2 Unlikely	3 Occasional	4 Probable	5 Likely
Catastrophic	5	TR-OPS-4	TR-OPS-1			
Critical	4	TR-DES-6/7/9 TR-OPS-17	TR-DES-3 TR-OPS-5/18/20			
Relevant	3	TR-DES-8/13	TR-OPS-6/7/12/13/15/16 TR-DES-4/10	TR-DES-1/2 TR-OPS-2/8		
Marginal	2		TR-DES-5 TR-OPS-9/23	TR-DES-11 TR-OPS-10/14/21/22	TR-OPS-3/11	
Negligible	1				TR-DES-12	
		Likelihood →				

Figure 14.2: *Post mitigation technical risk map*

15

Discussion

A final design has been reached but there is more optimisation that can be done with more time and resources. Several limitations of this study are given in Section 15.1 and recommendations of potential future research are discussed in Section 15.2,

15.1. Limitations

The limitations of this study primarily relate to the level of depth that was able to be achieved for each subsystem. While the conventional aspects of the design, such as the wing and empennage, can certainly be improved with more detailed analysis primarily through an improved aerodynamics model, more research is needed. This is especially true in aspects of the design that are more unique such as the hydromechanics of the aircraft and the fuel containment system.

Regarding the boat aspects of the aircraft, several limitations of this study have been identified due to the inherent chaotic nature of water making analysis difficult. First, water stability and control during take-off and taxi should be analysed further. Along with this, the drag at take-off is a point that required further attention. As of now, a study has been conducted and it has been determined that water capabilities are not a critical condition for the technical capabilities of the design but the specifics of how the aircraft would behave is not well understood. Due to this, the comfort of the passengers during take-off and landing could not be accurately determined. The assurance of such comfort was an initial stakeholder requirement and its compliance has not yet been confirmed.

The hydrogen fuel aspect of the aircraft is another area in which more research is needed. This is the area of the design with the lowest real-world technological readiness level and the actual implementation is not yet fully worked out and understood. As for the design that was produced, inevitably several assumptions were made; one of which is that the mechanical properties of the fuel tanks are assumed those of regular cylinders, rather than the unique shapes they actually are. The true tank mass would likely be greater than currently estimated due to the possible inefficiencies of the real shapes. Lastly, the details of hydrogen boil-off management remains an area that can be improved upon. It may be found that true boil-off is greater than estimated and thus the system would need more fuel. Due to these uncertainties, contingencies were put in place throughout the design but it would be wise to try and reduce these as much as possible through further research.

Despite the niche aspects requiring more research, other more general limitations exist as well. One limitation is the level of depth of the current wing box design. For this study, only the main forces were considered but analyses on the buckling and fatigue properties were not done. Multiple loading cases should also be considered to increase confidence in the design. Overall, more validation should also be done to increase the confidence in the final design but this would require more resources. Several other limitations refer mainly to surrounding processes rather than the technical limitations of the design. Once more specifics are known about the materials being used, the recyclability and reusability of materials can more accurately be assessed. A study into the materials would also allow for a more accurate cost analysis to be done. Another limitation to the realism of the design would come from a need to further develop the logistics of operating a liquid hydrogen, sea-based passenger aircraft. To do this, a much larger feasibility study should be done which should focus on infrastructure, operations and logistics as well as the exact laws and regulations that would need to be complied with for the design to get certified.

15.2. Recommendations

Given the limitations of the current design, several recommendations can be given for further study. The easiest to implement with the greatest impact on improving the design may be a computational fluid dynamic (CFD) study into the aerodynamics and hydrodynamics of the aircraft. These are two aspects which have not been sufficiently validated and this would be a large step in increasing the overall confidence in the design. Along with CFD, finite element methods (FEM) could be used to more accurately analyse the aircraft structure. This would help to validate and improve the current model and could lead to significant weight reductions. The next logical recommendation would be to construct a scale model of the aircraft. Testing this in a wind tunnel as well as in a water tunnel would further help to validate the aerodynamics, hydrodynamics and hydrostatic stability of the aircraft model.

Along with improving the accuracy of the model, the depth of the design could be improved with a more in depth material study as was discussed in Section 15.1. This would improve the understanding of sustainability characteristics as well as improve the accuracy of the cost analysis. One exciting study that could be done would be to develop a concept of a retractable hydrofoil that would let the aircraft get over the hump speed and increase passenger comfort and then retract to avoid the adverse effects of cavitation. The results of such a study could be beneficial to future seaplane design.

16

Conclusion and Reflection

This chapter aims to conclude the report regarding the Emperor. This shall be done by providing the conclusion in Section 16.1, where the most important information concerning the Emperor and the designing process is stated. Finally, a reflection on the feasibility of the Emperor in near-future society is discussed in Section 16.2.

16.1. Conclusion

"With sustainability being a driving design factor in current-day aviation, hydrogen-powered flight offers a promising solution. This report aimed at exploring and presenting a design of a hydrogen electrically powered by fuel cells, transatlantic aircraft, competitive in payload capacity, travel time, cost, reliability, and safety.

After laying out the initial project objectives and requirements, several primary concepts were generated. By analysing the key design features such as the potential structure, lift generation method, propulsion strategy as well as others, the initial concepts were made to represent different degrees of hydrogen fuel compression. These ranged from a zeppelin-like airship with a fuel compression ratio of 3 to a more conventionally shaped, cryogenic, liquid hydrogen aircraft. It was found in general that the more the fuel is compressed, the better the potential performance of the aircraft. A formal trade off was done and the liquid hydrogen concept was selected for further development. "[1].

To develop this concept into a complete design, a computational model was produced which takes various input parameters and converged to a final product, called "Emperor", which is able to fulfil the requirements as set previously. Several noteworthy results were an operating empty mass of $7.52 \cdot 10^5$ $[kg]$, a fuel mass of $1.37 \cdot 10^5$ $[kg]$ a fuselage length of 133.60 $[m]$, a wing span of 125.78 $[m]$, a fan count of 82, a cruise speed of 720 $[km/h]$, and a range of 8,000 $[km]$.

Once this design was reached, further analysis has been conducted to provide further detail. The performance, noise and RAMS characteristics are addressed for the established design. The sensitivity analysis shows the design to be both feasible and robust, by changing various parameters, such as velocity, range, fuel mass, and assessing the effect on the design. Following, several data diagrams were produced to show interactions of various subsystems regarding hardware, software, data handling, electrical power, and communication. The production process includes the course of action following this Design Synthesis Exercise, highlighting the extension of detailed design, marketing, manufacturing, and deliveries. The operations and logistics are focused on sea-based operations, thus the airport will be stationed in coastal area. Loading of passengers, cargo and fuel is done on a two-floor floating dock, which is also used for pre- and post-flight inspections and maintenance.

The sustainability of the aircraft is examined on environmental, economic, and social domains. The main aspects for sustainability include the elimination of greenhouse gases, reuse of materials, use of renewable energy, lean manufacturing, and fair wages for employees. Furthermore, the potential market and costs were analysed. It was found that the aircraft would have a delivery price of 1456.75 $[M\$]$, an operational return on investment (ROI) of 40.30 % with a program ROI of 12.44 %. "Finally, the technical risks were assessed, and the most pressing were found to be a potential overestimation of material properties, faulty programming code, leakage in or fatal damage to the hydrogen tanks, the inability to assure passenger comfort, or corrosion; all of which have been sufficiently mitigated." [1].

Overall, this study has resulted in a compelling design of a sustainable, transatlantic air travel alternative to current-day civil aviation, which is competitive in payload capacity, travel time, cost, reliability, and safety.

16.2. Reflection on Possible Real World Adoption

This reflection contains a discussion on whether building the Emperor in the near-future with its technology and problems is recommended. The Emperor comes with both advantages and disadvantages, which will be discussed in this section.

The Emperor appears to possess various difficulties. The main issue is that this concept is extremely expensive to both design and manufacture. The innovative technology used in the Emperor has a low technology readiness level, which requires an extensive, and expensive, development program. Due to the unconventional design, it will be quite an endeavour to ensure proper certifications and confidence from airlines and passengers. As a consequence of the large size of the aircraft, a lot of material is needed which greatly increases manufacturing costs. Due to these money constraints, a substantial amount of subsidies would be required.

Another potential issue could be that the passengers' demand for flights would be less than the frequency and availability that can be provided by the Emperor, as this would reduce the operational profits for the airlines. Thus even though the Emperor is profitable in case of sufficient demand, this still poses a risk for airlines.

The sea-based operations cause a barrier due to the need for new infrastructure and logistics centered in coastal areas. This complicates operations as this has to be sufficiently in place by the time of the first delivery of the Emperor. Take-off and landing from sea also limits the number of routes which can be flown to solely coastal areas or interior areas with bodies of water of sufficient size.

However, sea-ports can also be seen as a chance to ease the development of airports. They allow for flexibility regarding their location and require less use of land due to the floating platform and runway being positioned at sea. Furthermore, they can be placed in large coastal cities without having to resort to the outskirts of the city, making it more accessible and comfortable for passengers.

One of the main issues in current-day society is the exhaust of emission by the use of fossil fuels, with disastrous consequences for the environment. The Emperor is currently the only solution for fast, long-range sustainable aviation. It is emission-free due to the use of hydrogen in fuel cells, and ensures sustainability over the entire range of operations and manufacturing.

The Emperor's operations are effective due to its ability of transporting a lot of passengers at once. In order to make the Emperor compete with current aviation, a change in the mindset of airlines and travelers is needed. Not being able to fill up the aircraft every flight was presented as a problem, but this can be avoided by limiting the amount of flights per day and week, ensuring there is sufficient demand for the available seats. This would limit the choice for the passengers as to when they can travel but is a small sacrifice that will allow sustainable long-range travel to become a possibility.

The aircraft is not only appealing for airlines due to its operational profitability, but also due to the added value brought by its sustainable nature, which considerably increases the reputation of the airline. The Emperor is a step forward in the energy transition quest, and is an exciting advertisement for sustainable aviation. This concept could even be explored further for its ability to be transformed into a cargo aircraft version, which aids the energy transition quest by replacing polluting cargo ships for this emission-free aviation alternative. Another possibility is to scale down the payload capacity of the Emperor, to allow for land-based operations. This avoids the risks associated with the sea-based operations, as well as the uncertainty in passenger demand.

Overall, it can be established that the Emperor will probably be a challenge to be built, especially from a business standpoint since money constraints are the most pressing issue. However, limited money resources are the largest challenge for almost all sustainable alternatives. There is no substantial economic incentive for companies to invest in these alternatives, as it usually takes a long time for these alternatives to become profitable. It is time for the leaders in this world to take on their responsibility and allow sustainable solutions to become viable through government funding. From this point forward, their decisions should reflect that they value human life and environmental well-being over money.

In conclusion, the Emperor can be seen as a step forward in achieving long-range, zero-emission aviation, allowing airlines and passengers to play a larger role in the green energy transition. As a group, we hope that this project contributes to the survival of future generations and opens a door to pursue innovative, green aviation alternatives.

Bibliography

[1] M. van Bart, P. Méndez Chácon, A. Harmsen, R. Heckmanns, P. Diaz Garcia, K. Vanaken, A. Kiselev, T. Potgieter, M. Doorenbosch, and J. Van Nauta Lemke. Midterm Report - Heavier than air fast hydrogen seagoing Airship. Technical report, TU Delft, 2022.

[2] J. Sinke. Ae3211-ii: Miscellaneous topics. Production of Aerospace Systems, 2022.

[3] M. van Bart, P. Méndez Chácon, A. Harmsen, R. Heckmanns an P. Diaz Garcia, K. Vanaken, A. Kiselev, T. Potgieter, M. Doorenbosch, and J. Van Nauta Lemke. Baseline Report - Heavier than air fast hydrogen seagoing Airship. Technical report, TU Delft, 2022.

[4] E. Gill. Ae3211 systems engineering and aerospace design. Delft University of Technology, 2022.

[5] P. Lobner. Megalifter - semi-buoyant hybrid aircraft, 2022. URL https://lynceans.org/wp-content/uploads/2021/08/Megalifter-hybrid-aircraft_R1-converted-compressed.pdf.

[6] V. A. Yartys and M. V. Lototsky. An overview of hydrogen storage methods. In T. Nejat Veziroglu, Svetlana Yu. Zaginaichenko, Dmitry V. Schur, B. Baranowski, Anatofliy P. Shpak, and Valeriy V. Skorokhod, editors, *Hydrogen Materials Science and Chemistry of Carbon Nanomaterials*, pages 75–104, Dordrecht, 2005. Springer Netherlands. ISBN 978-1-4020-2669-0.

[7] G. Daniel Brewer. *Hydrogen Aircraft Technology*. CRC Press Inc., 1991.

[8] S. Gudmundsson. *GENERAL AVIATION AIRCRAFT DESIGN: APPLIED METHODS AND PROCEDURES*. Elsevier, first edition, 2014. ISBN: 978-0-12-397308-5.

[9] C. Bertorello, D. Bruzzone, P. Cassella, and I. Zotti. Trimaran model test results and comparison with different high speed craft, 2007.

[10] H. B. Suydam. Hydrodynamic characteristics of a low-drag planing-tail flying-boat hull, 1952.

[11] R. Vos, J.A. Melkert, and B.T.C. Zandbergen. AE1222-II: Class I weight estimation + payload-range diagrams version 14-Feb-20. Internal communication, 2020. Accessed: 8-06-2022.

[12] D.P. Raymer. *Aircraft Design: A Coneptual Aproach*. American Institute of Aeronautics and Astronautics, Inc., 1989.

[13] O. Al-Shamma and R. Ali. Aircraft weight estimation in interactive design process. *University of Hertfordshire*.

[14] Egbert Torenbeek. *Synthesis of subsonic airplane design: An introduction to the preliminary design of subsonic general aviation and transport aircraft, with emphasis on layout, aerodynamic design, propulsion and performance*. Kluwer, 1996.

[15] R. D. Finck. Usaf (united states air force) stability and control datcom (data compendium). Technical report, Flight Control Division, Air Force Flight Dynamics Labaratory, apr 1978.

[16] F. Oliviero. AE2111-II: Aerospace Design and Systems Engineering Elements II, Lift & Drag Estimation. Internal communication, 2021. Accessed: 24-05-2022.

[17] Alan Canamar. Seaplane conceptual design and sizing. Master's thesis, University of Glasgow, nov 2012.

[18] R.P. Liem A. Seth. Takeoff analysis of amphibious aircraft with implementation of a hydrofoil. Technical report, Manipal Institute of Technology, The Hong Kong University of Science and Technology, 2018. URL http://www.i-asem.org/publication_conf/structures18/11.ICAAS18/XH3A.6.AS1708_5081F1.pdf.

[19] M. Burston, K. Ranasinghe, A. Gardi, V. Parezanović, R. Ajaj, and R. Sabatini. Design principles and digital control of advanced distributed propulsion systems. *Energy*, 241, 2022. doi: 10.1016/j.energy.2021.122788.

[20] P. Lv. Theoretical and Experimental Investigation of Boundary Layer Ingestion for Aircraft Application | TU Delft Repositories, 04 2019. URL https://repository.tudelft.nl/islandora/object/uuid:6d8bd168-e057-4ee9-854c-32c84015e4c4?collection=research.

[21] M. Mennicken, D. Schoenweitz, M. Schnoes, and R. Schnell. Fan design assessment for BLI propulsion systems. *CEAS Aeronautical Journal*, 13(1):3–19, 2021. doi: 10.1007/s13272-021-00532-8.

[22] Filippone, A. *Advanced Aircraft Flight Performance*. Cambridge university press, 2012.

[23] The United States Department of Energy. *Improving Fan System Performance*. U.S. Department of Energy, Energy Efficiency and Renewable Energy, 2003.

[24] TLT-Turbo. The mojet - the next generation of jet fans for tunnel ventilation. Technical report, MoJet, 2018.

[25] S. Bozhko, C.I. Hill, and T. Yang. *More-Electric Aircraft: Systems and Modeling*, pages 1–31. John Wiley & Sons, Ltd, 2018. ISBN 9780471346081. doi: https://doi.org/10.1002/047134608X.W8367. URL https://onlinelibrary.wiley.com/doi/abs/10.1002/047134608X.W8367.

[26] T. Kadyk, C. Winnefeld, R. Hanke-Rauschenbach, and U. Krewer. Analysis and design of fuel cell systems for aviation. *Energies*, 11, 2018. doi: 10.3390/en11020375.

[27] Fuel Cells and Hydrogen 2 Joint Undertaking. *Hydrogen-powered aviation : a fact-based study of hydrogen technology, economics, and climate impact by 2050*. Publications Office, 2020. URL https://data.europa.eu/doi/10.2843/471510.

[28] Thomas Kadyk, René Schenkendorf, Sebastian Hawner, Bekir Yildiz, and Ulrich Römer. Design of fuel cell systems for aviation: Representative mission profiles and sensitivity analyses. *Frontiers in Energy Research*, 7, 2019. doi: 10.3389/fenrg.2019.00035. URL https://www.frontiersin.org/article/10.3389/fenrg.2019.00035.

[29] P. M. Sutheesh and A. Chollackal. Thermal performance of multilayer insulation: A review. In *IOP Conference Series: Materials Science and Engineering*, 2018. URL https://iopscience.iop.org/article/10.1088/1757-899X/396/1/012061/pdf#:~:text=The%20effective%20thermal%20conductivity%20of,conduction%20modes%20of%20heat%20transfer.

[30] A.J. Colozza. Hydrogen storage for aircraft applications overview, Sep 2002. URL https://ntrs.nasa.gov/citations/20020085127.

[31] C. Winnefeld, T. Kadyk, B. Bensmann, U. Krewer, and R. Hanke-Rauschenbach. Modelling and designing cryogenic hydrogen tanks for future aircraft applications. *Energies*, 11:105, 01 2018. doi: 10.3390/en11010105.

[32] Aerocorner. What materials are aircraft made of (& why) - plane design priorities. blog. URL https://aerocorner.com/blog/what-are-planes-made-of/#why-are-planes-made-of-aluminum.

[33] V. S. Saji and R. M. Cook. *Corrosion Protection and Control Using Nanomaterials*. Woodhead Publishing, 2012.

[34] H.D. Curtis. *Fundamentals of Aircraft Structural Analysis*. Mcgraw-Hill Education - Europe, 1996.

[35] C. Rans J. Melkert. Ae2135-i structural analysis & design. Formula Sheet and Lecture Slides, 2020.

[36] F. Oliviero. AE3211-I: System Engineering & Aerospace Design, Aircraft balance. Internal communication, 2022. Accessed: 02-06-2022.

[37] D. Batema et al. Dynamics and control 1 pdr. Power Point, 2006. Purdue University.

[38] F. Fossati. *Aero-Hydrodynamics and the Performance of Sailing Yachts*. Bloomsbury Publishing Plc, London, 2009.

[39] C. Wang et al. Seawater density variations in the north atlantic and the atlantic meridional overturning circulation. *Climate Dynamics*, 34:953–968, 2010. doi: 10.1007/s00382-009-0560-5.

[40] Federal Aviation Administration. Sec. 23.751 - main float buoyancy, 2011.

[41] H.R. van Nauta Lemke, J. van Amerongen, and P.G.M. van der Klugt. Rudder roll stabilization for ships. *Automatica*, 26:679–690, 1990. doi: doi.org/10.1016/0005-1098(90)90045-J.

[42] R. Abdel-Fadil and A. Eid. 3rd international conference on energy systems and technologies. In *Fuzzy Logic Control of Modern Aircraft Actuators*, volume 16-19, pages 149–158, Cairo, Egypt, 2015. Springer.

[43] M. Cavalieri and R. Wilson. The trend towards increasing use of electrical actuators in the aerospace and defense industry. pdf, 2015. URL https://www.google.com/url?sa=t&rct=j&q=&esrc=s&source=web&cd=&ved=2ahUKEwjZ97fq_az4AhW_h_0HHTLHBGMQFnoECD0QAQ&url=https%3A%2F%2Fwww.kollmorgen.com%2Fen-us%2Fservice-and-support%2Fknowledge-center%2Fwhite-papers%2Ftrend-towards-increasing-electrical-actuators-in-aerospace-and-defense%2F&usg=AOvVaw1QVBfz94wC-J-gCCTI4Mey.

[44] G. Qiao et al. A review of electromechanical actuators for more/all electric aircraft systems. *Journal of Mechanical Engineering Science*, 232(22):4128–4151, 2017. doi: 10.1177/0954406217749869.

[45] National Research Council (US) Committee on Airliner Cabin Air Quality. *Environmental Control Systems on Commercial Passenger Aircraft*, chapter 2 Environmental Control Systems on Commercial Passenger Aircraft. National Academies Press, 1986. doi: 10.17226/913. URL https://www.ncbi.nlm.nih.gov/books/NBK219009/#ddd00034.

[46] EASA eRules. Easy access rules for large aeroplanes (cs-25) (amendment 26). Technical report, European Union Aviation Safety Agency, October 2021. https://www.easa.europa.eu/document-library/easy-access-rules/online-publications/easy-access-rules-large-aeroplanes-cs-25?page=30.

[47] European Union Aviation Safety Agency. *Certification Specifications and Acceptable Means of Compliance for Large Aeroplanes CS-25*. European Union Aviation Safety Agency, March 2018.

[48] A. Synodinos, R. Self, and A. Torija. Preliminary noise assessment of aircraft with distributed electric propulsion. *AIAA*, jun 2018. https://arc.aiaa.org/doi/pdf/10.2514/6.2018-2817.

[49] Maurice Q Lourdes. *AC 36-1H - Noise Levels for U.S. Certificated and Foreign Aircraft Document Information*. Federal Aviation Administration, may 2012.

[50] Justin D. Salciccioli, Yves Crutain, Matthieu Komorowski, and Dominic C. Marshall. *Sensitivity Analysis and Model Validation*, pages 263–271. Springer International Publishing, Cham, 2016. ISBN 978-3-319-43742-2. doi: 10.1007/978-3-319-43742-2_17. URL https://doi.org/10.1007/978-3-319-43742-2_17.

[51] J. Hoeflinger and P. Hofmann. Air mass flow and pressure optimisation of a pem fuel cell range extender system. *International Journal of Hydrogen Energy*, 45:29246–29258, 2020. doi: https://doi.org/10.1016/j.ijhydene.2020.07.176. URL https://www.sciencedirect.com/science/article/pii/S0360319920327841.

[52] Ming He, Cui Lv, Linghui Gong, Jihao Wu, Weiping Zhu, Yu Zhang, Meimei Zhang, Wentao Sun, and Li Sha. The design and optimization of a cryogenic compressed hydrogen refueling process. *International Journal of Hydrogen Energy*, 2021. doi: https://doi.org/10.1016/j.ijhydene.2020.11.061. URL https://www.sciencedirect.com/science/article/pii/S0360319920342634.

[53] J. Sinke. Ae3211-i production of aerospace systems. Delft University of Technology, 2022.

[54] J. Markish. Valuation techniques for commercial aircraft program design. Master's thesis, Massachusetts Institute of Technology, http://hdl.handle.net/1721.1/16871, jun 2002.

[55] G. Kleen and E. Padgett. Durability-adjusted fuel cell system cost. *Department of Energy United States of America*, jan 2021.

[56] J. Hoelzen, D. Silberhorn, T. Zill, B. Bensmann, and R. Hanke-Rauschenbach. Hydrogen-powered aviation and its reliance on green hydrogen infrastructure – review and research gaps. *International Journal of Hydrogen Energy*, 47:3108–3130, January 2022. URL https://www.sciencedirect.com/science/article/pii/S0360319921043184#appsec1.

A Task Distribution

Table A.1 shows the contributions of each member of the group to the project. It should be noted that the hours contributed to the tasks differ. Some people focused a large amount of time, such as tasks for the design which including programming. Others worked on various tasks, thus their names will be more present in the table. In the end, everyone participated the same amount of time and contributed equally to the report.

Table A.1: *Work Division*

Chapter	**Contribution**
0. Executive Overview	Julie, Kato, Paula & Thomas
1. Introduction	Julie & Kato
2. Objectives and requirements	Julie & Paula
3. Functional analysis	Atze, Mika & Paloma
4. Preliminary Design and Trade-off summary	Alexander, Julie, Kato, Max, Mika, Rowan & Thomas
5. Initialising Detailed Design	Alexander, Max, Thomas & Rowan
6. Design Characteristics	Everyone
7. Characteristics Analysis and Summary	Alexander, Atze, Julie, Max, Mika & Rowan
8. Verification, Validation, and Sensitivity	Alexander, Max & Thomas
9. Data Diagrams	Kato, Paloma, Paula & Rowan
10. Production, Operations and Logistics	Julie, Kato, Mika, Thomas, Paloma, Paula & Rowan
11. Sustainability	Julie, Paula & Paloma
12. Market analysis	Atze, Mika, Kato & Thomas
13. Costs and Revenue Analysis	Atze, Mika & Thomas
14. Risks	Kato
15. Discussion	Julie & Thomas
16. Conclusion and Reflection	Julie, Paula & Thomas
CATIA	Paloma & Rowan
Renders	Max